

WL-TR-93-4126

HIGH PERFORMANCE ELASTOMERS

K.J.L. PACIOREK

TECHNOLUBE PRODUCTS CO.
3365 E. SLAUSON AVE.
VERNON CA 90058



OCTOBER 1993

FINAL REPORT FOR 02/24/87-09/30/93

APPROVED FOR PUBLIC RELEASE; DISTRIBUTION IS UNLIMITED.

MATERIALS DIRECTORATE
WRIGHT LABORATORY
AIR FORCE MATERIEL COMMAND
WRIGHT PATTERSON AFB OH 45433-7734

19960708 032

DTIC QUALITY INSPECTED 1

DISCLAIMER NOTICE



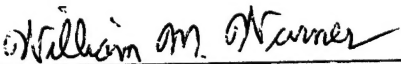
THIS DOCUMENT IS BEST QUALITY AVAILABLE. THE COPY FURNISHED TO DTIC CONTAINED A SIGNIFICANT NUMBER OF PAGES WHICH DO NOT REPRODUCE LEGIBLY.


NOTICE


When Government drawings, specifications, or other data are used for any purpose other than in connection with a definitely Government-related procurement, the United States Government incurs no responsibility or any obligation whatsoever. The fact that the government may have formulated or in any way supplied the said drawings, specifications, or other data, is not to be regarded by implication, or otherwise in any manner construed, as licensing the holder, or any other person or corporation; or as conveying any rights or permission to manufacture, use, or sell any patented invention that may in any way be related thereto.

This report is releasable to the National Technical Information Service (NTIS). At NTIS, it will be available to the general public, including foreign nations.

This technical report has been reviewed and is approved for publication.


WILLIAM M. WARNER
Nonstructural Materials Branch
Nonmetallic Materials Division
Materials Directorate


KENT J. EISENTRAUT, Chief
Nonstructural Materials Branch
Nonmetallic Materials Division
Materials Directorate


CHARLES E. BROWNING, Chief
Nonmetallic Materials Division
Materials Directorate

If your address has changed, if you wish to be removed from our mailing list, or if the addressee is no longer employed by your organization please notify WL/MLBT, WPAFB, OH 45433 -7750 to help us maintain a current mailing list.

Copies of this report should not be returned unless return is required by security considerations, contractual obligations, or notice on a specific document.

REPORT DOCUMENTATION PAGE

Form Approved
OMB No. 0704-0188

Public reporting burden for this collection of information is estimated to average 1 hour per response, including the time for reviewing instructions, searching existing data sources, gathering and maintaining the data needed, and completing and reviewing the collection of information. Send comments regarding this burden estimate or any other aspect of this collection of information, including suggestions for reducing this burden, to Washington Headquarters Services, Directorate for Information Operations and Reports, 1215 Jefferson Davis Highway, Suite 1204, Arlington, VA 22202-4302, and to the Office of Management and Budget, Paperwork Reduction Project (0704-0188), Washington, DC 20503.

1. AGENCY USE ONLY (Leave blank)		2. REPORT DATE OCT 1993	3. REPORT TYPE AND DATES COVERED FINAL 02/24/87--09/30/93	
4. TITLE AND SUBTITLE HIGH PERFORMANCE ELASTOMERS			5. FUNDING NUMBERS C F33615-86-C-5080 PE 62102 PR 2421 TA 01 WU 45	
6. AUTHOR(S) K.J.L. PACIOREK				
7. PERFORMING ORGANIZATION NAME(S) AND ADDRESS(ES) TECHNOLUBE PRODUCTS CO. 3365 E. SLAUSON AVE. VERNON, CA 90058			8. PERFORMING ORGANIZATION REPORT NUMBER SN-3514-F	
9. SPONSORING/MONITORING AGENCY NAME(S) AND ADDRESS(ES) MATERIALS DIRECTORATE WRIGHT LABORATORY AIR FORCE MATERIEL COMMAND WRIGHT-PATTERSON AFB OH 45433-7734 POC: W. Warner, WL/MLBT, 255-9016			10. SPONSORING/MONITORING AGENCY REPORT NUMBER WL-TR-93-4126	
11. SUPPLEMENTARY NOTES				
12a. DISTRIBUTION/AVAILABILITY STATEMENT APPROVED FOR PUBLIC RELEASE; DISTRIBUTION IS UNLIMITED			12b. DISTRIBUTION CODE	
13. ABSTRACT (Maximum 200 words) The investigations of processes leading to high performance elastomer systems based on quinoxaline- or imide rings linked by perfluoroalkylether chains, initiated in February 1987 and described in part in three Interim Reports, were completed. In the final portion of the program mono-, dumbbell-, and polymeric quinoxalines linked by perfluoroalkylether chains, either directly to the heterocycle or via a phenyl group, were synthesized and evaluated. Two types of linking groups were studied: $-\text{CF}_2\text{CF}_2(\text{OCF}_2\text{CF}_2)_5-$ ("A" arrangement) and $-\text{CF}_2\text{CF}_2\text{CF}_2\text{O}(\text{CF}_2)_4\text{O}(\text{CF}_2)_4\text{OCF}_2\text{CF}_2\text{CF}_2-$ ("B" arrangement). The thermal stability of the quinoxalines based on the "A" linkage was $\sim 316^\circ\text{C}$. Materials linked by the "B" arrangement to the quinoxaline via p-phenylene units gave dumbbell- and polymeric quinoxalines of thermal and thermal oxidative stability exceeding 330°C , proving the validity of the approach taken. Investigations of perfluoroalkylether-linked imides were limited; the yields were low and purifications tedious.				
14. SUBJECT TERMS HIGH PERFORMANCE ELASTOMERS WIDE TEMPERATURE RANGE THERMOOXIDATIVE STABILITY			15. NUMBER OF PAGES 178	
SEAL TECHNOLOGY ELASTOMER SYNTHESIS FLUORINE CHEMISTRY			16. PRICE CODE	
17. SECURITY CLASSIFICATION OF REPORT UNCLASSIFIED	18. SECURITY CLASSIFICATION OF THIS PAGE UNCLASSIFIED	19. SECURITY CLASSIFICATION OF ABSTRACT UNCLASSIFIED	20. LIMITATION OF ABSTRACT SAR	

TABLE OF CONTENTS

<u>SECTION</u>	<u>PAGE</u>
1. EXECUTIVE SUMMARY.....	1
2. INTRODUCTION.....	5
3. RESULTS AND DISCUSSION.....	9
3.1 QUINOXALINE I.....	10
3.2 QUINOXALINE II.....	19
3.3 QUINOXALINE III.....	20
3.4 QUINOXALINE IV.....	23
3.5 QUINOXALINE V.....	25
3.6 QUINOXALINE VI.....	27
3.7 QUINOXALINE VII.....	30
3.8 QUINOXALINES VIII and IX.....	32
3.9 IMIDES.....	39
4. EXPERIMENTAL DETAILS AND PROCEDURES.....	47
5. REFERENCES.....	166

LIST OF FIGURES

FIGURE	PAGE
1. Infrared spectrum of $\text{C}_6\text{H}_5\text{C}(\text{O})\text{C}(\text{O})\text{CF}_2\text{CF}_2(\text{OCF}_2\text{CF}_2)_5\text{C}(\text{O})\text{C}(\text{O})\text{C}_6\text{H}_5$	56
2. Infrared spectrum of Quinoxaline I.....	58
3. TGA scan of Quinoxaline I in N_2	59
4. TGA scan of Quinoxaline I in air.....	60
5. Infrared spectrum of $\text{C}_7\text{F}_{15}\text{C}(\text{O})\text{C}(\text{O})\text{C}_6\text{H}_5$	64
6. Infrared spectrum of Quinoxaline II.....	67
7. DSC scan of Quinoxaline II.....	68
8. TGA scan of Quinoxaline II in N_2	69
9. TGA scan of Quinoxaline II in air.....	70
10. Infrared spectrum of $\text{C}_6\text{H}_5\text{C}(\text{O})\text{C}(\text{O})\text{C}_6\text{H}_4(\text{CF}_2\text{CF}_2\text{O})_5\text{CF}_2\text{CF}_2\text{C}_6\text{H}_4\text{C}(\text{O})\text{C}(\text{O})\text{C}_6\text{H}_5$	72
11. Infrared spectrum of Quinoxaline III.....	74
12. DSC scan of Quinoxaline III.....	75
13. TGA scan of Quinoxaline III in N_2	76
14. TGA scan of Quinoxaline III in air.....	77
15. Infrared spectrum of Quinoxaline IV.....	79
16. DSC scan of Quinoxaline IV.....	80
17. TGA scan of Quinoxaline IV in N_2	81
18. TGA scan of Quinoxaline IV in air.....	82
19. Infrared spectrum of $\text{C}_3\text{F}_7\text{OCF}(\text{CF}_3)\text{CF}_2\text{OCF}(\text{CF}_3)\text{C}(\text{O})\text{C}(\text{O})\text{C}_6\text{H}_5$	84
20. Infrared spectrum of Quinoxaline V.....	88
21. DSC scan of Quinoxaline V.....	89
22. TGA scan of Quinoxaline V in N_2	90
23. TGA scan of Quinoxaline V in air.....	91
24. Infrared spectrum of Quinoxaline VI.....	95

LIST OF FIGURES

<u>FIGURE</u>	<u>PAGE</u>
25. TGA scan of Quinoxaline VI in N ₂	96
26. TGA scan of Quinoxaline VI in air.....	97
27. Infrared spectrum of [MeO ₂ CC ₃ F ₆ OC ₄ F ₈] ₂ O.....	99
28. Infrared spectrum of [C ₆ H ₅ C(O)C(O)C ₃ F ₆ OC ₄ F ₈] ₂ O.....	101
29. Infrared spectrum of Quinoxaline VII.....	105
30. DSC scan of Quinoxaline VII.....	106
31. DSC scan of Quinoxaline VII after a prior DSC run up to 100°C.....	107
32. DSC scan of Quinoxaline VII following exposure to 316°C for 72 hours.....	108
33. TGA scan of Quinoxaline VII in N ₂	109
34. TGA scan of Quinoxaline VII in air.....	110
35. Infrared spectrum of [HO ₂ CC ₃ F ₆ OC ₄ F ₈] ₂ O.....	112
36. Infrared spectrum of [AgO ₂ CC ₃ F ₆ OC ₄ F ₈] ₂ O.....	113
37. Infrared spectrum of [IC ₃ F ₆ OC ₄ F ₈] ₂ O.....	116
38. Infrared spectrum of [C ₆ H ₅ C(O)C(O)C ₆ H ₄ C ₃ F ₆ OC ₄ F ₈] ₂ O.....	119
39. Infrared spectrum of Quinoxaline VIII.....	120
40. TGA scan of Quinoxaline VIII in N ₂	122
41. TGA scan of Quinoxaline VIII in air.....	123
42. Infrared spectrum of Quinoxaline IX-1.....	124
43. TGA scan of the hexafluorobenzene-soluble portion of Quinoxaline IX-1 in N ₂	125
44. TGA scan of the hexafluorobenzene-insoluble portion of Quinoxaline IX-1 in N ₂	126
45. Infrared spectrum of Quinoxaline IX-2.....	127
46. TGA scan of Quinoxaline IX-2 in N ₂	128
47. TGA scan of Quinoxaline IX-2 in air.....	129

LIST OF FIGURES

<u>FIGURE</u>	<u>PAGE</u>
48. Infrared spectrum of Quinoxaline IX-3 (in C ₆ F ₆ ; solvent subtracted).....	130
49. TGA scan of Quinoxaline IX-3 in N ₂	131
50. TGA scan of Quinoxaline IX-3 in air.....	132
51. Infrared spectrum of Quinoxaline IX-4 (in C ₆ F ₆ ; solvent subtracted).....	133
52. TGA scan of Quinoxaline IX-4 in N ₂	134
53. TGA scan of Quinoxaline IX-4 in air.....	135
54. Infrared spectrum of Quinoxaline IX-5 (in C ₆ F ₆ ; solvent subtracted).....	136
55. TGA scan of Quinoxaline IX-5 in N ₂	137
56. Infrared spectrum of Quinoxaline IX-6.....	138
57. TGA scan of Quinoxaline IX-6 in N ₂	139
58. Infrared spectrum of Imide II.....	147
59. TGA scan of Imide II in N ₂	148
60. TGA scan of Imide II in air.....	149
61. Infrared spectrum of BrC ₆ H ₄ C(O)CF ₂ CF ₂ (OCF ₂ CF ₂) ₅ C(O)C ₆ H ₄ Br.....	152
62. Infrared spectrum of BrC ₆ H ₄ C ₃ F ₆ O(CF ₂ CF ₂ O) ₄ C ₃ F ₆ C ₆ H ₄ Br.....	157
63. Infrared spectrum of Imide III.....	161
64. TGA scan of Imide III in N ₂	162
65. TGA scan of Imide III in air.....	163
66. DSC scan of Imide III.....	164
67. DSC scan of Imide III exposed in vacuum to 316°C for 72 hours.....	165

LIST OF TABLES

<u>TABLE</u>	<u>PAGE</u>
1 ION FRAGMENTS AND INTENSITIES RELATIVE TO BASE PEAK OF $C_6H_5CCl=CClC_6H_5$	12
2 ION FRAGMENTS AND INTENSITIES RELATIVE TO BASE PEAK OF $C_6H_5CCl_2C(O)CF_2CF_2(OCF_2CF_2)_5CO_2Me$	13
3 QUINOXALINE DATA SUMMARY.....	14
4 SUMMARY OF THERMAL TESTING OF QUINOXALINES.....	17
5 PREPARATION OF QUINOXALINE IX SERIES.....	36
6 QUINOXALINE IX SERIES.....	37
7 IMIDE DATA SUMMARY.....	40
8 SUMMARY OF THERMAL TESTING OF IMIDES.....	41
9 ION FRAGMENTS AND INTENSITIES RELATIVE TO BASE PEAK OF $C_3F_7[OCF(CF_3)CF_2]_2C_6H_4NH_2$	44
10 ION FRAGMENTS AND INTENSITIES RELATIVE TO BASE PEAK OF $EtO_2C(CF_2CF_2O)_5CF_2CF_2CO_2Et$	51
11 ION FRAGMENTS AND INTENSITIES RELATIVE TO BASE PEAK OF $C_6H_5CCl_2C(O)(CF_2CF_2O)_5CF_2CF_2C(O)CCl_2C_6H_5$	53
12 ION FRAGMENTS AND INTENSITIES RELATIVE TO BASE PEAK OF $C_6H_5C(O)C(O)CF_2CF_2(OCF_2CF_2)_5C(O)C(O)C_6H_5$	55
13 ION FRAGMENTS AND INTENSITIES RELATIVE TO BASE PEAK OF QUINOXALINE I.....	57
14 ION FRAGMENTS AND INTENSITIES RELATIVE TO BASE PEAK OF $C_6H_5CCl_2C(O)C_7F_{15}$	62
15 ION FRAGMENTS AND INTENSITIES RELATIVE TO BASE PEAK OF $C_6H_5C(O)C(O)C_7F_{15}$	63
16 ION FRAGMENTS AND INTENSITIES RELATIVE TO BASE PEAK OF QUINOXALINE II.....	66
17 ION FRAGMENTS AND INTENSITIES RELATIVE TO BASE PEAK OF $C_6H_5C(O)C(O)C_6H_4(CF_2CF_2O)_5CF_2CF_2C_6H_4C(O)C(O)C_6H_5$	71
18 ION FRAGMENTS AND INTENSITIES RELATIVE TO BASE PEAK OF $C_3F_7OCF(CF_3)CF_2OCF(CF_3)C(O)CCl_2C_6H_5$	83

<u>TABLE</u>	<u>PAGE</u>
19 ION FRAGMENTS AND INTENSITIES RELATIVE TO BASE PEAK OF $C_3F_7OCF(CF_3)CF_2OCF(CF_3)C(O)C(O)C_6H_5$	84
20 ION FRAGMENTS AND INTENSITIES RELATIVE TO BASE PEAK OF QUINOXALINE V.....	87
21 SUMMARY OF ULTRAVIOLET SPECTROSCOPIC ANALYSES OF AMINES, KETONES, AND QUINOXALINES.....	93
22 ION FRAGMENTS AND INTENSITIES RELATIVE TO BASE PEAK OF $[MeO_2CC_3F_6OC_4F_8]_2O$ (MW, 866).....	98
23 ION FRAGMENTS AND INTENSITIES RELATIVE TO BASE PEAK OF $[C_6H_5CCl_2C(O)C_3F_6OC_4F_8]_2O$ (MW, 1122).....	100
24 ION FRAGMENTS AND INTENSITIES RELATIVE TO BASE PEAK OF $[C_6H_5C(O)C(O)(CF_2)_3O(CF_2)_4]_2O$ (MW, 1014).....	102
25 ION FRAGMENTS AND INTENSITIES RELATIVE TO BASE PEAK OF QUINOXALINE VII.....	104
26 ION FRAGMENTS AND INTENSITIES RELATIVE TO BASE PEAK OF $[ICF_2CF_2CF_2OCF_2CF_2CF_2CF_2]_2O$ (MW, 1002).....	115
27 ION FRAGMENTS AND INTENSITIES RELATIVE TO BASE PEAK OF $[C_6H_5C(O)C(O)C_6H_4C_3F_6OC_4F_8]_2O$ (MW, 1166).....	118
28 ION FRAGMENTS AND INTENSITIES RELATIVE TO BASE PEAK OF $C_3F_7OCF(CF_3)CF_2OCF(CF_3)C(O)C_6H_4Br$	141
29 ION FRAGMENTS AND INTENSITIES RELATIVE TO BASE PEAK OF $C_3F_7O[CF(CF_3)CF_2O]_2CF(CF_3)C(O)C_6H_4Br$	142
30 ION FRAGMENTS AND INTENSITIES RELATIVE TO BASE PEAK OF $C_3F_7[OCF(CF_3)CF_2]_2C_6H_4Br$	143
31 ION FRAGMENTS AND INTENSITIES RELATIVE TO BASE PEAK OF IMIDE II.....	145
32 ION FRAGMENTS AND INTENSITIES RELATIVE TO BASE PEAK OF $C_3F_7[OCF(CF_3)CF_2]_3C_6H_4[N(CO)_2]C_6H_4$	146
33 ION FRAGMENTS AND INTENSITIES RELATIVE TO BASE PEAK OF $C_6H_5C(O)CF_2CF_2(OCF_2CF_2)_5C(O)C_6H_4Br$	151
34 ION FRAGMENTS AND INTENSITIES RELATIVE TO BASE PEAK OF $BrC_6H_4C(O)CF_2CF_2(OCF_2CF_2)_5C(O)C_6H_4Br$	153
35 ION FRAGMENTS AND INTENSITIES RELATIVE TO BASE PEAK OF $[BrC_6H_3(CF_2)_3O(CF_2CF_2O)_4(CF_2)_3C_6H_3Br]S_2$	154

TABLEPAGE

36	ION FRAGMENTS AND INTENSITIES RELATIVE TO BASE PEAK OF $\text{BrC}_6\text{H}_4\text{C}_3\text{F}_6\text{O}(\text{CF}_2\text{CF}_2\text{O})_4\text{C}_3\text{F}_6\text{C}_6\text{H}_4\text{Br}$ (MW, 1090).....	156
37	ION FRAGMENTS AND INTENSITIES RELATIVE TO BASE PEAK OF $\text{C}_6\text{H}_5\text{C}_3\text{F}_6\text{O}(\text{CF}_2\text{CF}_2\text{O})_4\text{C}_3\text{F}_6\text{C}_6\text{H}_4\text{Br}$ (MW, 1012).....	158
38	ION FRAGMENTS AND INTENSITIES RELATIVE TO BASE PEAK OF $\text{BrC}_6\text{H}_4\text{C}_3\text{F}_6\text{O}(\text{CF}_2\text{CF}_2\text{O})_4\text{C}_3\text{F}_6\text{C}_6\text{H}_4[\text{N}(\text{CO})_2]\text{C}_6\text{H}_4$	160

FOREWORD

This report was prepared by Technolube Products Division, Lubricating Specialties Co., Vernon, California, under Contract No. F33615-86-C-5080 " High Performance Elastomers" and covers work performed during the period 24 February 1987 through 30 September 1993. The investigations were carried out by K.J.L. Paciorek, Project Manager, with contributions by R.H. Kratzer, S.R. Masuda, W-H. Lin and J.H. Nakahara of Technolube, and J.G. Shih, K.K. Johri, J.S. Wroblewski and K.G. Podejko of Ultrasystems Defense. This contract was administered under the direction of Wright Laboratory/Materials Directorate with Dr. William M. Warner (WL/MLBT) as the Project Engineer.

We wish to acknowledge the contribution of Wright Laboratory/Materials Directorate, Nonstructural Materials Branch personnel for providing difunctional perfluoroalkylether precursors.

1. EXECUTIVE SUMMARY

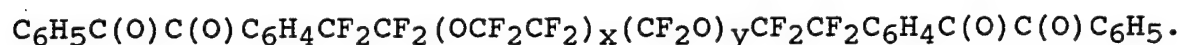
This is the Final Report under this contract; it contains detailed description of the work carried out during the fourth period. The details of investigations performed during the preceeding three years are given in the corresponding Interim Reports. The results of these studies are summarized below. The objective of this program was to develop thermally stable elastomeric materials usable over the temperature range from -54 to 371°C in the presence of fluids and air. A system consisting of polyquinoxaline rings linked by pefluoroalkylether chains based on a literature survey carried out during the first year of this undertaking, offered the best potential for attaining the program goals.

First year investigations were devoted to assessing the feasibility of the concept of perfluoroalkylether linked polyquinoxaline sytems by preparing and evaluating perfluoroalkyl-substituted model compounds. Also in the first year, a practical synthesis of 4-iodobenzil, a key comonomer, was developed. During the second year, a perfluoroalkylether-substituted model quinoxaline system, having a $n\text{-C}_8\text{F}_{17}\text{OCF}_2\text{CF}_2\text{-}$ group linked to the aromatic ring, was synthesized and shown to possess excellent thermal stability which validated the original postulation. Attempts to utilize commercially available difunctional precursors of the general formula $\text{HO}_2\text{C}(\text{CF}_2\text{CF}_2\text{O})_x(\text{CF}_2\text{O})_y\text{CF}_2\text{CO}_2\text{H}$ (Fomblin Z) were not successful. It

was subsequently shown that materials having difluoroformyl groups (OCF_2) adjacent to phenyl rings cannot be formed via coupling of the corresponding iodides with aromatic iodides.

The investigations performed during the third year of the program, were directed at developing processes leading to the production of a modified system derived from the commercially available $\text{HO}_2\text{C}(\text{CF}_2\text{CF}_2\text{O})_x(\text{CF}_2\text{O})_y\text{CF}_2\text{CO}_2\text{H}$,

namely, the benzil intermediate:



Model studies using $\text{ICF}_2\text{CF}_2\text{O}(\text{CF}_2)_5\text{OCF}_2\text{CF}_2\text{I}$ were conducted concurrently. This work revealed that an arrangement such as that present in the Fomblin Z system, having repeating perfluoroalkylether units, behaves differently from the one where the oxygens are separated by relatively long perfluoroalkyl segments. The major problem is the apparent instability of the perfluoroalkylethercopper compound at the elevated temperatures required for its formation. The attendant decomposition mechanisms were identified. The use of palladium catalyst and active copper reagents were explored to circumvent these problems; none were successful. The heterogeneous nature of Fomblin Z derived materials presented great difficulties in separation and analysis of the products and hindered mechanistic evaluations.

The work performed during the final period of the contract was centered on synthesis and evaluation of quinoxalines based on two difunctional monomolecular perfluoroalkylethers

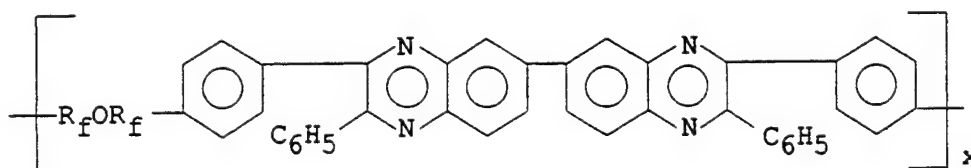
supplied by WL/MLBT. Limited effort was directed at the synthesis and evaluation of perfluoroalkylether linked imide systems; these investigations were initiated during the third year of the program. Synthesis yields were low; thermal stabilities were lower than that of the most promising polyquinoxalines. Two perfluoroalkylether linking arrangements were studied $-(CF_2CF_2O)_5CF_2CF_2-$ and $-(CF_2)_3O(CF_2)_4O(CF_2)_4O(CF_2)_3-$ in two types of quinoxalines. Specifically, a system in which the perfluoroalkylether chains are linked to the heterocyclic rings through phenyl groups, and a system where the perfluoroalkylether bridges are directly attached to the heterocyclic ring. Neither system exhibited the required thermal stability using the $-CF_2CF_2(OCF_2CF_2)_5-$ bridging units. Apparently the arrangement, $Ar-CF_2CF_2(OCF_2CF_2)_x-$, incorporates an inherent thermal instability. For compositions wherein the attachment to the phenyl rings was via perfluoro-n-propyl group (as illustrated by the linkage, $-(CF_2)_3O(CF_2)_4O(CF_2)_4O(CF_2)_3-$), both the model and polymeric quinoxalines exhibited thermal and thermal oxidative stability above 330°C by experimental evaluations. Thermal gravimetric analyses point to stabilities above 370°C. These results prove the validity of the original concept and provide feasible premises for development of thermally and oxidatively stable elastomers for the advanced aircraft applications. Limitation of time and funds prevented further evaluation of the applicability of these novel

compositions to preparation of practical high temperature elastomers.

2. INTRODUCTION

The objective of this program was to develop a thermally stable elastomeric material usable over the temperature range from -54 to 371°C in the presence of fluids and air. The envisioned approach was to chain-extend low glass transition temperature (T_g) perfluoro-alkylether segments through thermally and oxidatively stable aromatic units. A selected number of these chain extension units was to be capable of forming cross-links between chains and/or, as desired, chemical bonds to reactive fillers to reinforce the high temperature modulus of the elastomer.

A system composed of phenylquinoxaline rings joined by perfluoroalkylether chains was the primary elastomeric gum



candidate with the pendant phenyl-groups the most likely sites for introduction of functional groups for cross-linking or binding to the modulus reinforcing reactive fillers.

The investigations were carried out from 24 February 1987 through 31 September 1993, with a lapse from 24 February 1991 to 24 June 1992. This is the Final Report under subject contract. Only the work performed since February 1990 is discussed in detail. To maintain continuity and to provide basis for the approaches chosen, as the program proceeded, a brief

summary of the work described in the previous three Interim Reports [Ref. 1-3] is summarized below.

The first year program [Ref. 1] was devoted to assessing the feasibility of the concept of perfluoroalkylether linked polyquinoxaline systems by preparing and evaluating perfluoroalkyl-substituted model compounds. Also in the first year, a practical synthesis of 4-iodobenzil, a key comonomer, was developed. Only preliminary investigations of the extended chain perfluoroalkylether diiodide were carried out at that stage. During the second year [Ref. 2], a perfluoroalkylether-substituted model quinoxaline system, having a $n\text{-C}_8\text{F}_{17}\text{OCF}_2\text{CF}_2\text{-}$ group linked to the aromatic ring, was synthesized and shown to possess an excellent thermal stability, which validated the original postulation. The analogous material having the -OCF_2 group next to the aromatic ring could be not synthesized since the benzil intermediate could not be formed from the corresponding $\text{-OCF}_2\text{I}$ precursor. This finding explained the problems associated with forming Fomblin Z based bisbenzil from Fomblin Z diiodide since in the latter the $\text{-OCF}_2\text{I}$ groups are present. Investigations were then directed at producing "modified" Fomblin Z diiodides where the OCF_2I end-groups were replaced by $\text{-OCF}_2\text{CF}_2\text{OCF}_2\text{CF}_2\text{I}$ moieties.

The investigations performed during the third year of the program [Ref. 3], were directed at developing processes leading to the production of the desired modified Fomblin Z bisbenzil. Model studies using $\text{ICF}_2\text{CF}_2\text{O}(\text{CF}_2)_5\text{OCF}_2\text{CF}_2\text{I}$ were

conducted concurrently. This work revealed that an arrangement such as that present in the Fomblin Z system, having repeating perfluoroalkylether units, behaves differently from the one where the oxygens are separated by relatively long perfluoroalkyl segments. The major problem is the apparent instability of the perfluoroalkylethercopper compound at the elevated temperatures required for its formation. The attendant decomposition mechanisms were identified. The use of palladium catalyst and active copper reagents was explored to circumvent these problems; none were successful. The heterogeneous nature of Fomblin Z derived materials presented great difficulties in separation and analysis of the products and hindered mechanistic evaluations.

As an alternative to the polyquinoxaline system a polyimide arrangement was explored. The deficiency of the specific type of compounds studied was the presence of a $-CH_2$ attachment to the aromatic ring which presents potential oxidative instability. Although the model compound derived from monofunctional materials exhibited good thermal stability at $371^\circ C$, the last step did not proceed to completion (for the difunctional Fomblin Z derived material). Due to the inherent oxidative instability of such a structure, no attempts were made to further study the process.

Also during the third year of the program, a unimolecular perfluoroalkylether diester, $MeO_2C(CF_2CF_2O)_5CF_2CF_2CO_2Me$, became available from WL/MLBT. This material was successfully transformed into the corresponding

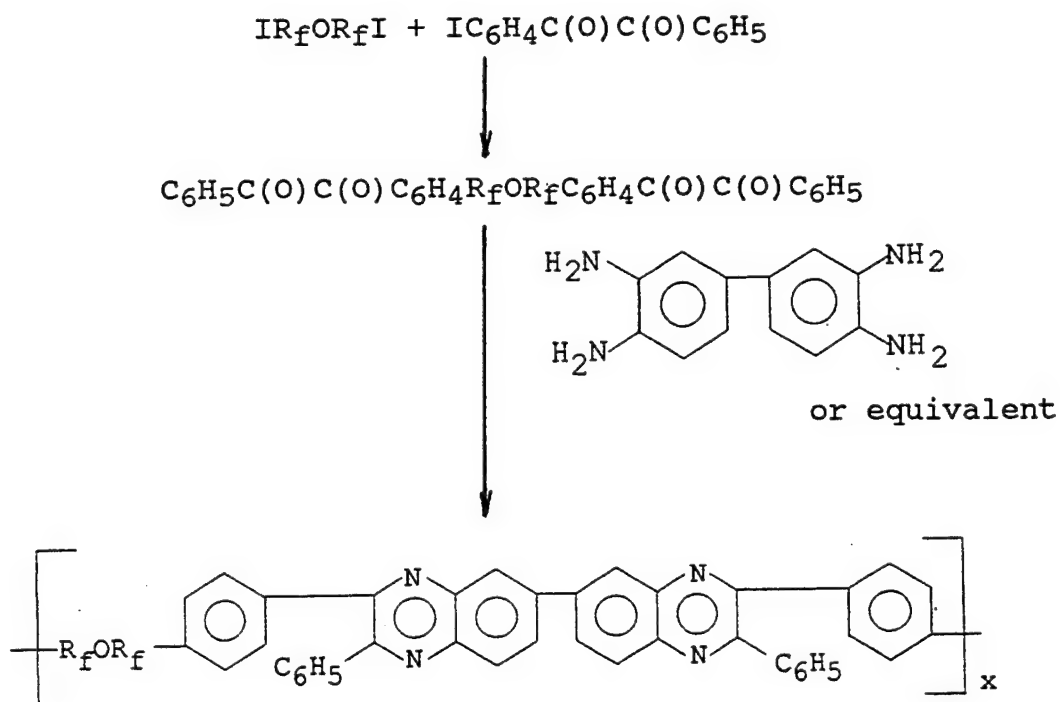
diiodide, $\text{I}(\text{CF}_2\text{CF}_2\text{O})_5\text{CF}_2\text{CF}_2\text{I}$, a key intermediate for the synthesis of the perfluoroalkylether-linked quinoxaline systems.

The work performed during the last period of the program, described in this Final Report, was in many aspects a direct continuation of the efforts summarized above. Thus the specific avenues chosen were based largely on the results and experience acquired in the earlier phases of the subject contract. Accordingly, $\text{MeO}_2\text{C}(\text{CF}_2\text{CF}_2\text{O})_5\text{CF}_2\text{CF}_2\text{CO}_2\text{Me}$ and its derivatives were utilized in the synthesis of two kinds of perfluoroalkylether-linked quinoxaline systems. One had all the linkups with the heterocyclic rings through phenyl groups, the other had the perfluoroalkyl groups directly attached to the heterocyclic ring. Neither system exhibited the required thermal stability. Apparently the arrangement, $\text{Ar}-\text{CF}_2\text{CF}_2(\text{OCF}_2\text{CF}_2)_x-$ incorporates inherent thermal instability. A related polyimide system exhibited a promising stability; unfortunately, the synthesis process did not lend itself to polymeric materials production.

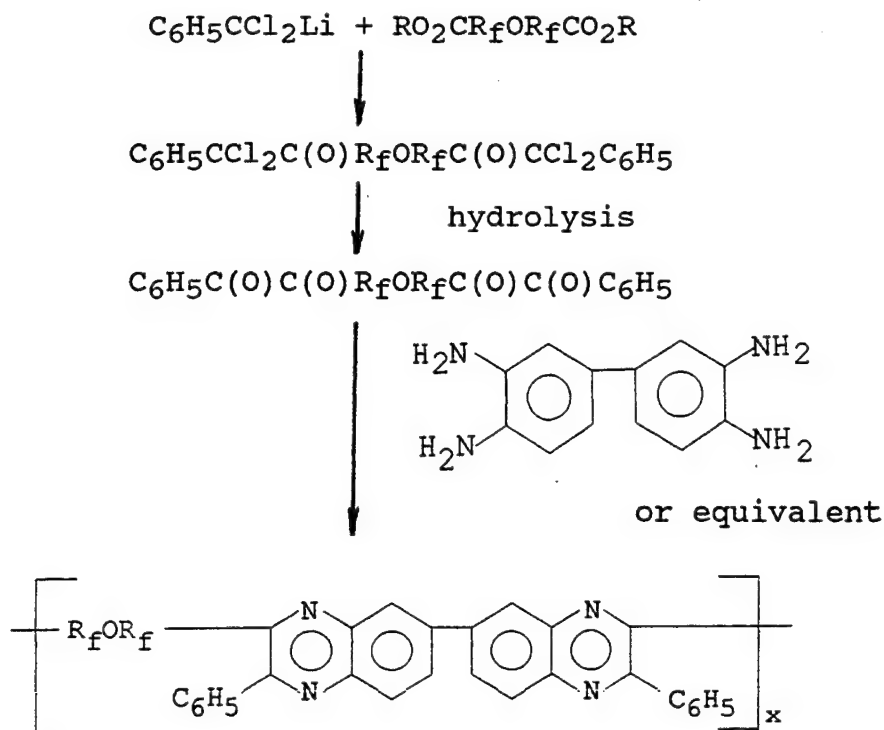
In view of the above findings, subsequent efforts were directed at a system wherein the attachment to the aromatic rings was via perfluoro-n-propyl group. Both the model and polymeric quinoxalines, wherein the perfluoroalkylether attachment was via a phenyl ring, exhibited thermal and thermal oxidative stability above 330°C , proving the validity of the original concept and providing a basis for the development of thermally and oxidatively stable elastomers for advanced aircraft applications.

3. RESULTS AND DISCUSSION

The investigations performed during the first three years of the subject program [Ref. 1-3], as described in Section 2, were devoted almost entirely to identifying and developing processes leading to polyquinoxaline systems by the general route depicted below:



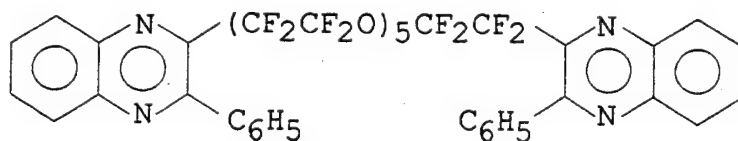
An alternative route leading to a quinoxaline system linked directly through the heterocyclic ring was also explored during the last phase of the program. The overall synthesis path is depicted below:



In addition a limited, effort was devoted to the study of imides. The availability, from WL/MLBT, of two unimolecular perfluoroalkylethers allowed the investigation of the effect of specific arrangements on the ease of reaction and stability of the final product.

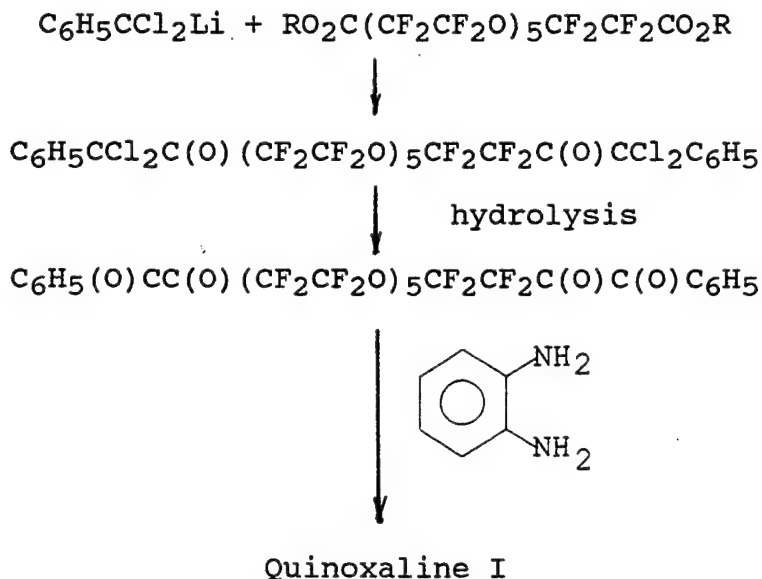
For ease of presentation, the synthesis and evaluations of the heterocyclics will be discussed in a separate section.

3.1 QUINOXALINE I



Quinoxaline I

The synthesis path to Quinoxaline I is depicted below:



Tetraketones have been prepared from $\text{C}_6\text{H}_5\text{CCl}_2\text{Li}$ and perfluoro-ethyl esters [Ref. 4]. This reaction was attempted using dimethyl ester $\text{MeO}_2\text{C}(\text{CF}_2\text{CF}_2\text{O})_5\text{CF}_2\text{CF}_2\text{CO}_2\text{Me}$. Unfortunately the reaction proceeded only to a very low extent, approximately 15% yield with the major portion of the dimethyl ester being recovered unreacted. The major byproduct was $\text{C}_6\text{H}_5\text{CCl}=\text{CClC}_6\text{H}_5$ identified by its mass spectrum (see Table 1). Among the other byproducts observed was the partially reacted ester, $\text{C}_6\text{H}_5\text{CCl}_2\text{C}(\text{O})\text{CF}_2\text{CF}_2(\text{OCF}_2\text{CF}_2)_5\text{CO}_2\text{Me}$ (identified by its MS given in Table 2). Utilizing the diethyl ester (obtained from the corresponding dimethyl ester by transesterification) and modifying the reaction conditions resulted in an essentially quantitative yield of $\text{C}_6\text{H}_5\text{CCl}_2\text{C}(\text{O})\text{CF}_2\text{CF}_2(\text{OCF}_2\text{CF}_2)_5\text{C}(\text{O})\text{CCl}_2\text{C}_6\text{H}_5$. The next step proceeded readily and the pure

TABLE 1

ION FRAGMENTS AND INTENSITIES RELATIVE TO BASE PEAK OF
 $\text{C}_6\text{H}_5\text{CCl}=\text{CClC}_6\text{H}_5$

m/e	%	m/e	%	m/e	%	m/e	%
18	6.8	88	48.9	139	14.3	211	11.1
26	10.0	89	24.4	147	15.2	212	56.8
27	7.6	93	23.1	148	10.4	213	64.0
28	9.3	94	11.8	149	32.1	214	46.4
29	8.1	98	10.5	150	30.2	215	39.4
35	9.3	99	9.8	151	35.1	216	13.8
36	36.4	100	8.0	152	35.3	233	19.5
37	6.6	101	9.3	153	9.7	234	6.3
38	21.2	102	13.2	159	10.3	235	16.0
39	14.1	105	17.3	161	9.2	236	8.9
50	15.7	106	34.4	163	9.1	237	6.3
51	20.6	107	13.3	174	11.8	246	9.5
52	9.4	108	6.3	175	42.2	247	24.2
61	6.4	111	7.0	176	82.7	248	82.8M ⁺
62	9.5	113	6.7	177	76.3	249	50.0
63	16.0	115	7.2	178	<u>100.0</u>	250	73.6
73	6.5	125	11.1	179	59.4	251	30.2
74	18.9	126	16.7	180	14.5	252	33.9
75	23.7	127	11.2	181	8.4	253	11.9
76	29.4	128	10.1	183	44.0	866	5.5
77	15.6	136	15.3	184	14.8		
86	9.3	137	8.5	185	10.9		
87	22.2	138	11.5	186	11.4		

Peaks having intensities lower than 6% of the base peak and lower than m/e 18 are not reported.

Significant Ions in Support of Structure and Composition

m/e
 89 - $\text{C}_6\text{H}_5\text{C}^+$
 178 - $[\text{M} - 2 \text{ Cl}]^+$
 213 - $[\text{M} - \text{Cl}]^+$

TABLE 2

ION FRAGMENTS AND INTENSITIES RELATIVE TO BASE PEAK OF
 $\text{C}_6\text{H}_5\text{CCl}_2\text{C}(\text{O})\text{CF}_2\text{CF}_2(\text{OCF}_2\text{CF}_2)_5\text{CO}_2\text{Me}$

m/e	%	m/e	%	m/e	%	m/e	%
15	33.7	66	19.5	126	10.6	215	9.0
18	10.8	69	18.4	127	9.2	217	9.9
20	15.4	73	6.0	131	26.6	223	7.0
28	32.3	75	8.8	135	8.4	225	7.5
29	18.2	77	8.8	139	6.3	275	20.3
30	7.5	78	8.2	143	10.7	287	10.0
31	14.4	81	25.2	152	23.9	289	7.0
32	7.0	85	6.7	154	11.6	391	11.5
35	7.2	89	25.5	159	<u>100.0</u>	403	11.3
36	21.8	90	6.5	160	24.0	405	8.6
38	10.2	97	19.4	161	82.9	507	7.5
39	9.8	100	22.2	162	19.7	519	6.3
44	15.5	101	9.4	163	24.3	850	6.2
47	17.3	105	12.2	164	6.0	871	20.1
50	17.8	109	16.8	167	7.3	872	7.1
51	11.1	119	48.9	174	6.5	873	9.4
59	39.7	122	6.6	185	6.6	891	6.2
62	8.3	123	13.6	201	26.0		
63	15.2	124	23.0	202	8.7		
65	7.1	125	10.2	203	11.8		

Peaks having intensities lower than 6% of the base peak and lower than m/e 15 are not reported.

Significant Ions in Support of Structure and Composition

m/e	m/e
59 - CO_2Me^+	287 - $\text{C}_6\text{H}_5\text{CCl}_2\text{C}(\text{O})\text{CF}_2\text{CF}_2^+$
89 - $\text{C}_6\text{H}_5\text{C}^+$	403 - $\text{C}_6\text{H}_5\text{CCl}_2\text{C}(\text{O})\text{CF}_2\text{CF}_2\text{OCF}_2\text{CF}_2^+$
109 - $\text{CF}_2\text{CO}_2\text{Me}^+$	891 - $[\text{M} - \text{Cl}]^+$
124 - $\text{C}_6\text{H}_5\text{CCl}^+$	907 - $[\text{M} - \text{F}]^+$ (2.7%)
159 - $\text{CF}_2\text{CF}_2\text{CO}_2\text{Me}^+$ and $\text{C}_6\text{H}_5\text{CCl}_2^+$	

$\text{C}_6\text{H}_5\text{C}(\text{O})\text{C}(\text{O})\text{CF}_2\text{CF}_2(\text{OCF}_2\text{CF}_2)_5\text{C}(\text{O})\text{C}(\text{O})\text{C}_6\text{H}_5$ was obtained in a 68% yield. Quinoxaline I was readily formed from the reaction of 1,2-phenylenediamine and the tetraketone. As can be seen from the results of thermal stability evaluations, (listed in Tables 3 and 4; procedure fully described in Section 4), the sample was completely degraded after exposure in vacuum to 371°C for 72 hours; no starting material could be detected in the residue. The high production of volatile compounds and their nature (CO , CO_2 , SiF_4 , CF_3H) points clearly to an extensive breakdown of the perfluoroalkylether chain. It should be noted that CO_2 and SiF_4 are derived from the reaction of COF_2 (one of the primary decomposition products) with glass, SiO_2 . At 343°C the extent of degradation was significantly reduced as shown by approximately 50% recovery of Quinoxaline I. Lowering the temperature to 316°C resulted only in a low degree of degradation; 84% starting material recovery and a low production of volatiles. Apparently, the degradation process is catalyzed by small quantities of impurities since subjecting Quinoxaline I, of somewhat lower purity (approximately 98%) to testing, promoted complete material degradation even at 300°C. In the case of Quinoxaline I, thermogravimetric analysis (TGA) in N_2 does not provide information regarding elevated temperature stability due to its volatility. The TGA in air indicates possibly some oxidation to be taking place at 125°C.

TABLE 3

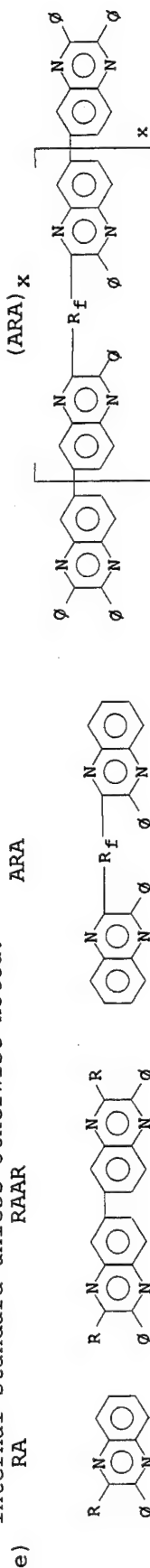
QUINOXALINE DATA SUMMARY

ID	Type ^e	Compound	MW		Yield % ^a	Purity %	MP °C	TGA		Thermal Stability ^c		
			calcd	osm				onset°C N ₂ /air	T ₁₀ °C ^b N ₂ /air	% S.M. ^d (vol. mmol/mmol S.M.)		
										371°C	343°C	316°C
af	RA	C ₈ F ₁₇ O	700	-	57	97	161-162	-	-	94 (none)	-	-
bg	RA	C ₈ F ₁₇ OC ₂ F ₄ O	816	-	29	99	101	-	-	99 (none)	-	-
c	RAAR	C ₈ F ₁₇ O	1399	-	36	NA ^h	191-197	-	-	-	-	-
dg	RAAR	C ₈ F ₁₇ OC ₂ F ₄ O	1631	1650	45	NA	185-190	-	-	-	-	-
I	ARA	(C ₂ F ₄ O) ₅ C ₂ F ₄	1091	1100	25	99	72-75	170/175	335/333	0 (12.2)	47 (5.48)	84 (1.05)
II	RA	C ₇ F ₁₅	574	590	42	100	118-119	115/120	200/215	91 (0.04)	94 (none)	-
III	ARA	O(C ₂ F ₄ O) ₅ C ₂ F ₄ O	1243	1300	13	NA	91-93	270/265	410/403	ND ⁱ (14.0)	-	ND (0.50)
IV	RAAR	C ₇ F ₁₅	1147	NA	65	NA	>200	265/115	366/362	-	ND (0.48)	-
V	RA	F[CF(CF ₃)CF ₂ O] ₂ CF(CF ₃)	656	680	55	99	liquid	85/78	178/185	-	-	34 (1.69)
VI	(ARA) ₃	(C ₂ F ₄ O) ₅ C ₂ F ₄	1089j	4200	20	NA	87-89	320/260	536/529	-	-	ND (10.85)
VII	ARA	C ₃ F ₆ O(C ₄ F ₈ O) ₂ C ₃ F ₆	1158	1150	22	99	68-70	229/227	355/344	-	-	85 (0.58)
VIII	ARA	O(C ₃ F ₆ O)(C ₄ F ₈ O) ₂ C ₃ F ₆ O	1310	1250	23	NA	135-138	315/280	427/423	-	93k (0.14)	96k (0.12)
IX-1	(ARA) _x	O(C ₃ F ₆ O)(C ₄ F ₈ O) ₂ C ₃ F ₆ O	1309j	3600	23	NA	>200	100/-	637/-	-	-	ND (2.63)
IX-2	(ARA) _x	O(C ₃ F ₆ O)(C ₄ F ₈ O) ₂ C ₃ F ₆ O	1309j	5400	18	NA	>200	395/390	612/601	-	-	96k (0.33)
IX-3	(ARA) _x	O(C ₃ F ₆ O)(C ₄ F ₈ O) ₂ C ₃ F ₆ O	1309j	13700	19	NA	-	400/397	615/597	-	-	ND ^m (1.14)
IX-4	(ARA) _x	O(C ₃ F ₆ O)(C ₄ F ₈ O) ₂ C ₃ F ₆ O	1309j	12000	19	NA	-	365/365	630 ^l /606	-	-	-
IX-5	(ARA) _x	O(C ₃ F ₆ O)(C ₄ F ₈ O) ₂ C ₃ F ₆ O	1309j	15300	20	NA	-	375/-	625 ^l /-	-	-	-
IX-6	(ARA) _x	O(C ₃ F ₆ O)(C ₄ F ₈ O) ₂ C ₃ F ₆ O	1309j	15900	20	NA	-	365/-	625 ^l /-	-	-	-

TABLE 3 (continued)

QUINOXALINE DATA SUMMARY

- a) Overall yield starting from perfluoroalkylidide for compounds a-d and starting from perfluoroalkylmethyl ester for compounds I-(IX1-6).
 b) $T_{1/2}$ is the temperature where only half the sample remains in the Thermogravimetric Analysis (TGA).
 c) In each instance the material was exposed in vacuo at the denoted temperature for 72 hours.
 d) Percent starting material recovered, calculated by quantitative gas chromatography using tetradecane as an internal standard unless otherwise noted.



- f) This compound is described in SN-3514-A1, AFWAL-TR-88-4129.
 g) This compound is described in SN-3514-A2, WRDC-TR-89-4067.
 h) NA: not available.
 i) ND: not determined.
 j) This is the theoretical molecular weight for one repeating unit.
 k) Percent starting material recovered, calculated by quantitative infrared spectroscopy.
 l) This is for a 40% weight loss.
 m) Residue was insoluble in hexafluoroisopropanol and hexafluorobenzene.

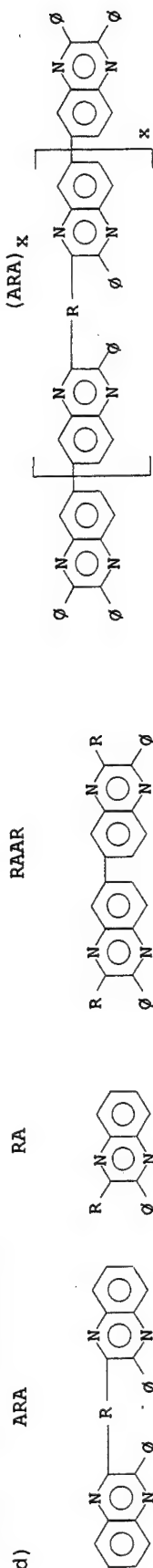
TABLE 4
SUMMARY OF THERMAL TESTING OF QUINOXALINES^a

Conditions										Invol.		Noncondensables									
Condensables ^b																					
Compound		Test		Quantity		Type	Temp	% S.M.		mmol/mmol S.M.		Total		mmol/mmol S.M. c							
ID	Type ^d	R		mg	mmol	atm	°C	Recov.	CO	N ₂	O ₂	mg	mmol	CO ₂	SiF ₄	CF ₃ H	Unk.				
I	ARA	(C ₂ F ₄ O) ₅ C ₂ F ₄	1	361.3	0.33	vac	371	0	2.11	NA ^e	NA	208.4	3.22	5.50	2.82	1.32	0.09				
			2	182.3	0.17	vac	371	0	2.61	NA	NA	106.3	1.61	6.09	2.54	0.67	0.28				
			3	103.0	0.09	vac	343	47	1.08	NA	NA	25.9	0.41	4.39	2.66	1.23	0.24				
			4	104.2	0.10	vac	316	84	0.19	NA	NA	5.4	0.08	0.66	0.19	0.02	--				
II	RA	C ₇ F ₁₅	1	363.0	0.63	vac	371	91	none	NA	NA	1.4	0.02	none	ND ^f	none	none				
			2	129.2	0.22	air	371	59	0.52	2.15	none	19.6	0.32	1.03	0.20	0.10	0.11				
			3	96.1	0.17	vac	343	94	none	NA	NA	none	none	none	none	none	none				
III	ARA	Ø(C ₂ F ₄ O) ₅ C ₂ F ₄ Ø	1	100.3	0.08	vac	371	ND	4.15	NA	NA	49.2	0.77	6.47	2.88	0.29	0.22				
			2	56.8	0.04	vac	316	ND	none	NA	NA	0.9	0.02	none	0.06	none	0.28				
IV	RAAR	C ₇ F ₁₅	1	108.9	0.10	vac	343	ND	none	NA	NA	13.2	0.11	0.59	0.37	none	0.13				
			2	84.3	0.07	vac	343	ND	none	NA	NA	2.0	0.04	0.34	0.10	none	0.16				
			3	85.6	0.07	vac	343	ND	none	NA	NA	1.1	0.04	0.07	0.05	none	0.36				
V	RA	F(HFPO) ₂ CF(CF ₃)	1	112.0	0.17	vac	316	17	none	NA	NA	43.5	0.50	1.71	0.94	0.18 ^g	0.18				
			2	107.6	0.16	vac	316	34	none	NA	NA	21.1	0.27	1.10	0.49	0.08 ^g	ND				
VI	(ARA) ₃	(C ₂ F ₄ O) ₅ C ₂ F ₄	1	98.5	0.02	vac	316	ND	2.46	NA	NA	11.3	0.20	5.88	1.42	0.42	0.67				
VII	ARA	C ₃ F ₆ O(C ₄ F ₈ O) ₂ C ₃ F ₆	1	103.6	0.09	vac	316	75	0.77	NA	NA	3.8	0.05	0.34	0.15	none	0.08				
			2	101.2	0.09	vac	316	85	0.14	NA	NA	1.1	0.04	0.26	0.10	none	0.08				
VIII	ARA	ØC ₃ F ₆ O(C ₄ F ₈ O) ₂ C ₃ F ₆ Ø	1	106.5	0.08	vac	316	96	none	NA	NA	0.3	0.01	none	none	none	0.12				
			2	116.0	0.09	vac	330	93	none	NA	NA	0.9	0.01	none	none	none	0.11				
			3h	107.6	0.08	air	330	92	none	NA	NA	0.7	0.02	none	none	none	0.25				
IX-1	(ARA) _x	ØC ₃ F ₆ O(C ₄ F ₈ O) ₂ C ₃ F ₆ Ø	1	99.6	0.03	vac	316	ND	none	NA	NA	4.1	0.07	1.09	0.10	none	1.24				
IX-2	(ARA) _x	ØC ₃ F ₆ O(C ₄ F ₈ O) ₂ C ₃ F ₆ Ø	1	102.3	0.02	vac	316	96	none	NA	NA	0.1	0.01	none	none	none	0.50				
IX-3	(ARA) _x	ØC ₃ F ₆ O(C ₄ F ₈ O) ₂ C ₃ F ₆ Ø	1	101.6	0.01	vac	316	ND	none	NA	NA	0.8	0.01	none	none	none	1.00				
			2h	101.6	0.01	air	316	ND	none	NA	NA	0.5	0.03	none	none	none	3.00				
			3h	101.7	0.01	air	330	ND	none	NA	NA	1.3	0.04	none	none	none	4.00				

TABLE 4 (continued)

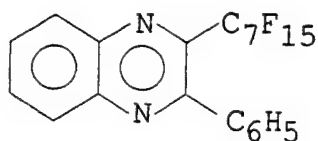
SUMMARY OF THERMAL TESTING OF QUINOXALINES

- a) Thermal evaluations were conducted in sealed ampoules (Volume ~18-20 mL) over a period of 72 hours, unless stated otherwise, in the denoted atmosphere at the denoted temperature.
 b) Condensables identified and quantified by infrared spectroscopy.
 c) S.M.: starting material.



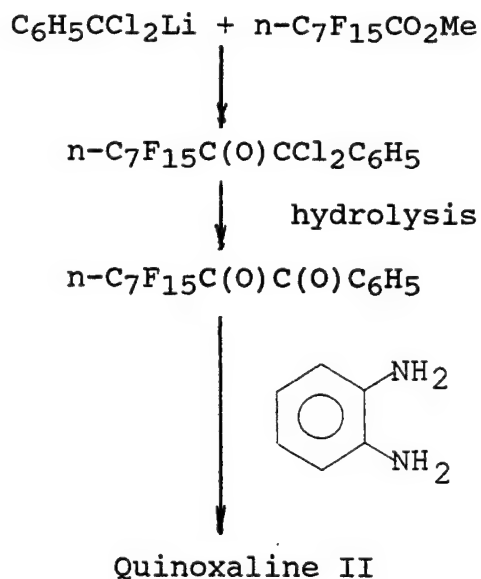
- e) NA: not applicable.
 f) ND: not determined.
 g) C₃F₇OCF(CF₃)H, identified by its mass spectrum and quantified by average molecular weight.
 h) This test was run for 24 h.

3.2 QUINOXALINE II



Quinoxaline II

In view of the relatively low stability of Quinoxaline I, wherein -OCF₂CF₂ is attached to the hetero-ring, it became of importance to determine whether the system is inherently unstable or whether the observed instability is caused by the oxygen next to the β -carbon. The synthesis route employed was analogous to that employed for the preparation of Quinoxaline I, i.e:

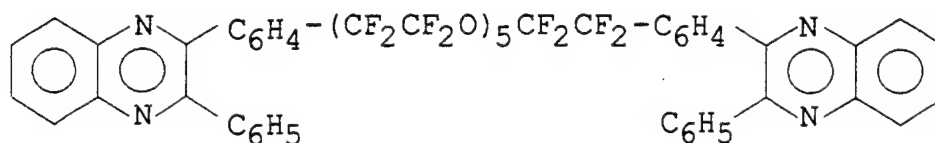


In this case it was not necessary to use the ethyl ester since 74% yield of the dichloro-intermediate was obtained with the methyl ester. The next step, the formation of the diketone,

$n\text{-C}_7\text{F}_{15}\text{C}(\text{O})\text{C}(\text{O})\text{C}_6\text{H}_5$, proceeded in an essentially quantitative yield.

Pure Quinoxaline II was isolated in 59% yield. This material was essentially thermally stable at 371°C over 72 hours in vacuum (91% starting material recovery, trace of volatiles formed; see Table 4). However, in the presence of air, under the above conditions, only 59% of the starting material was recovered. Most likely the extent of degradation was limited only by the availability of oxygen in the sealed ampoule. At 343°C in vacuum Quinoxaline II was not degraded over the 72 hour period. Due to limited funds and since the perfluoroalkyl-substituted compounds (due to the rigidity of the chains) are not suitable for elastomer applications, oxidative stability was not tested at 343°C .

3.3 QUINOXALINE III



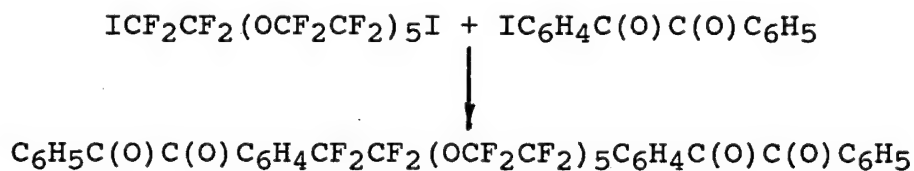
Quinoxaline III

As discussed in Section 2, polyquinoxaline systems wherein the heterocyclic rings are joined via phenyl group to the perfluoroalkylether chains was the originally proposed system. The advantage of this arrangement over that present in Quinoxalines I and II is the potentially better hydrolytic

stability and thermal oxidative stability that could be obtained. The major drawback here is the low yield of the coupling process i.e. the reaction of the diiodide and 4-iodobenzil. The problems encountered in the past with this process are fully described in the Interim Reports [Ref. 1-3] generated under the subject contract. This was one of the reasons to investigate the system represented by Quinoxalines I and II. However, in view of the unacceptable thermal stability of the perfluoroalkylether linked model, namely Quinoxaline I, it was decided to investigate the alternate arrangement as illustrated by Quinoxaline III.

The preparation of the diiodide, $\text{I}(\text{CF}_2\text{CF}_2\text{O})_5\text{CF}_2\text{CF}_2\text{I}$, was described previously [Ref. 3]. The synthesis of the coreagent, 4-iodobenzil, was developed early under this program [Ref. 1], however, scaleup did not give pure material. Accordingly, during the current phase of the program the synthesis was optimized, not so much with respect to the yield itself, as to obtaining a reasonable, readily achieved yield of very pure, >99%, product. The attained overall yield was 30%.

As noted above the coupling process;



did not proceed readily and difficulties were encountered in the tetraketone purification. In the previously performed coupling reactions of the diiodide, $\text{ICF}_2\text{CF}_2\text{O}(\text{CF}_2)_5\text{OCF}_2\text{CF}_2\text{I}$, with

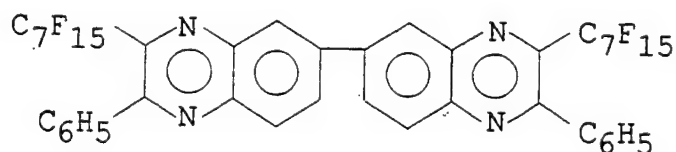
4-iodobenzil using copper bronze and $\text{Pd}(\text{PPh}_3)_4$, the product mixture usually contained a significant amount of $\text{ICF}_2\text{CF}_2\text{O}(\text{CF}_2)_5\text{OCF}_2\text{CF}_2\text{C}_6\text{H}_4\text{COCOC}_6\text{H}_5$ [Ref. 3]. This finding tends to indicate that the dicopper intermediate is either not formed or that the second copper does not react readily with 4-iodobenzil and regenerates the iodide upon air exposure. This is a process described by McLoughlin and Thrower [Ref. 5]. A potential alternative route to the dicopper intermediate is through a cadmium intermediate. Perfluoroalkyl cadmium compounds have been prepared by the reaction of perfluoroalkyl iodides with cadmium powder [Ref. 6]. The metathesis of perfluoroalkyl cadmium compounds with copper bromide was found to result in the desired perfluoroalkylcopper products [Ref. 7 and 8].

Unfortunately, none of the investigated cadmium processes seemed to work. Either no reaction took place or all the starting diiodide was consumed in some degradation process during the initial reaction of the diiodide with cadmium metal. This occurred faster than the subsequent copper exchange. Apparently, the intermediates $\text{ICdCF}_2\text{CF}_2(\text{OCF}_2\text{CF}_2)_5\text{CdI}$ and $\text{ICF}_2\text{CF}_2(\text{OCF}_2\text{CF}_2)_5\text{CdI}$, are unstable since upon hydrolysis prior to introduction of CuX neither $\text{HCF}_2\text{CF}_2(\text{OCF}_2\text{CF}_2)_5\text{I}$ nor $\text{HCF}_2\text{CF}_2(\text{OCF}_2\text{CF}_2)_5\text{H}$ were detected.

The optimized direct coupling using essentially the method of McLoughlin and Thrower [Ref. 5] gave 24.5% yield of 99% pure $\text{C}_6\text{H}_5\text{C}(\text{O})\text{C}(\text{O})\text{C}_6\text{H}_4\text{CF}_2\text{CF}_2(\text{OCF}_2\text{CF}_2)_5\text{C}_6\text{H}_4\text{C}(\text{O})\text{C}(\text{O})\text{C}_6\text{H}_5$.

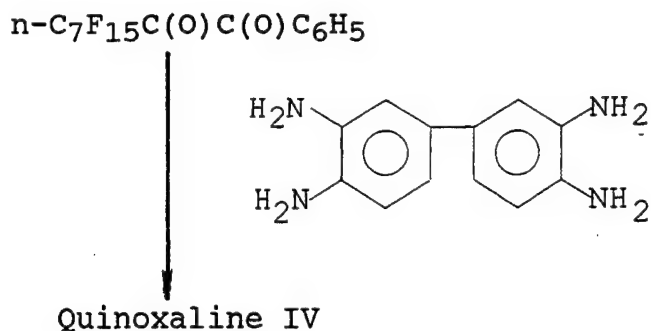
Reaction of the tetraketone with 1,2-phenylenediamine gave Quinoxaline III in a 52% yield, which is comparable to that attained in the case of the other quinoxalines (see Table 3). However, the overall yield from the methyl ester is significantly lower due to the low yield of the tetraketone. Quinoxaline III was found to undergo catastrophic degradation at 371°C as shown by the quantity and nature of the volatiles produced. Due to the involatility of the starting material the starting material recovery, if any, could not be determined. On the other hand, the nature of the residue, black/charred, and the quantity of volatiles, point to complete decomposition directly comparable to that of Quinoxaline I. At 316°C the material appeared to be stable. Based on the absence of carbon monoxide and the insignificant quantity of volatiles formed, this material has better stability than Quinoxaline I at 316°C. The TGA data do not provide any information regarding the material stability since the weight loss onset at 270°C appears to be due to evaporation and not to decomposition. No significant differences were observed between the TGA scans conducted in nitrogen and air.

3.4 QUINOXALINE IV



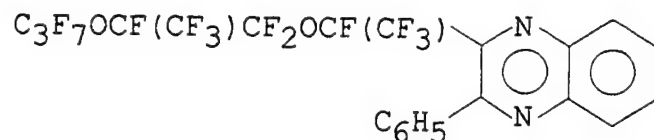
Quinoxaline IV

This dumbbell quinoxaline was obtained in an essentially quantitative yield by the reaction of the diketone with the tetramine, i.e.:



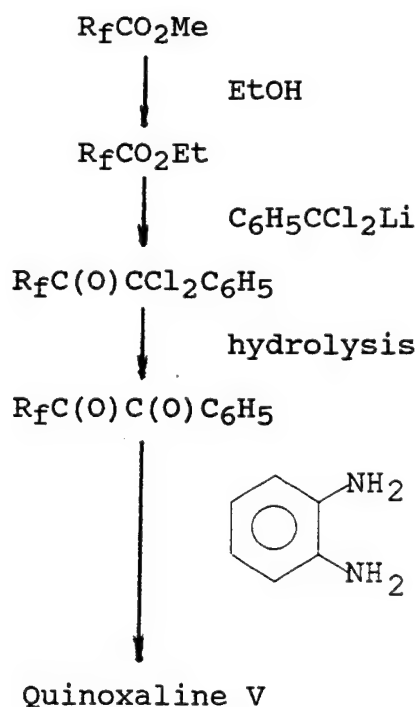
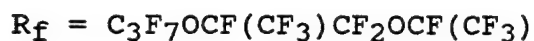
This material was prepared to determine whether there is a difference in stability between a dumbbell arrangement and the model monoquinoxaline represented by Quinoxaline II. As evident from data listed in Table 4, this material was less thermally stable than Quinoxaline II. Whereas in the case of Quinoxaline II a minimal degradation was observed at 371°C and no degradation at 343°C. Quinoxaline IV under these conditions did undergo some decomposition. Three tests of different purity Quinoxaline IV were carried out at 343°C, showing that the purity greatly affects the thermal stability. The sample used in Test 3 was twice recrystallized from hexafluoroisopropanol. After examining the TGA scans in nitrogen and air, it is obvious that the material is oxidatively unstable (see Table 3). It is of interest that in the vicinity of 375°C the decomposition process in air becomes exothermic (see actual TGA scans given in Section 4).

3.5 QUINOXALINE V



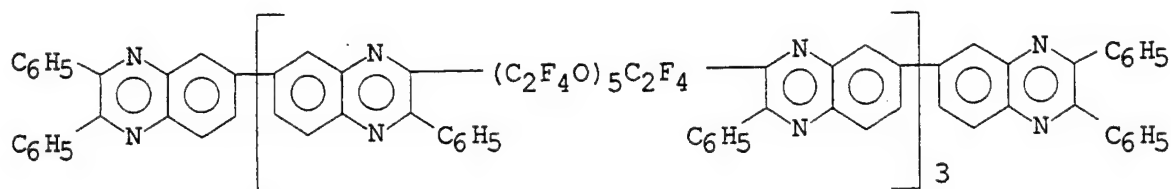
Quinoxaline V

It has been found that the presence of $-\text{CF}(\text{CF}_3)$ group adjacent to a heterocyclic ring in the the case of triazines and phospho-s-triazines enhances thermal , thermal oxidative and hydrolytic stability. It was of importance to explore whether this applies also to the quinoxalines. The synthesis route followed was analogous to that employed for Quinoxaline I, i.e.:



As observed in the earlier preparations of the chloro-intermediate, utilization of the methyl ester gave only a low yield (here approximately 18%) of the desired product. Thus the employment of the ethyl ester was mandatory to achieve reaction completion. Otherwise, each of the intermediates was readily formed and purified. From the diketone Quinoxaline V was obtained in an essentially quantitative yield. The material was unstable at 316°C as evident from the starting material recovery and the volatiles produced (see Table 4). In Test 1 the purity of the sample tested was 96%; in Test 2 it was 99.9%. It is obvious that purity has a significant effect on the material stability, especially under borderline conditions (which seems to be the case here). Purification procedures available to model compounds are not applicable to polymeric systems. Thus, the data obtained for a high purity model compound provides information regarding the inherent stability of the given arrangement, not the practically attainable stability of the equivalent polymer. It is clear however, that the system represented by Quinoxaline V is of significantly lower stability than that of Quinoxaline I. In view of its high volatility, due to low molecular weight, the TGA data for Quinoxaline V do not give any guidance regarding the thermal and/or oxidative stability.

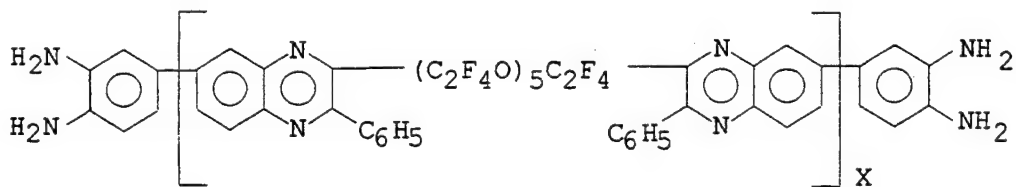
3.6 QUINOXALINE VI



Quinoxaline VI

Even though the model of this arrangement, namely Quinoxaline I, did not exhibit the required thermal stability it was of importance to determine: a) the feasibility of producing a polyquinoxaline system, and b) the effect of molecular weight increase on the overall thermal stability

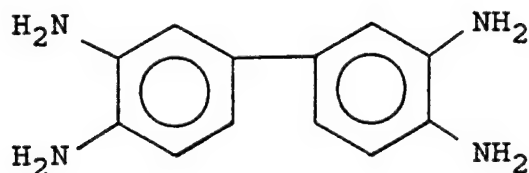
The reaction between the tetraketone $C_6H_5C(O)C(O)CF_2CF_2(OCF_2CF_2)_5C(O)C(O)C_6H_5$ and 3,3'-diaminobenzidine was monitored by ultraviolet spectroscopy to elucidate the operative mechanism. It appears that when the tetraketone is first introduced to the tetraamine, it quickly reacts with two molecules of 3,3'-diaminobenzidine to form A:



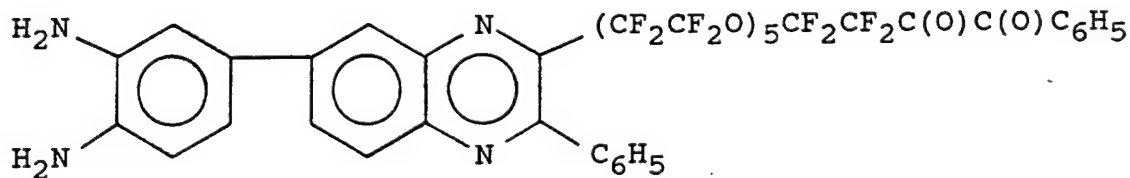
A

where $x = 1$. At the stage when the ratio of the tetraketone to the tetraamine reaches 1:2, all the 3,3'-diaminobenzidine is consumed, leaving all the available amino end-groups in the form of the molecule A with $x = 1$. As tetraketone addition continues,

molecules of $x = 1$ will combine with the additional tetraketone to form molecules with $x = 3$. Subsequently, the molecules with $x = 3$ can generate compound A with $x = 7$. The quantity of tetraketone employed was sufficient to convert all of the 3,3'-diaminobenzidine into 0.554 mmol of material where $x = 3$ and 0.027 mmol of material where $x = 7$. A mixture of such a composition, after end-capping with benzil, would have an average molecular weight of 4030. This is consistent with the measured molecular weight of 4200. This mechanism requires the compound with $x = 1$ to be formed first, followed by the $x = 3$ and $x = 7$ compositions in a stepwise fashion. For this to occur, the rate of reaction of a given tetraamine must be faster than that of the diamine-diketone species, e.g.,



fast reacting



slow reacting

This assumption is reasonable since the tetraamines (3,3'-diaminobenzidine, Compounds A with $x = 1$ and $x = 3$) would

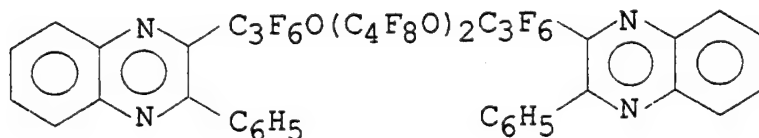
be of a lower molecular weight than the corresponding diamine-diketone intermediates and would have the capability to react at either end with both the tetraketone and the diketone.

This reaction was expected to give a broad spectrum of products but the narrow melting range (87-89°C) supports the formation of an essentially unimolecular species. This is further confirmed, as mentioned above, by the measured average molecular weight of 4200. These data are in agreement with a theoretical composition of 95.4% of the material $x = 3$ (molecular weight 3828) and 4.6% of material $x = 7$ (molecular weight 8183).

The degree of degradation at 316°C of Quinoxaline VI was high as measured by the quantity of volatiles produced. When comparing the volatiles produced, in terms of a ratio mmol/mmol starting material, Quinoxaline VI is substantially less stable than Quinoxaline I (10.85 vs 1.05 mmol; see Table 3). This comparison is not entirely valid since Quinoxaline VI is of a substantially higher molecular weight than Quinoxaline I. If one considers that in the "polymer" Quinoxaline VI there are three times as many sites to attack (CF_2 next to the ring) as in Quinoxaline I and each attack will produce three times as many volatiles and assuming complete degradation, the ratio of volatiles per mole of Quinoxaline VI to Quinoxaline I should be 9:1. The actual ratio of volatiles per mole was 10:1. These results show clearly that the inherent stability of Quinoxaline VI may be identical to that of Quinoxaline I. However, these results also show that a low degree of degradation in a model

compound is translated into an extensive degradation in a polymer. The effect must increase with molecular weight. The TGA data are in good agreement with the sealed tube results. The onset of weight loss in an inert atmosphere at 325°C supports fully the degree of decomposition reached during the 72 hours at 316°C. It is believed that in the case of these involatile, relatively high molecular weight materials the TGA provides a reasonable guidance to the composition's stability. Inasmuch as there is no drastic difference between the appearance of the TGA scans carried out in nitrogen and in air, at least up to 500°C, this would imply that here the oxidative stability corresponds to the thermal stability.

3.7 QUINOXALINE VII

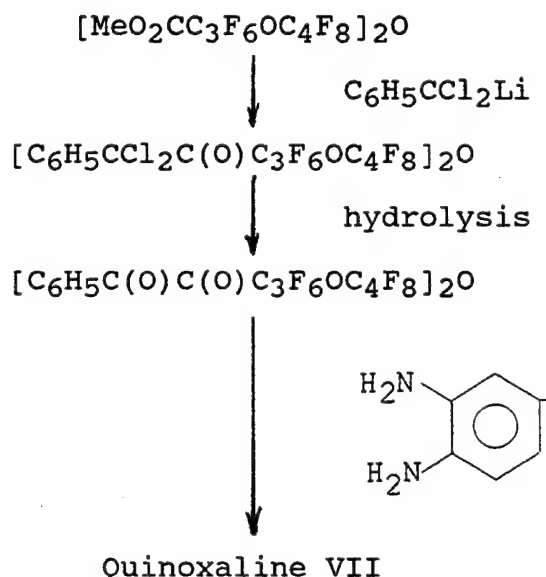


Quinoxaline VII

Based on the investigations performed up to this point, including the work reported in the past [Ref. 1-3], it became increasingly obvious that to have a thermally stable hybrid perfluoroalkylether linked quinoxaline polymer requires a n-perfluoropropyl, $-OCF_2CF_2CF_2$, attachment to the aromatic rings. To test the validity of this postulate, studies were carried out

using the precursor $[\text{MeO}_2\text{C}(\text{CF}_2)_3\text{O}(\text{CF}_2)_4]_2\text{O}$ kindly provided by WL/MLBT.

To prepare Quinoxaline VII synthesis path analogous to that employed in the case of Quinoxaline I was followed, i.e.,

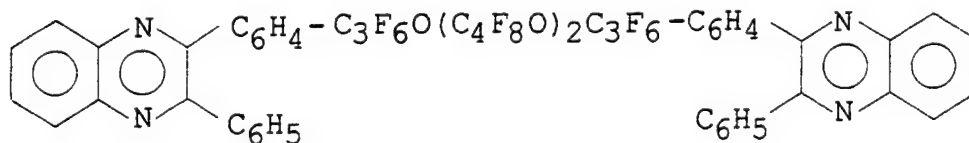


In contrast to the past reactions, there was no need to transform the methyl ester to the corresponding ethyl ester to obtain a reasonable yield of the chloro-intermediate (65% yield). The next step, to give the tetraketone, also proceeded readily. Finally, reaction of 1,2-phenylenediamine with the tetraketone afforded Quinoxaline VIII in a 52% yield. It is of interest that this material exhibited an altered DSC scan following heating up to 100°C. Specifically, Quinoxaline VII, crystallized from methanol, had MP 72-74°C. This corresponds to a DSC endotherm at 75°C. However, after heating in a DSC apparatus to 100°C, a double endotherm at 62 and 72°C appeared. This would imply the

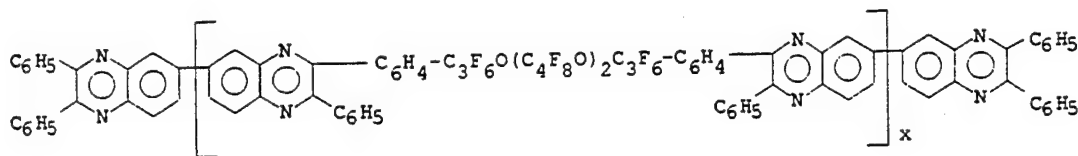
presence of different crystalline forms. The material recovered after exposure at 316°C for 72 hours, also had two endotherms at 55 and 65°C. It should be mentioned that quantitative DSC provided means to determine the quinoxaline content in a given sample (see Section 4).

Two thermal stability evaluations were carried out on Quinoxaline VII at 316°C. In Test 1 noncrystallized material was employed; in Test 2 the sample was crystallized from methanol. In both instances carbon monoxide was produced. The starting material recovery, 75% versus 85%, is not significantly different for the two tests. What is, however, of great importance is that the material was not significantly more stable than Quinoxaline I. This finding in turn implies that, at least for this type of quinoxaline, the perfluoroalkylether attachment to the hetero-ring via n-perfluoropropyl group does not impart better stability than the -OCF₂CF₂ moiety. The TGA data, in view of the compound volatility, are not useful in predicting stabilities.

3.8 QUINOXALINES VIII and IX

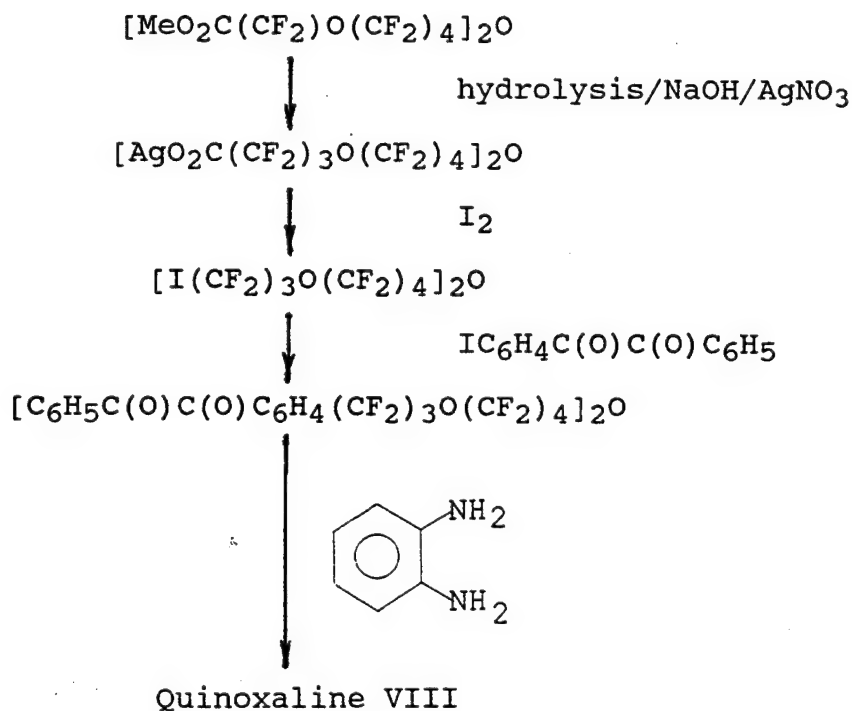


Quinoxaline VIII



Quinoxaline IX

In view of the relatively low thermal stability of the arrangement represented by Quinoxaline VII, the methyl ester, $[\text{MeO}_2\text{CC}_3\text{F}_6\text{OC}_4\text{F}_8]_2$, was utilized in the synthesis of Quinoxaline VIII and the Quinoxaline IX series. The reaction sequence employed was analogous to that followed in the case of Quinoxaline III:

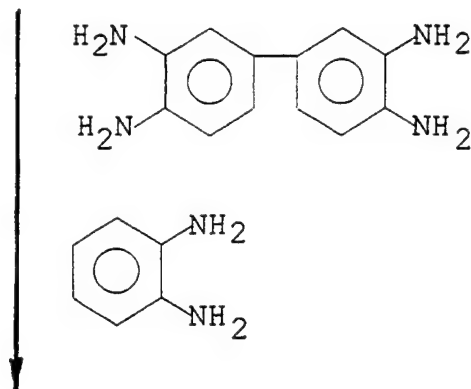
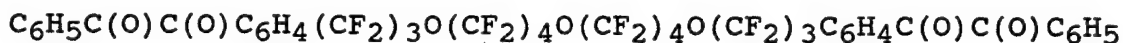


Every one of the steps delineated above up to the tetraketone proceeded readily and in high yield. In contrast to

the problems encountered with the coupling of $\text{ICF}_2\text{CF}_2(\text{OCF}_2\text{CF}_2)_5\text{I}$, described in Section 3.1, the process here gave high yield of the tetraketone (90%). It is of interest that in the case of $[\text{I}(\text{CF}_2)_3\text{O}(\text{CF}_2)_4]_2\text{O}$ the high tetraketone yield was achieved using dimethylsulfoxide solvent; only a very low yield (approximately 7%) was obtained in N,N-dimethylformamide. The opposite was true for $\text{ICF}_2\text{CF}_2(\text{OCF}_2\text{CF}_2)_5\text{I}$. The purification of Quinoxaline VIII was tedious due to the crystallization process.

Quinoxaline VIII exhibited the best thermal and thermal oxidative stability as compared to the quinoxalines discussed earlier. Based on the starting material recovery and the volatiles formed, (as listed in Table 4), the compound was thermally and oxidatively stable at least up to 330°C. The TGA data due to the material's relative volatility are of no value in stability assessment. No tests were carried out at higher temperatures due to limitation of funds and time. It was considered of more importance to investigate the corresponding polyquinoxaline system than to devote further efforts to a model compound.

A series of polymeric quinoxalines, represented by the general structure of Quinoxaline IX were synthesized by reaction of the tetraketone with 3,3'-diaminobenzidine, varying the reagents' stoichiometries. This was followed, in the case of Quinoxalines IX-2, IX-3 and IX-4, by end-capping with 1,2-phenylenediamine, i.e.:



Quinoxaline IX Series

The reactions carried out are summarized in Table 5. In the case of Quinoxaline IX-1 the ratio of tetraketone to tetraamine was 1:1.2. Problems were encountered with end-capping, part of the product was insoluble in hexafluorobenzene, the degree of polymerization of the C₆F₆-soluble portion was low ($X = 2.3$; Table 6), and most importantly, the material showed low thermal stability. This low stability is evident from the sealed ampoule results, as shown by the quantity of volatiles evolved on exposure to 316°C (see Table 4) and from the TGA data (see Table 3).

The molecular weights of the quinoxalines were increased by having the reactants ratio approach unity as indicated by the data given for Quinoxalines IX-4 and IX-5 (see Table 6). However, to determine the inherent thermal and oxidative stability of this system required skewed stoichiometries to allow for end-capping. This was accomplished in the case of Quinoxalines IX-2, IX-3 and IX-4 where the initial diketone

TABLE 5
PREPARATION OF QUINOXALINE IX SERIES^a

Q	Amine ^b mmol	Ketone ^c mmol	K/A	Solvent Type	CH ₃ CO ₂ H g	Conditions Temp(°C)Time(h)	Diamine ^d mmol	Q yield(%)
IX-1 ^e	1.03	0.857	1.00/1.20	HFI ^f	13	45-50	17 (0.65)9/0.67	73
IX-2	0.75	0.857	1.15/1	HFI/ch ^h	10/10	45-50	48	90
IX-3	0.7981	0.8370	1.05/1	HFI	15	50-55	91	94
IX-4	0.8522	0.8693	1.02/1	HFI	15	50-55	165	94
IX-5	0.8288	0.8292	1.00/1	HFI	15	50-55	168	97
IX-6 ⁱ	0.8345	0.8345	1.00/1	HFI	15	100	168	89

a) In a typical reaction (with the exception of X-1) the tetraamine solution was added to the stirred tetraketone solution (plus glacial acetic acid) at room temperature over 45 minutes. It was then stirred under reflux at the denoted temperature for the denoted time. To the cooled solution was added diamine and the mixture heated for 24-66 hours. The product was isolated by precipitation into methanol (twice) and dried in vacuo at 95°C.

b) 3,3'-Diaminobenzidine

c) [C₆H₅C(O)C(O)C₆H₄C₃F₆OC₄F₈]₂O

d) 1,2-Phenylenediamine

e) In this experiment the tetraketone solution (plus trifluoroacetic acid) was added to the tetraamine solution followed by benzil after 17 hours. The product showed carbonyl absorption thus, it was reacted in HFI with diamine. Only 50% of the final product was C₆F₆ soluble.

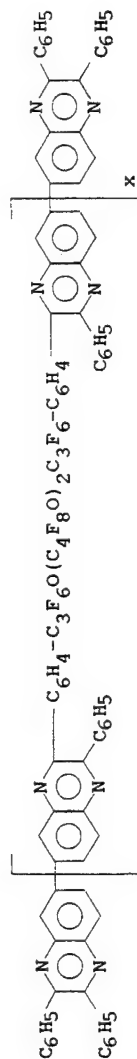
f) Hexafluoroisopropanol

g) The value in parenthesis corresponds to the quantity of benzil.

h) m-cresol

i) This test was performed in a sealed ampoule.

TABLE 6
QUINOXALINE IX SERIES



Material	MW Osm	x	IR(Fig.No.)	TGA(Fig.No.) N ₂ Air
Quinoxaline IX-1	3600	2.3	42	43 44 ^a
Quinoxaline IX-2	5390	3.7	45	46 47
Quinoxaline IX-3	13700	10.0	48	49 50
Quinoxaline IX-4	12000	8.7	51	52 53
Quinoxaline IX-5	15300 ^b	11.7	54	55
Quinoxaline IX-6	15900 ^b	12.1	56	57

a) Figure 43 is the TGA of the C₆F₆ soluble portion; Figure 44 is the TGA scan of the C₆F₆ insoluble portion of the Quinoxaline IX-1.
b) This material was not end-capped.

termination was quinoxaline end-capped by reaction with 1,2-phenylenediamine. The only studies conducted in Quinoxaline IX series were to optimize the polymerization process. As noted above, having the ratio of the comonomers as close as possible to unity gave the highest molecular weight (Quinoxalines IX-5 and IX-6). Raising the temperature from 55 to 100°C did not seem to have an effect. With the exception of Quinoxaline IX-1, only one catalyst, glacial acetic acid was investigated and all the tests were carried out in hexafluoroisopropanol.

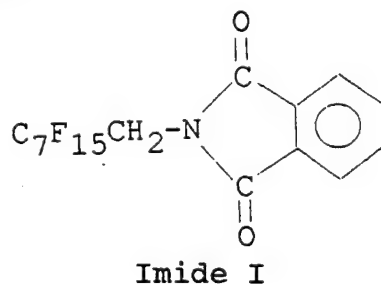
Based on the stability evaluations, given in Table 4, the polyquinoxalines were exceptionally stable as shown by the negligible volatiles production and the essentially quantitative starting material recovery exemplified by Quinoxaline IX-2. Unfortunately, in the case of Quinoxaline IX-3 the starting material could not be quantified due to the insolubility of the residue, both in hexafluorobenzene and hexafluoroisopropanol, following the exposure to 316°C. The same occurred at 330°C in vacuum and at 316°C in air. There are two possibilities, either the material was crosslinked or it changed its crystalline structure, rendering it insoluble in the above mentioned solvents. It has to be emphasized that Quinoxaline IX-3 was not very soluble in $(\text{CF}_3)_2\text{CHOH}$ and C_6F_6 prior to the heat treatment. Furthermore, its molecular weight is more than twice that of Quinoxaline IX-2 (see Table 6).

The TGA data point to stabilities, both in inert atmosphere and in air, of the order of 390°C for the end-capped

materials. Quinoxalines IX-5 and IX-6 were not end-capped and this probably led to the somewhat decreased thermal stabilities as determined by TGA weight loss. As mentioned above, these materials were prepared to investigate further the effect of stoichiometries and to assess the effect of temperature on the polymerization. Based on the investigations discussed above, with respect to Quinoxaline IX Series, these compositions prove clearly the validity of the original concept of perfluoroalkyl-ether linked polyquinoxalines as elastomeric raw gum systems.

3.9 IMIDES

Systems based on imide rings linked by $-\text{CH}_2(\text{CF}_2\text{CF}_2\text{O})_x(\text{CF}_2\text{O})_y\text{CF}_2\text{CH}_2-$ chains formed by reaction of Fomblin Z diamine with dianhydrides or tetracarboxylic acids, were claimed by Strepparola et al [Ref. 12] to offer thermally and oxidatively stable elastomers. Our earlier studies [Ref. 3] showed the model Imide I



to have high thermal stability (see Tables 7 and 8); no oxidative stability evaluations were carried out. The presence of the CH_2 group does provide sites for oxidative attack as well as for degradation via hydrogen fluoride elimination. Furthermore, we

TABLE 7
IMIDE DATA SUMMARY

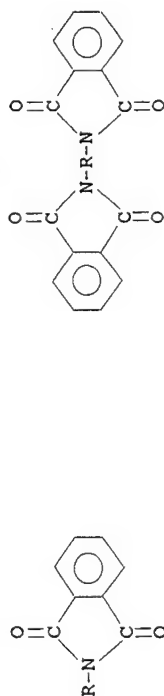
ID	Type ^d	Compound	R	MW		Yield % ^a	Purity %	MP °C	TGA		Thermal Stability ^b		
				calcd	osm				onset ^c N ₂ /air	T ₁₀ ^c N ₂ /air	% S.M.C 371°C	(vol. mmol/mmole S.M.) 343°C	316°C
Ie	RA	C ₇ F ₁₅ CH ₂		529	-	49	98	136-137	-	-	100	-	-
II	RA	C ₃ F ₇ [OCF(CF ₃)CF ₂] ₂ Ø		723	730	36	99	82-85	130/135	245/244	-	-	95 (none)
III	ARA	ØC ₃ F ₆ O(C ₂ F ₄ O) ₄ C ₃ F ₆ Ø		1224	1240	4	NA ^f	136-138	263/275	407/405	-	-	90g(0.14)

a) Overall yield starting from perfluoroalkylmethyl ester.

b) In each instance the material was exposed in vacuo at the denoted temperature for 72 hours.

c) Percent starting material recovered, calculated by quantitative gas chromatography using tetradecane as an internal standard.

d) RA ARA



e) This compound is described in SN-3514-A3, WRDC-TR-90-4105.

f) NA: not available.

g) Percent starting material recovered, calculated by quantitative infrared spectroscopy

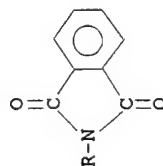
TABLE 8
SUMMARY OF THERMAL TESTING OF IMIDESa

ID	Compound		Test	Quantity		Conditions		Invol. % S.M. Recov.	Noncondensables		Condensables	
	Type ^c	R		mg	mmol	Type	Temp °C		mmol/mmol S.M. ^b	mmol/mmol S.M.	mg	mmol/mmol S.M.
I	RA	C ₇ F ₁₅ CH ₂	1	359.5	0.68	vac	371	100	none		1.3	
II	RA	C ₃ F ₇ [OCF(CF ₃)CF ₂] ₂ O	1	110.4	0.15	vac	316	95	none	NA ^d	none	
III	ARA	O(C ₃ F ₆ O(C ₂ F ₄ O) ₄ C ₃ F ₆ O)	1	102.0	0.08	vac	316	90	none		2.4	0.14

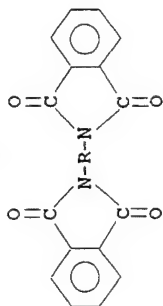
a) Thermal evaluations were conducted in sealed ampoules (Volume ~18-20 mL) over a period of 72 hours in the denoted atmosphere at the denoted temperature.

b) S.M.: starting material.

c) RA



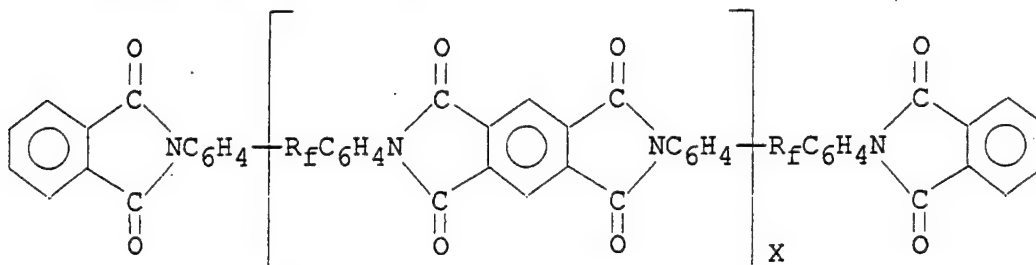
ARA



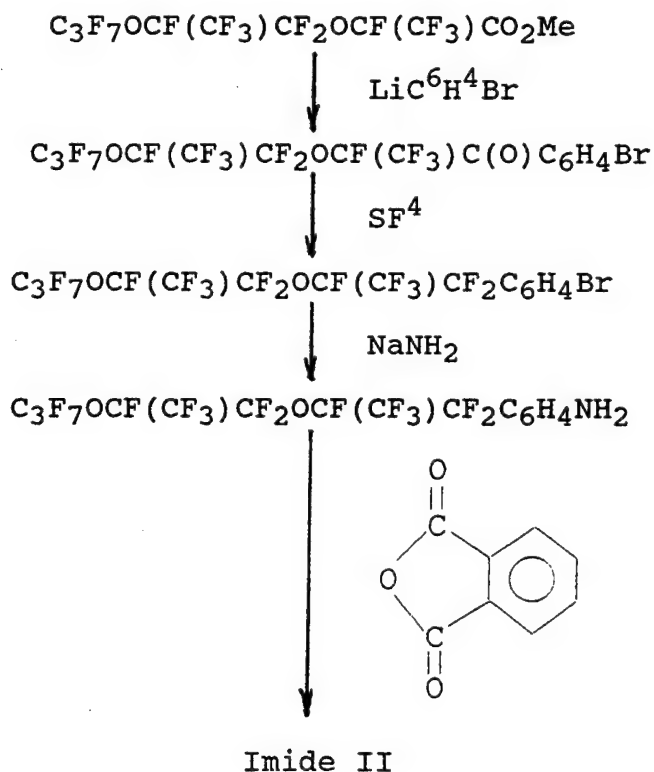
d) NA: not applicable.

have encountered difficulties in attempting to prepare the Fomblin Z linked diimide [Ref. 3]

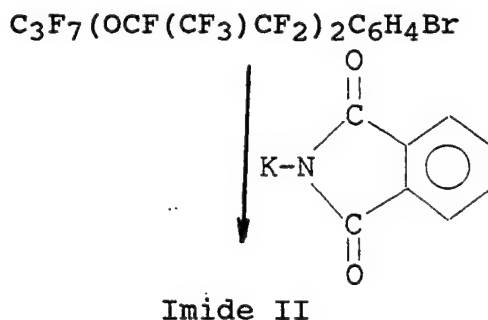
In view of the low stabilities of Quinoxaline I and even Quinoxaline III, some efforts were directed early during the last phase of this program at the synthesis of an imide system of the general structure shown below:



To determine the feasibility of the above undertaking a model system represented by Imide II needed to be synthesized first. The synthesis path is depicted below:



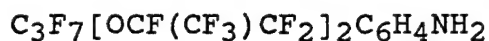
The first two steps proceeded readily to give $C_3F_7OCF(CF_3)CF_2OCF(CF_3)C(O)C_6H_5Br$ and $C_3F_7OCF(CF_3)CF_2OCF(CF_3)CF_2C_6H_4Br$ in 53 and 68% yields, respectively. Unfortunately, none of the reactions tried led to the production of the amino-compound. Different conditions tried employing the $NH_3/NaNH_2$ reagent system gave at best, 1% yield of $C_3F_7[OCF(CF_3)CF_2]_2C_6H_4NH_2$, identified by its mass spectrum presented in Table 9. Accordingly, another approach needed to be explored. The Gabriel reaction with the aid of copper catalysis [Ref. 13] has been used to convert aryl halides to aryl amines. It is a two-step process, the first step being the reaction of an aromatic halide with potassium imide to form the aromatic imide. Since the imide was the desired end product, the second step, hydrolysis or hydrazinolysis, was omitted, i.e.,



Using the above path Imide II was obtained in a 51% yield. No degradation was observed at $316^\circ C$. The starting material recovery was essentially quantitative. The appearance of the sample unchanged. This was not the case with the quinoxalines, where usually dark discoloration was observed. The

TABLE 9

ION FRAGMENTS AND INTENSITIES RELATIVE TO BASE PEAK OF



m/e	%	m/e	%	m/e	%	m/e	%
20	12.2	76	4.0	141	3.3	226	5.3
28	28.4	79	2.3	<u>142</u>	<u>100.0</u>	239	3.4
31	10.5	80	5.4	143	21.9	242	10.3
32	8.5	81	5.4	144	2.0	255	6.6
38	2.7	82	5.3	145	10.9	257	7.7
39	6.1	91	3.0	147	2.5	285	2.1
41	2.8	92	4.9	150	6.1	287	2.1
47	10.9	93	2.2	153	2.7	288	2.0
50	15.7	95	5.4	157	2.4	305	12.9
51	3.0	97	4.9	160	3.4	307	17.5
52	3.0	100	16.5	169	27.4	308	5.5
62	2.3	102	2.5	170	2.3	408	4.7
63	3.0	107	5.0	173	5.8	474	3.4
64	2.8	114	8.1	192	15.2	574	6.1
65	14.3	115	2.3	195	2.4	591	2.3
66	4.4	119	17.8	205	57.7	593	33.4M ⁺
69	47.2	122	2.2	206	9.3	594	10.1
70	2.0	125	11.4	207	52.0	633	6.6
71	4.2	126	26.5	208	11.2	636	8.9
73	3.3	127	4.8	219	2.3		
74	2.4	131	4.0	222	3.2		
75	10.6	140	3.4	223	2.2		

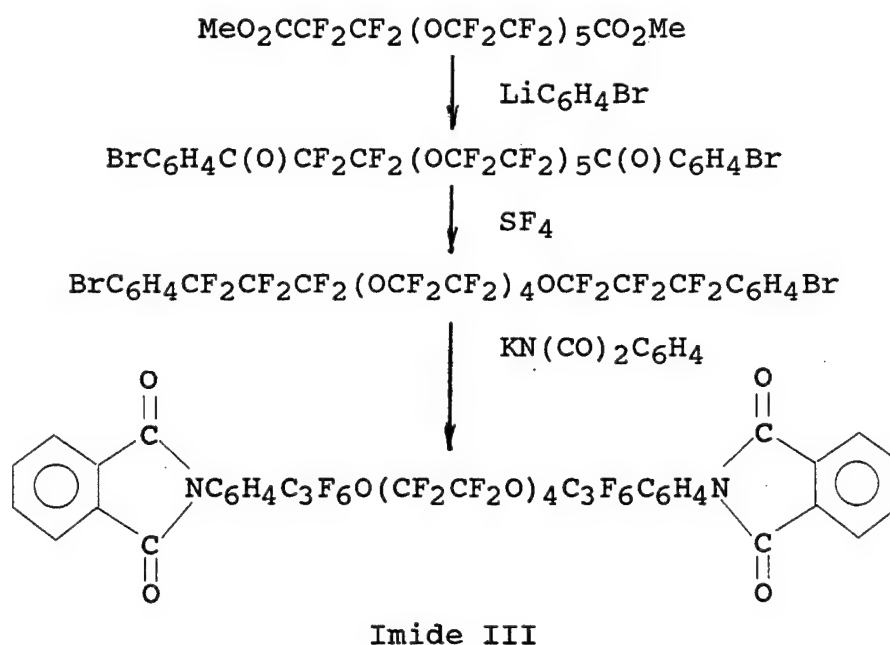
Peaks having intensities lower than 2% of the base peak and lower than m/e 20 are not reported.

Significant Ions in Support of Structure and Composition

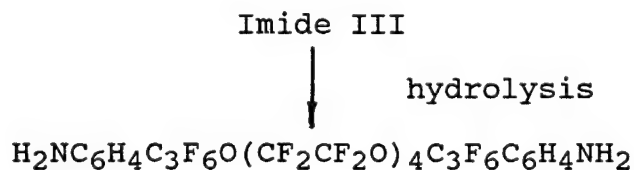
m/e	m/e
76 - C_6H_4^+	242 - $\text{CF}(\text{CF}_3)\text{CF}_2\text{C}_6\text{H}_4\text{NH}_2^+$
142 - $\text{CF}_2\text{C}_6\text{H}_4\text{NH}_2^+$	408 - $[\text{M} - \text{C}_3\text{F}_7\text{O}]^+$
169 - C_3F_7^+	574 - $[\text{M} - \text{F}]$

TGA data in this case do not give any information as to the material stability due to its relatively high volatility.

In view of the promising results obtained with Imide II the investigation of the synthesis and the stability of the Imide III, where two imide rings are joined by a perfluoroalkylether bridge, were carried out, i.e.:



It should be noted that the dumbbell Imide III can serve both as a model compound for the thermal stability evaluation and as an intermediate for the synthesis of the diamino reactant required for the polyimide synthesis, i.e.:



The first step proceeded readily, affording a 77% yield of the dibromide, $\text{BrC}_6\text{H}_4\text{C}(\text{O})\text{CF}_2\text{CF}_2(\text{OCF}_2\text{CF}_2)_5\text{C}(\text{O})\text{C}_6\text{H}_4\text{Br}$. The reaction with SF_4 was initially conducted at 220°C which resulted in an extensive by-product formation. Both polymeric and monomeric disulfides of the general formula

$[\text{BrC}_6\text{H}_4(\text{CF}_2)_3\text{O}(\text{CF}_2\text{CF}_2\text{O})_4(\text{CF}_2)_3\text{C}_6\text{H}_4\text{Br}]_n\text{S}_2$ were produced. Lowering the temperature to $150\text{--}160^\circ\text{C}$ eliminated these problems and gave $\text{BrC}_6\text{H}_4(\text{CF}_2)_3\text{O}(\text{CF}_2\text{CF}_2\text{O})_4(\text{CF}_2)_3\text{C}_6\text{H}_4\text{Br}$ in a 40% yield. The next step did not proceed to completion and the purification of the product was very tedious. Imide III was thermally stable at 316°C , however, it has undergone discoloration. Its stability appeared lower than that of the Imide II. The TGA data are not very informative, inasmuch as the observed weight loss onset at approximately 270°C , both in nitrogen and air atmospheres, is most likely caused by evaporation. In view of the low yield of Imide III, the synthesis of the diamine

$\text{H}_2\text{NC}_6\text{H}_4\text{C}_3\text{F}_6\text{O}(\text{CF}_2\text{CF}_2\text{O})_4\text{C}_3\text{F}_6\text{C}_6\text{H}_4\text{NH}_2$ was not even attempted.

Furthermore, the Quinoxaline IX arrangement appeared to offer a better system both with respect to the synthesis and performance.

4. EXPERIMENTAL DETAILS AND PROCEDURES

General

All solvents used were reagent grade and were dried and distilled prior to use. The commercially available starting materials were usually purified by distillation, crystallization or other appropriate means. Operations were carried out either in an inert-atmosphere enclosure (Vacuum/Atmospheres Model HE-93B), under nitrogen bypass or in vacuum.

All the melting points are uncorrected and were determined in evacuated, sealed capillaries, unless otherwise stated. Infrared spectra (IR) were recorded on Perkin-Elmer Corp. Model 1330 infrared spectrophotometer either neat (liquids) or as double mulls (Kel-F oil No. 10 and Nujol). Molecular weights were determined in hexafluorobenzene using a Mechrolab Model 302 vapor pressure osmometer. Ultraviolet (UV) spectra were recorded on Beckman Corp. Model 35 spectrophotometer. Gas chromatography (GC) was performed by employing either a 10 ft x 1/8 in stainless steel column packed with 4% OV-101 on 80/100 mesh Chromosorb GAW or a 3 ft x 1/8 in stainless steel column packed with 3% Dexsil 300 on 100/120 mesh Chromosorb WAW and using a programming rate of 8°C/min from 35-300°C. The mass spectrometric analyses were obtained with 21-491B double focusing mass spectrometer attached to Varian Aerograph Model 2700 gas chromatograph equipped with a flame ionization detector and a Du Pont 21-094 data acquisition and processing system. The mass

spectra were obtained by direct insertion probe and combined gas chromatography/mass spectrometry (GC/MS). Thermal gravimetric analyses (TGA) were carried out in inert atmospheres and in air, from room temperature to 700°C at 10°C/min with a Du Pont 990/951 system. Differential Scanning Calorimetry (DSC) was carried out using Du Pont 990 system. Vacuum line techniques were utilized where applicable. The elemental analyses were performed by Schwarzkopf Microanalytical Laboratory, Woodside, NY.

Pyrolyses

The tests were performed in 18-20 mL ampoules. The samples were weighted in and then the tubes were evacuated using the vacuum line assembly. If the test was to be conducted in air at this stage dry air, 600 mm Hg, was introduced and then the tube sealed. Otherwise, once good vacuum, 0.001 mm Hg, was attained, the tubes were sealed in vacuum. Following the heating regime, the tubes were cooled to -196°C, opened to the vacuum system and the -196°C noncondensibles, if any, separated and analyzed by infrared spectrometry. Subsequently, the tube contents were warmed to room temperature and collected in the calibrated portion of the vacuum line. If the quantities were larger than 0.2 mmol, the condensibles were fractionated through -78°C into -196°C cooled traps. The resultant fractions were analyzed by quantitative infrared spectroscopy. On quantities smaller than 0.2 mmol, quantitative infrared spectroscopy was directly performed. The starting material remaining in the involatile portion was quantified either by quantitative GC using

an internal standard, or by quantitative DSC (decrease in the endotherm associated with fusion), or by quantitative infrared spectroscopy using the matched cell technique. The procedure used depended on the starting material nature. The tests are summarized in Tables 3, 4, 7 and 8 wherein the method to determine starting material recovery is identified.

Starting Materials

The $n\text{-C}_8\text{F}_{17}\text{I}$ was obtained from Du Pont De Nemours and Co.; $\text{MeO}_2\text{C}(\text{CF}_2\text{CF}_2\text{O})_5\text{CF}_2\text{CF}_2\text{CO}_2\text{Me}$ and $\text{Me}_2\text{O}_2\text{C}(\text{CF}_3)_3\text{O}(\text{CF}_2)_4\text{O}(\text{CF}_2)_4\text{O}(\text{CF}_2)_3\text{CO}_2\text{Me}$, products of Exfluor Inc., were provided by WL/MLBT. 3,3'-Diaminobenzidine and 1,2-phenylenediamine were obtained from Aldrich Chemical Co. 3,3'-Diaminobenzidine was first washed with m-cresol, then it was recrystallized from m-cresol (5 g in 20 mL) to give white crystals, MP 175-176°C. 1,2-Phenylenediamine was recrystallized twice from methanol to give white crystals, MP 100-101°C. 4-Iodobenzaldehyde was prepared in quantitative yield following the reported procedure [Ref. 1]. 4-Iodobenzil was resynthesized and the procedure optimized to achieve the required >99% purity.

Preparation of 4-iodobenzil

To a stirring solution of 4-iodobenzaldehyde (103 g, 0.445 mol) and benzaldehyde (99 g, 0.934 mol) in ethanol (210 mL) was added potassium cyanide (7.2 g, 0.11 mol) in water (200 mL) and the solution was subsequently refluxed at 110°C for 3 hours. After cooling to room temperature, water (170 mL) was added and the reaction mixture extracted with dichloromethane (4x300 mL).

The organic layer was washed with water (2x400 mL), dried over anhydrous magnesium sulfate and evaporated to give 186 g of the iodobenzoin. A mixture of the crude benzoin, ammonium nitrate (303 g, 3.8 mol) and copper acetate (6.1 g, 30 mmol) in 80% acetic acid (1500 mL) was heated at 120°C for 3 hours. After the reaction mixture was cooled to room temperature, a large quantity of a yellow solid appeared. Following refrigeration the precipitate was filtered, washed with concentrated acetic acid (100 mL) and water (3x100 mL). Air drying resulted in 133 g of crude 4-iodobenzil. Extraction with dichloromethane followed by solvent removal and drying in vacuum gave 82 g of material which based on GC analysis contained 70% of 4-iodobenzil. Two recrystallizations from 80% acetic acid (5 mL/g) gave 49 g (32% yield) of 97% purity. Another crystallization gave 44 g (29% yield) of 99% pure material.

Transesterification of $\text{MeO}_2\text{C}(\text{CF}_2\text{CF}_2\text{O})_5\text{CF}_2\text{CF}_2\text{CO}_2\text{Me}$

$\text{MeO}_2\text{C}(\text{CF}_2\text{CF}_2\text{O})_5\text{CF}_2\text{CF}_2\text{CO}_2\text{Me}$ (10.0 g, 12.5 mmol) was refluxed with ethanol (10 mL, 172 mmol) and concentrated sulfuric acid (0.5 mL, 9.4 mmol) at 95°C for 16 hours, followed by removal of ~5 mL of a mixture of ethanol and the produced methanol by distillation at atmospheric pressure. Upon addition of another 10 mL of ethanol refluxing was continued for another 5 hours and the alcohols distilled off. The ethyl ester, $\text{EtO}_2\text{C}(\text{CF}_2\text{CF}_2\text{O})_5\text{CF}_2\text{CF}_2\text{CO}_2\text{Et}$ (8.4 g, 81% yield), was then distilled, BP 69-74°C/0.001 mm Hg. The MS is given in Table 10.

TABLE 10

ION FRAGMENTS AND INTENSITIES RELATIVE TO BASE PEAK OF
 $\text{EtO}_2\text{C}(\text{CF}_2\text{CF}_2\text{O})_5\text{CF}_2\text{CF}_2\text{CO}_2\text{Et}$

m/e	%	m/e	%	m/e	%	m/e	%
26	11.3	75	15.4	171	7.5	473	19.8
27	32.0	77	7.2	173	22.7	493	9.0
28	29.5	78	18.4	174	9.7	495	6.5
29	46.7	79	9.0	185	10.2	570	9.7
30	19.3	93	6.4	191	10.0	589	50.6
31	22.4	95	10.3	211	9.1	609	41.4
43	6.9	97	36.3	213	37.7	635	13.6
44	9.5	98	24.5	214	7.9	705	26.4
45	35.2	100	41.7	216	9.3	714	7.1
47	21.5	101	16.2	239	10.8	734	25.6
50	10.5	117	18.5	241	10.1	745	10.7
51	10.4	119	40.8	261	28.0	753	25.1
55	7.2	120	8.3	263	12.4	772	38.6
56	6.4	125	14.7	289	11.0	779	7.1
57	6.4	126	9.9	329	12.4	783	15.7
66	6.0	143	7.7	357	10.9	799	45.5
67	6.1	145	24.7	377	21.8	820	6.3
69	25.4	146	7.0	379	10.0	827	<u>100.0</u>
73	8.0	163	10.1	445	6.5		

Peaks having intensities lower than 6% of the base peak and lower than m/e 26 are not reported.

Significant Ions in Support of Structure and Composition

m/e	m/e
45 - OEt^+	753 - $[\text{M} - \text{CO}_2\text{Et}]^+$
173 - $\text{CF}_2\text{CF}_2\text{CO}_2\text{Et}^+$	827 - $[\text{M} + 1]^+$
289 - $\text{CF}_2\text{CF}_2\text{OCF}_2\text{CF}_2\text{CO}_2\text{Et}^+$	

Preparation of $\text{C}_6\text{H}_5\text{CCl}_2\text{C}(\text{O})\text{CF}_2\text{CF}_2(\text{OCF}_2\text{CF}_2)_5\text{C}(\text{O})\text{CCl}_2\text{C}_6\text{H}_5$

Into a 250 mL three-neck round bottom flask equipped with a mechanical stirrer, thermometer, nitrogen inlet and addition funnel with septum was introduced α,α,α -trichlorotoluene (11.15 g, 57.04 mmol). Under a flow of nitrogen, to the trichlorotoluene were added tetrahydrofuran (125 mL) and ethyl ether (125 mL) and the solution was cooled to -111°C (using Freon-11). n-Butyllithium (25 mL, 2.5 M) was then transferred to the addition funnel, via a syringe, and added dropwise over 1 hour period creating a dark blue solution. The reaction mixture was subsequently stirred for 1 hour at -111°C . Under an increased nitrogen flow, the addition funnel was exchanged for an addition funnel containing $\text{EtO}_2\text{C}(\text{CF}_2\text{CF}_2\text{O})_5\text{CF}_2\text{CF}_2\text{CO}_2\text{Et}$ (29.34 g, 35.51 mmol). The ester was added over 20 minutes and the reaction mixture was stirred for 3 hours at -111°C . It was then quenched (at -111°C) by a solution of cold, concentrated hydrochloric acid (10 mL) in ethanol (20 mL). The resultant mixture was poured into 2 N hydrochloric acid (250 mL). The organic layer was separated; the aqueous layer was extracted with ether (175 mL) and combined with the original organic solution. After drying over anhydrous magnesium sulfate and solvent removal in vacuum the crude product (35.65 g, 95% yield) was distilled in vacuum, the fraction (21.3 g, 57% yield), BP $159\text{--}162^\circ\text{C}/0.001\text{ mm Hg}$ consisted of 86% of $\text{C}_6\text{H}_5\text{CCl}_2\text{C}(\text{O})\text{CF}_2\text{CF}_2(\text{OCF}_2\text{CF}_2)_5\text{C}(\text{O})\text{CCl}_2\text{C}_6\text{H}_5$ based on GC analysis. The MS is given in Table 11.

TABLE 11

ION FRAGMENTS AND INTENSITIES RELATIVE TO BASE PEAK OF
 $\text{C}_6\text{H}_5\text{CCl}_2\text{C}(\text{O})(\text{CF}_2\text{CF}_2\text{O})_5\text{CF}_2\text{CF}_2\text{C}(\text{O})\text{CCl}_2\text{C}_6\text{H}_5$

m/e	%	m/e	%	m/e	%	m/e	%
20	13.4	78	9.5	137	9.5	201	38.1
28	35.2	81	9.8	139	11.3	202	11.3
31	14.8	85	16.0	143	15.7	203	17.3
35	16.0	87	13.7	145	9.0	223	14.1
36	47.5	88	8.3	151	7.6	251	9.3
37	8.0	89	57.5	152	34.8	287	15.4
38	20.8	90	13.3	153	7.8	289	13.2
39	17.5	97	16.9	154	15.0	403	14.7
44	7.3	99	10.4	158	10.4	405	13.0
47	23.6	100	32.6	159	<u>100.0</u>	519	9.3
50	22.8	101	10.0	160	44.6	982	4.8
51	14.8	105	7.9	161	82.7	983	16.6
62	14.8	109	7.8	162	31.3	984	10.8
63	29.3	119	51.2	163	52.9	985	14.9
66	17.7	120	7.8	164	11.6	986	7.6
69	19.3	123	15.7	167	12.2	987	5.4
70	8.2	124	45.2	169	8.8	1001	5.1
72	8.9	125	21.8	174	11.2	1019	7.8
73	11.6	126	20.5	177	7.8	1021	7.4
75	12.5	127	17.4	185	9.1		
77	9.5	135	15.7	189	9.9		

Peaks having intensities lower than 5% of the base peak and lower than m/e 20 are not reported.

Significant Ions in Support of Structure and Composition

m/e	m/e
89 - $\text{C}_6\text{H}_5\text{C}^+$	403 - $\text{C}_6\text{H}_5\text{CCl}_2\text{C}(\text{O})\text{CF}_2\text{CF}_2\text{OCF}_2\text{CF}_2^+$
124 - $\text{C}_6\text{H}_5\text{CCl}^+$	519 - $\text{C}_6\text{H}_5\text{CCl}_2\text{C}(\text{O})\text{CF}_2\text{CF}_2(\text{OCF}_2\text{CF}_2)_2^+$
159 - $\text{C}_6\text{H}_5\text{CCl}_2^+$	1019 - $[\text{M} - \text{Cl}]^+$
287 - $\text{C}_6\text{H}_5\text{CCl}_2\text{C}(\text{O})\text{CF}_2\text{CF}_2^+$	1035 - $[\text{M} - \text{F}]^+ (1.4\%)$

Preparation of $\text{C}_6\text{H}_5\text{C}(\text{O})\text{C}(\text{O})\text{CF}_2\text{CF}_2(\text{OCF}_2\text{CF}_2)_5\text{C}(\text{O})\text{C}(\text{O})\text{C}_6\text{H}_5$

In a 500 mL round bottom flask, a mixture of $\text{C}_6\text{H}_5\text{CCl}_2\text{C}(\text{O})\text{CF}_2\text{CF}_2(\text{OCF}_2\text{CF}_2)_5\text{C}(\text{O})\text{CCl}_2\text{C}_6\text{H}_5$ (9.2 g, 8.7 mmol) was stirred with silver nitrate (11.8 g, 69.6 mmol) in ethanol (150 mL) and water (150 mL) under gentle reflux for 94 hours. After cooling to room temperature the solid was filtered and washed with diethylether (150 mL). In the filtrate the organic layer was separated, washed with water, dried over anhydrous MgSO_4 and the solvent removed in vacuum. The crude product (9.9 g) was distilled and the fraction (5.2 g, 68% yield), BP 130-133°C/0.001 mm Hg was found to consist of 94% of $\text{C}_6\text{H}_5\text{C}(\text{O})\text{C}(\text{O})\text{CF}_2\text{CF}_2(\text{OCF}_2\text{CF}_2)_5\text{C}(\text{O})\text{C}(\text{O})\text{C}_6\text{H}_5$. The MS and IR spectra are given in Table 12 and Figure 1.

Preparation of Quinoxaline I

Under nitrogen bypass to a solution of $\text{C}_6\text{H}_5\text{C}(\text{O})\text{C}(\text{O})\text{CF}_2\text{CF}_2(\text{OCF}_2\text{CF}_2)_5\text{C}(\text{O})\text{C}(\text{O})\text{C}_6\text{H}_5$ (2.2 g, 2.3 mmol) in m-cresol (5 mL) was added 1,2-phenylenediamine (0.6 g, 5.5 mmol). The resulting mixture was stirred at room temperature for 24 hours. Subsequently, it was poured onto stirred methanol (25 mL). No precipitate was formed; thus, the solution was heated at 50°C in vacuum to remove methanol and cresol. The addition of methanol (10 mL) to the residue followed by cooling to -15°C and subsequent stirring at room temperature for 2 hours resulted in white solid (1 g), MP 72-75°C, purity 99.4% (GC). Anal. Calcd for $\text{C}_{40}\text{H}_{18}\text{F}_{24}\text{N}_4\text{O}_5$: C, 44.05; H, 1.67; F, 41.81; MW, 1090.62. Found: C, 44.12; H, 1.60; F, 40.91; MW, 1100. The MS is

TABLE 12

ION FRAGMENTS AND INTENSITIES RELATIVE TO BASE PEAK OF
 $\text{C}_6\text{H}_5\text{C}(\text{O})\text{C}(\text{O})\text{CF}_2\text{CF}_2(\text{OCF}_2\text{CF}_2)_5\text{C}(\text{O})\text{C}(\text{O})\text{C}_6\text{H}_5$

m/e	%	m/e	%	m/e	%	m/e	%
20	7.2	75	12.5	120	4.4	223	4.2
26	5.4	76	17.2	123	8.5	233	17.1
27	9.7	77	66.9	124	12.8	234	9.6
28	29.7	78	33.2	125	5.2	299	5.8
31	11.6	79	5.0	126	7.1	320	7.9
38	5.3	81	6.7	127	10.3	349	15.9
39	8.2	89	4.2	139	4.1	350	5.6
47	14.6	95	4.5	145	5.2	415	6.3
50	27.4	96	13.1	154	7.2	437	5.6
51	51.0	97	13.7	167	4.2	465	14.4
52	10.6	100	29.6	173	7.6	466	5.1
56	11.2	101	5.7	177	5.4	531	4.2
62	4.1	104	12.2	181	4.5	581	7.7
63	5.3	105	<u>100.0</u>	182	5.8	784	8.5
66	11.8	106	54.2	185	4.1	813	4.0
69	14.4	107	12.9	191	4.4	814	4.0
70	4.7	109	4.0	204	4.9	927	5.8
74	10.2	119	38.1	221	6.3		

Peaks having intensities lower than 4% of the base peak and lower than m/e 20 are not reported.

Significant Ions in Support of Structure and Composition

m/e

- 105 - $\text{C}_6\text{H}_5\text{CO}^+$
- 233 - $\text{C}_6\text{H}_5\text{C}(\text{O})\text{C}(\text{O})\text{CF}_2\text{CF}_2^+$
- 349 - $\text{C}_6\text{H}_5\text{C}(\text{O})\text{C}(\text{O})\text{CF}_2\text{CF}_2\text{OCF}_2\text{CF}_2^+$
- 465 - $\text{C}_6\text{H}_5\text{C}(\text{O})\text{C}(\text{O})\text{CF}_2\text{CF}_2(\text{OCF}_2\text{CF}_2)_2^+$
- 927 - $[\text{M} - \text{F}]^+$
- 947 - $[\text{M} + 1]^+$ (2.4%)

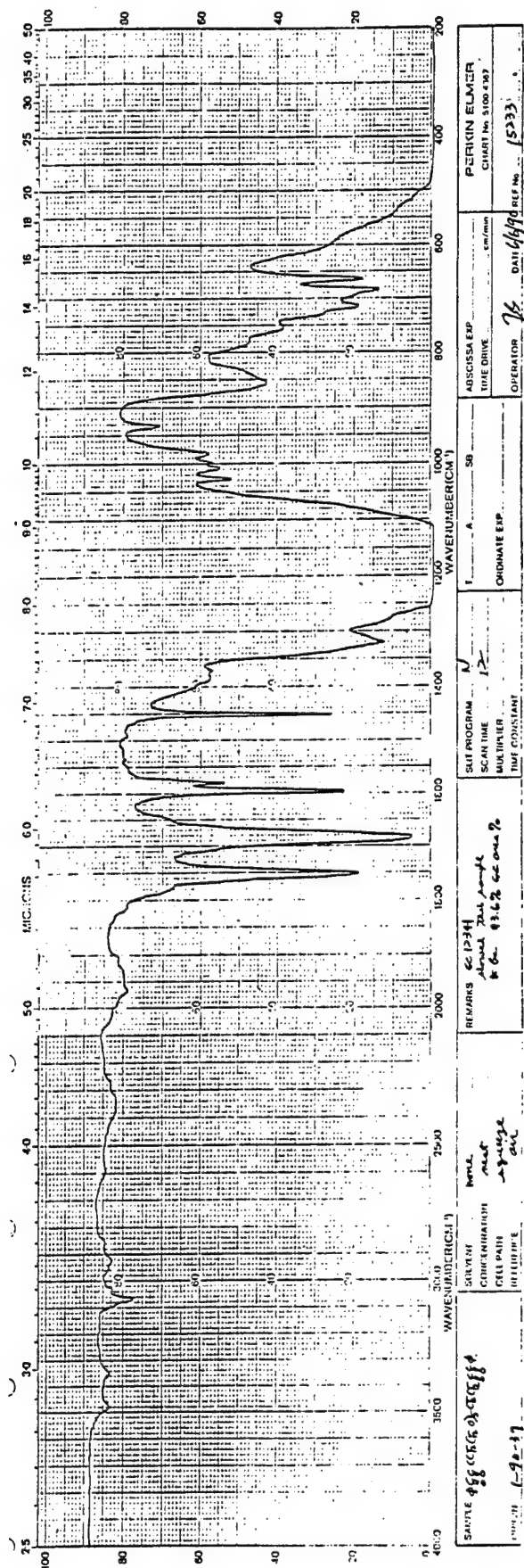
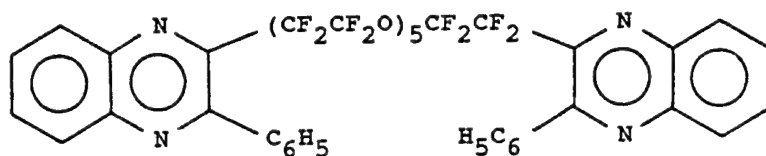


Figure 1. Infrared spectrum of $\text{C}_6\text{H}_5\text{C}(\text{O})\text{C}(\text{O})\text{CF}_2\text{CF}_2(\text{OCF}_2\text{CF}_2)_5\text{C}(\text{O})\text{C}(\text{O})\text{C}_6\text{H}_5$ (1-90-37).

TABLE 13

ION FRAGMENTS AND INTENSITIES RELATIVE TO BASE PEAK OF

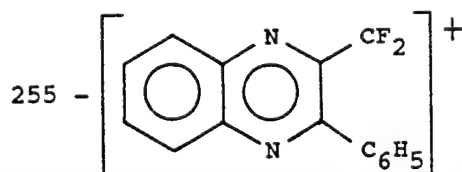
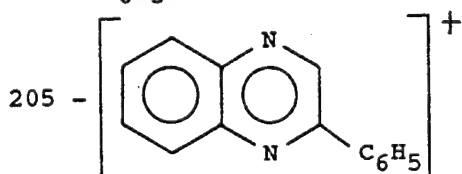


m/e	%	m/e	%	m/e	%	m/e	%
18	3.6	101	5.0	223	8.6	421	18.1
20	22.3	102	29.3	224	13.2	422	7.4
28	19.9	103	17.8	235	21.9	534	9.3
31	11.8	104	9.6	236	10.7	535	3.2
32	3.0	118	4.7	253	6.0	536	3.0
36	5.4	119	21.3	254	17.1	537	5.6
39	3.3	126	6.4	255	19.7	545	28.5
47	22.6	127	15.5	256	4.7	650	6.8
50	27.5	128	5.9	266	4.1	766	5.4
51	18.3	151	9.5	281	5.2	885	3.5
52	3.4	152	14.2	282	5.1	1004	3.4
66	19.2	153	5.3	285	17.3	1013	3.0
69	9.2	177	7.8	286	7.9	1024	4.7
74	4.6	178	16.8	302	3.0	1049	5.4
75	17.0	179	33.0	303	4.6	1050	9.8
76	26.2	180	7.8	304	13.8	1052	8.0
77	40.3	197	3.4	305	28.5	1053	5.2
78	7.2	204	3.9	306	10.1	1055	3.8
81	4.5	205	100.0	324	4.8		
97	6.7	206	36.2	371	4.5		
100	14.1	207	5.7	418	9.9		

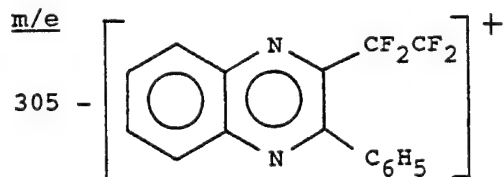
Peaks having intensities lower than 3% of the base peak and lower than m/e 18 are not reported.

Significant Ions in Support of Structure and Composition

m/e

77 - C_6H_5^+ 

m/e

885 - $[\text{M} - 205]^+$ 1052 - $[\text{M} - 2\text{F}]^+$

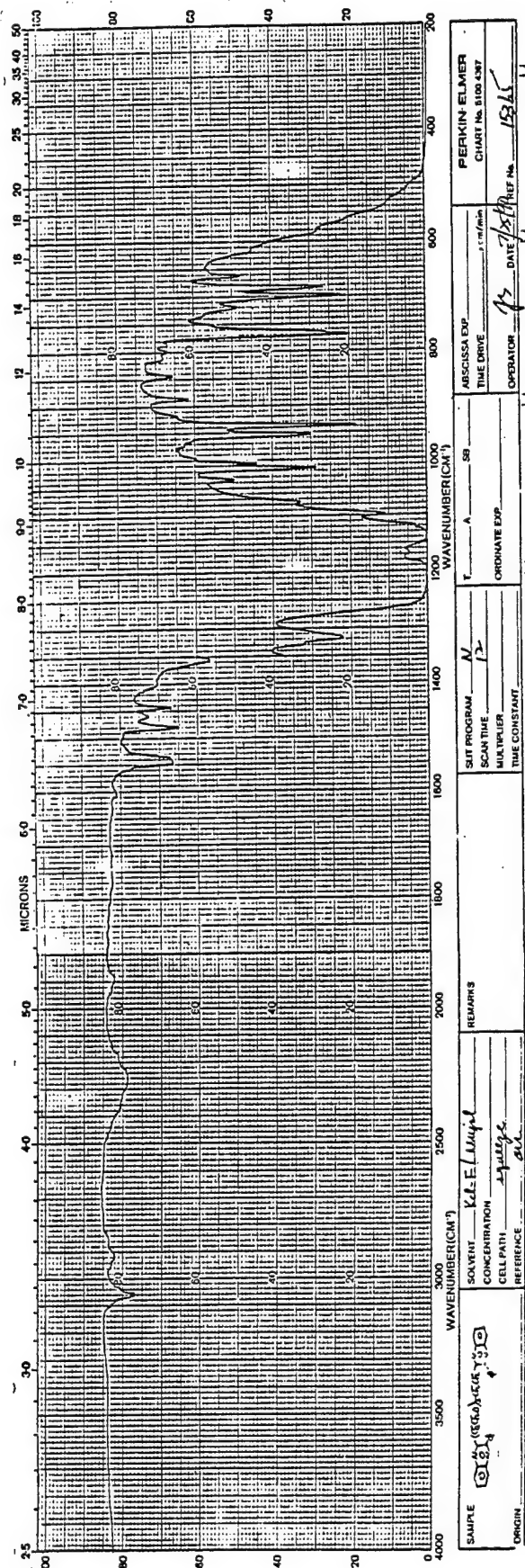


Figure 2. Infrared spectrum of Quinoxaline I.

PART NO. 990088

TGA RUN NO. <u>100193</u> OPERATOR <u>DRM</u> SAMPLE <u>Quinoxaline I</u> <u>GC 12387</u> ATM. <u>N₂</u> @ <u>0</u> FLOW RATE _____		T-AXIS SCALE, °C/in. <u>50</u> PROG. RATE, °C/min _____ HEAT, COOL, ISO _____ SHIFT, in. <u>0</u>		DTA-DSC SCALE, °C/in. _____ (mcal/sec)/in. _____ WEIGHT, mg _____ REFERENCE _____		TGA SCALE, mg/in. _____ SUPPRESSION, mg _____ WEIGHT, mg <u>1.85</u> TIME CONST., sec _____ dY, (mg/min)/in. _____		TMA SCALE, mils/in. _____ MODE _____ SAMPLE SIZE _____ LOAD, g _____ dY, (10X), (mils/min)/in. _____	
---	--	--	--	--	--	--	--	--	--

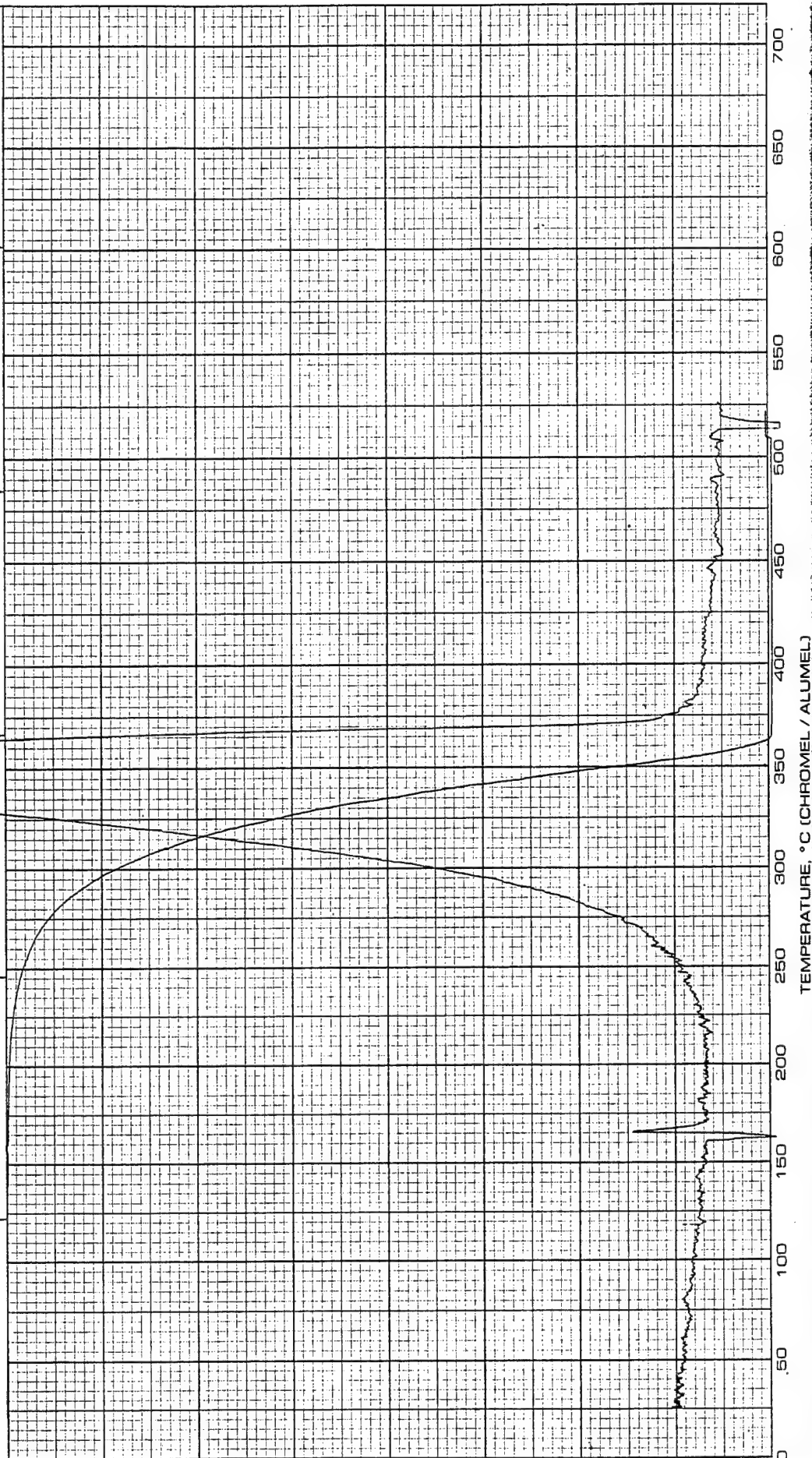


Figure 3. TGA scan of Quinoxaline I in N₂.

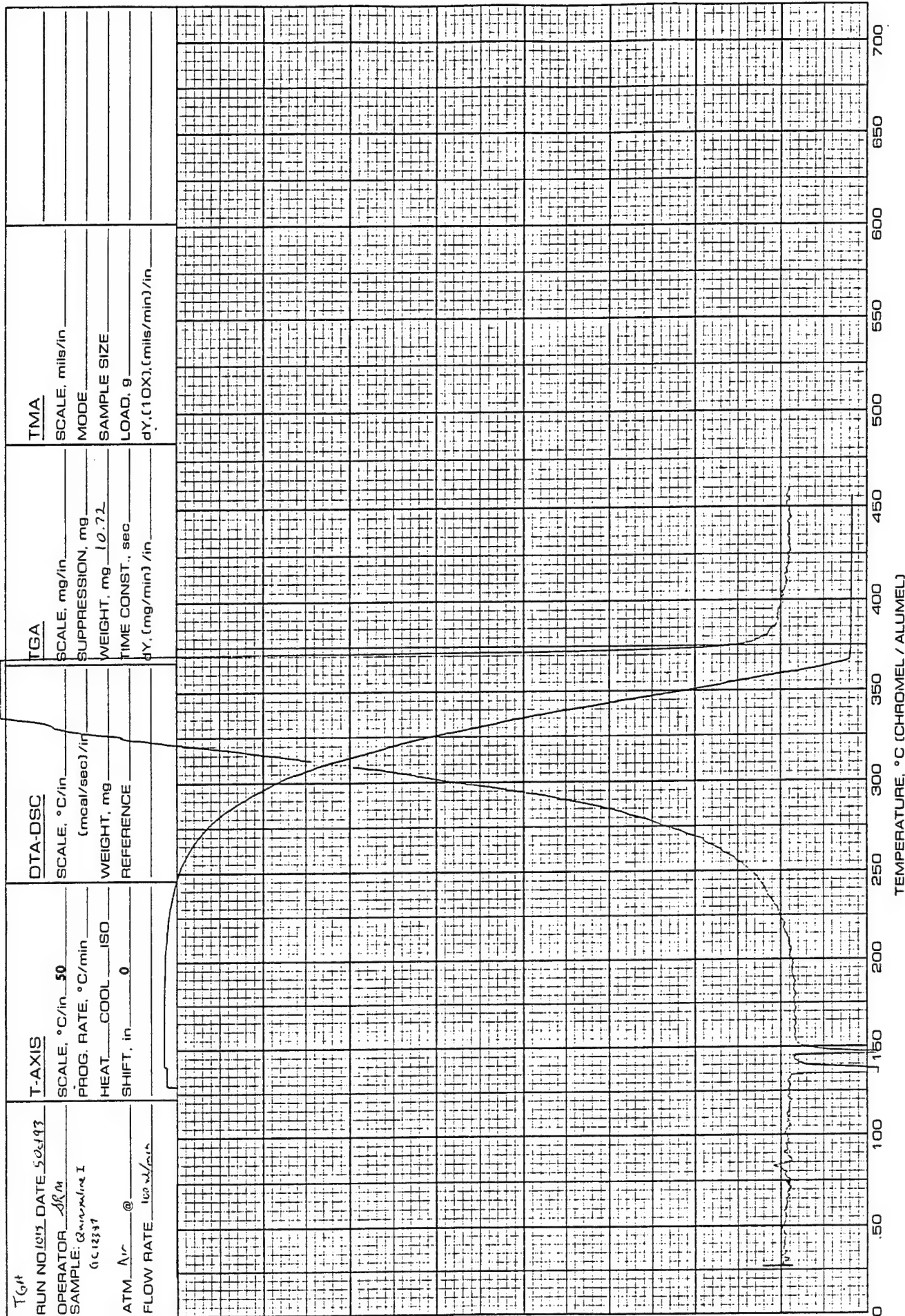


Figure 4. TGA scan of Quinoxaline I in air.

presented in Table 13, the IR in Figure 2, and TGA scans, in nitrogen and air, in Figure 3 and 4, respectively.

Preparation of $n\text{-C}_7\text{F}_{15}\text{C}(\text{O})\text{CCl}_2\text{C}_6\text{H}_5$

Using the conditions described for the preparation of $\text{C}_6\text{H}_5\text{CCl}_2\text{C}(\text{O})\text{CF}_2\text{CF}_2(\text{OCF}_2\text{CF}_2)_5\text{C}(\text{O})\text{CCl}_2\text{C}_6\text{H}_5$, the ester $n\text{-C}_7\text{F}_{15}\text{CO}_2\text{Me}$ (4.8 g, 11.2 mmol) was added to the product of reaction of trichlorotoluene (25 g, 13.8 mmol) and *n*-butyllithium (5.5 mL, 2.5 M). The realized yield was 74%. The MS is given in Table 14.

Preparation of $n\text{-C}_7\text{F}_{15}\text{C}(\text{O})\text{C}(\text{O})\text{C}_6\text{H}_5$

Using the conditions described for the preparation of $\text{C}_6\text{H}_5\text{C}(\text{O})\text{C}(\text{O})\text{CF}_2\text{CF}_2(\text{OCF}_2\text{CF}_2)_5\text{C}(\text{O})\text{C}(\text{O})\text{C}_6\text{H}_5$, $n\text{-C}_7\text{F}_{15}\text{C}(\text{O})\text{CCl}_2\text{C}_6\text{H}_5$ (4.5 g, 8.1 mmol) was treated with silver nitrate (5.5 g, 32 mmol) in aqueous ethanol over 64 hours. This resulted in 98% yield (4.0 g) of $n\text{-C}_7\text{F}_{15}\text{C}(\text{O})\text{C}(\text{O})\text{C}_6\text{H}_5$, BP 69–70°C/0.001 mm Hg (purity 95%). The MS is given in Table 15 and the IR in Figure 5.

Preparation of Quinoxaline II

Under nitrogen bypass to a stirred mixture of $n\text{-C}_7\text{F}_{15}\text{C}(\text{O})\text{C}(\text{O})\text{C}_6\text{H}_5$ (1.5 g, 3.0 mmol) and *m*-cresol (5 mL) was added a solution of 1,2-phenylenediamine (0.4 g, 3.7 mmol) in *m*-cresol (10 mL) over 15 minutes at room temperature. After 30 minutes a thick solid layer was formed on top of the reaction mixture. The reaction mixture was allowed to stir at room temperature for 22 hours. Subsequently, it was poured into methanol (20 mL), filtered and the solid rinsed with an

TABLE 14
ION FRAGMENTS AND INTENSITIES RELATIVE TO BASE PEAK OF
 $C_6H_5CCl_2C(O)C_7F_{15}$

m/e	%	m/e	%	m/e	%	m/e	%
28	18.2	88	7.0	133	6.6	167	10.0
31	14.5	89	51.6	135	6.0	169	15.3
35	7.4	90	13.8	138	17.4	174	21.1
36	20.1	93	6.4	139	15.0	175	6.2
37	6.3	99	8.7	140	10.7	176	13.2
38	15.5	100	28.1	143	13.8	180	17.1
39	15.3	101	7.6	145	15.2	181	12.7
50	19.8	102	6.0	150	7.3	182	9.6
51	12.2	103	11.8	151	18.1	201	12.3
62	18.5	115	20.5	152	44.9	203	8.2
63	26.1	116	9.7	153	15.4	219	6.2
64	6.6	119	19.1	154	21.1	231	6.8
69	33.8	123	15.4	158	9.0	493	9.6
73	10.4	124	49.5	159	<u>100.0</u>	521	22.0
75	8.5	125	14.2	160	36.1	522	11.4
77	9.5	126	23.1	161	82.6	523	15.0
81	14.3	127	11.1	162	26.3	537	7.5
85	9.9	128	7.6	163	40.8		
87	10.2	131	21.8	164	9.7		

Peaks having intensities lower than 6% of the base peak and lower than m/e 28 are not reported.

Significant Ions in Support of Structure and Composition

m/e	m/e
89 - $C_6H_5C^+$	159 - $C_6H_5CCl_2^+$
119 - $CF_2CF_3^+$	169 - $CF_2CF_2CF_3^+$
124 - $C_6H_5CCl^+$	521 - $[M - Cl]^+$
131 - $C_3F_5^+$	537 - $[M - F]^+$

TABLE 15

ION FRAGMENTS AND INTENSITIES RELATIVE TO BASE PEAK OF
 $C_7F_{15}C(O)C(O)C_6H_5$

m/e	%	m/e	%	m/e	%	m/e	%
18	6.3	56	22.9	95	4.4	131	31.0
20	10.7	57	6.2	96	12.2	132	4.0
26	10.3	62	6.3	100	35.4	139	3.4
27	13.5	63	6.1	101	5.6	150	6.9
28	36.2	69	42.8	104	15.1	151	3.8
29	3.5	70	6.3	105	<u>100.0</u>	154	3.2
31	17.6	73	5.3	106	52.5	162	3.8
33	5.2	74	14.0	107	13.1	169	14.0
37	5.4	75	14.4	109	7.8	181	11.6
38	9.8	76	21.4	112	5.2	182	4.4
39	13.0	77	82.8	117	4.0	219	3.5
49	6.3	78	45.1	119	19.2	231	7.1
50	41.9	79	6.2	121	3.1	427	3.8
51	62.8	81	12.9	122	3.1	455	5.0
52	18.2	89	6.0	123	5.3	483	8.2
53	4.9	93	9.4	124	12.2	503	4.1

Peaks having intensities lower than 3% of the base peak and lower than m/e 18 are not reported.

Significant Ions in Support of Structure and Composition

<u>m/e</u>	<u>m/e</u>
105 - $C_6H_5CO^+$	169 - $CF_3CF_2CF_2^+$
119 - $CF_3CF_2^+$	483 - $[M - F]^+$
131 - $C_3F_5^+$	503 - $[M + 1]^+$

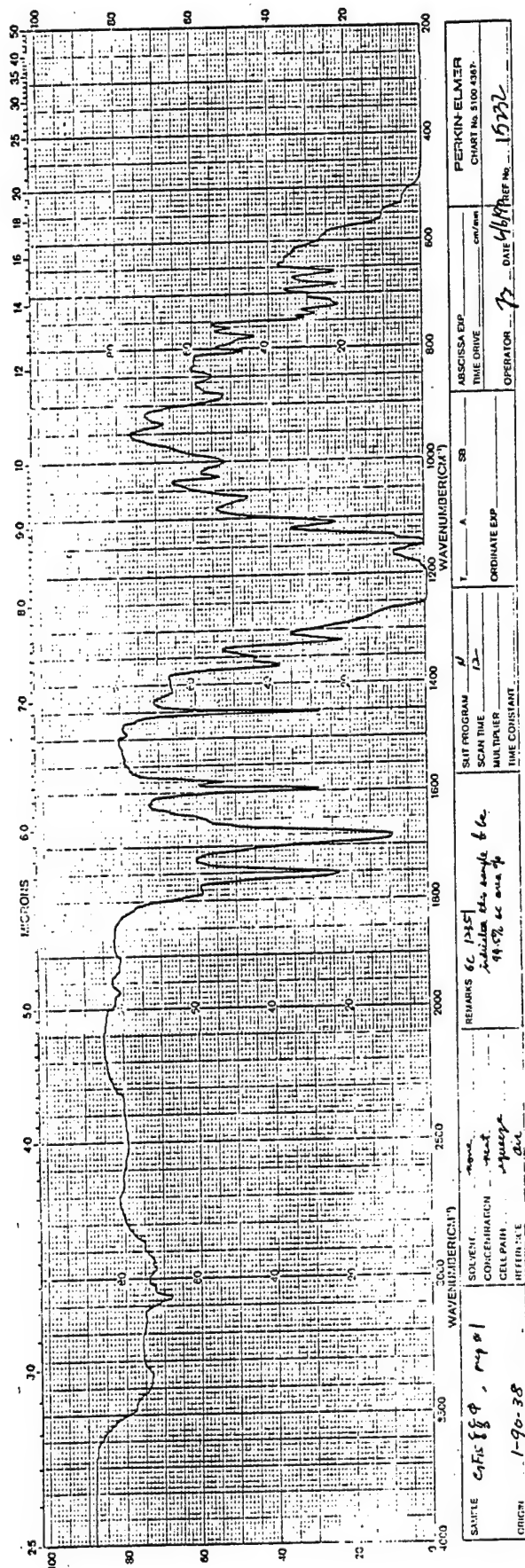


Figure 5. Infrared spectrum of $C_7F_{15}C(O)C(O)C_6H_5$ (1-90-38).

additional ~50 mL of methanol. Quinoxaline II (1.0 g, 59% yield), MP 118-119°C was obtained and was shown by gas chromatography to be free of impurities. Anal. Calcd for $C_{21}H_9F_{15}N_2$: C, 43.91; H, 1.58; F, 49.62; MW, 574.32. Found: C, 44.06; H, 1.44; F, 49.03; MW, 590. The MS is presented in Table 16, the IR in Figure 6, the DSC scan in Figure 7, and TGA scans, in nitrogen and air, in Figures 8 and 9, respectively.

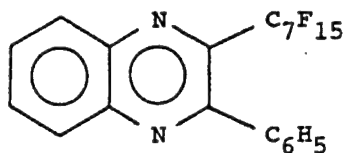
Preparation of $C_6H_5C(O)C(O)C_6H_4(CF_2CF_2O)_5CF_2CF_2C_6H_4C(O)C(O)C_6H_5$

In an inert atmosphere enclosure, 4-iodobenzil (10.35 g, 30 mmol), copper bronze (42.8 mmol), and $I(CF_2CF_2O)_5CF_2CF_2I$ (5.00 g, 5.35 mmol) were weighed into a 100 mL round bottom flask, followed by N,N-dimethylformamide (DMF, 60 mL). The round bottom flask was equipped with a 1/2 in stir bar, water cooled condenser, and nitrogen inlet. The set-up was connected to nitrogen bypass and heated at 105°C for 160 hours. After the reaction mixture was filtered, the insoluble residue was washed with CH_2Cl_2 , and the washing combined with the DMF filtrate.

The solvent was removed from the filtrate in vacuum at room temperature, and the residue (19.0 g) was extracted with Freon-113 (25 mL) and then with CH_2Cl_2 (25 mL). The combined product (12.1 g), after solvent removal, was heated at 80°C for 64 hours to sublime out the more volatile impurities. The 1:1 ether/hexane soluble portion of the residue (2.83 g) was filtered through silica column (1.8 x 30 cm) with 1:1 ether/hexane to give a bright yellow product (1.44 g, 24.5% yield), MP 66-68°C;

TABLE 16

ION FRAGMENTS AND INTENSITIES RELATIVE TO BASE PEAK OF



m/e	%	m/e	%	m/e	%	m/e	%
18	6.7	78	8.7	131	11.1	237	2.5
20	7.7	81	8.8	132	2.0	253	3.4
26	3.9	88	2.1	143	2.9	254	20.6
27	6.3	89	5.5	150	4.0	255	26.2
28	11.6	90	3.9	151	12.4	256	9.7
29	5.5	93	2.1	152	14.8	266	6.1
31	11.0	99	3.2	153	5.5	267	4.2
32	3.3	100	14.1	169	7.8	278	2.6
36	10.2	101	7.5	176	3.3	284	2.4
38	7.2	102	31.5	177	11.2	285	2.0
39	6.6	103	24.6	178	16.2	286	3.5
50	26.3	104	11.3	179	26.8	287	6.5
51	22.4	105	2.5	180	9.1	304	5.3
52	6.7	107	2.0	181	2.8	305	2.9
62	3.2	112	2.1	203	4.7	555	20.0
63	5.7	114	2.9	204	7.4	556	8.5
64	2.5	118	21.2	205	100.0	574	99.4
69	27.2	119	15.6	206	46.5	575	36.4
73	5.0	125	3.0	207	9.9	576	11.5
74	9.6	126	5.4	208	2.1	577	2.1
75	20.4	127	14.6	224	2.5		
76	27.2	128	11.9	235	11.0		
77	40.9	129	2.1	236	10.5		

Peaks having intensities lower than 2% of the base peak and lower than m/e 18 are not reported.

Significant Ions in Support of Structure and Composition

m/e

77 - C_6H_5^+
 119 - CF_3CF_2^+
 131 - C_3F_5^+
 179 - $[\text{M} - \text{C}_7\text{F}_{15}\text{CN}]^+$

m/e

205 - $[\text{M} - \text{C}_7\text{F}_{15}]^+$
 255 - $[\text{M} - \text{C}_6\text{F}_{13}]^+$
 555 - $[\text{M} - \text{F}]^+$

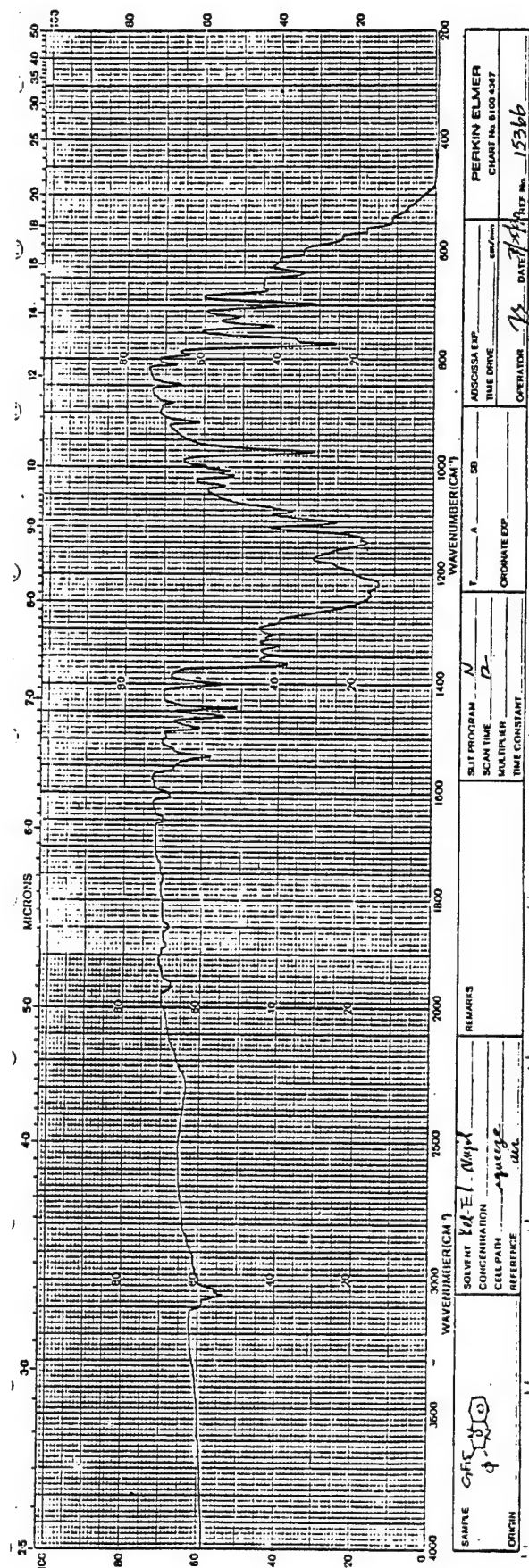


Figure 6. Infrared spectrum of Quinoxaline II.

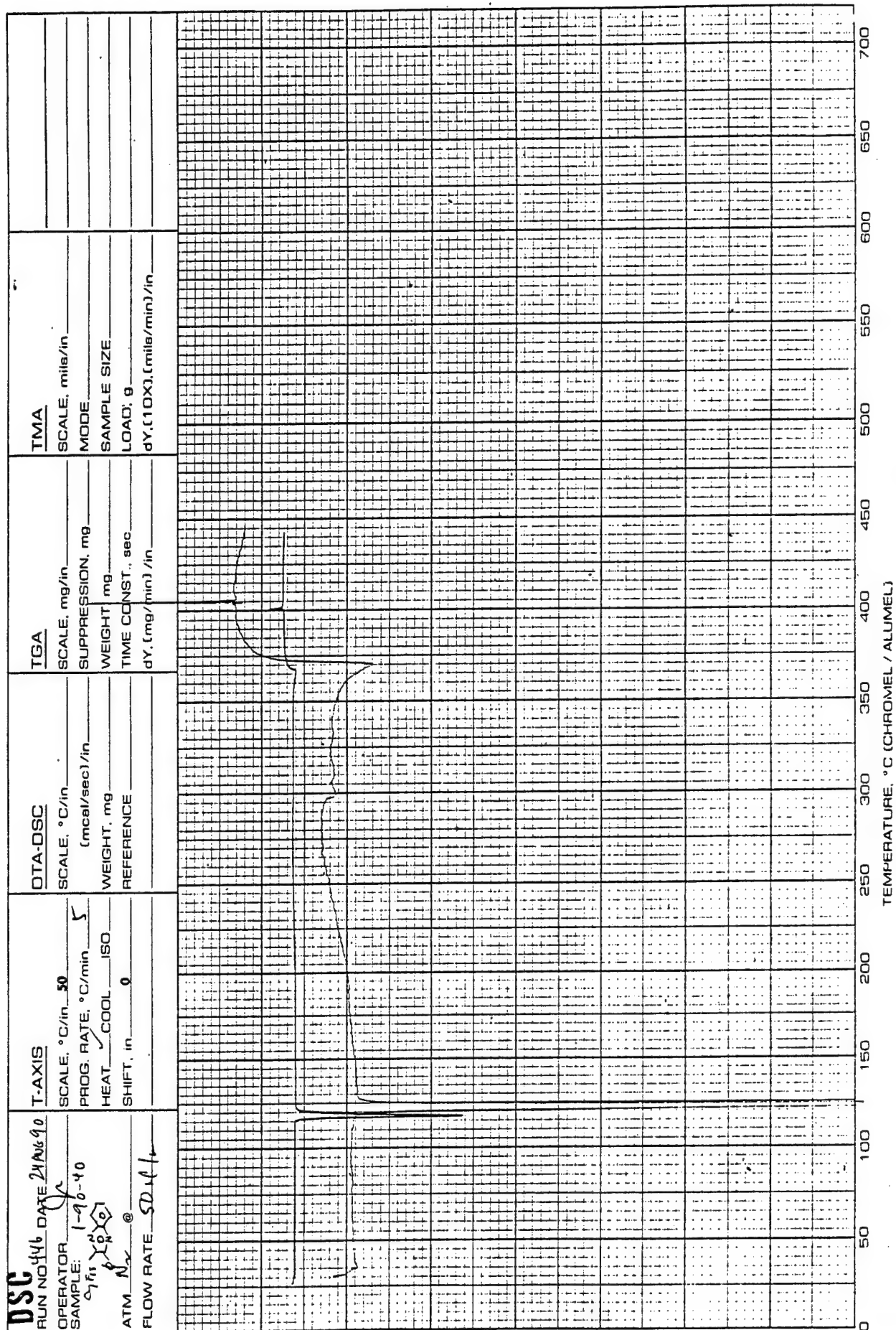
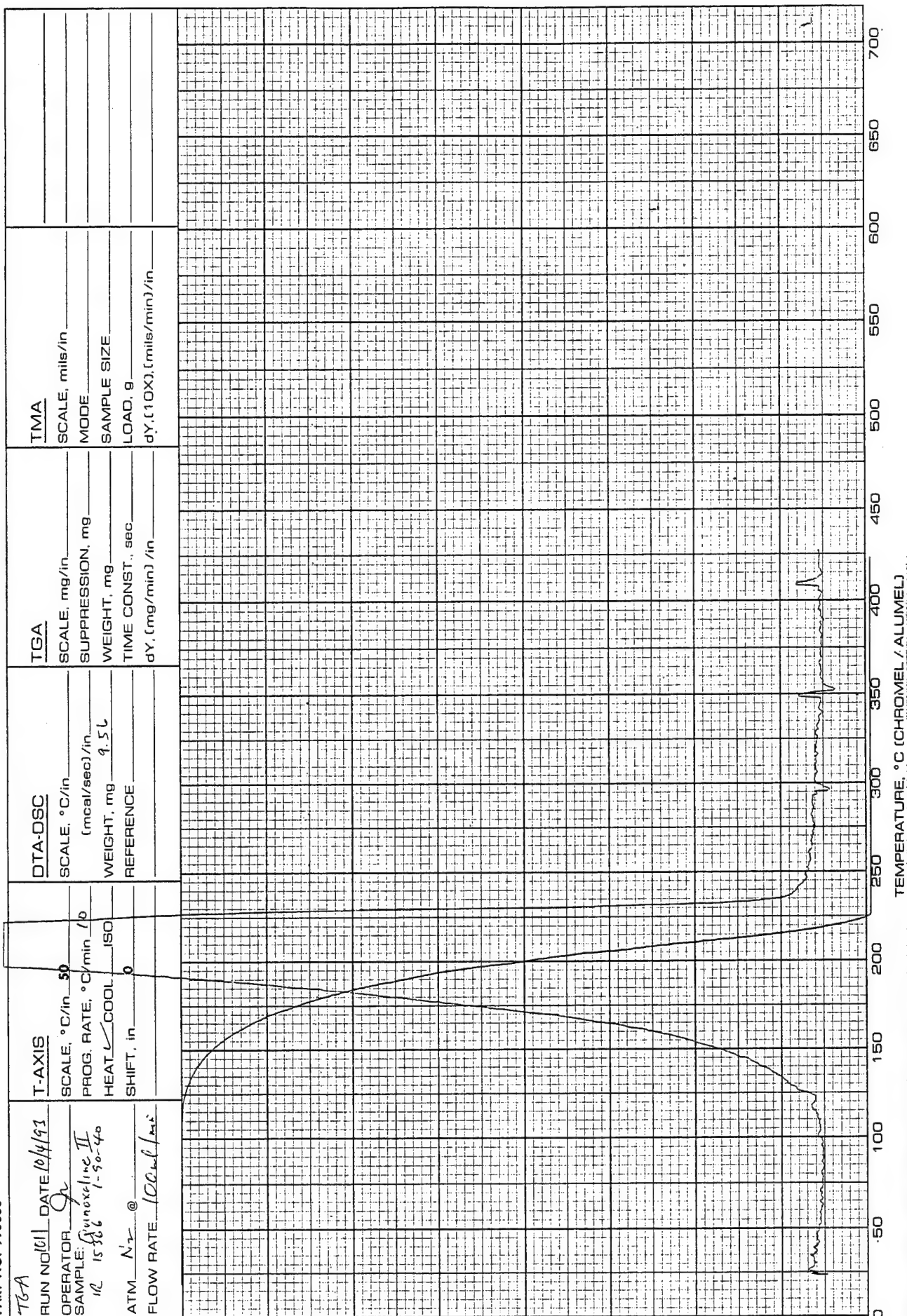


Figure 7. DSC scan of Quinoxaline II.

Figure 8. TGA scan of Quinoxaline II in N₂.

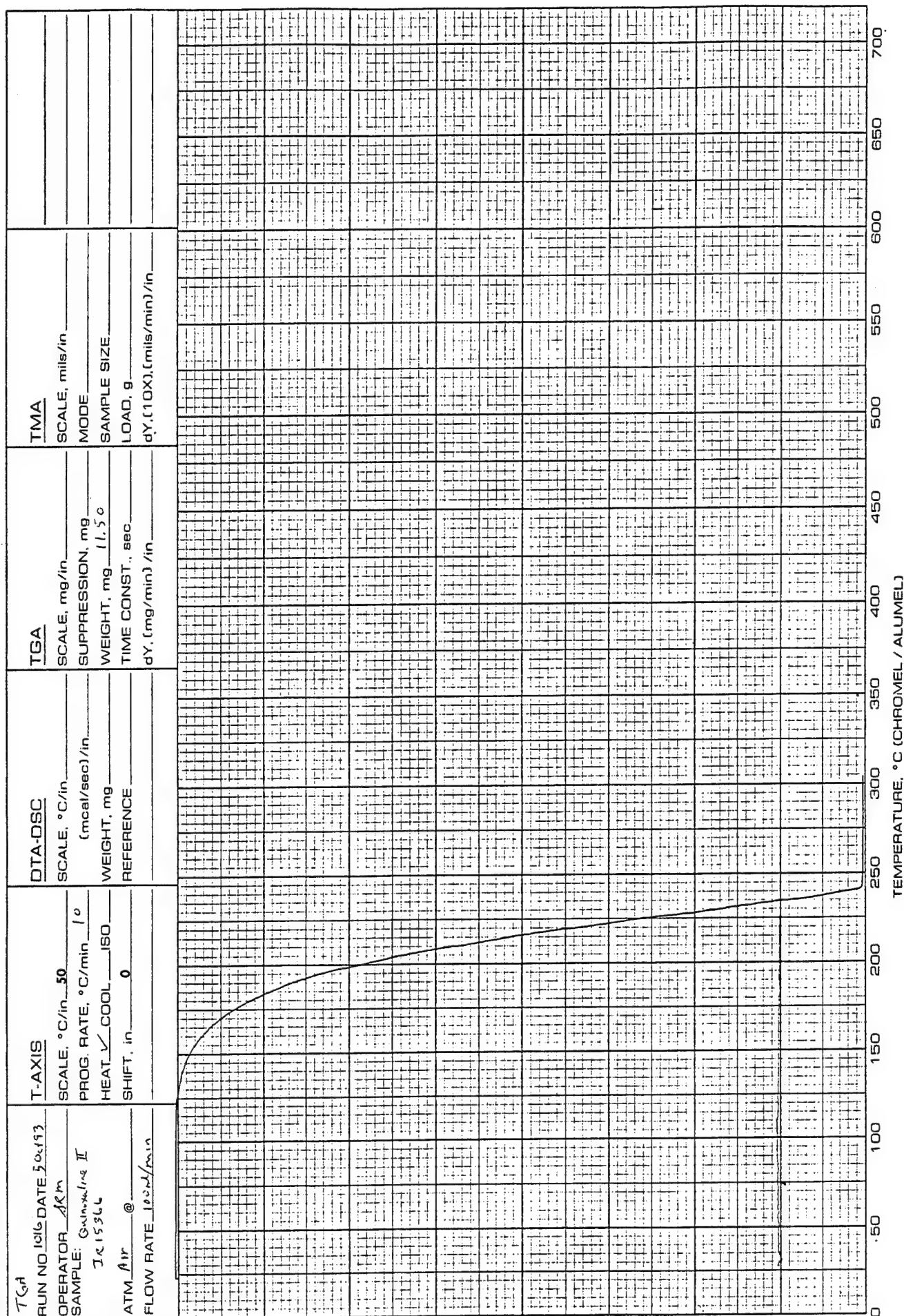


Figure 9. TGA scan of Quinoxaline II in air.

TABLE 17

ION FRAGMENTS AND INTENSITIES RELATIVE TO BASE PEAK OF
 $\text{C}_6\text{H}_5\text{C}(\text{O})\text{C}(\text{O})\text{C}_6\text{H}_4(\text{CF}_2\text{CF}_2\text{O})_5\text{CF}_2\text{CF}_2\text{C}_6\text{H}_4\text{C}(\text{O})\text{C}(\text{O})\text{C}_6\text{H}_5$

m/e	%	m/e	%	m/e	%	m/e	%
20	14.1	76	10.9	124	9.8	320	5.2
28	23.8	77	58.8	125	6.4	861	5.4
31	7.8	78	18.7	126	16.7	909	7.4
39	5.7	96	11.6	127	8.3	936	7.1
44	7.1	97	7.7	145	10.9	937	11.0
47	18.0	100	8.9	154	10.5	938	5.7
50	22.0	104	6.8	173	13.0	965	8.4
51	23.1	105	<u>100.0</u>	176	6.5	966	8.0
52	5.4	106	56.2	201	8.8	993	35.4
66	15.2	107	12.7	204	6.1	994	18.0
69	11.5	119	17.5	230	8.6	995	8.4
74	6.0	122	8.0	260	5.6	1060	9.3
75	8.1	123	7.7	317	5.6		

Peaks having intensities lower than 5% of the base peak and lower than m/e 20 are not reported.

Significant Ions in Support of Structure and Composition

m/e

- 77 - C_6H_5^+
- 105 - $\text{C}_6\text{H}_5\text{CO}^+$
- 126 - $\text{C}_6\text{H}_4\text{CF}_2^+$

m/e

- 993 - $[\text{M} - \text{C}_6\text{H}_5\text{CO}]^+$
- 1060 - $[\text{M} - 38]^+$

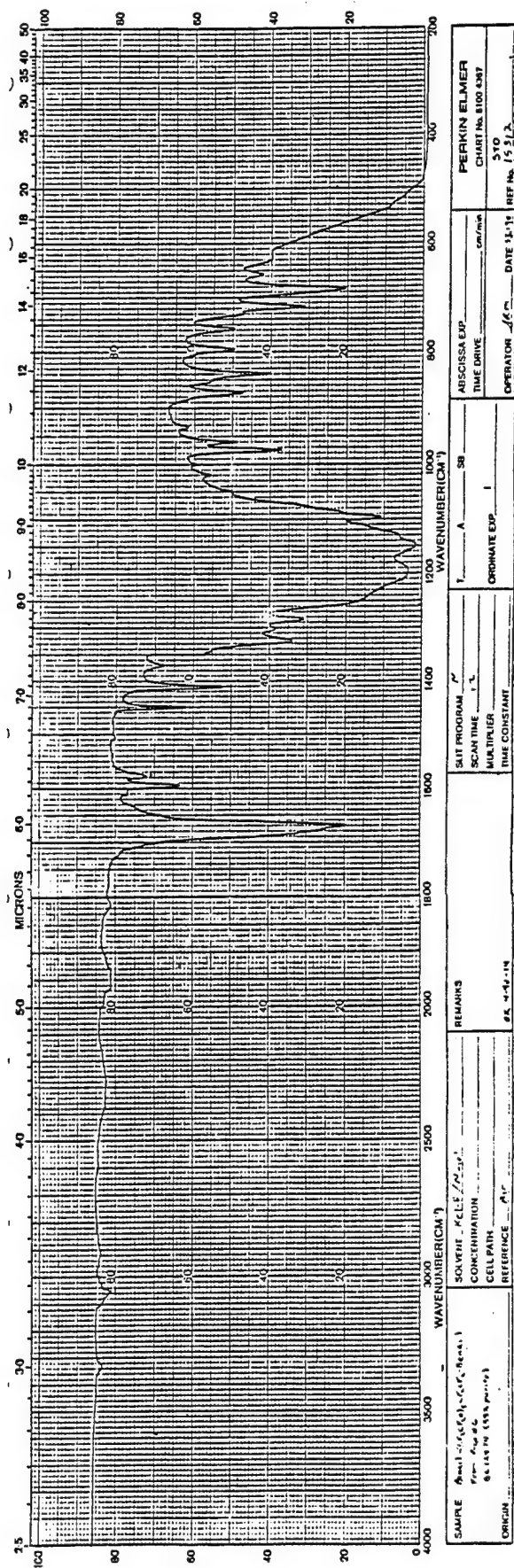


Figure 10. Infrared spectrum of $\text{C}_6\text{H}_5\text{C}(\text{O})\text{C}(\text{O})\text{C}_6\text{H}_4(\text{CF}_2\text{CF}_2\text{O})_5\text{CF}_2\text{CF}_2\text{C}_6\text{H}_4\text{C}(\text{O})\text{C}(\text{O})\text{C}_6\text{H}_5$ (4-90-14).

purity, 99% (GC). The MS is given in Table 17, the IR in Figure 10.

Preparation of Quinoxaline III

$\text{C}_6\text{H}_5\text{C}(\text{O})\text{C}(\text{O})\text{C}_6\text{H}_4(\text{CF}_2\text{CF}_2\text{O})_5\text{CF}_2\text{CF}_2\text{C}(\text{O})\text{C}_6\text{H}_4\text{C}(\text{O})\text{C}_6\text{H}_5$ (0.40 g, 0.36 mmol) was stirred with 1,2-phenylenediamine (0.10 g, 0.92 mmol) in m-cresol (15 mL) over a period of 24 hours at room temperature. Subsequently, m-cresol was removed by distillation at 50°C in vacuum (<0.001 mm Hg). Then methanol (30 mL) was added and the mixture stirred 16 hours at room temperature. The resulting precipitate was filtered, washed with methanol (35 mL), and the white solid dried in vacuum giving Quinoxaline III (0.24 g, 52% yield), MP 91.5-93°C. Due to material's involatility its purity (GC) and MS could not be determined. Anal. Calcd for $\text{C}_{52}\text{H}_{26}\text{F}_{24}\text{N}_4\text{O}_5$: C, 50.25; H, 2.11; F, 36.69; MW, 1242.83. Found: C, 50.25; H, 1.88; F, 36.47; MW, 1300. The IR is given in Figure 11, DSC scan in Figure 12, and TGA scans, in nitrogen and air, in Figures 13 and 14, respectively.

Preparation of Quinoxaline IV

In nitrogen atmosphere to 3,3'-diaminobenzidine (0.4 g, 1.7 mmol) in m-cresol (10 mL) was added $\text{C}_7\text{F}_{15}\text{C}(\text{O})\text{C}(\text{O})\text{C}_6\text{H}_5$ (2.1 g, 4.2 mmol) in m-cresol (5 mL). Heavy precipitation formed after half of the tetraketone solution was added. The reaction mixture was allowed to stir for 24 hours at room temperature. Then it was poured onto stirring methanol (50 mL); the precipitate filtered, washed with 50 mL of methanol and dried in vacuum to give a pale yellow-beige solid (1.93 g, 92% yield). The material

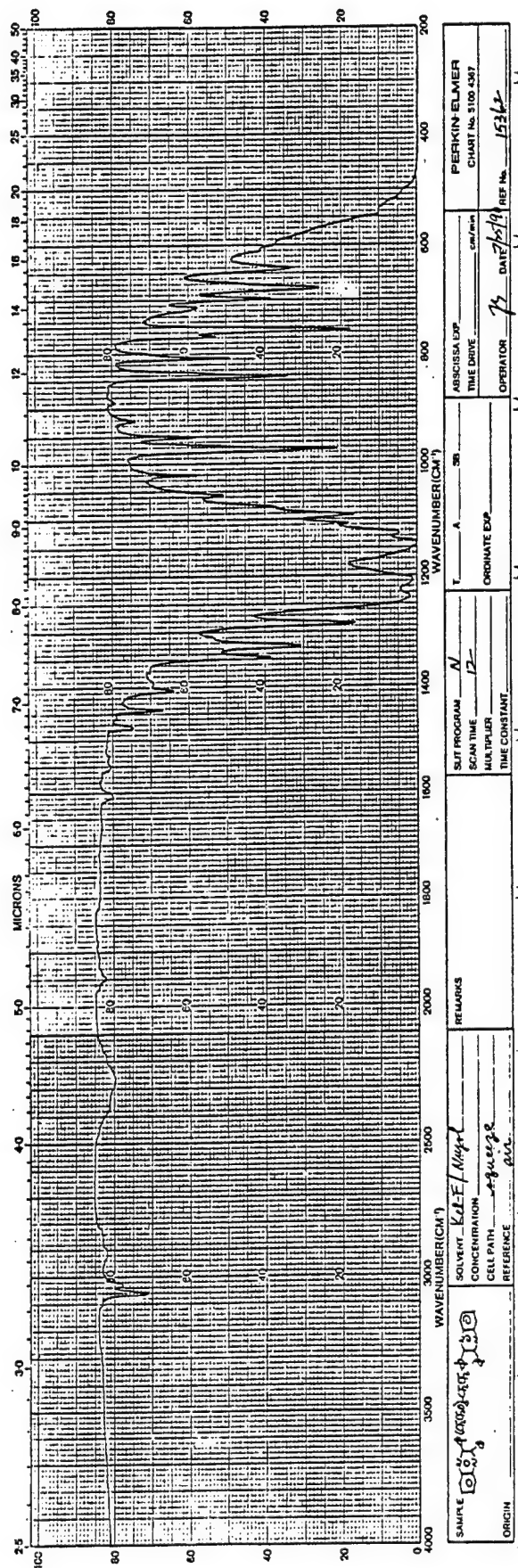


Figure 11. Infrared spectrum of Quinoxaline III.

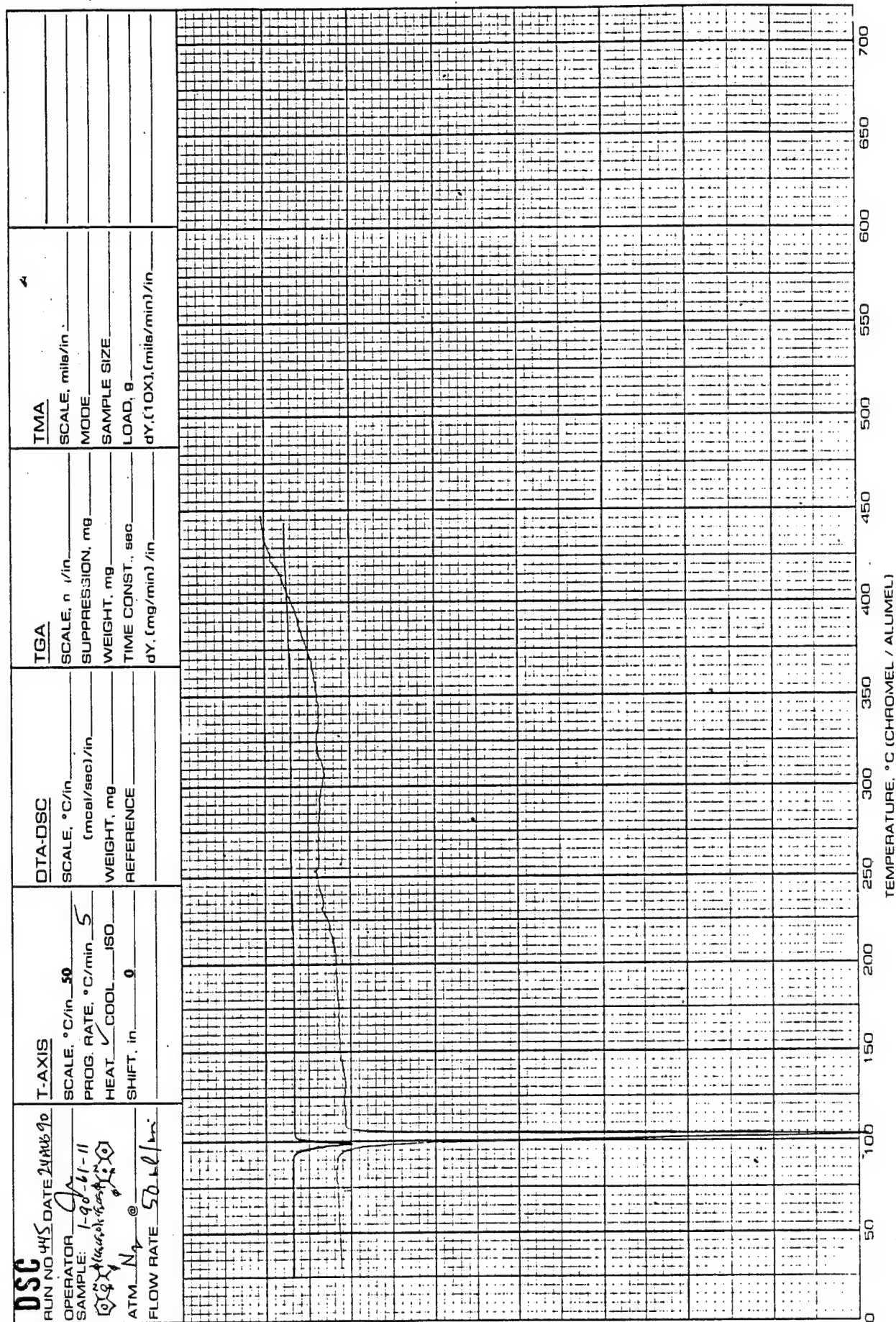


Figure 12. DSC scan of Quinoxaline III.

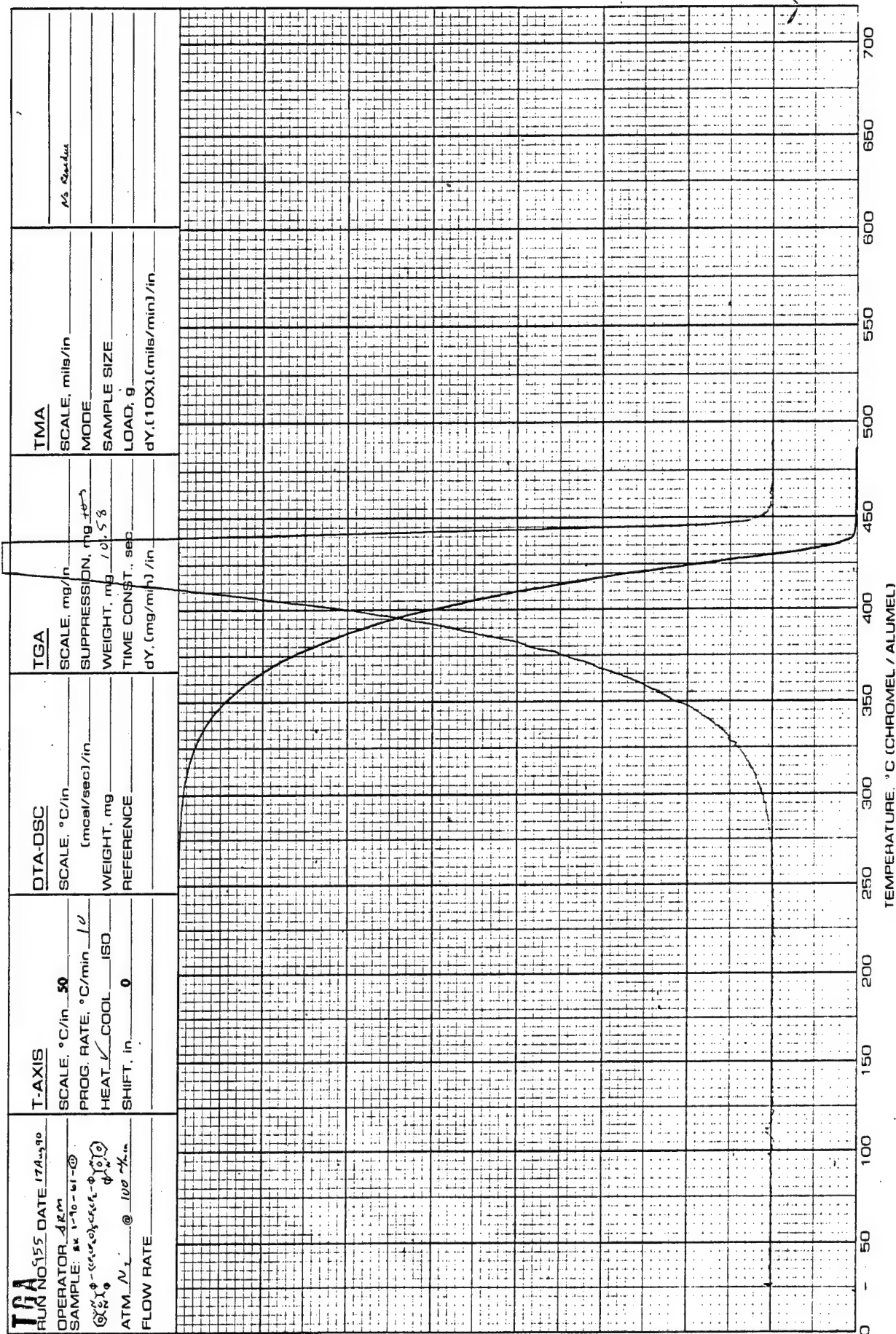


Figure 13. TGA scan of Quinoxaline III in N₂.

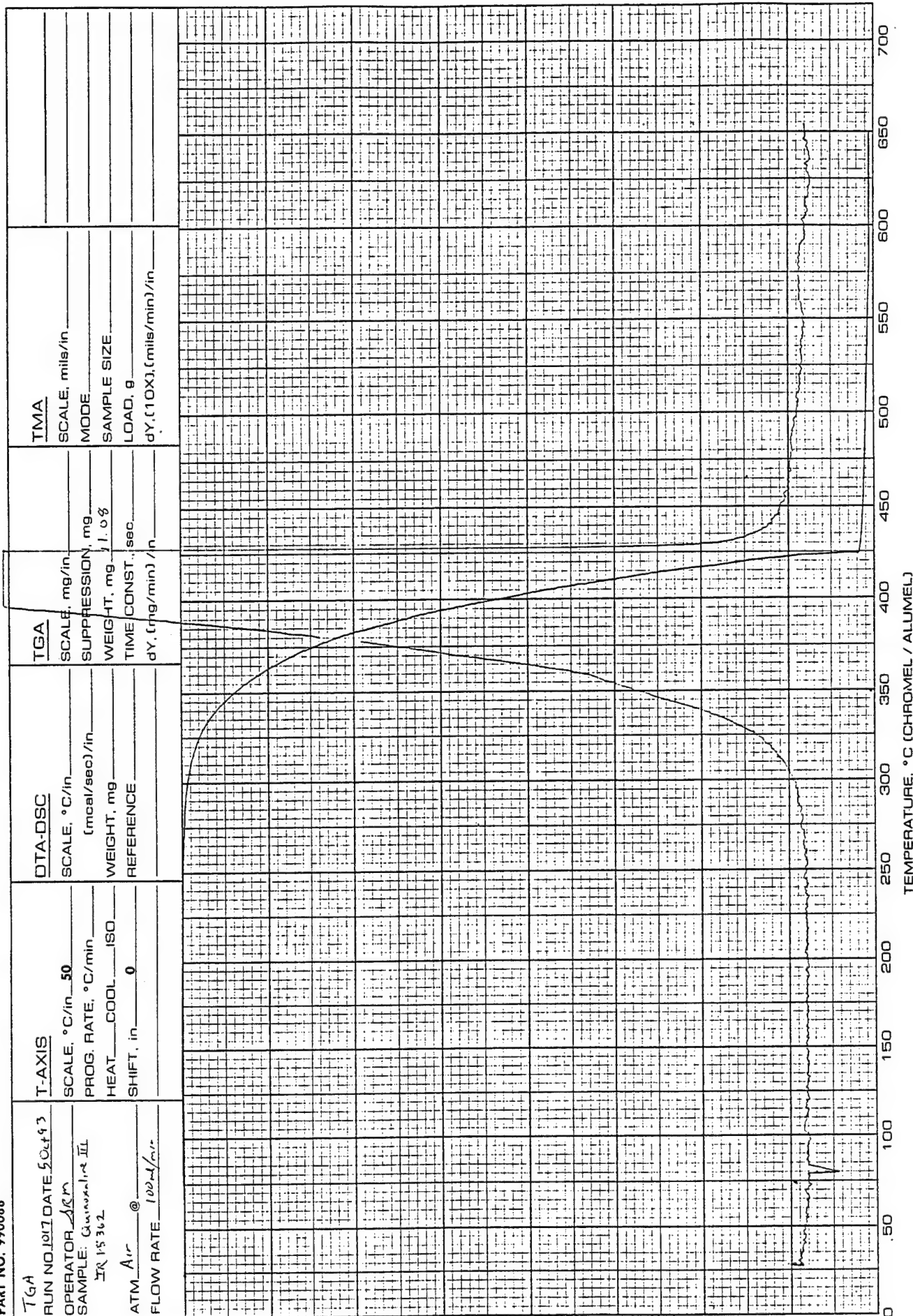


Figure 14. TGA scan of Quinoxaline III in air.

was not soluble in Freon-113, methylene chloride, benzene, and hexafluorobenzene. It was recrystallized from hexafluoroisopropanol/ethanol MP >200°C. Due to the compound involatility the purity (GC) and MS could not be determined. Anal. Calcd for $C_{42}H_{16}F_{30}N_4$: C, 43.99; H, 1.41; F, 49.71; MW, 1146.62. Found: C, 43.96; H, 1.27; F, 49.66; MW, not determined due to insolubility in conventional solvents. The IR is presented in Figure 15, DSC scan in Figure 16, and TGA scans, in nitrogen and air, in Figure 17 and 18, respectively.

Preparation of $C_3F_7OCF(CF_3)CF_2OCF(CF_3)C(O)CCl_2C_6H_5$

Using the conditions described for the preparation of $C_6H_5CCl_2C(O)CF_2CF_2(OCF_2CF_2)_5C(O)CCl_2C_6H_5$ the ester, $C_3F_7OCF(CF_3)CF_2OCF(CF_3)CO_2Et$ (4.5 g, 8.6 mmol) was added to the product of reaction of trichlorotoluene (2.2 g, 11.4 mmol) with n-butyllithium (5 mL, 2.5 M). The yield of $C_3F_7OCF(CF_3)CF_2OCF(CF_3)C(O)CCl_2C_6H_5$ was 73% (4.2 g). The MS is given in Table 18.

Preparation of $C_3F_7OCF(CF_3)CF_2OCF(CF_3)C(O)C(O)C_6H_5$

Using the conditions described for the preparation of $C_6H_5C(O)C(O)CF_2CF_2(OCF_2CF_2)_5C(O)C(O)C_6H_5$, $C_3F_7OCF(CF_3)CF_2OCF(CF_3)C(O)CCl_2C_6H_5$ (4.2 g, 6.6 mmol) was treated with silver nitrate (6.2 g, 36.5 mmol) in aqueous ethanol for 91 hours. This resulted in 78% yield (3.0 g) of $C_3F_7OCF(CF_3)CF_2OCF(CF_3)C(O)C(O)C_6H_5$ BP 49-50°C/0.001 mm Hg (purity 95%, GC). The IR is given in Figure 19 and the MS in Table 19.

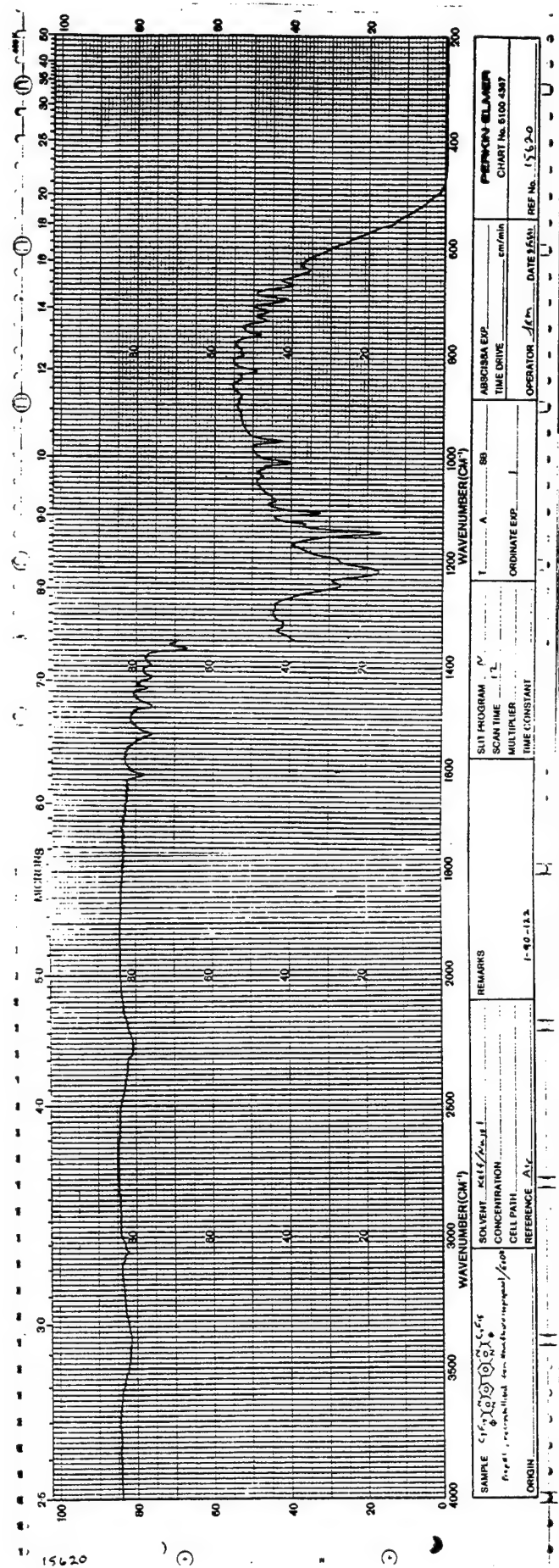


Figure 15. Infrared spectrum of Quinoxaline IV.

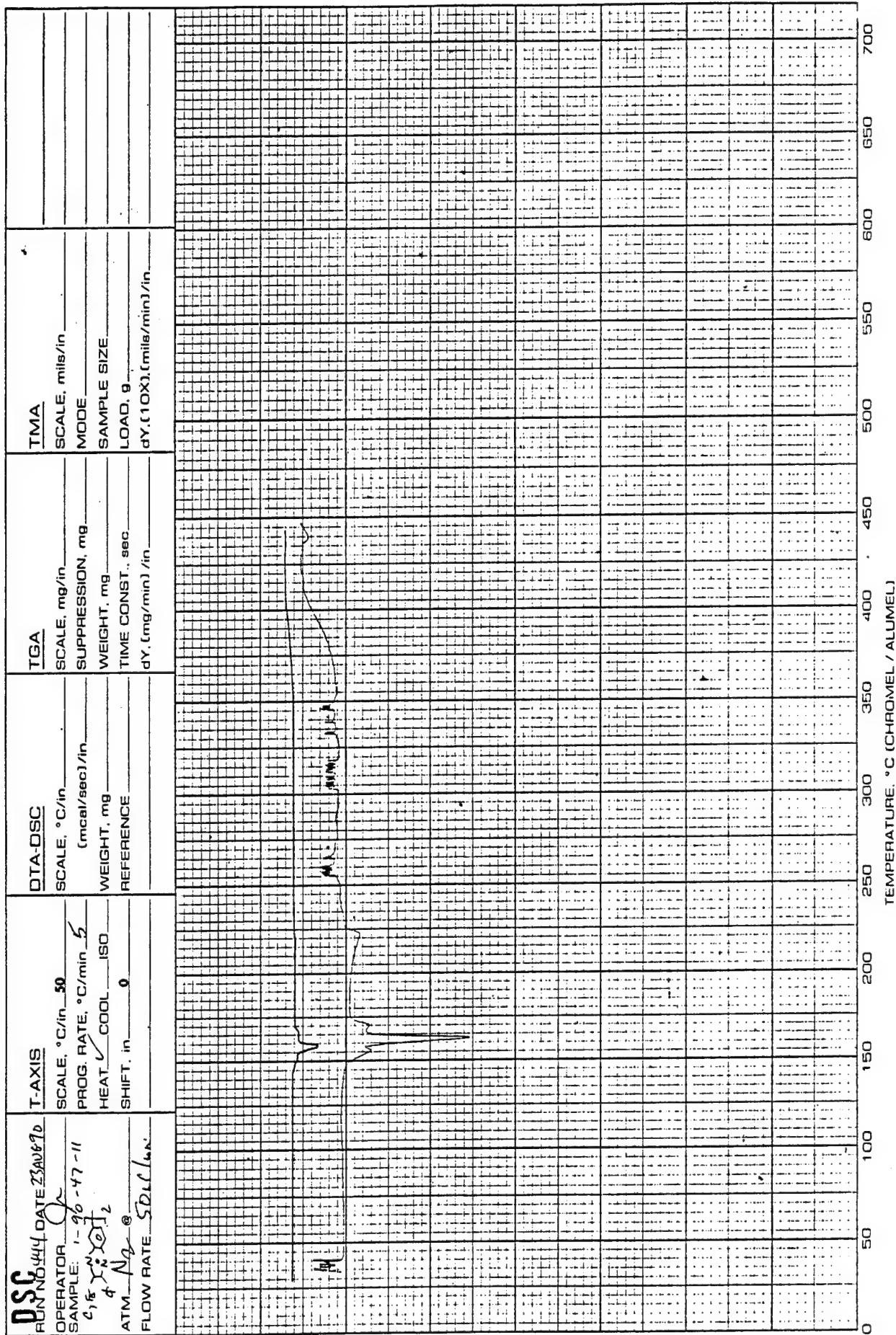


Figure 16. DSC scan of Quinoxaline IV.

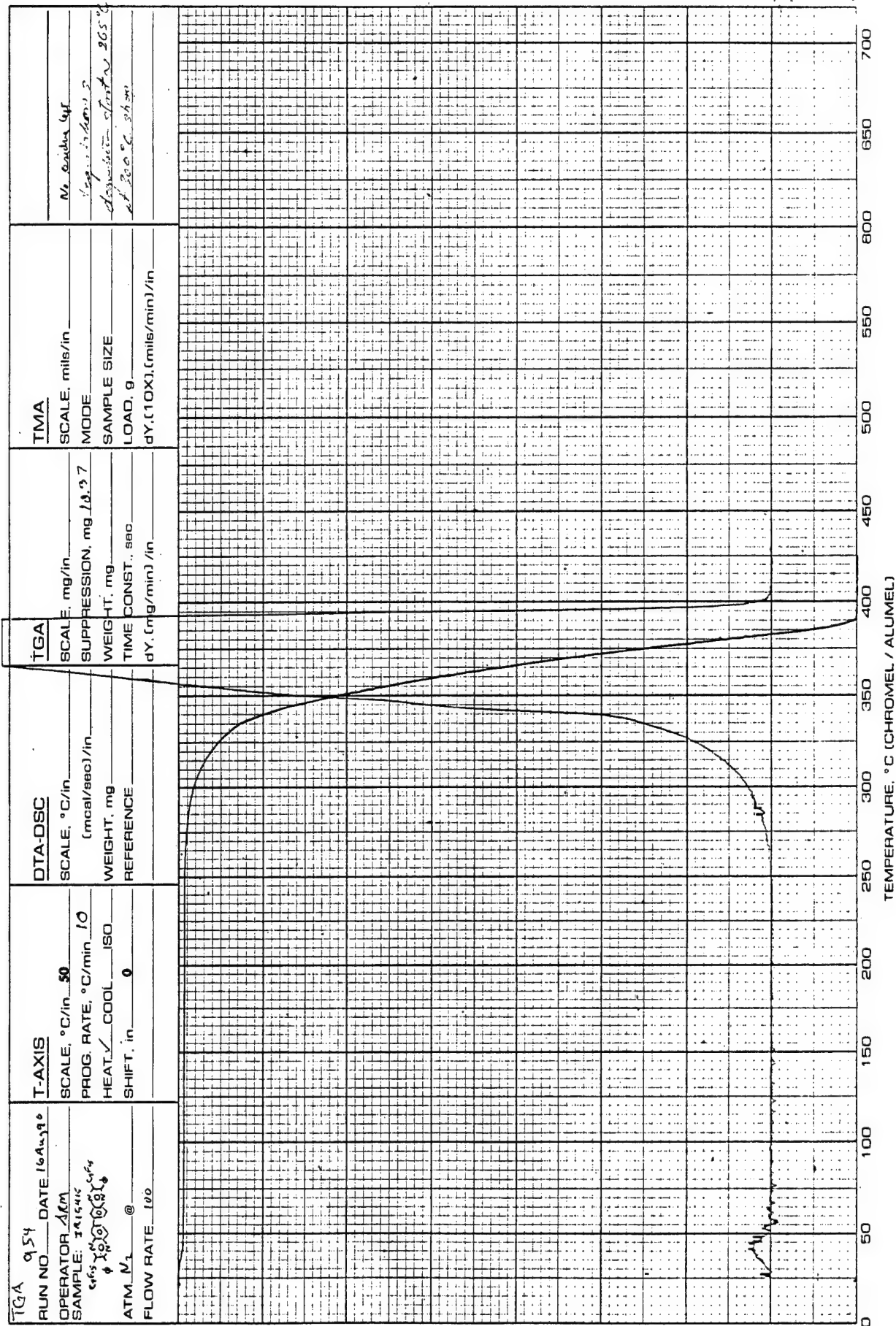


Figure 17. TGA scan of Quinoxaline IV in N₂.

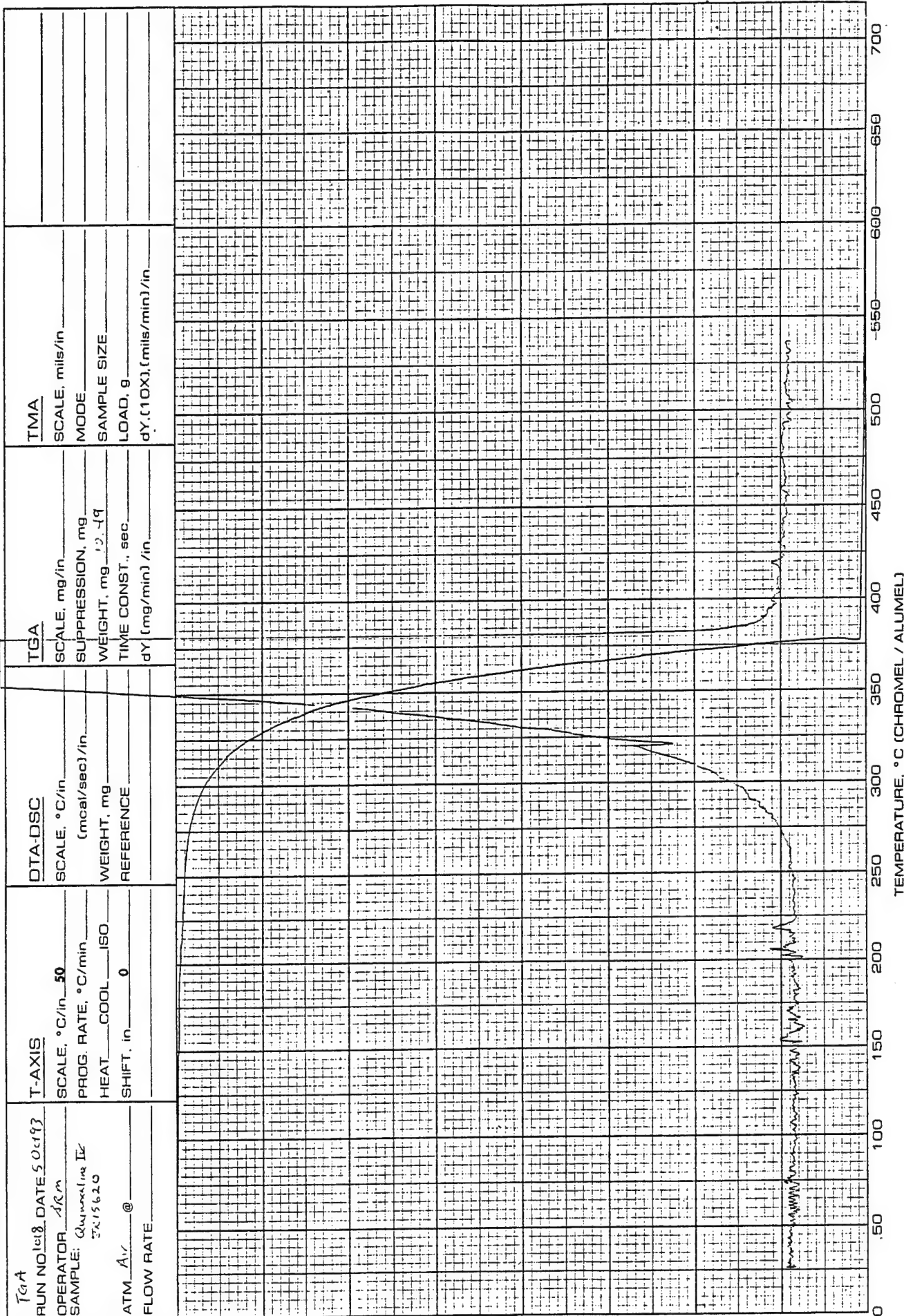
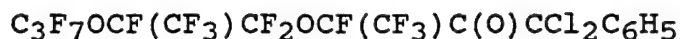


Figure 18. TGA scan of Quinoxaline IV in air.

TABLE 18

ION FRAGMENTS AND INTENSITIES RELATIVE TO BASE PEAK OF



m/e	%	m/e	%	m/e	%	m/e	%
18	9.0	78	7.6	131	10.9	171	15.6
28	20.9	81	8.0	133	6.6	173	10.3
31	18.0	85	9.3	135	6.3	177	6.4
35	6.8	86	6.1	136	7.1	185	7.5
36	19.1	87	10.6	143	16.0	189	9.3
37	6.9	88	7.1	145	7.5	217	6.2
38	15.6	89	54.7	147	8.7	223	10.7
39	17.5	90	12.8	150	20.0	224	6.1
47	17.6	97	15.5	152	53.4	225	6.1
50	23.9	99	9.8	153	13.8	251	12.0
51	12.8	100	25.0	154	25.9	253	6.6
61	7.5	101	8.3	155	8.7	259	7.0
62	18.8	107	6.7	158	7.5	261	6.0
63	27.6	108	6.6	159	100.0	335	7.7
66	7.9	119	22.9	160	39.6	353	6.2
69	70.6	120	7.7	161	89.0	519	8.4
70	8.0	123	16.8	162	27.1	521	6.3
73	9.5	124	48.1	163	47.5	603	21.5
74	6.1	125	18.5	164	11.2	604	10.5
75	9.0	126	22.1	169	56.3	605	13.4
77	8.7	127	14.8	170	8.0	619	6.2

Peaks having intensities lower than 6% of the base peak and lower than m/e 18 are not reported.

Significant Ions in Support of Structure and Composition

m/e

- 89 - $\text{C}_6\text{H}_5\text{C}^+$
 124 - $\text{C}_6\text{H}_5\text{CCl}^+$
 159 - $\text{C}_6\text{H}_5\text{CCl}_2$
 169 - C_3F_7^+

m/e

- 335 - $\text{C}_3\text{F}_7\text{OCF}(\text{CF}_3)\text{CF}_2$
 603 - $[\text{M}-\text{Cl}]^+$
 619 - $[\text{M}-\text{F}]^+$

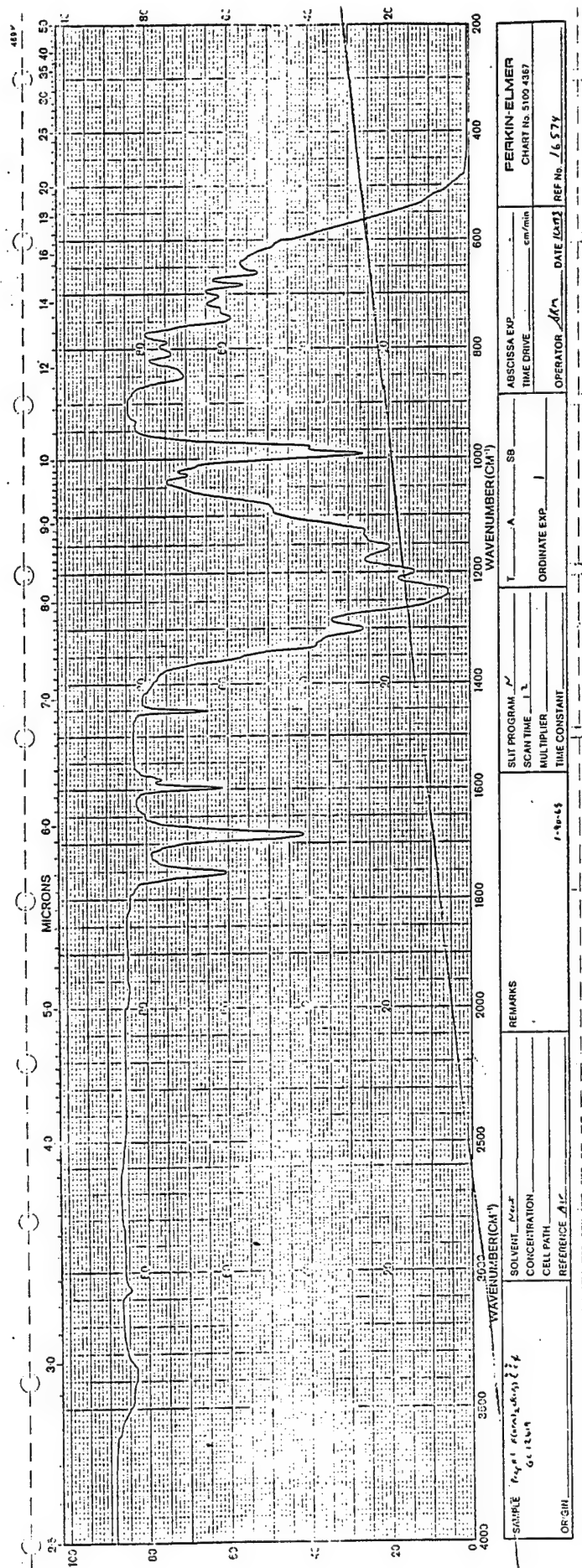


Figure 19. Infrared spectrum of $\text{C}_3\text{F}_7\text{OCF}(\text{CF}_3)\text{CF}_2\text{CF}(\text{CF}_3)\text{C}(\text{O})\text{C}(\text{O})\text{C}_6\text{H}_5$

TABLE 19

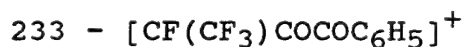
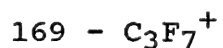
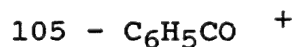
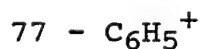
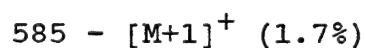
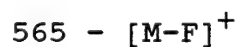
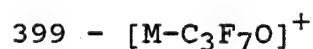
ION FRAGMENTS AND INTENSITIES RELATIVE TO BASE PEAK OF



m/e	%	m/e	%	m/e	%	m/e	%
12	4.0	56	18.5	95	4.7	133	4.4
20	6.5	57	7.7	96	15.6	147	7.0
26	7.8	58	3.2	97	14.4	150	23.9
27	12.9	62	6.8	100	26.2	151	6.2
28	32.0	63	6.3	101	4.8	169	34.0
29	3.6	66	8.9	104	14.5	170	5.0
31	19.3	69	53.2	105	100.0	177	13.6
34	4.8	70	8.7	106	53.6	189	8.4
37	4.6	73	4.2	107	13.1	205	4.8
38	6.4	74	15.1	108	3.0	233	15.7
39	10.3	75	14.8	117	6.9	234	5.1
44	3.1	76	21.7	119	17.2	299	4.9
47	15.1	77	70.3	122	5.3	335	5.7
49	5.1	78	46.5	123	6.4	371	6.1
50	39.7	79	6.2	124	10.9	399	5.7
51	58.3	81	8.3	127	5.5	465	7.7
52	16.7	89	9.6	128	5.3	565	8.2
53	4.0	93	3.6	131	11.7		

Peaks having intensities lower than 3% of the base peak and lower than m/e 12 are not reported.

Significant Ions in Support of Structure and Composition

m/em/e

Preparation of Quinoxaline V

1,2-Phenylenediamine (0.46 g, 4.3 mmol) in m-cresol (10 mL) was added to a stirred solution of $\text{C}_3\text{F}_7\text{OCF}(\text{CF}_3)\text{CF}_2\text{OCF}(\text{CF}_3)\text{C}(\text{O})\text{C}(\text{O})\text{C}_6\text{H}_5$ (2.0 g, 3.4 mmol) in m-cresol (10 mL). The reaction mixture was stirred for 24 hours at room temperature. The m-cresol was removed via vacuum distillation leaving a viscous liquid (2.2 g). The crude material was purified by column chromatography using silica gel (2.5 cm x 29 cm) and ether/hexanes (1/3) as eluant. The product (2.0 g, 91% yield) consisted of 94.5 percent of the HFPO trimer-substituted quinoxaline and 1.1% of the HFPO tetramer-substituted quinoxaline for a total of 95.6% HFPO-substituted quinoxalines. Overall yield starting from the methyl ester was 55%. Further purification by sublimation of 1.20 g onto a cold finger followed by passing the residue through silica gel (1 cm x 17 cm) and elution with ether/hexanes (1/10) gave 0.62 g of 99.9% HFPO-substituted quinoxaline (98.1% trimer-, 1.8% tetramer-substituted; GC data). Anal. Calcd for $\text{C}_{22}\text{H}_9\text{F}_{17}\text{N}_2\text{O}_2$: C, 40.26; H, 1.38; F, 49.21; MW, 656.33. Found: C, 40.38; H, 1.41; F, 50.56; MW, 680. The MS is presented in Table 20, the IR in Figure 20, DSC scan in Figure 21, and TGA scans, in nitrogen and air, in Figures 22 and 23, respectively.

Preparation of Quinoxaline VI

The tetraketone, $\text{C}_6\text{H}_5\text{C}(\text{O})\text{C}(\text{O})\text{CF}_2\text{CF}_2(\text{OCF}_2\text{CF}_2)_5\text{C}(\text{O})\text{C}(\text{O})\text{C}_6\text{H}_5$, (0.87 g, 0.92 mmol) in hexafluoroisopropanol (5 mL) was added dropwise to 3,3'-

TABLE 20

ION FRAGMENTS AND INTENSITIES RELATIVE TO BASE PEAK OF
QUINOXALINE V

m/e	%	m/e	%	m/e	%	m/e	%
27	7.2	89	8.6	142	15.2	223	8.7
31	14.0	95	6.0	143	5.4	224	9.4
39	7.9	97	7.0	147	5.7	234	5.4
47	15.4	100	20.7	150	12.9	235	28.8
50	32.3	101	9.2	151	13.6	236	23.9
51	25.3	102	36.1	152	14.9	237	6.7
52	7.9	103	22.9	153	7.4	254	7.1
62	5.6	104	14.7	169	26.6	285	14.7
63	7.8	107	5.1	177	16.9	286	7.2
64	7.4	117	24.0	178	19.8	304	21.9
66	7.3	118	16.9	179	27.8	305	29.8
69	54.1	119	19.1	180	11.2	306	12.4
74	5.8	126	9.8	203	7.0	471	10.2
75	19.1	127	12.6	204	13.1	637	9.9
76	29.1	128	7.5	<u>205</u>	<u>100.0</u>	656	83.6M ⁺
77	40.2	129	5.7	206	55.9	657	29.6
78	10.6	131	8.0	207	14.3	658	12.0
81	7.0	133	5.1	208	5.6		

Peaks having intensities lower than 5% of the base peak and lower than m/e 27 are not reported.

Significant Ions in Support of Structure and Composition

<u>m/e</u>	<u>m/e</u>
77 - C ₆ H ₅ ⁺	305 - [M-C ₃ F ₇ OCF(CF ₃)CF ₂ O] ⁺
169 - C ₃ F ₇ ⁺	471 - [M-C ₃ F ₇ O] ⁺
179 - [M-C ₃ F ₇ OCF(CF ₃)CF ₂ OCF(CF ₃)CN] ⁺	637 - [M-F] ⁺
205 - [M-C ₃ F ₇ OCF(CF ₃)CF ₂ OCF(CF ₃)] ⁺	

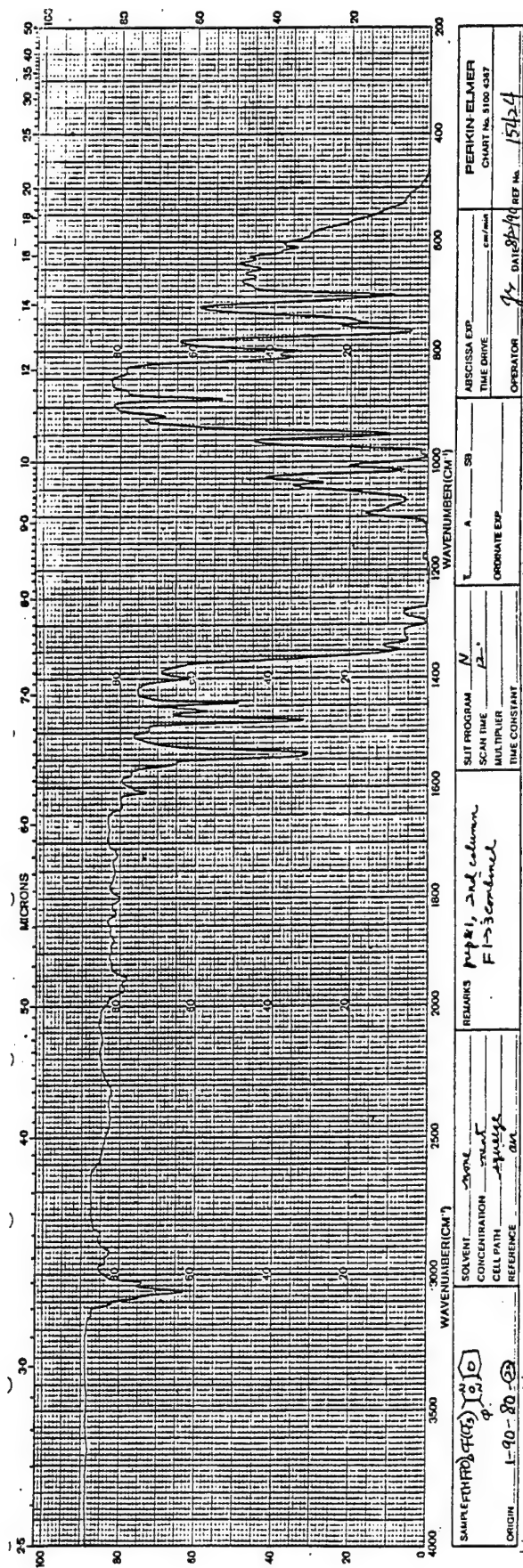


Figure 20. Infrared spectrum of Quinoxaline V.

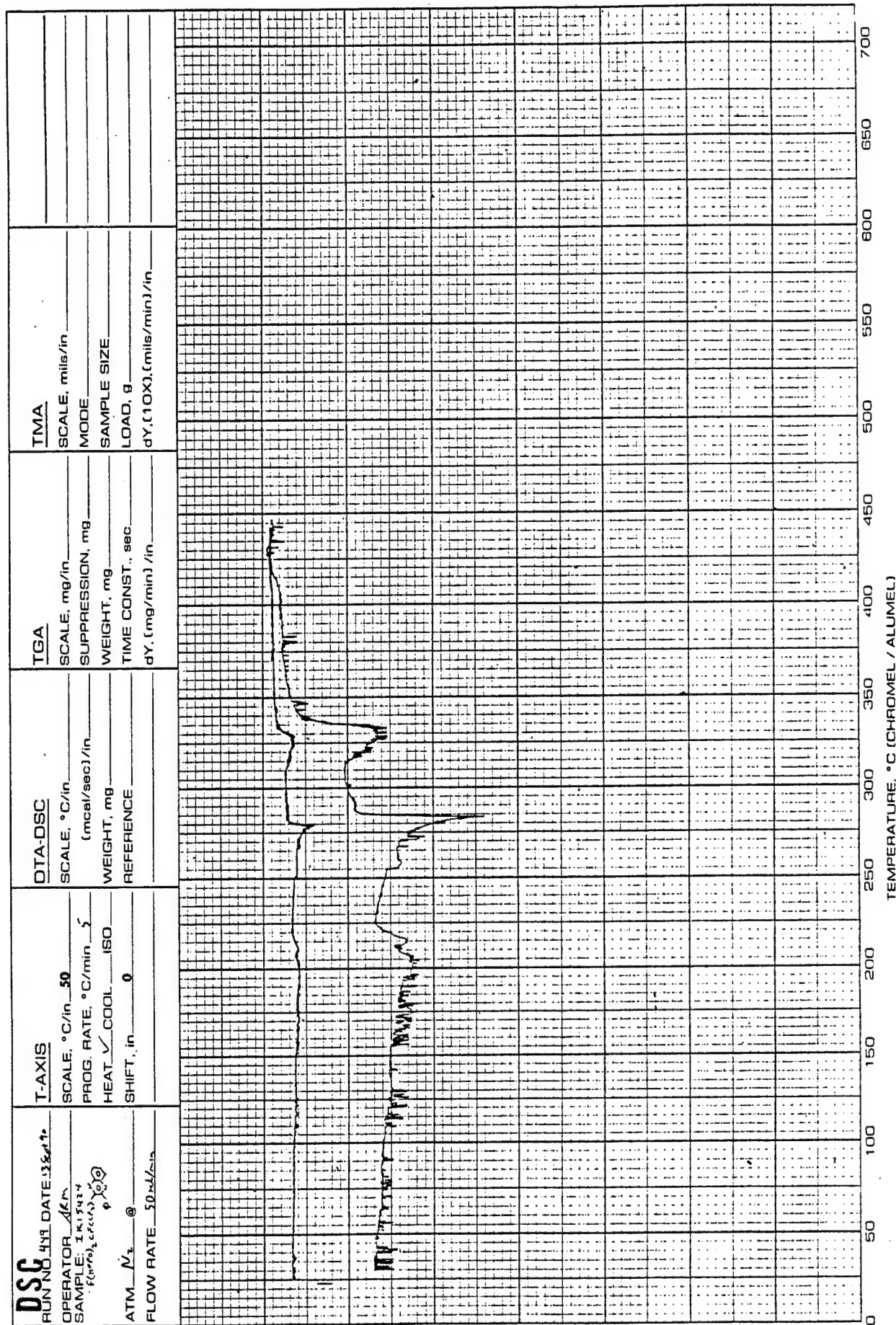
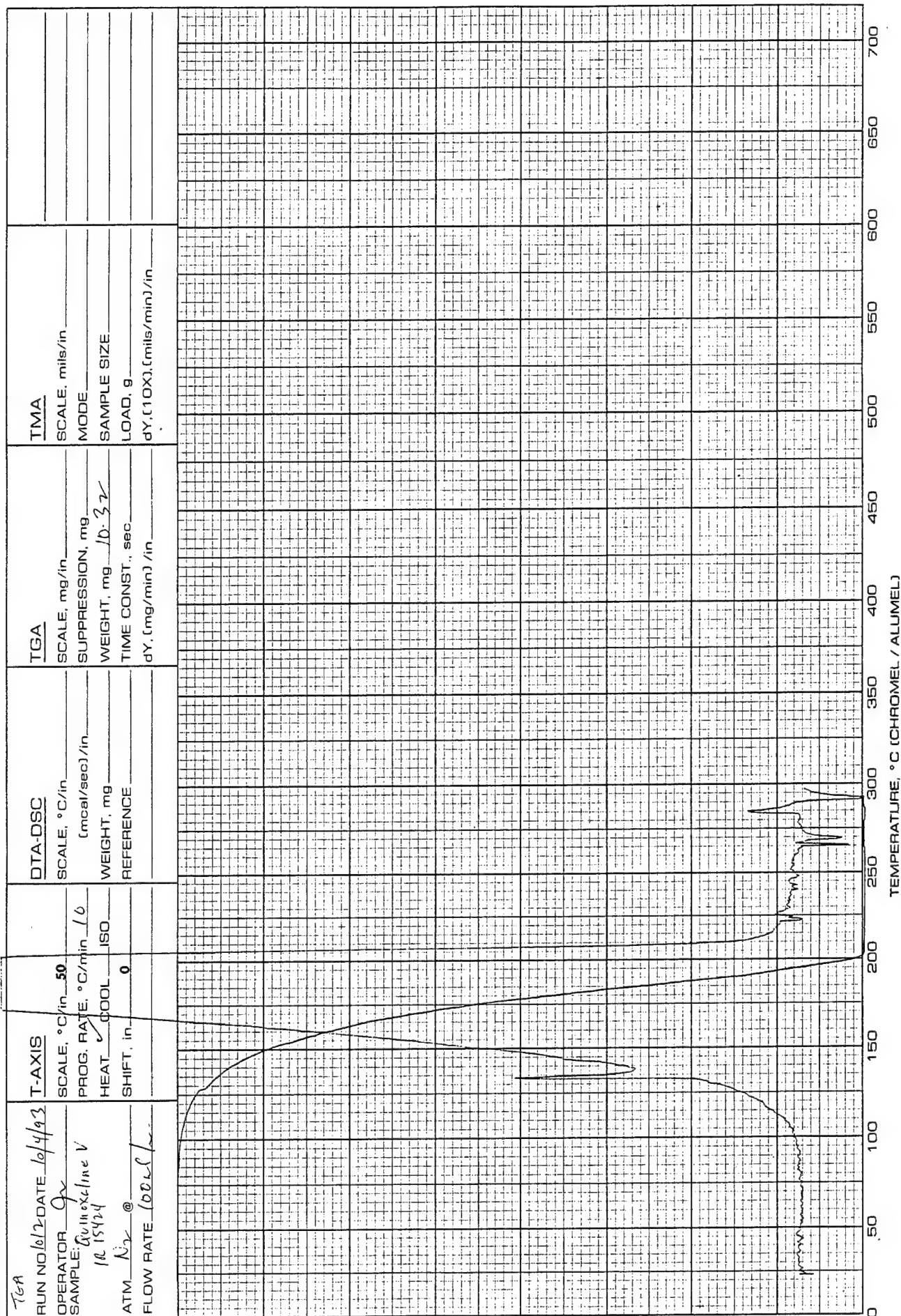


Figure 21. DSC scan of quinoxaline V.

Figure 22. TGA scan of Quinoxaline V in N₂.

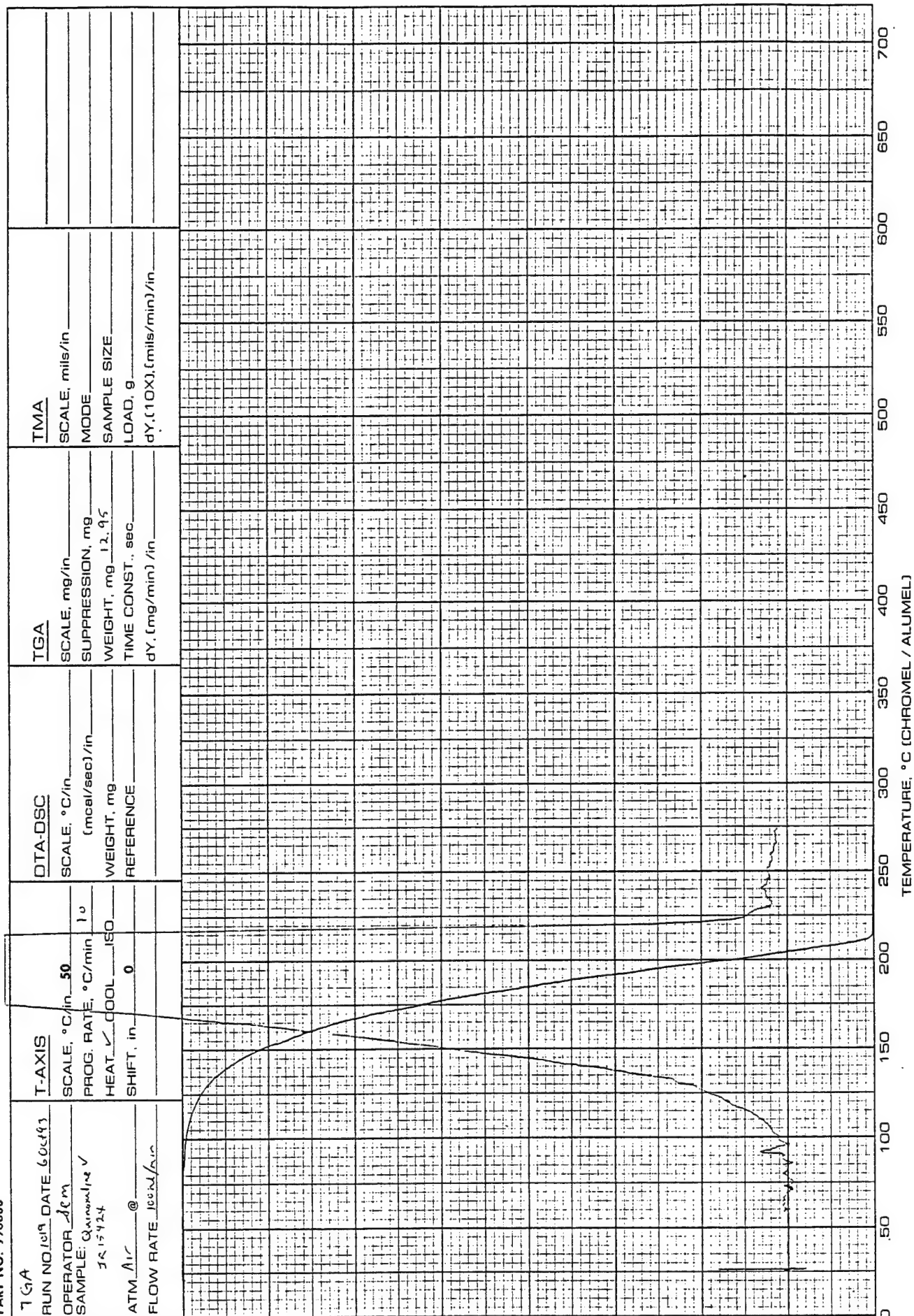


Figure 23. TGA scan of Quinoxaline V in air.

diaminobenzidine (0.26 g, 1.21 mmol) in hexafluoroisopropanol (5 mL) solution over a period of 15 minutes. Both reagents prior to mixing and following the addition were sampled for UV analysis. The specific absorptions are listed in Table 21. Based on the absence of the 312 nm absorption at that stage, it can be deduced that the 3,3'-diaminobenzidine had completely reacted (possibly only at one end). The appearance of absorption at 269 nm confirmed the formation of quinoxaline. The absorbance of 0.558 (1/5000 dilution with ethanol) indicated a concentration of 4×10^{-2} M ($\epsilon = 6.70 \times 10^4$) of quinoxaline with respect to Quinoxaline IV standard. After stirring for 18 hours at room temperature, the reaction mixture was again sampled (diluted 1/8000 in hexafluoroisopropanol). The absorbance at 268 nm was 0.310. After stirring an additional 5 hours, the absorption was essentially unchanged (absorbance 0.325, 1/8000 dilution with hexafluoroisopropanol). Since a 20% excess of 3,3'-diaminobenzidine was used, the polymer would be expected to be amine terminated. To form the inactive quinoxaline end-groups, benzil (0.17 g, 0.81 mmol) in hexafluoroisopropanol (1 mL) was added. After an additional 16 hours, the reaction mixture was concentrated to half its volume, and dripped into vigorously stirred methanol (50 mL) to give 1.08 g of a pale yellow solid. The process was repeated by dissolving the solid in hexafluoroisopropanol (3.5 mL) and dripping into methanol (35 mL). This resulted in a pale yellow solid (0.67 g, 55% yield),

TABLE 21

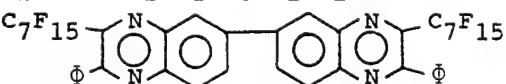
SUMMARY OF ULTRAVIOLET SPECTROSCOPIC ANALYSIS OF AMINES, KETONES, AND QUINOXALINES

UV No.	Components	Concentration		Solvent ^a EtOH/HFIP	UV Data		
		mg/l	M(x10 ⁻⁵)		λ_{\max} nm	ABS	$\epsilon \times 10^{4b}$
701	3,3'-diaminobenzidine	5.3	2.47	100/0	223	>1	
					281	0.352	1.42
					312	0.357	1.45
702	$\Phi C(O)C(O)R_f C(O)C(O)\Phi^c$	22.6	2.39	100/0	204	0.550	2.30
					255	0.553	2.31
704	quinoxaline IV ^d	4.0	0.35	0/100	210	0.417	11.8
					270	0.470	13.4
					358	0.188	5.34
705	3,3'-diaminobenzidine $\Phi C(O)C(O)R_f C(O)C(O)\Phi$	2.6	1.24	100/0	206	0.570	4.75
		11.3	1.20		214	0.565	
					220	0.550	
					250	0.453	3.78
					280	0.216	1.74
					312	0.188	1.52
706	3,3'-diaminobenzidine $\Phi C(O)C(O)R_f C(O)C(O)\Phi$ quinoxaline IV	1.3	0.62	50/50	206	>1	
		5.6	0.60		227	0.277	
		2.0	0.18		240	0.273	
					243	0.304	
					249	0.350	
					255	0.395	
					260	0.400	
					264	0.375	
707	quinoxaline IV	2.0	0.18	50/50	206	>1	
					229	0.148	8.22
					240	0.165	9.17
					244	0.185	10.3
					249	0.216	12.0
					255	0.246	13.7
					261	0.252	14.0
					268	0.236	13.1
708	3,3'-diaminobenzidine quinoxaline IV	10.6	4.94	100/0	<244	>1	
		4.0	0.35		277	0.737	1.49
					313	0.643	1.30
709	3,3'-diaminobenzidine quinoxaline IV	2.6	1.24	50/50	206	>1	
		10.1	0.88		226	0.670	
					243	0.543	
					249	0.580	
					255	0.645	
					262	0.730	
					269	0.783	

(a) EtOH = ethanol, HFIP = hexafluoroisopropanol; in all the measurements, with the exception of quinoxaline IV (UV 704), EtOH was used as the reference.

(b) ϵ = molar absorptivity.

(c) $R_f = -(CF_2CF_2O)_5CF_2CF_2-$

(d) 

in this case hexafluoroisopropanol was used as reference.

MP 87-89°C; MW, 4200. The IR is given in Figure 24 and the TGA scans, in nitrogen and air, in Figures 25 and 26, respectively.

Preparation of $[\text{C}_6\text{H}_5\text{CCl}_2\text{C}(\text{O})\text{C}_3\text{F}_6\text{OC}_4\text{F}_8]_2\text{O}$

Using the conditions described for the preparation of $\text{C}_6\text{H}_5\text{CCl}_2\text{C}(\text{O})\text{CF}_2\text{CF}_2(\text{OCF}_2\text{CF}_2)_5\text{C}(\text{O})\text{CCl}_2\text{C}_6\text{H}_5$, the ester, $[\text{MeO}_2\text{CC}_3\text{F}_6\text{OC}_4\text{F}_8]_2\text{O}$ (12.9 g, 14.9 mmol; MS given in Table 22, IR in Figure 27) was added to the product of reaction of trichlorotoluene (6.7 g, 3.43 mmol) with n-butyllithium (15 mL, 2.5 M, 37.5 mmol). The yield of $[\text{C}_6\text{H}_5\text{CCl}_2\text{C}(\text{O})\text{C}_3\text{F}_6\text{OC}_4\text{F}_8]_2\text{O}$ was 65% (10.8 g). The MS is given in Table 23.

Preparation of $[\text{C}_6\text{H}_5\text{C}(\text{O})\text{C}(\text{O})\text{C}_3\text{F}_6\text{OC}_4\text{F}_8]_2\text{O}$

Using conditions described for preparation of $\text{C}_6\text{H}_5\text{C}(\text{O})\text{C}(\text{O})\text{CF}_2\text{CF}_2(\text{OCF}_2\text{CF}_2)_5\text{C}(\text{O})\text{C}(\text{O})\text{C}_6\text{H}_5$, $[\text{C}_6\text{H}_5\text{CCl}_2\text{C}(\text{O})\text{C}_3\text{F}_6\text{OC}_4\text{F}_8]_2\text{O}$ (10.8 g, 9.6 mmol) was treated with silver nitrate (13.2 g, 77.7 mmol) in aqueous ethanol for 41 hours. This resulted in 61% yield (5.9 g) of $[\text{C}_6\text{H}_5\text{C}(\text{O})\text{C}(\text{O})\text{C}_3\text{F}_6\text{OC}_4\text{F}_8]_2\text{O}$, BP 163-165°C/0.001 mm Hg (purity 93%, GC). The IR is given in Figure 28 and the MS in Table 24.

Preparation of Quinoxaline VII

Under nitrogen atmosphere to $[\text{C}_6\text{H}_5\text{C}(\text{O})\text{C}(\text{O})\text{C}_3\text{F}_6\text{OC}_4\text{F}_8]_2\text{O}$ (1.84 g, 1.81 mmol) in m-cresol (15 mL) was added 1,2-phenylenediamine (0.48 g, 4.45 mmol) in m-cresol (10 mL). The resultant light brown solution was allowed to stir at room temperature for 22 hours. After reaction, m-cresol (12 mL) was distilled in vacuo at 60-70°C. To the residue was added methanol (10 mL) and on cooling the solution in ice-water for a few

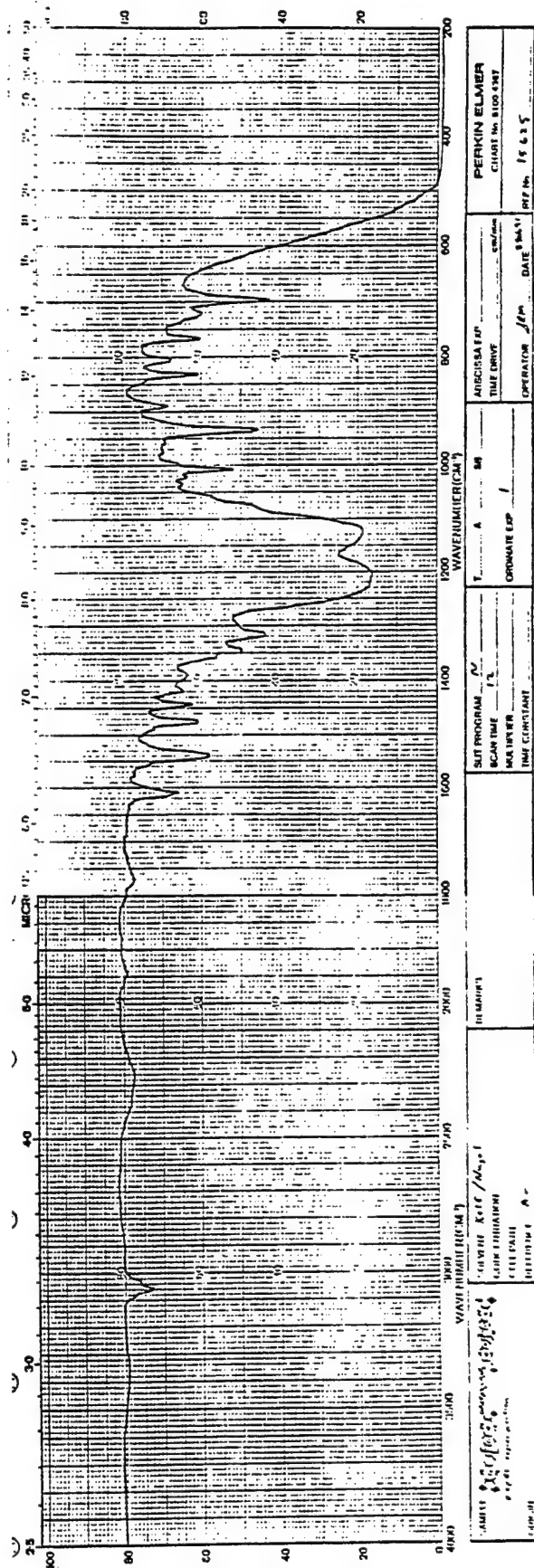


Figure 24. Infrared spectrum of Quinoxaline VI.

PART NO. 990088

RUN NO. <u>1613</u> DATE <u>10/6/97</u> OPERATOR <u>JP</u> SAMPLE <u>Quinoxaline VI</u> <u>1st run</u> ATM <u>N₂</u> @ <u>100 mL</u> FLOW RATE <u>100 mL</u>	T-AXIS SCALE, °C/in <u>50</u> PROG. RATE, °C/min <u>10</u> HEAT <input checked="" type="checkbox"/> COOL <input type="checkbox"/> ISO SHIFT, in <u>0</u>	DTA-DSC SCALE, °C/in <u>10</u> (mcal/sec)/in WEIGHT, mg REFERENCE	TGA SCALE, mg/in SUPPRESSION, mg WEIGHT, mg TIME CONST., sec dY, (mg/min) /in	TMA SCALE, mils/in MODE SAMPLE SIZE LOAD, g dY, (10X), (mils/min) /in
--	--	---	--	--

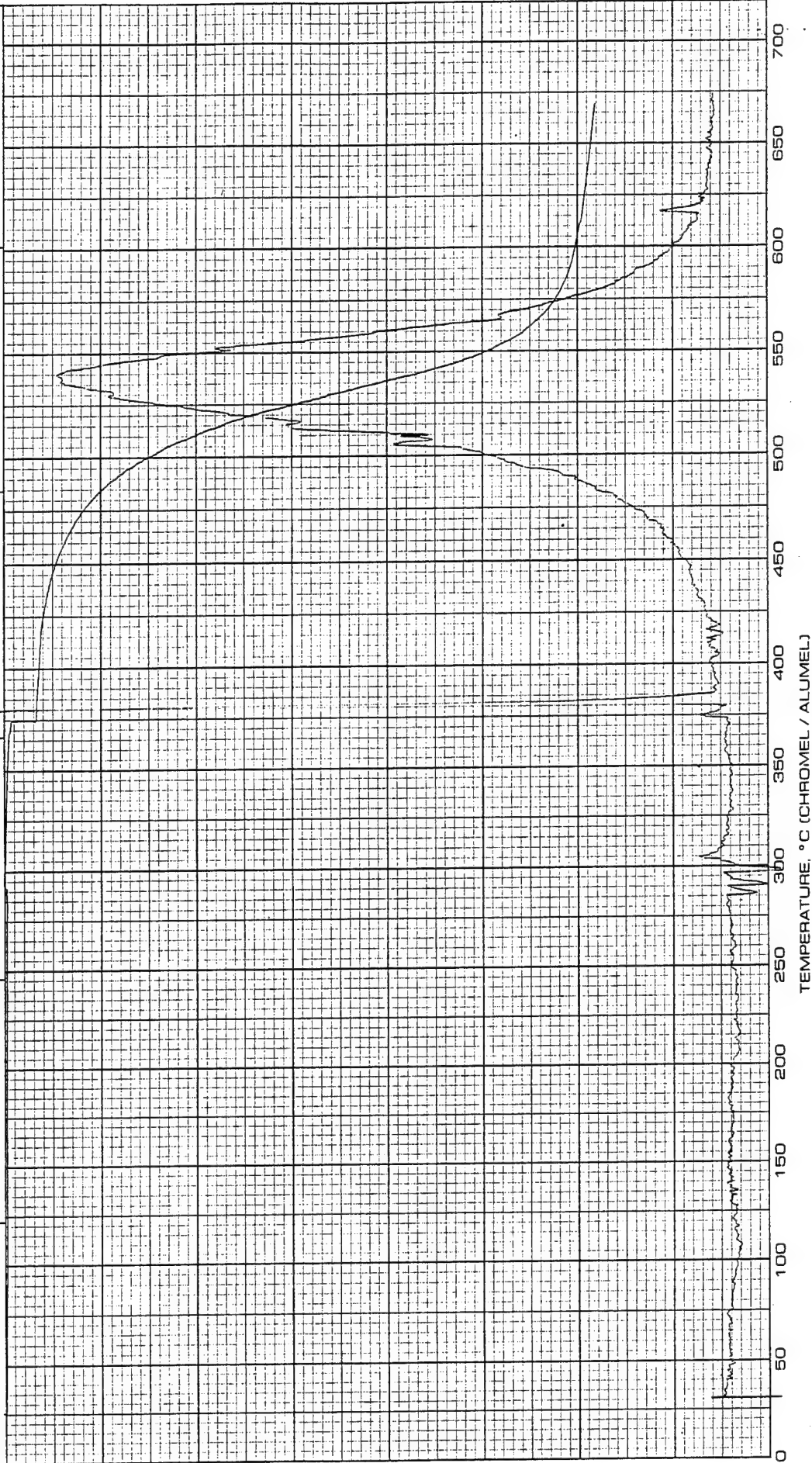


Figure 25. TGA scan of Quinoxaline VI in N₂.

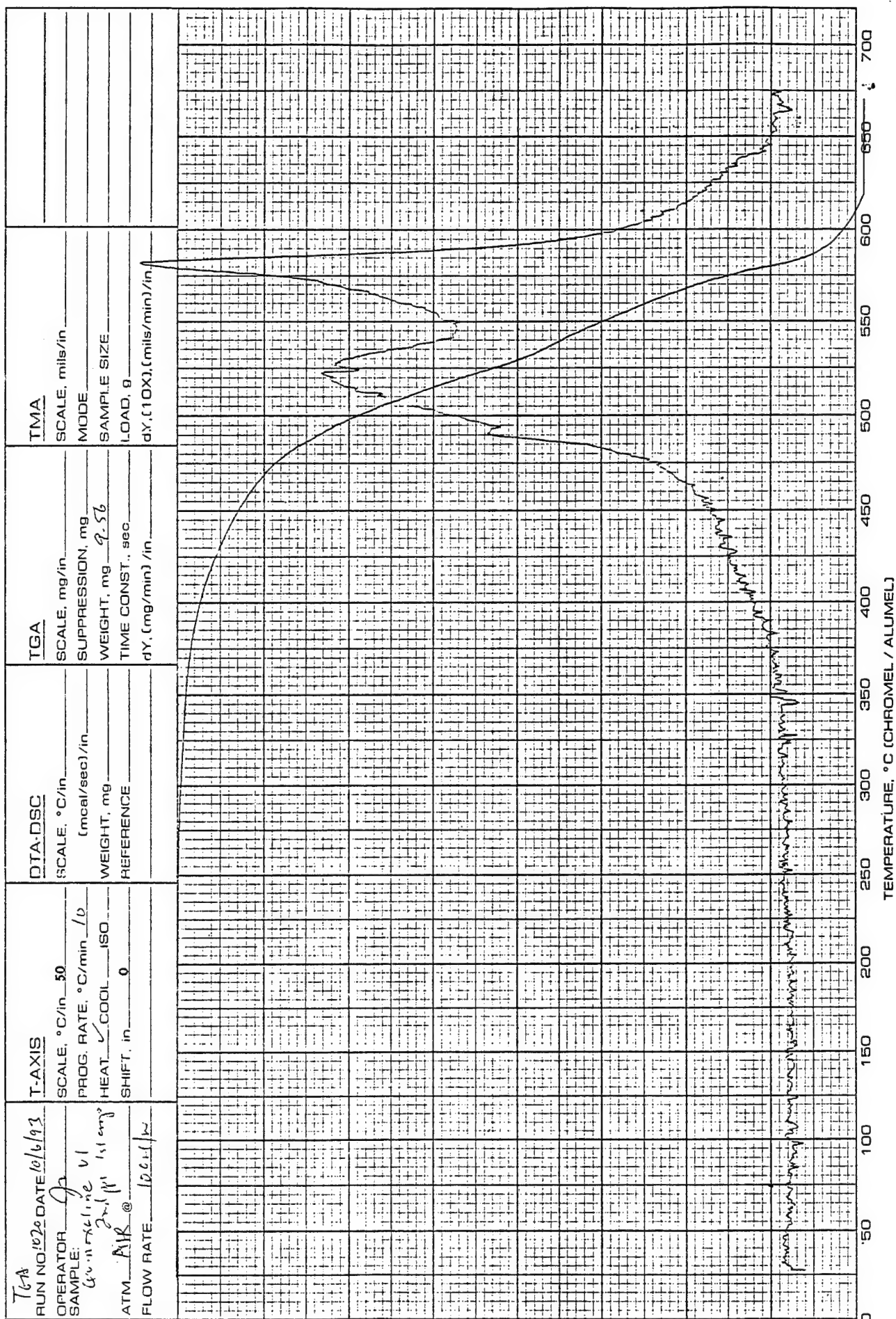
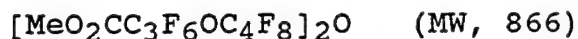


Figure 26. TGA scan of Quinoxaline VI in air.

TABLE 22

ION FRAGMENTS AND INTENSITIES RELATIVE TO BASE PEAK OF



m/e	%	m/e	%	m/e	%	m/e	%
14	4.0	61	3.8	128	3.1	219	3.4
15	75.4	62	2.2	131	33.4	275	4.7
16	7.4	64	3.3	132	2.8	425	17.0
20	7.0	65	21.3	147	31.5	557	4.1
28	19.6	66	9.7	150	40.1	607	4.1
29	17.5	69	36.4	151	12.4	657	11.1
30	12.6	70	1.7	157	3.3	789	6.1
31	29.5	78	5.4	158	5.7	801	9.7
32	2.3	81	32.8	159	6.1	803	3.2
33	7.1	82	3.2	162	4.1	807	17.1
34	3.5	93	6.2	169	26.6	808	3.8
43	6.9	97	4.0	179	3.7	819	2.7
44	14.4	100	52.6	181	55.7	822	74.1
45	13.9	101	7.8	182	7.7	823	26.7
47	15.5	109	11.7	197	8.0	824	7.3
50	14.2	112	5.2	208	2.8	847	21.3
51	6.4	113	6.6	209	<u>100.0</u>	848	6.6
59	86.5	119	66.9	210	26.0	881	3.6
60	14.4	120	8.6	211	4.4		

Peaks having intensities lower than 2% of the base peak and lower than m/e 14 are not reported.

Significant Ions in Support of Structure and Composition

m/e

15 - Me^+
 31 - MeO^+
 59 - CO_2Me^+
 209 - $\text{C}_3\text{F}_6\text{CO}_2\text{Me}^+$
 425 - $\text{C}_4\text{F}_8\text{OC}_3\text{F}_6\text{CO}_2\text{Me}^+$

m/e

657 - $[\text{M}-\text{C}_3\text{F}_6\text{CO}_2\text{Me}]^+$
 807 - $[\text{M}-\text{CO}_2\text{Me}]^+$
 822 - $[\text{M}-\text{CO}_2]^+$
 847 - $[\text{M}-\text{F}]^+$
 881 - $[\text{M}+\text{Me}]^+$

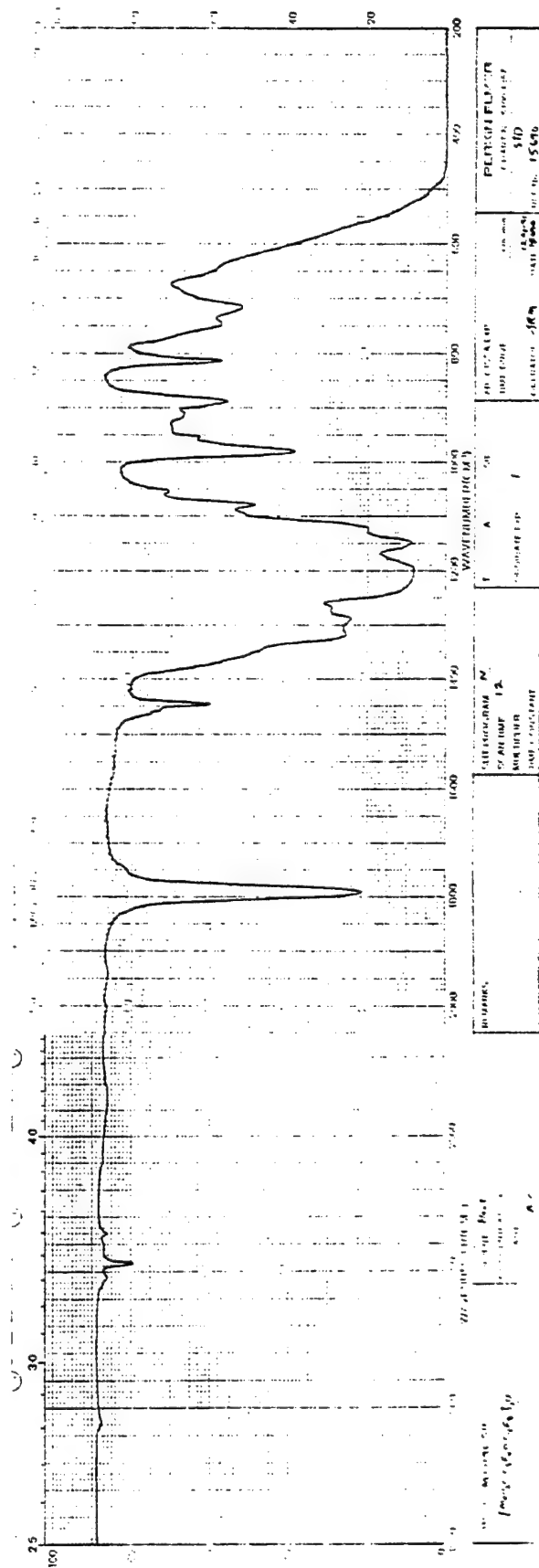
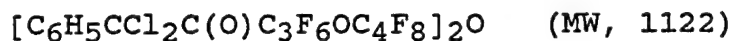


Figure 27. Infrared spectrum of $[\text{MeO}_2\text{CC}_3\text{F}_6\text{OC}_4\text{F}_8]_2\text{O}$.

TABLE 23

ION FRAGMENTS AND INTENSITIES RELATIVE TO BASE PEAK OF



m/e	%	m/e	%	m/e	%	m/e	%
31	10.5	85	8.8	150	11.5	203	12.9
35	9.1	87	7.1	151	5.2	219	4.1
36	26.1	89	33.6	152	23.0	239	6.0
37	5.4	90	9.0	154	10.1	273	4.6
38	14.0	97	4.0	159	<u>100.0</u>	301	13.5
39	12.5	99	5.2	160	28.0	302	7.9
47	10.7	100	25.4	161	82.8	303	8.3
50	12.3	118	4.0	162	24.5	337	21.5
51	7.6	119	9.9	163	26.6	338	4.4
62	11.4	123	9.7	164	5.2	339	16.0
63	18.7	124	28.6	167	6.8	1015	4.9
66	6.0	125	21.1	169	11.8	1051	23.4
69	20.9	126	13.8	174	8.8	1052	8.9
73	5.7	127	11.5	176	4.1	1053	15.6
75	4.3	131	12.3	185	8.7	1054	5.5
77	4.6	139	6.7	201	29.0		
81	6.1	143	9.0	202	4.7		

Peaks having intensities lower than 4% of the base peak and lower than m/e 31 are not reported.

Significant Ions in Support of Structure and Composition

m/e

89 - $\text{C}_6\text{H}_5\text{C}^+$
 124 - $\text{C}_6\text{H}_5\text{CCl}^+$
 159 - $\text{C}_6\text{H}_5\text{CCl}_2^+$

m/e

337 - $\text{C}_6\text{H}_5\text{CCl}_2\text{C}(\text{O})\text{C}_3\text{F}_6^+$
 1051 - $[\text{M}-\text{Cl}-\text{HCl}]^+$

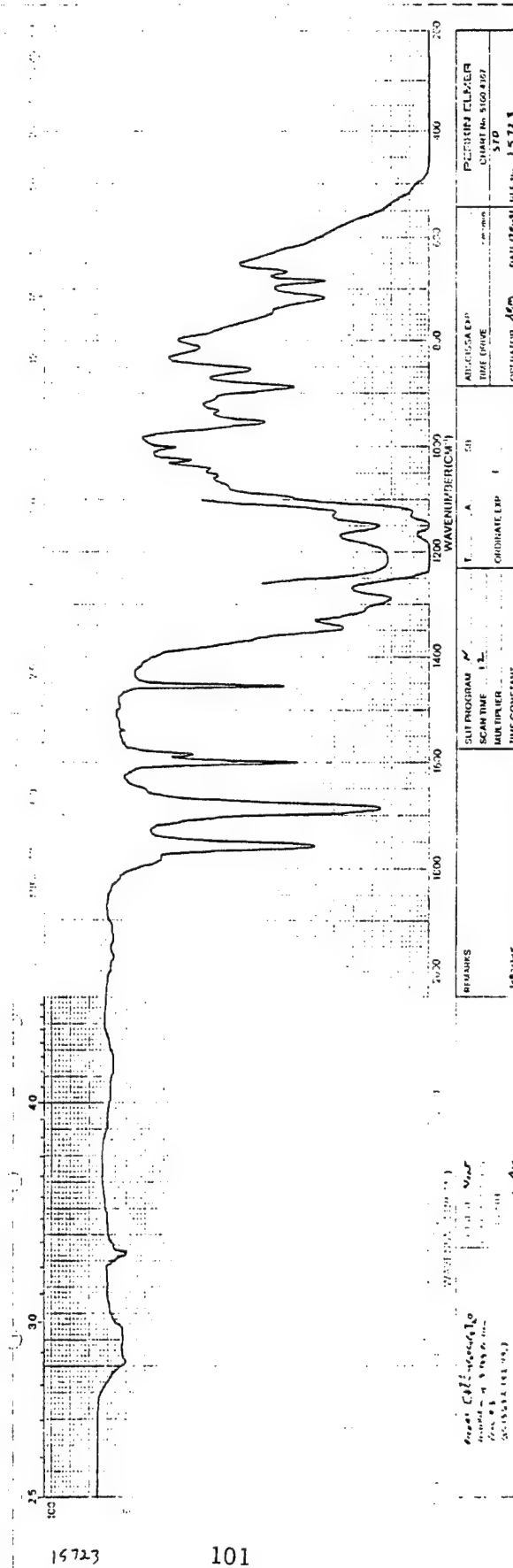
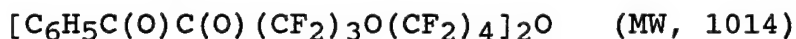


Figure 28. Infrared spectrum of $[\text{C}_6\text{H}_5\text{C}(\text{O})\text{C}(\text{O})(\text{CF}_2)_3\text{O}(\text{CF}_2)_4]_2\text{O}$.

TABLE 24

ION FRAGMENTS AND INTENSITIES RELATIVE TO BASE PEAK OF



m/e	%	m/e	%	m/e	%	m/e	%
20	5.2	69	15.0	105	100.0	255	29.2
27	6.1	74	5.7	106	32.7	256	6.1
28	19.1	75	6.7	107	5.5	283	24.2
31	9.9	76	11.9	119	5.2	284	5.4
39	4.7	77	63.7	123	7.6	349	5.6
47	8.7	78	16.6	124	8.0	499	7.1
50	19.5	81	4.3	127	3.3	565	3.0
51	38.7	89	3.1	131	11.6	715	1.6
52	4.5	96	10.6	150	13.3	881	3.2
57	3.3	100	22.9	169	7.9	975	5.4
66	3.6	104	5.0	227	5.3	995	5.3

Peaks having intensities lower than 3% of the base peak and lower than m/e 15 are not reported except for m/e 715.

Significant Ions in Support of Structure and Composition

<u>m/e</u>	<u>m/e</u>
28 - CO^+	499 - $\text{C}_6\text{H}_5\text{COCO}(\text{CF}_2)_3\text{O}(\text{CF}_2)_4^+$
77 - C_6H_5^+	715 - $[\text{M}-\text{C}_6\text{H}_5\text{COCO}(\text{CF}_2)_3\text{O}]^+$
105 - $\text{C}_6\text{H}_5\text{CO}^+$	881 - $[\text{M}-\text{C}_6\text{H}_5\text{COCO}]^+$
283 - $\text{C}_6\text{H}_5\text{COCO}(\text{CF}_2)_3^+$	995 - $[\text{M}-\text{F}]^+$

minutes, a solid was formed which was filtered and washed 8 times with a total of 65 mL of methanol. Drying in vacuum at 40°C for 3 hours gave 1.14 g (54% yield) of white solid MP 68-70°C (purity >99%, GC) Anal. Calcd for $C_{42}H_{18}F_{28}N_4O_3$: MW, 1158.64. Found: MW, 1150. The overall yield starting from the methyl ester was 22% and is comparable to that obtained for Quinoxaline I. A portion of Quinoxaline VII (0.79 g) was crystallized from methanol to give product (0.57 g), MP 72-74°C. The MS is presented in Table 25. The IR is given in Figure 29, the DSC scans in Figures 30-32, and the TGA scans, in nitrogen and air, in Figures 33 and 34, respectively.

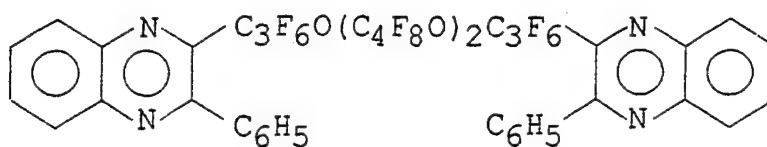
Hydrolysis of $[MeO_2CC_3F_6OC_4F_8]_2O$

The ester, $[MeO_2CC_3F_6OC_4F_8]_2O$ (50.01 g, 57.73 mmol) was hydrolyzed in 210 mL of a 10% solution of sodium hydroxide. The reaction was quenched with 50 mL of concentrated hydrochloric acid and extracted with ether (3x100 mL), washed with water (8x50 mL) and dried over anhydrous magnesium sulfate. Solvent removal gave 47 g (98% yield) of the diacid, MP 50-53°C. The diacid was titrated with a solution of sodium hydroxide (0.1014 M) and the equivalent weight was found to be 431.6 (theory 419.09). Mass spectral analysis did not show any diester so the material contained most likely 5.8% of the monoacid ester.

A 16.4 g portion was retreated at pH 9 with sodium hydroxide at 50°C for 24 hours. After acidification the diacid was extracted with ether (4x75 mL) and the ether layer washed with water (4x50 mL) then dried over anhydrous magnesium sulfate.

TABLE 25

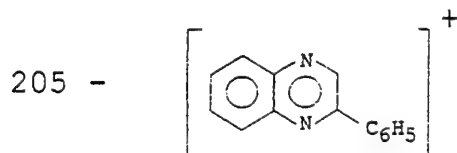
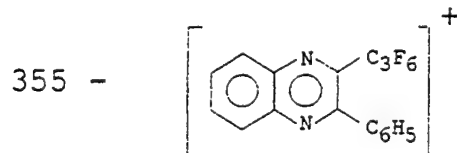
ION FRAGMENTS AND INTENSITIES RELATIVE TO BASE PEAK OF



m/e	%	m/e	%	m/e	%	m/e	%
17	4.7	102	13.3	224	2.7	568	5.3
18	24.7	103	4.2	235	6.3	579	6.8
20	17.9	118	2.7	236	6.4	784	3.7
29	2.8	127	5.0	237	2.0	953	3.9
31	2.2	128	2.2	253	2.4	1012	3.1
40	2.6	151	3.1	254	5.8	1025	2.8
47	7.5	152	3.1	255	6.3	1138	12.7
50	3.5	177	2.1	266	2.9	1139	17.6
51	3.7	178	5.8	297	2.2	1140	12.2
66	5.9	179	14.7	304	3.3	1141	4.4
75	5.4	180	2.0	355	24.2	1157	17.0
76	3.8	205	100.0	356	3.9	1158	89.7M ⁺
77	18.5	206	17.2	373	2.9	1159	40.5
100	2.1	223	3.6	374	5.4	1160	10.5

Peaks having intensities lower than 2% of the base peak and lower than m/e 17 are not reported.

Significant Ions in Support of Structure and Composition

m/e1139 - [M-F]⁺77 - C₆H₅⁺

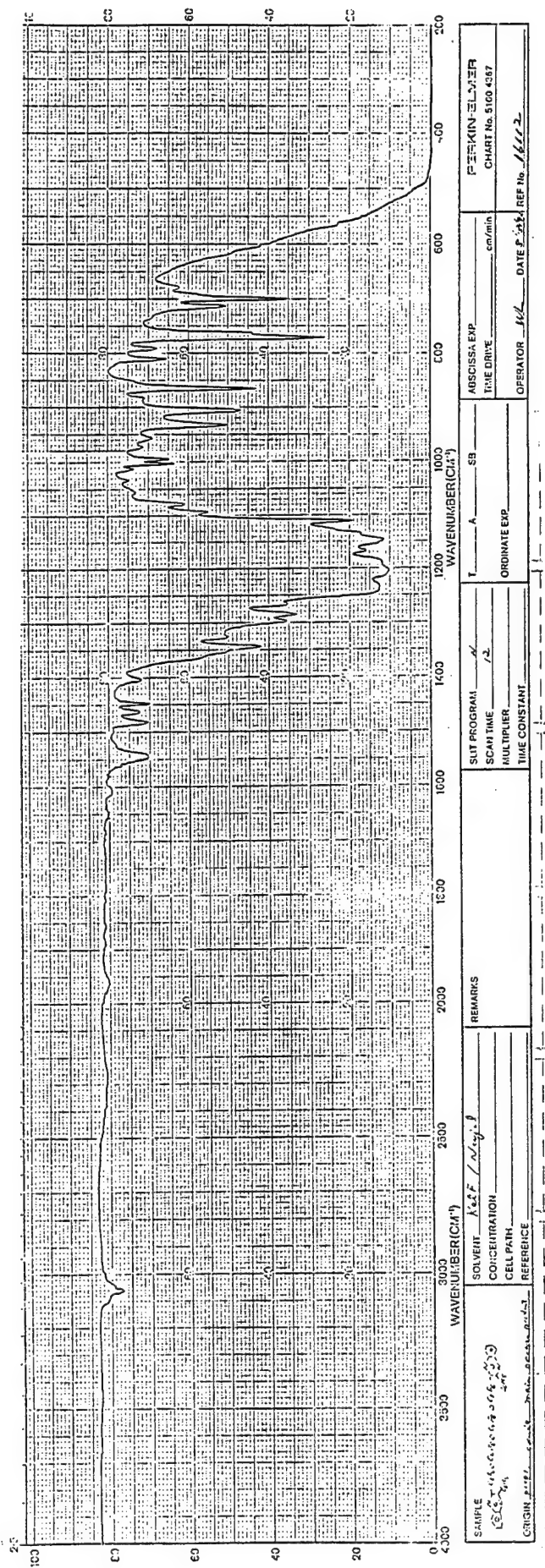


Figure 29. Infrared spectrum of Quinoxaline VII.

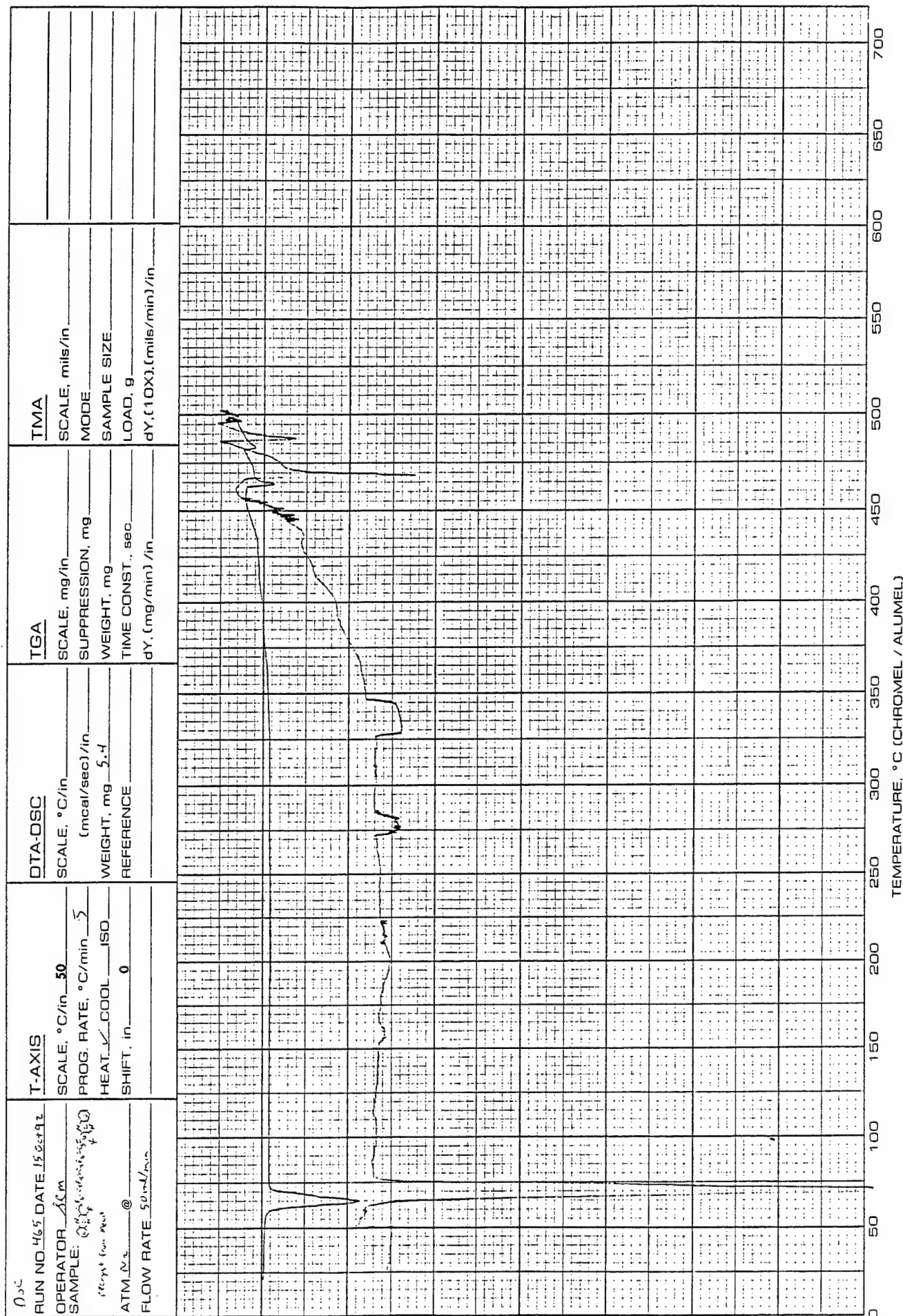


Figure 30. DSC scan of Quinoxaline VII.

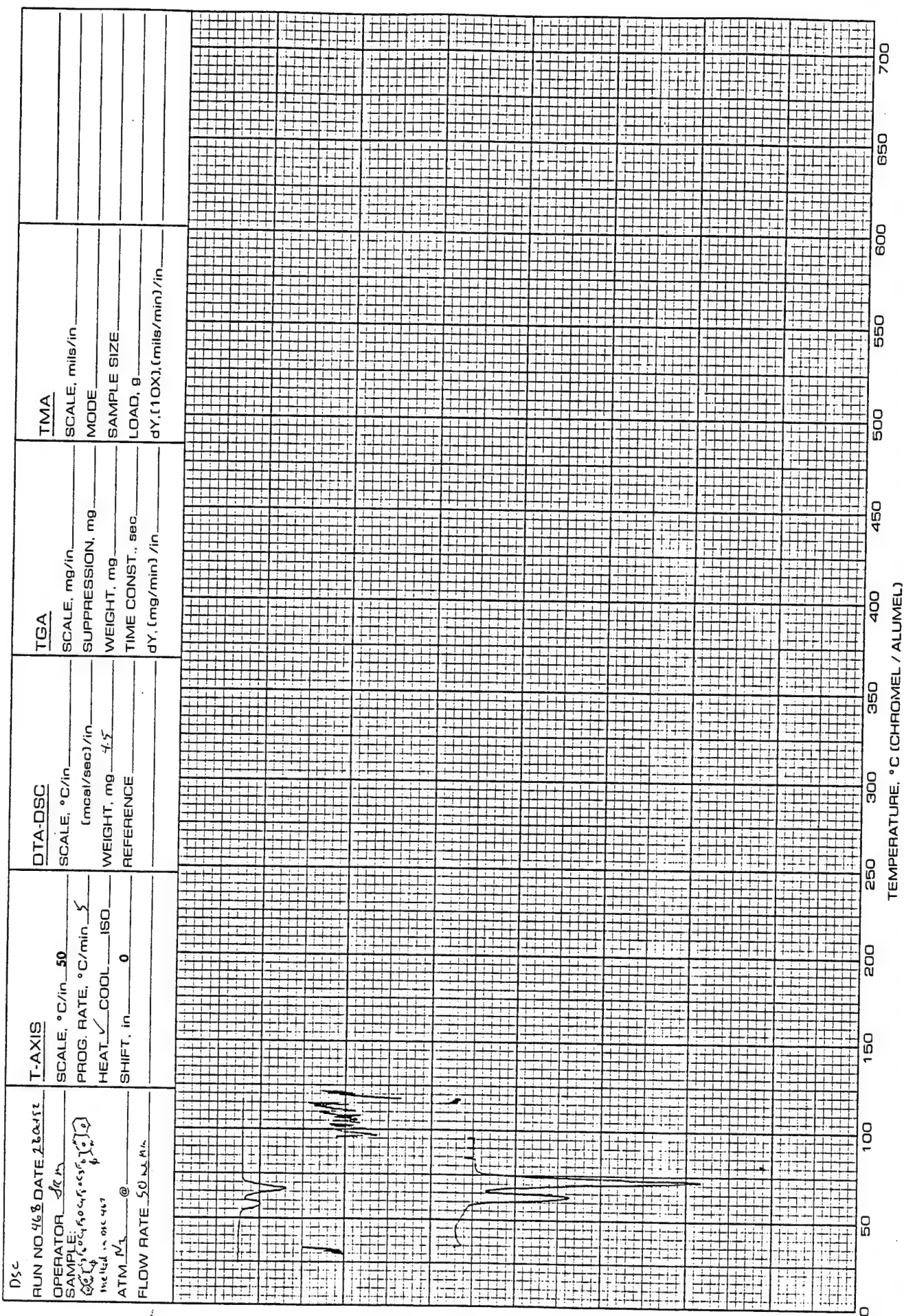


Figure 31. DSC scan of Quinoxaline VII after a prior DSC run up to 100°C.

TEMPERATURE, °C (CHROMEL / ALUMEL)

Figure 32. DSC scan of Quinoxaline VII following exposure to 316°C for 72 hours.

TGA
 RUN NO. 1014 DATE 10/4/93
 OPERATOR ON
 SAMPLE: Quinacridone VII
 4-90-49
 ATM N₂ @ 100 mL/min
 FLOW RATE 100 mL/min

T-AXIS
 SCALE, °C/in 50
 PROG. RATE, °C/min 10
 HEAT, COOL, ISO
 SHIFT, in 0

DTA-DSC
 SCALE, °C/in
 (mcal/sec)/in
 WEIGHT, mg
 REFERENCE

TGA
 SCALE, mils/in
 MODE
 SAMPLE SIZE
 LOAD, g
 dY, (10X), (mils/min)/in

TEMPERATURE, °C (CHROMEL / ALUMEL)

Figure 33. TGA scan of Quinoxaline VII in ~~N₂~~.

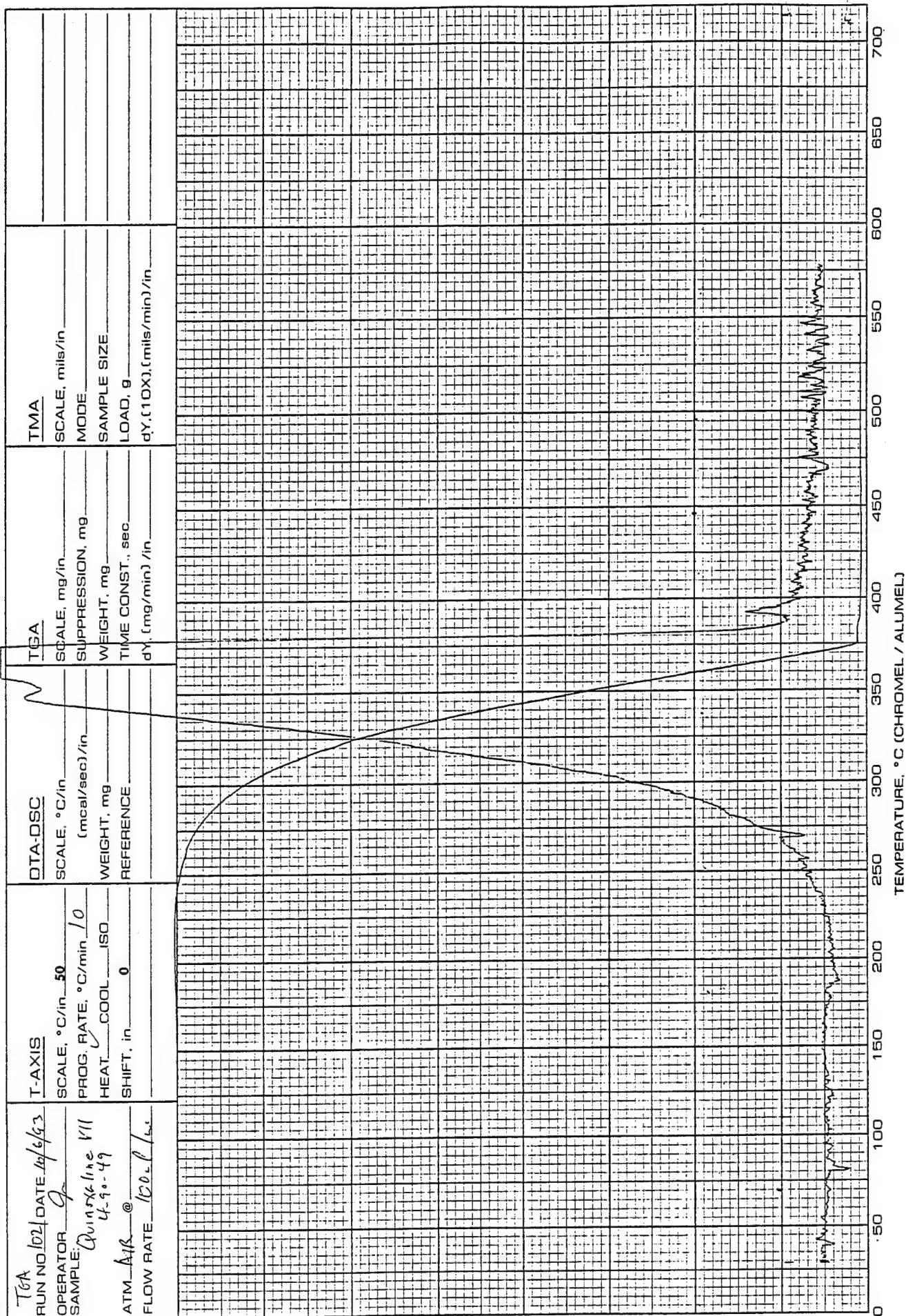


Figure 34. TGA scan of Quinoxaline VII in air.

Following solvent removal, the diacid was dried under vacuum (<0.001 mm Hg) for 6 hours at 45°C to give 15.9 g (97% recovery). The acid isolated after solvent removal had an equivalent weight of 425.3 which corresponds to a purity of 99% versus 94% after the first treatment with sodium hydroxide. The IR is given in Figure 35.

Preparation of $[\text{AgO}_2\text{CC}_3\text{F}_6\text{OC}_4\text{F}_8]_2\text{O}$

To a stirred solution of the diacid, $[\text{HO}_2\text{CC}_3\text{F}_6\text{OC}_4\text{F}_8]_2\text{O}$, (14.3 g, 17.1 mmol) in water (125 mL; titrated to a pH of 9.05 with a ~ 2.5 M solution of sodium hydroxide) was added silver nitrate (8.7 g, 51 mmol, in 9 mL water) at 10°C over ~ 10 minutes. A precipitate formed immediately and the solution became thick with solid. Stirring was continued for 1 hour prior to filtration; the isolated solid was washed with water (5x80 mL), then transferred to an ampoule and dried on the vacuum line (< 0.001 mm Hg) for 6 hours resulting in 16.6 g (92% yield) of $[\text{AgO}_2\text{CC}_3\text{F}_6\text{OC}_4\text{F}_8]_2\text{O}$ (MP $>200^{\circ}\text{C}$); Ag, 19.5%; theory, 20.5%. The IR is given in Figure 36.

Preparation of $[\text{IC}_3\text{F}_6\text{OC}_4\text{F}_8]_2\text{O}$

Iodine (18.6 g, 73 mmol) was ground to a fine powder using a mortar and pestle. The silver salt $[\text{AgO}_2\text{CC}_3\text{F}_6\text{OC}_4\text{F}_8]_2\text{O}$ (7.00 g, 6.65 mmol) was mixed with a portion of the iodine (9.0 g) and placed on top of iodine (8.0 g) in a 45 mm tube; the rest of the iodine (1.6 g) was put on top of the mixture. The tube was then attached to a nitrogen bypass placed in an oil bath (preheated to 120°C) and heated for 2 hours. This was followed

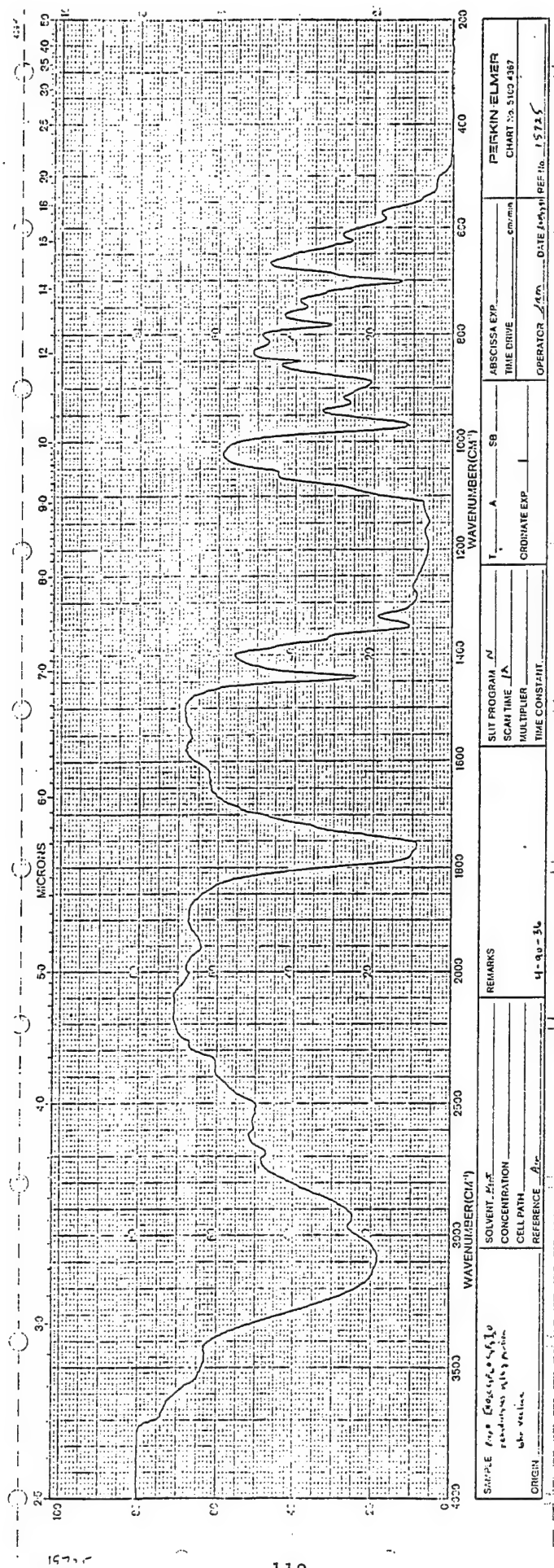


Figure 35. Infrared spectrum of $[\text{HO}_2\text{CC}_3\text{F}_6\text{OC}_4\text{F}_8]_2\text{O}$.

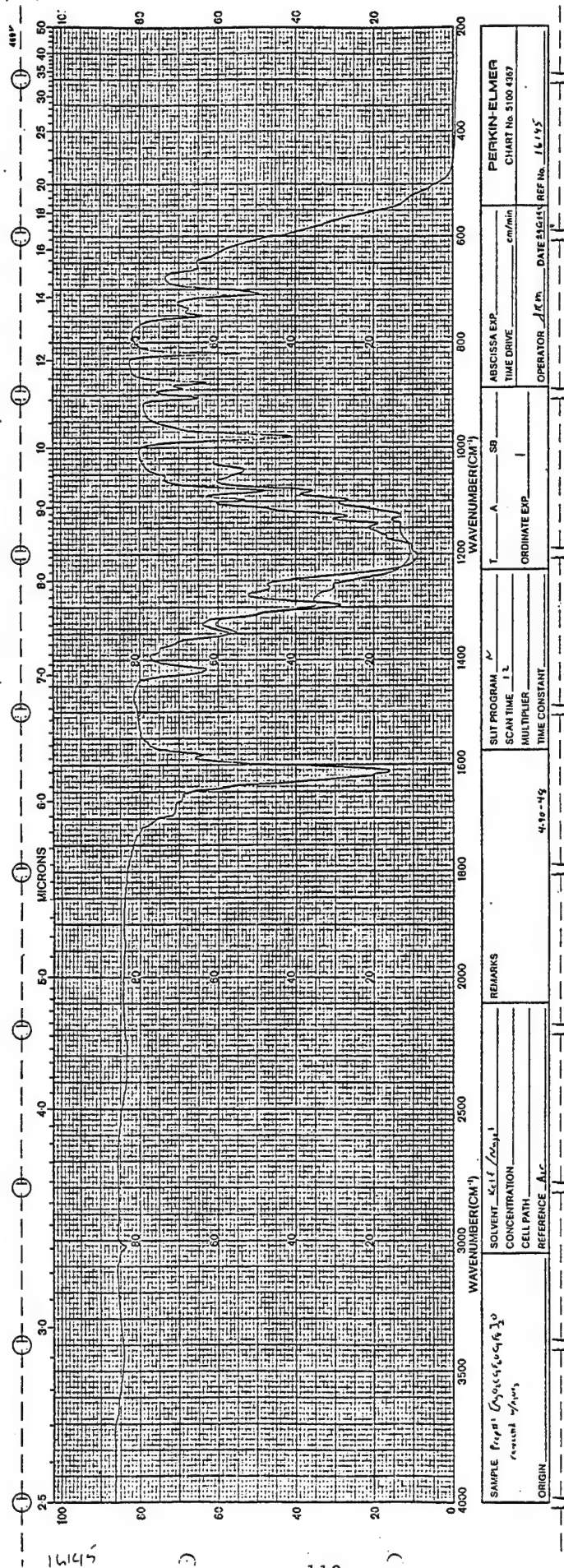


Figure 36. Infrared spectrum of $[AgO_2CC_3F_6OC_4F_8]_2O$.

by 3 hours at 140°C. After cooling, the residue together with the iodine from the bottom of the tube and the material sublimed in the adapter was ground and extracted with Freon-113 (30 mL). Solvent removal in vacuo resulted in 5.88 g (88% yield) of $[\text{IC}_3\text{F}_6\text{OC}_4\text{F}_8]_2\text{O}$ (purity 94%, GC). Treatment with copper bronze followed by filtration and washing with Freon-113 gave, after solvent removal and distillation, $[\text{IC}_3\text{F}_6\text{OC}_4\text{F}_8]_2\text{O}$, 5.05 g (76% yield); BP 60-62°C/0.001 mm Hg. The MS is presented in Table 26 and the IR in Figure 37.

Preparation of $[\text{C}_6\text{H}_5\text{C}(\text{O})\text{C}(\text{O})\text{C}_6\text{H}_4\text{C}_3\text{F}_6\text{OC}_4\text{F}_8]_2\text{O}$

In an inert atmosphere enclosure to 4-iodobenzil (7.46 g, 29.8 mmol), copper bronze (5.78 g, 91.0 mmol), and $[\text{IC}_3\text{F}_6\text{OC}_4\text{F}_8]_2\text{O}$ (13.55 g, 13.5 mmol) in a 250 mL round bottom flask was added via a syringe anhydrous DMSO (13.5 mL). The reaction mixture was subsequently stirred at 105-119°C for 24 hours under nitrogen bypass. After heating, two layers were present. Analysis by gas chromatography showed a trace of product in the top layer. The bottom layer consisted of 90% product. Dichloromethane (70 mL) was added to the bottom layer, the solution filtered and the remaining DMSO removed by washing with water (8x50 mL). After drying with MgSO_4 , solvent removal in vacuum resulted in a semisolid (12.83 g, 81% yield; purity 81%, GC). Heating under high vacuum (<0.001 mm Hg) for 4 hours at 110°C gave 11.74 g of residue (purity 94%, GC). This material was further purified using a silica gel column (110 g, 48 cm x 2.8 cm). The sample was placed on the column dissolved in 12 mL

TABLE 26

ION FRAGMENTS AND INTENSITIES RELATIVE TO BASE PEAK OF

 $[\text{ICF}_2\text{CF}_2\text{CF}_2\text{OCF}_2\text{CF}_2\text{CF}_2\text{CF}_2]_2\text{O}$ (MW, 1002)

m/e	%	m/e	%	m/e	%	m/e	%
15	2.1	93	6.3	150	24.8	219	4.0
31	16.6	97	2.2	158	2.9	227	5.8
47	13.8	100	45.7	162	3.0	231	3.2
50	8.4	101	2.8	169	24.4	239	3.3
59	3.1	109	2.0	170	2.2	254	9.1
62	2.2	112	4.1	177	40.1	277	<u>100.0</u>
63	2.6	119	18.9	181	7.6	278	8.8
66	3.3	127	41.4	189	2.2	1002	74.5M ⁺
69	36.2	131	46.8	197	8.4	1003	18.5
78	2.5	132	4.7	208	8.2	1004	3.1
81	6.5	146	14.9	209	2.4		

Peaks having intensities lower than 2% of the base peak are not reported.

Significant Ions in Support of Structure and Composition

m/e127 - I⁺177 - CF₂I⁺277 - CF₂CF₂CF₂I⁺1002 - M⁺

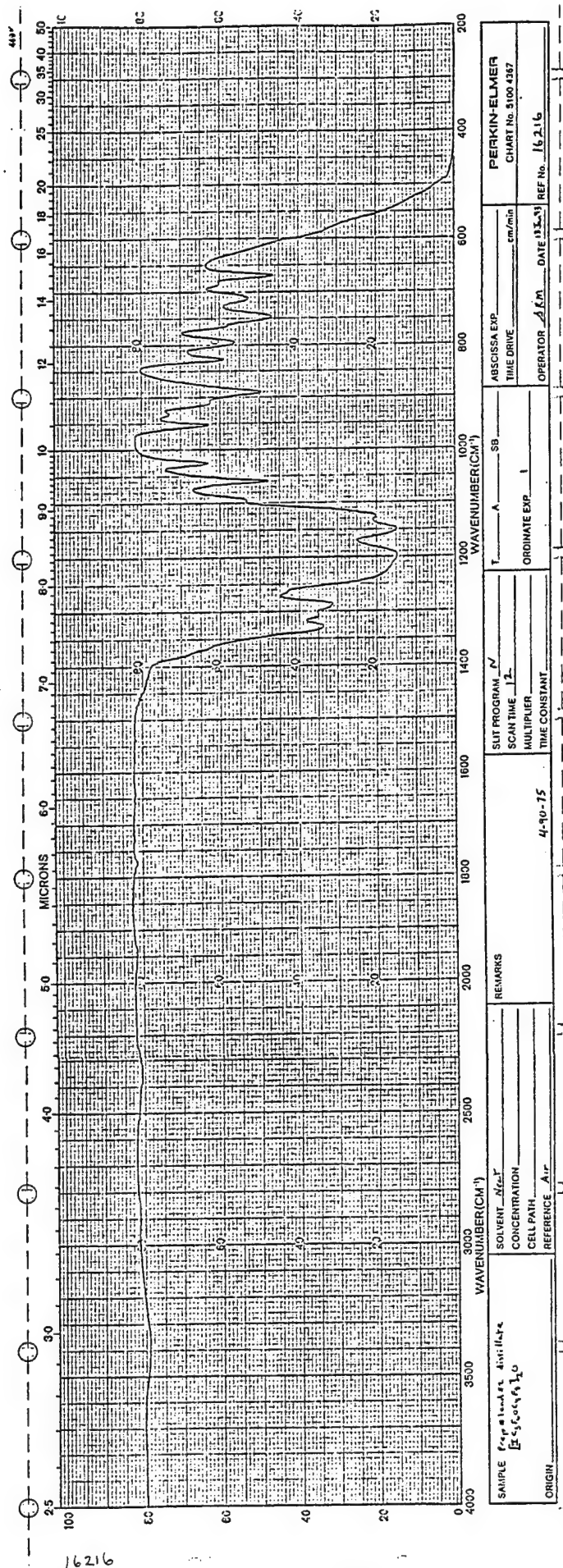


Figure 37. Infrared spectrum of $[\text{IC}_3\text{F}_6\text{OC}_4\text{F}_8]_2\text{O}$.

of 1:2 ether/hexanes. The first band (0.57 g) was eluted with 10% ether/hexanes (400 mL). The second band and the surrounding areas were eluted with 20% ether/hexanes. The third and fourth bands were eluted with 50% ether/hexanes. Only the bright yellow second band gave a powdery solid (6.78 g, 43% yield) MP 63-65°C (purity 99.5%, GC). All the other fractions consisted of viscous liquids. The MS of $[\text{C}_6\text{H}_5\text{C}(\text{O})\text{C}(\text{O})\text{C}_6\text{H}_4\text{C}_3\text{F}_6\text{OC}_4\text{F}_8]_2\text{O}$ is presented in Table 27 and the IR in Figure 38.

Preparation of Quinoxaline VIII

In an inert atmosphere enclosure, to a stirred solution of $[\text{C}_6\text{H}_5\text{C}(\text{O})\text{C}(\text{O})\text{C}_6\text{H}_4\text{C}_3\text{F}_6\text{OC}_4\text{F}_8]_2\text{O}$ (3.12 g, 2.67 mmol) and glacial acetic acid (1 mL) in m-cresol (30 mL) was added 1,2-phenylenediamine (0.58 g, 5.36 mmol) in m-cresol (30 mL), via an addition funnel, over a period of 30 minutes. After stirring for an additional 2 hours at room temperature, the addition funnel was replaced with a reflux condenser and the reaction mixture was stirred at 45-50°C for 18 hours under nitrogen bypass. m-Cresol (45 mL) was then distilled off under vacuum. The resultant viscous residue was added dropwise to a vigorously stirred methanol (100 mL). Following an overnight stirring, the solid was filtered and washed with methanol and after drying in vacuum, a solid 2.8 g (80% yield), MP 118-122°C, was obtained. Two recrystallizations from benzene/hexane gave 0.83 g (24% yield) of Quinoxaline VIII, MP 135-137°C. Anal. Calcd for $\text{C}_{54}\text{H}_{26}\text{F}_{28}\text{N}_4\text{O}_3$: MW 1310.84. Found: 1300. The IR is given in Figure 39 and the

TABLE 27

ION FRAGMENTS AND INTENSITIES RELATIVE TO BASE PEAK OF
 $[\text{C}_6\text{H}_5\text{C}(\text{O})\text{C}(\text{O})\text{C}_6\text{H}_4\text{C}_3\text{F}_6\text{OC}_4\text{F}_8]_2\text{O}$ (MW, 1166)

m/e	%	m/e	%	m/e	%	m/e	%
14	1.2	50	6.7	95	1.2	131	2.7
17	2.0	51	12.7	96	5.4	145	4.7
18	10.4	66	3.8	97	1.0	154	3.0
20	8.1	69	6.6	100	3.4	155	1.1
27	1.1	70	1.0	105	<u>100.0</u>	169	1.3
28	22.0	73	2.8	106	16.9	173	4.3
31	3.1	74	1.8	107	1.4	176	1.3
32	3.5	75	2.7	119	1.8	207	1.7
36	3.2	76	2.0	122	1.8	251	1.6
38	1.5	77	29.7	123	2.5	253	2.6
39	1.4	78	4.9	124	3.3	1061	5.8
44	5.1	79	1.2	125	1.5	1062	2.4
47	9.5	81	2.8	126	4.5		
49	1.3	85	2.5	127	1.8		

Significant ions in Support of Structure and Composition

<u>m/e</u>	
77	C_6H_5^+
105	$\text{C}_6\text{H}_5\text{CO}^+$
1061	$[\text{M} - \text{C}_6\text{H}_5\text{CO}]^+$

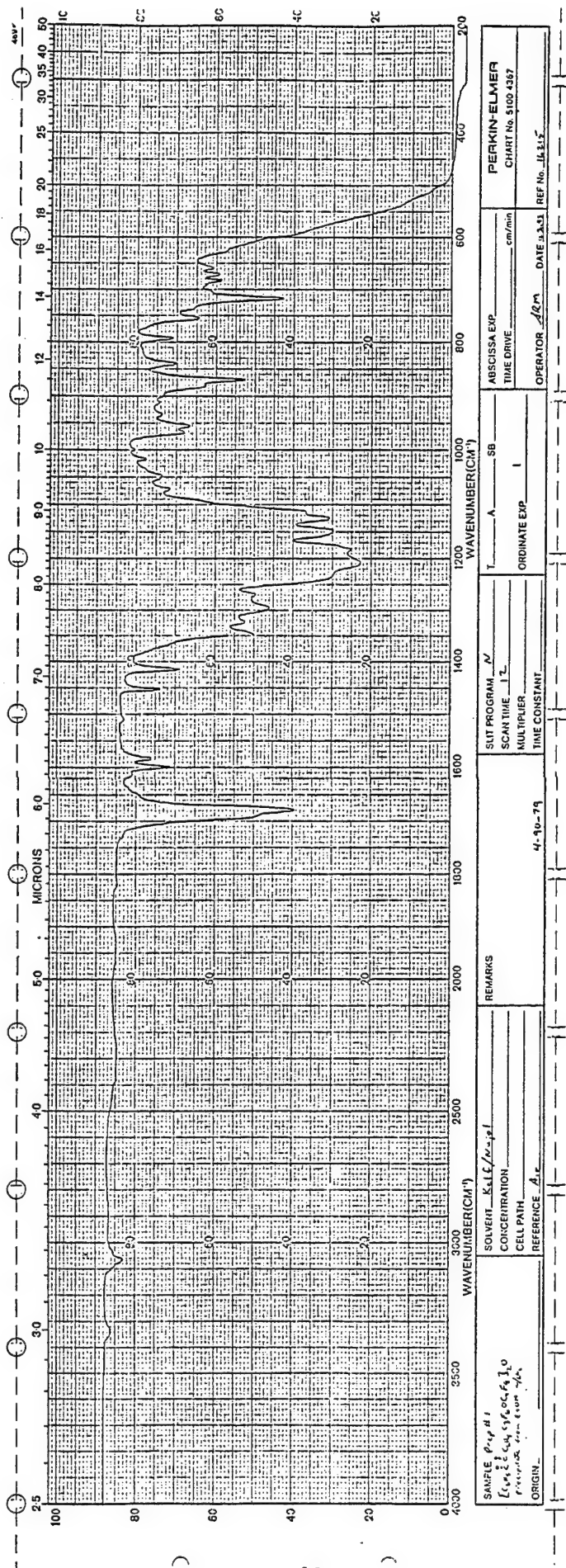


Figure 38. Infrared spectrum of $[\text{C}_6\text{H}_5\text{C}(\text{O})\text{C}(\text{O})\text{C}_6\text{H}_4\text{C}_3\text{F}_6\text{OC}_4\text{F}_8]_2\text{O}$.

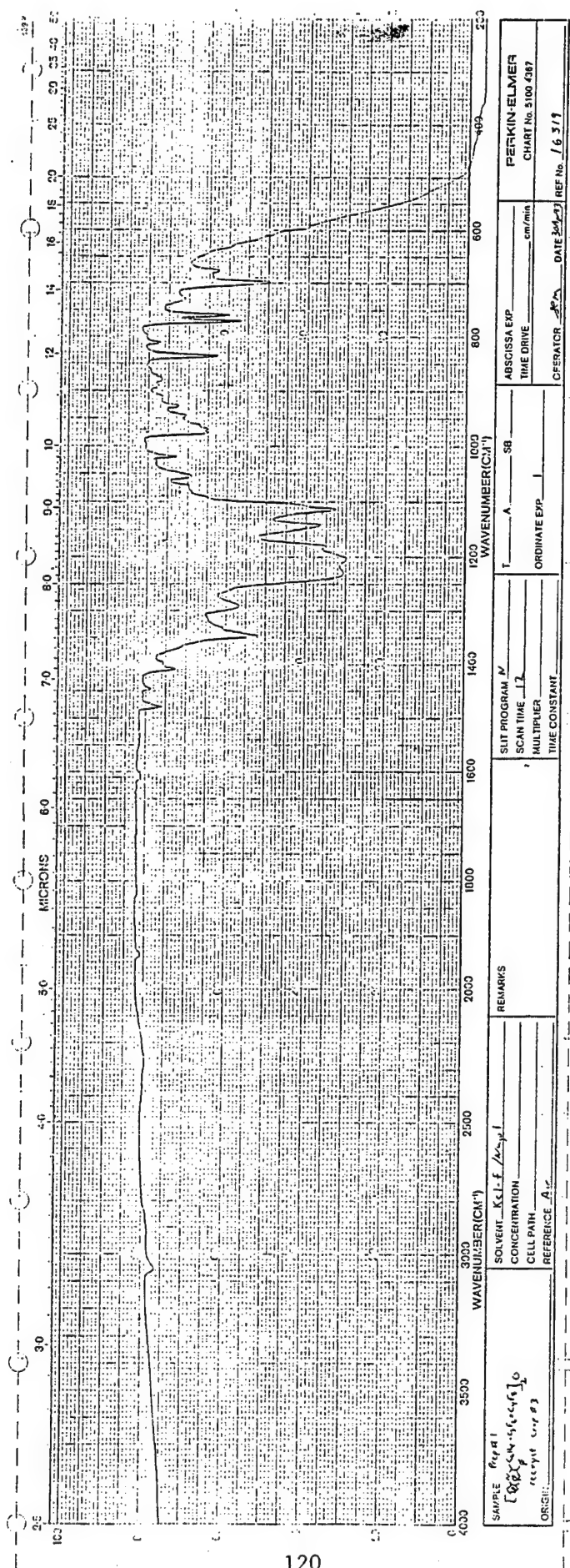


Figure 39. Infrared spectrum of Quinoxaline VIII.

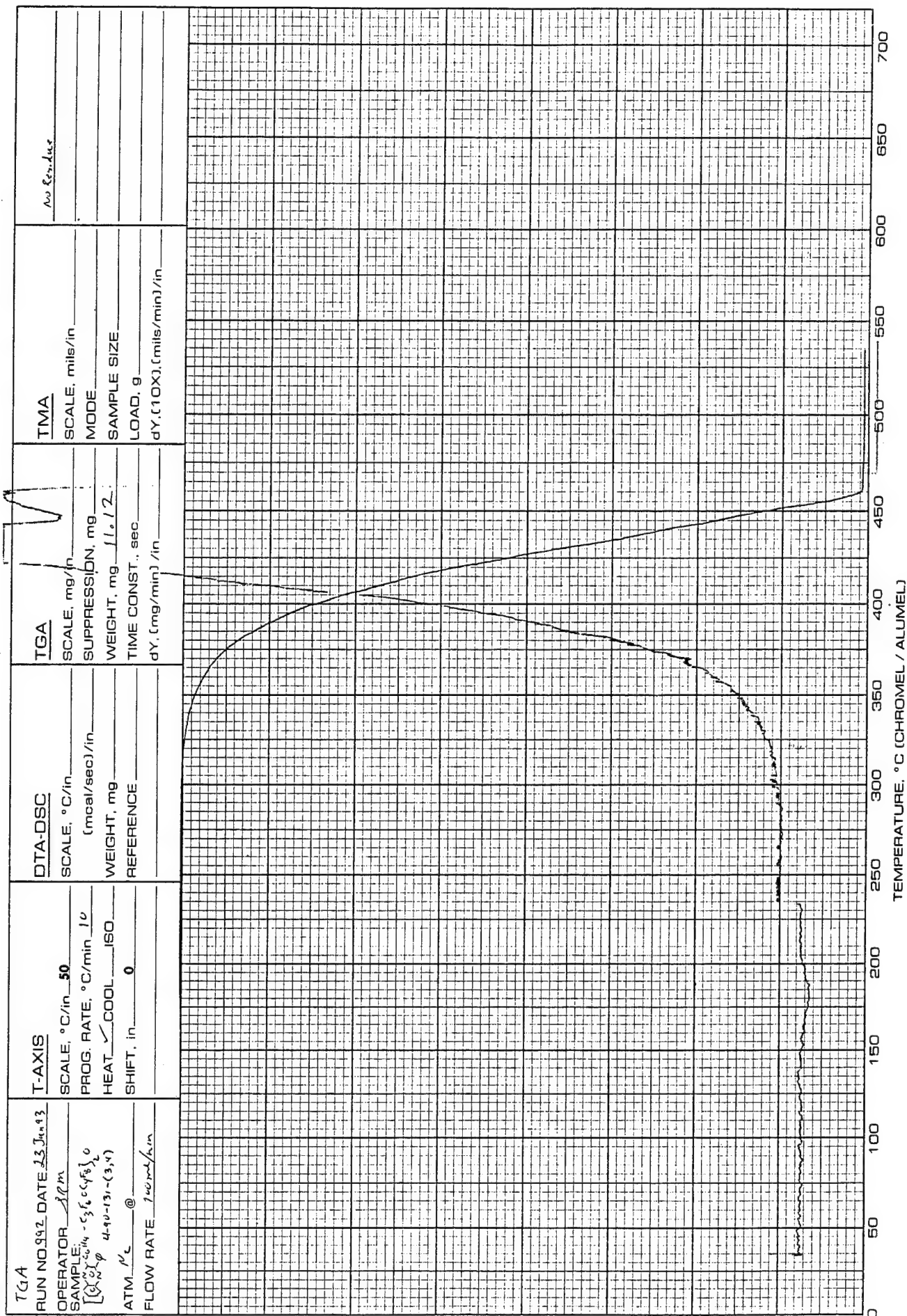
TGA scans, in nitrogen and air, in Figures 40 and 41, respectively.

Preparation of Quinoxaline IX Series

The syntheses and properties Of Quinoxalines IX-1 through IX-6 are given in Table 5. The corresponding IR and TGA scans, Figures 42-57, are listed there also.

Preparation of $C_3F_7OCF(CF_3)CF_2OCF(CF_3)C(O)C_6H_4Br$

p-Dibromobenzene (13.0 g, 55.1 mmol) was placed into a 300 mL 3 neck round bottom flask equipped with a magnetic stirrer, gas inlet, and 2 addition funnels, one containing n-butyllithium (20 mL, 2.5 M) and the other $C_3F_7OCF(CF_3)CF_2OCF(CF_3)CO_2Me$ (23.2 g, 45.5 mmol). The mixture was cooled to $-78^{\circ}C$ and n-butyllithium was added over a period of 50 minutes. After stirring for 80 minutes, the ester was added over a period of 10 minutes and the resulting solution was left stirring an additional 2.5 hours. The reaction mixture was quenched with hydrochloric acid (100 mL, 2N) as it warmed to room temperature. The aqueous layer was separated and extracted with ether (50 mL). The ether extract was combined with the organic layer, washed with water (25 mL) and dried over anhydrous magnesium sulfate. The crude material, obtained after solvent evaporation, was heated at $110^{\circ}C$ under vacuum (<0.001 mm Hg) to remove volatile impurities such as unreacted starting materials and $C_3F_7OCF(CF_3)CF_2OCF(CF_3)C(O)C_4H_9$ to give 16.7 g (58% yield) of a residue which consisted of 89% $C_3F_7OCF(CF_3)CF_2OCF(CF_3)C(O)C_6H_4Br$ and

Figure 40. TGA scan of Quinoxaline VIII in N₂.

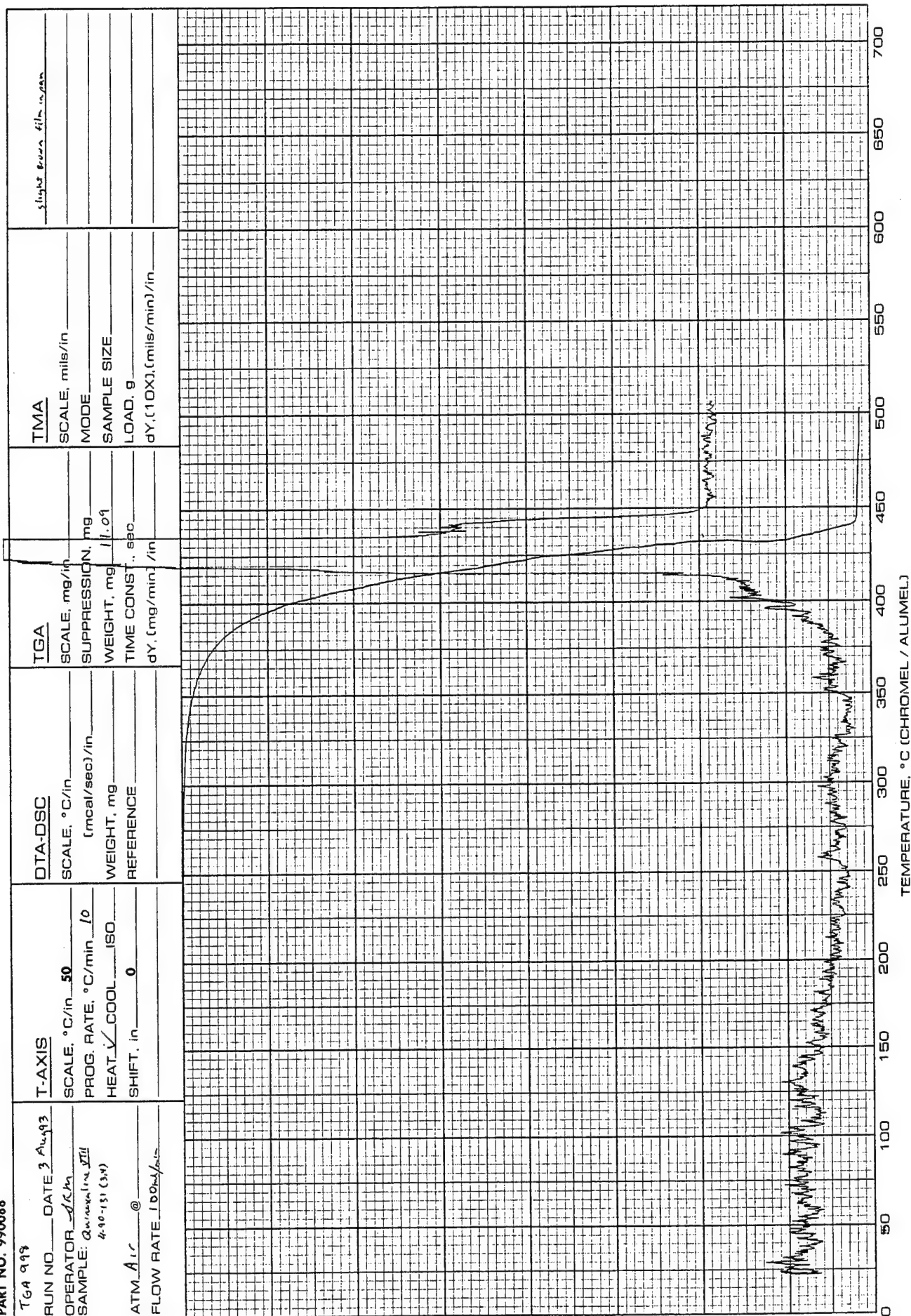


Figure 41. TGA scan of Quinoxaline VIII in air.

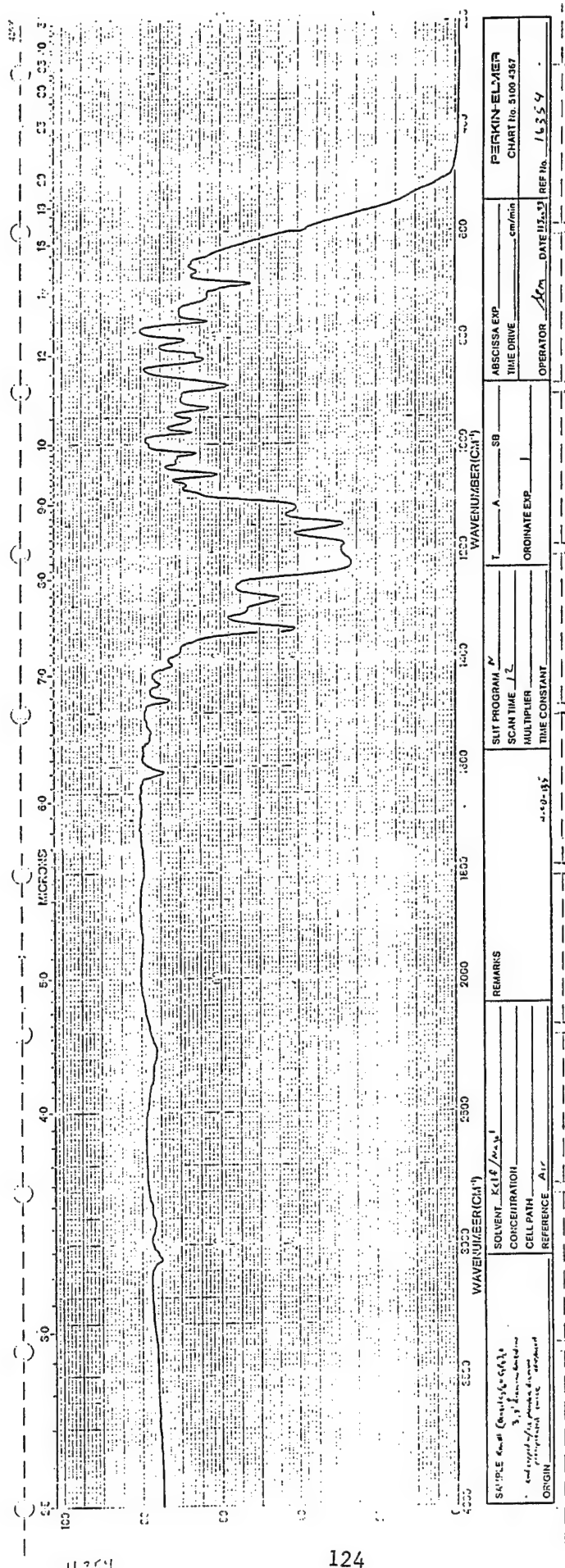
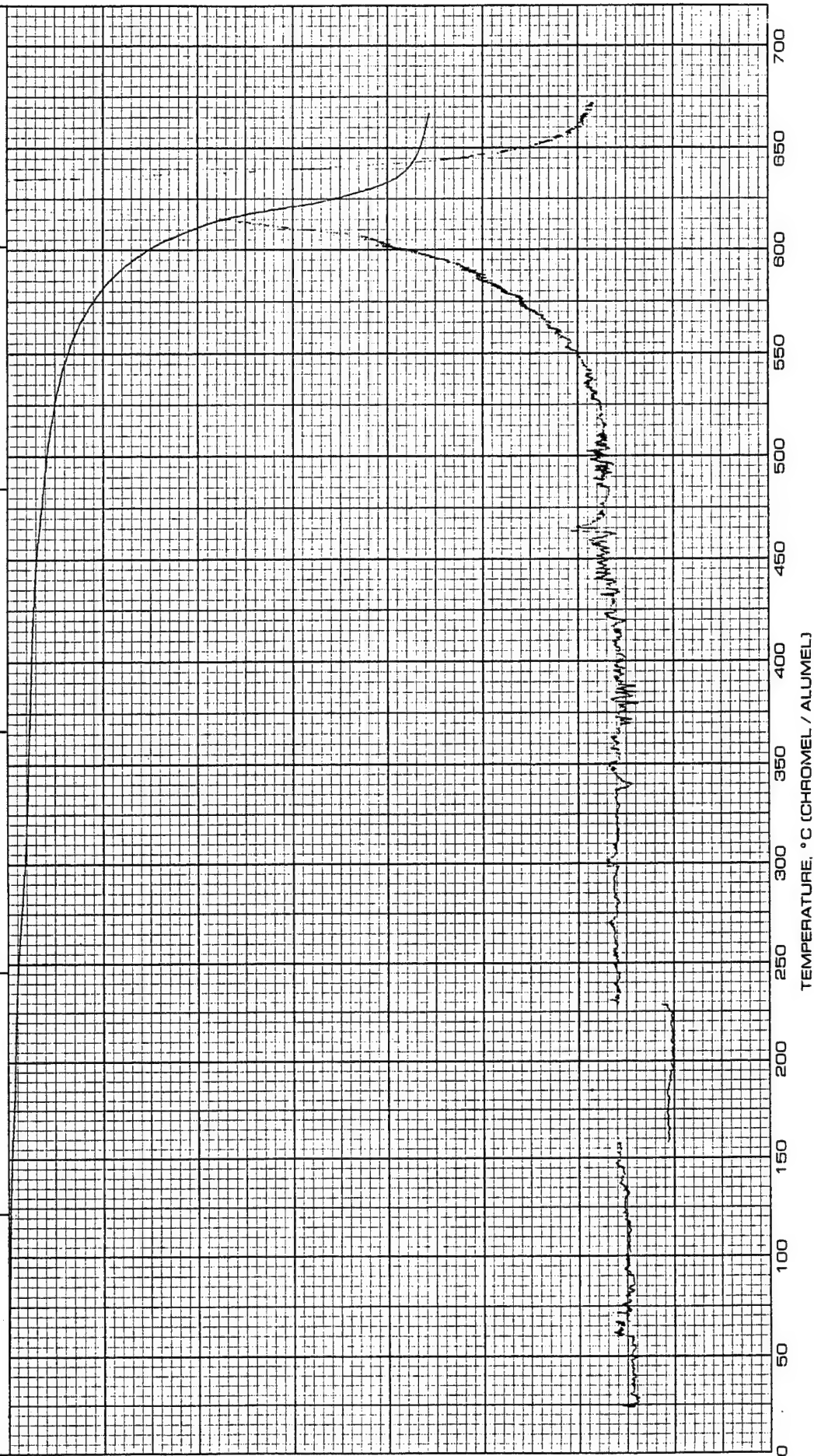
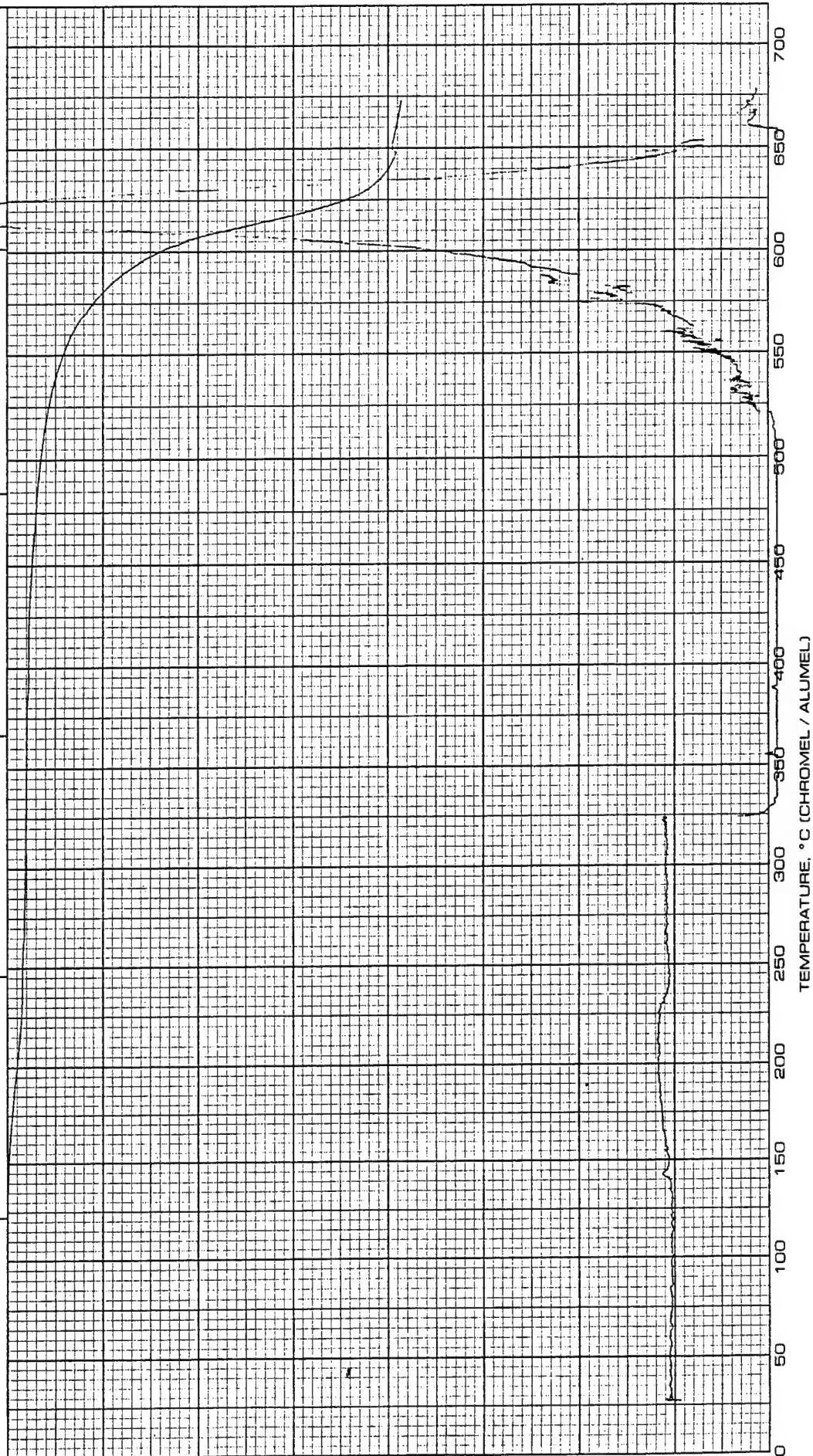


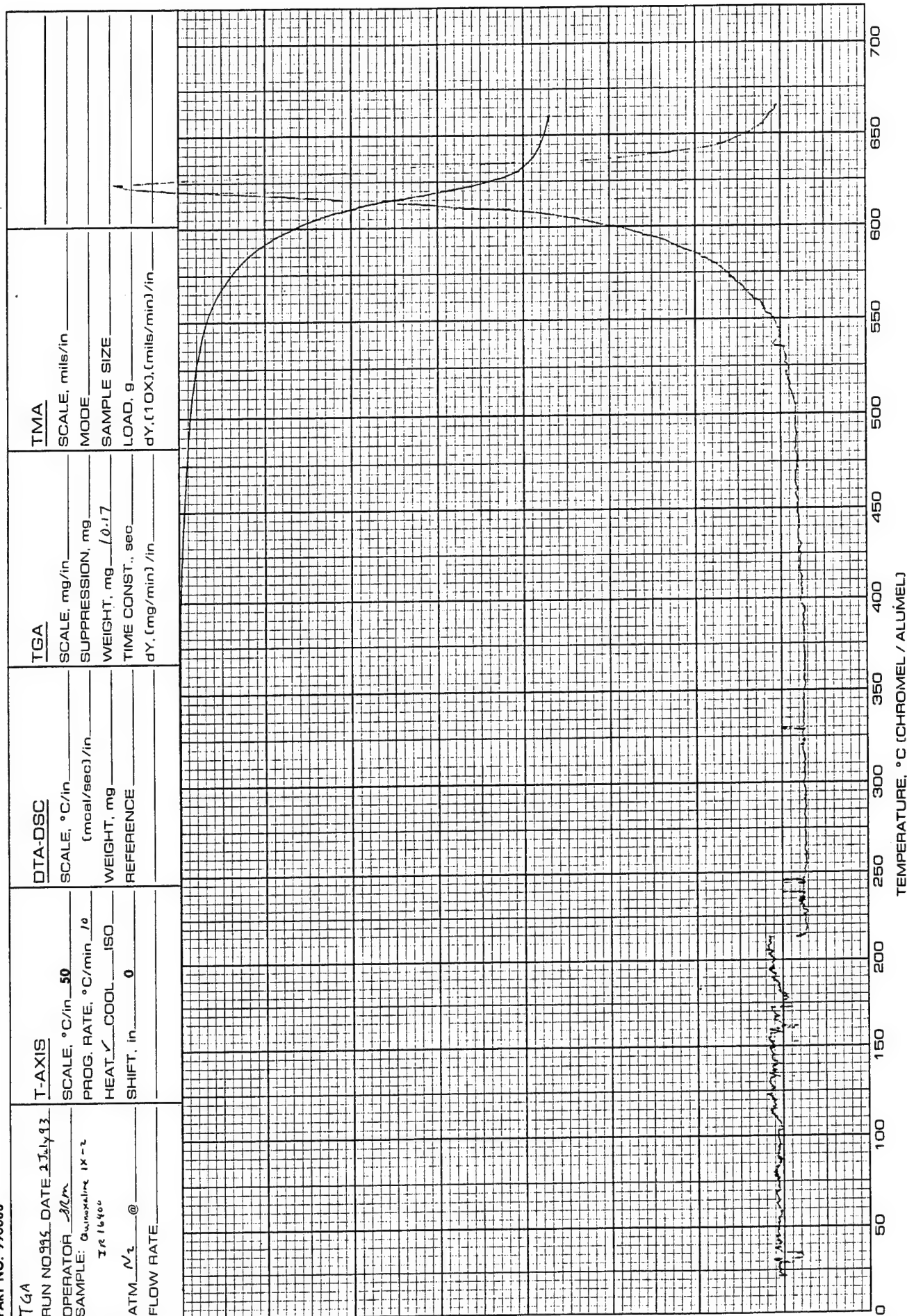
Figure 42. Infrared spectrum of Quinoxaline IX-1.

TGA RUN NO <u>991</u> DATE <u>23 July 63</u> OPERATOR <u>SEM</u> SAMPLE: <u>C₆F₆ sol IX-16354</u> <u>Quinoxaline IX-1</u>		T-AXIS SCALE, °C/in <u>50</u> PROG. RATE, °C/min <u>10</u> HEAT <input checked="" type="checkbox"/> COOL <u>ISO</u> SHIFT, in <u>0</u>		DTA-DSC SCALE, °C/in <u> </u> (mcal/sec)/in <u> </u> WEIGHT, mg <u> </u> REFERENCE <u> </u>		TGA SCALE, mg/in <u> </u> SUPPRESSION, mg <u> </u> WEIGHT, mg <u>10.4%</u> TIME CONST., sec <u> </u> dY, (mg/min) /in <u> </u>		TMA SCALE, mils/in <u> </u> MODE <u> </u> SAMPLE SIZE <u> </u> LOAD, g <u> </u> dY, (10X), (mils/min) /in <u> </u>		Blank Run
ATM <u>N₂</u> @ <u> </u> FLOW RATE <u>100 ml/min</u>										

Figure 43. TGA scan of the hexafluorobenzene-soluble portion of Quinoxaline IX-1 in N₂.

TGA RUN NO. 993 DATE 24 Jan 93 OPERATOR JRM SAMPLE: C ₆ F ₆ insol in 2,2,2-trifluoroethane Quinoxaline IX-1 ATM. N ₂ @ FLOW RATE 100 ml/min		T-AXIS SCALE, °C/in. 50 PROG. RATE, °C/min 10 HEAT V. COOL ISO SHIFT, in. 0		DTA-DSC SCALE, °C/in. (mcal/sec)/in. WEIGHT, mg REFERENCE		TGA SCALE, mg/in. SUPPRESSION, mg WEIGHT, mg 11.46 TIME CONST., sec dY, (mg/min)/in.		TMA SCALE, mils/in. MODE SAMPLE SIZE LOAD, g dY, (10X), (mils/min)/in.		Black residue	
---	--	--	--	--	--	--	--	--	--	---------------	--

Figure 44. TGA scan of the hexafluorobenzene-insoluble portion of Quinoxaline IX-1 in N₂.

Figure 46. TGA scan of Quinoxaline IX-2 in N₂.

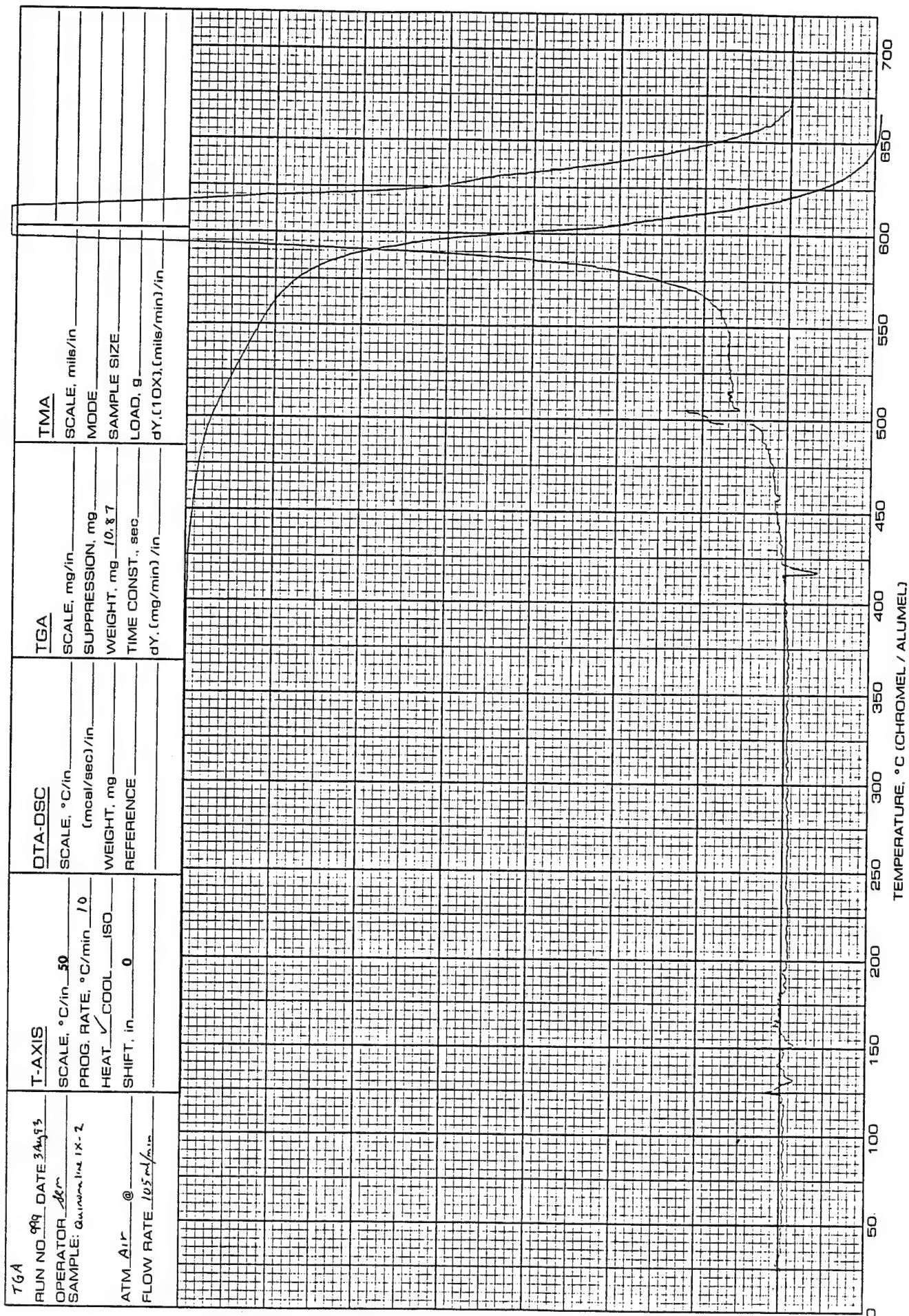


Figure 47. TGA scan of Quinoxaline IX-2 in air.

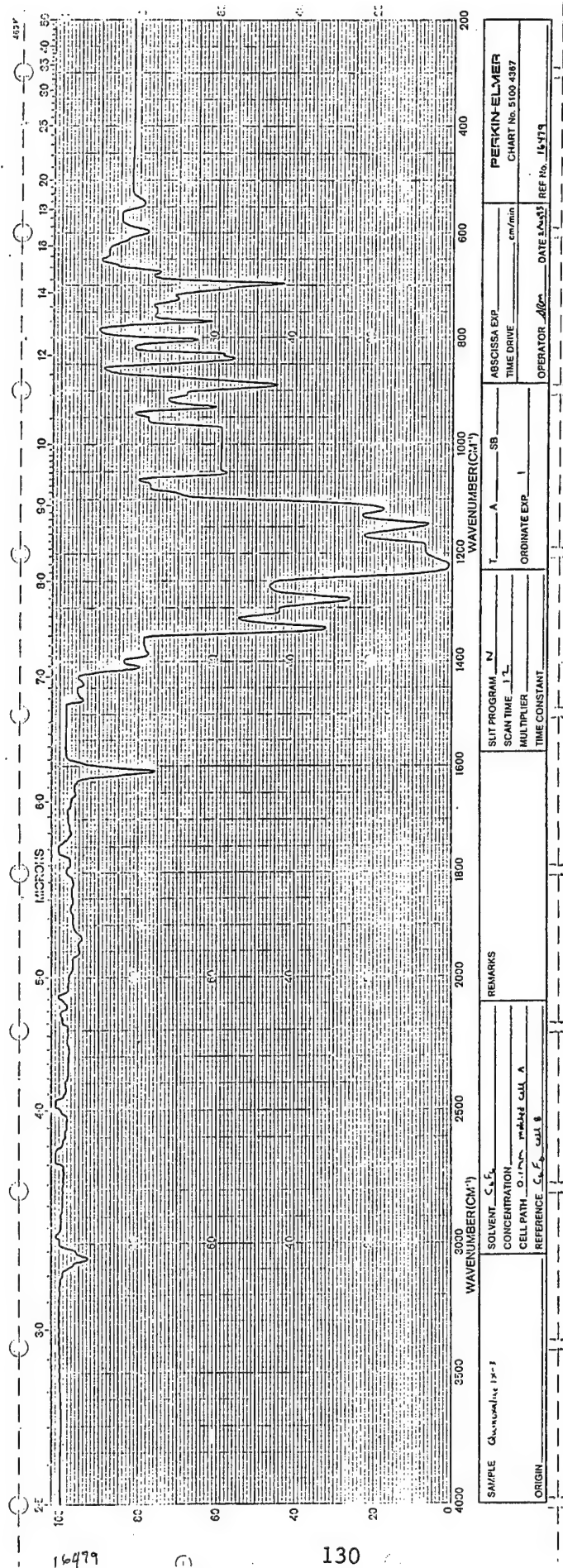
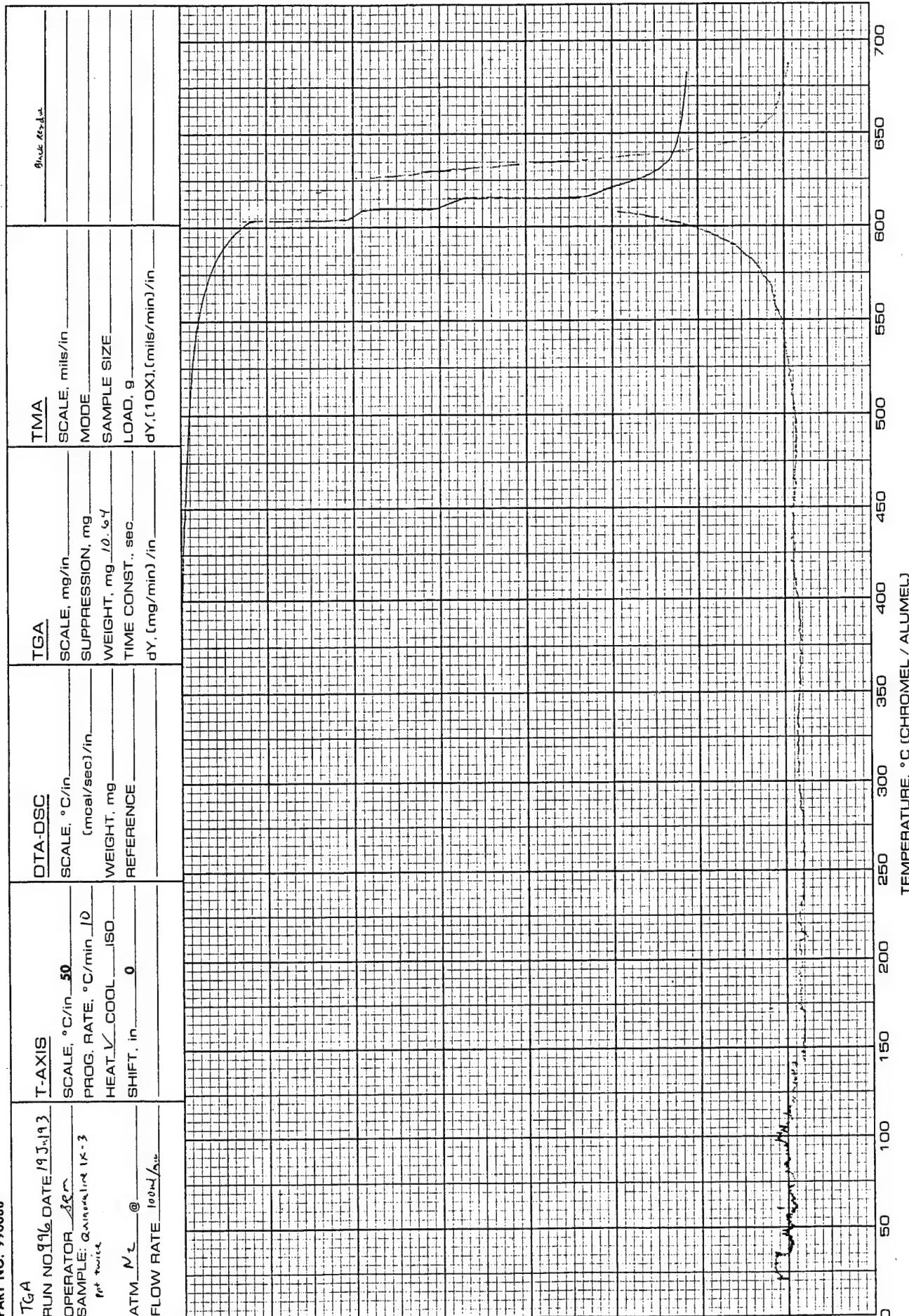


Figure 48. Infrared spectrum of Quinoxaline IX-3 (in C₆F₆; solvent subtracted).

Figure 49. TGA scan of Quinoxaline IX-3 in N₂.

PART NO. 990088

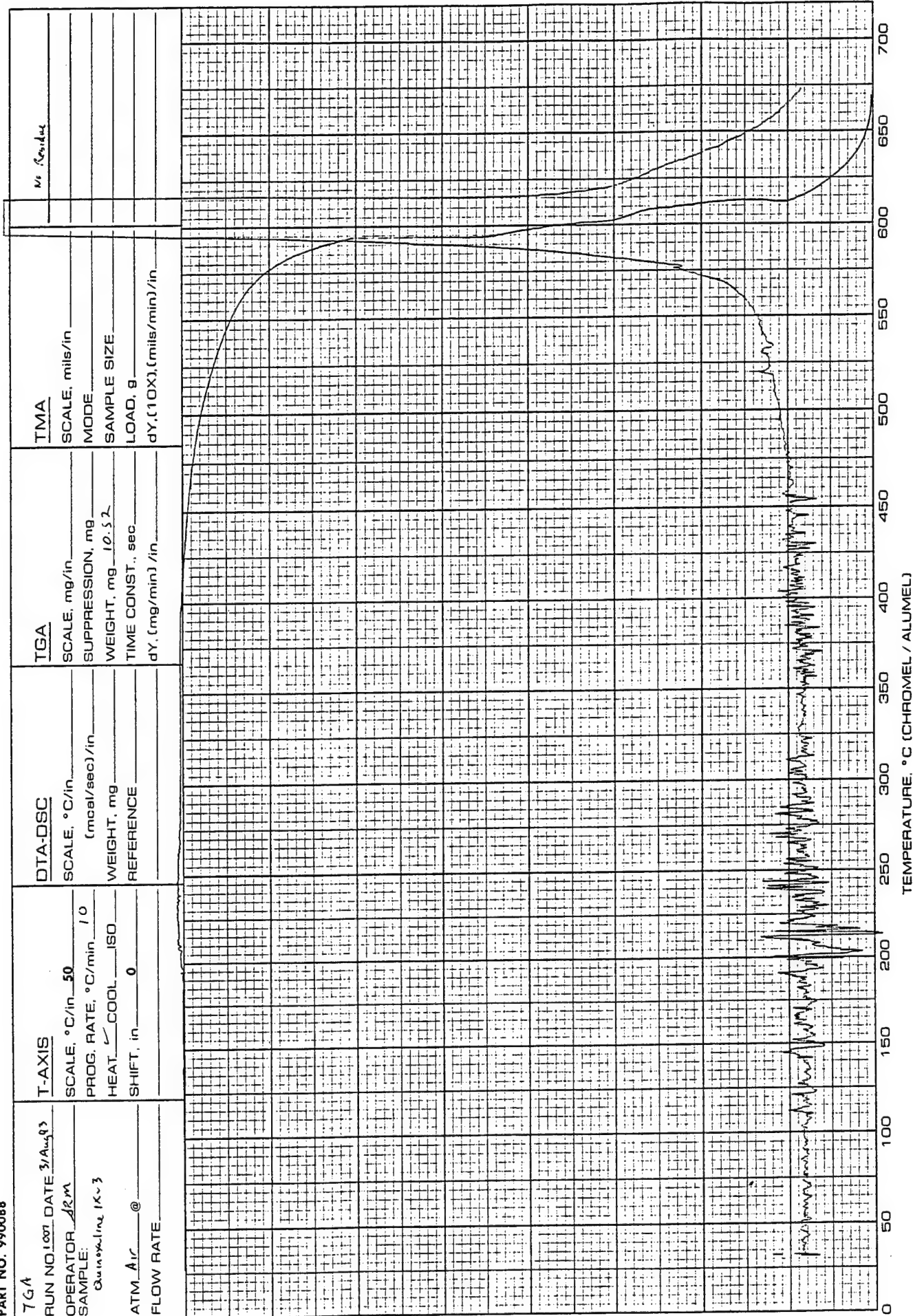
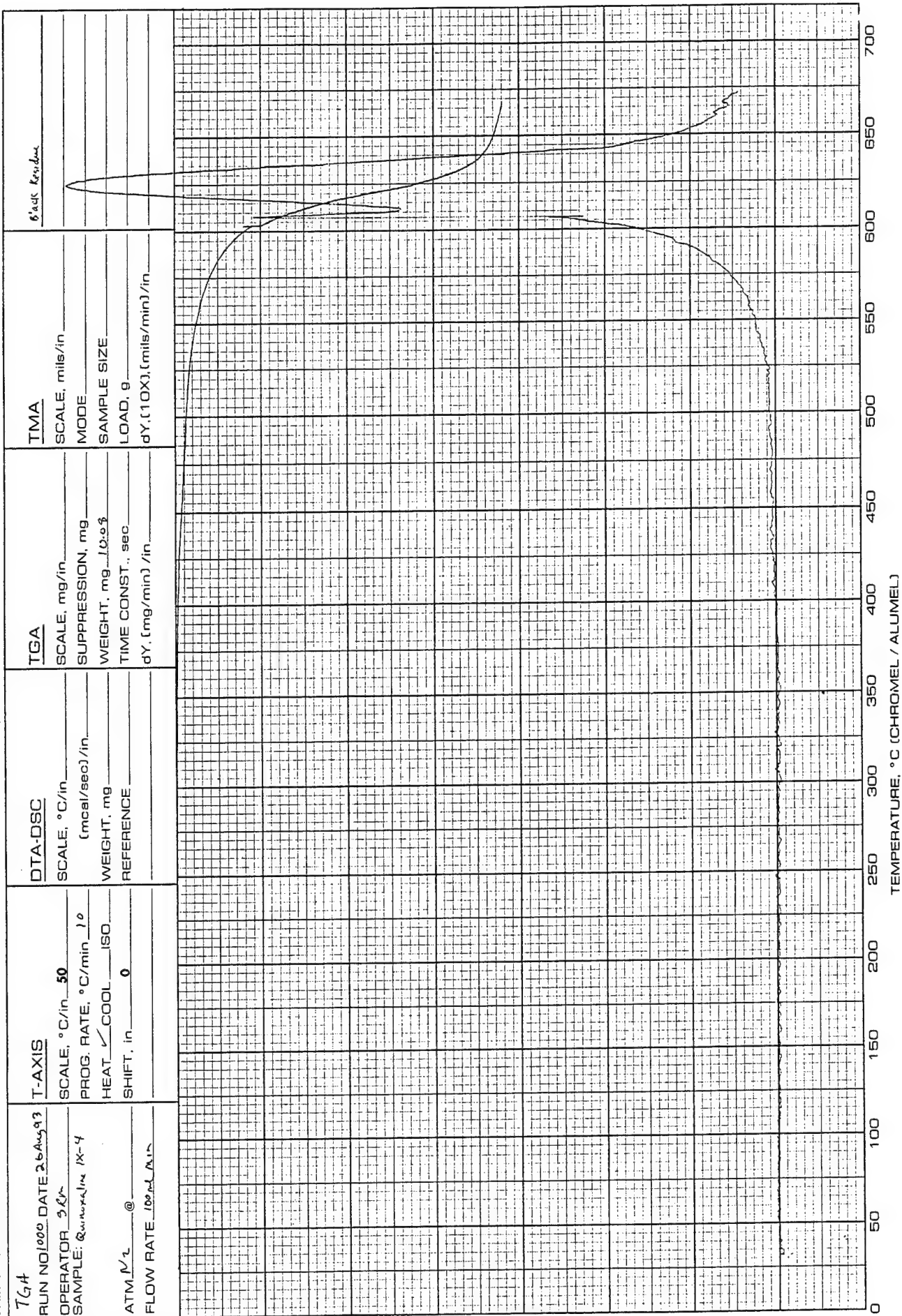


Figure 50. TGA scan of Quinoxaline IX-3 in air.

PART NO. 990088

Figure 52. TGA scan of Quinoxaline IX-4 in N₂.

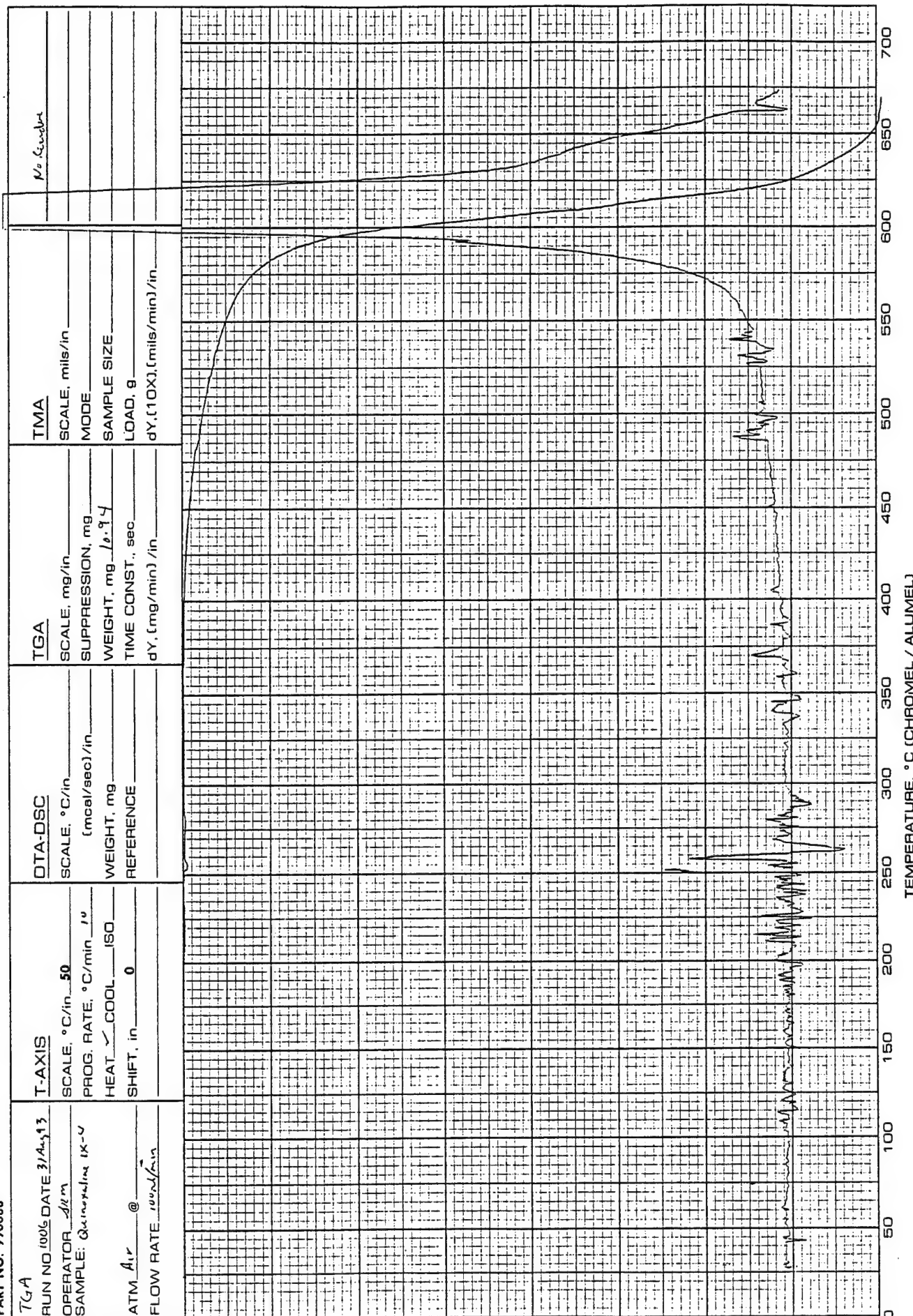


Figure 53. TGA scan of Quinoxaline IX-4 in air.

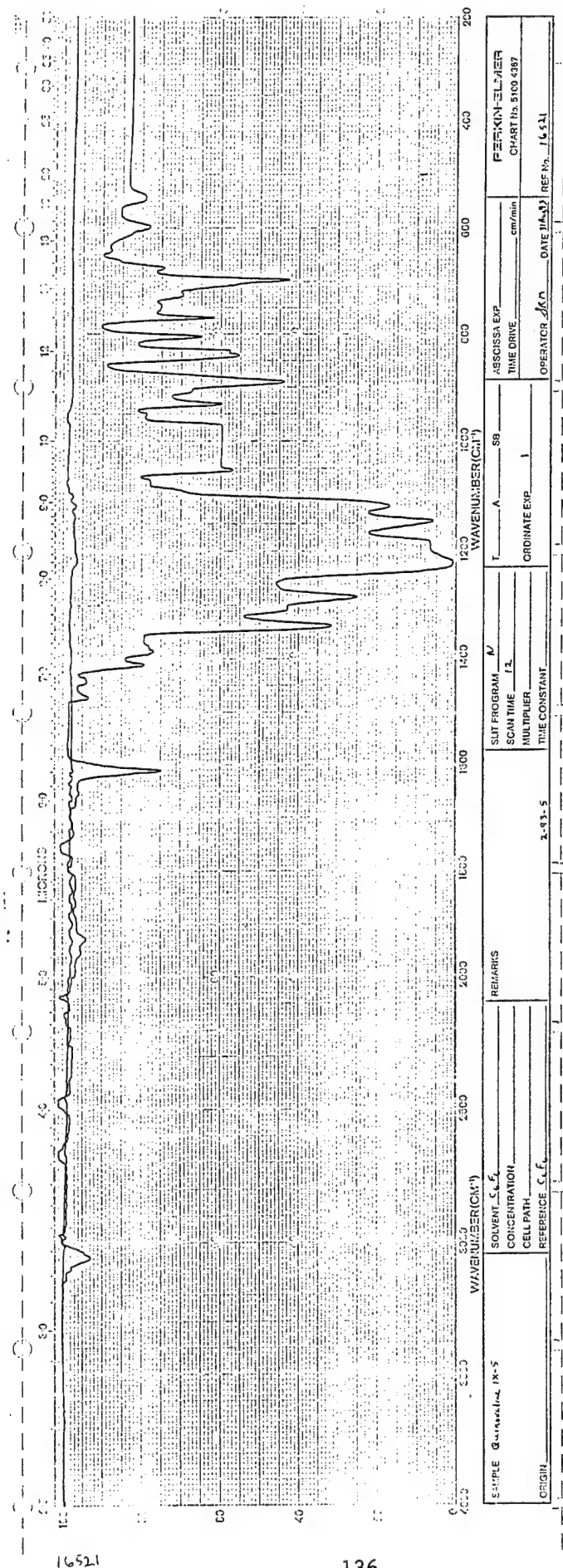
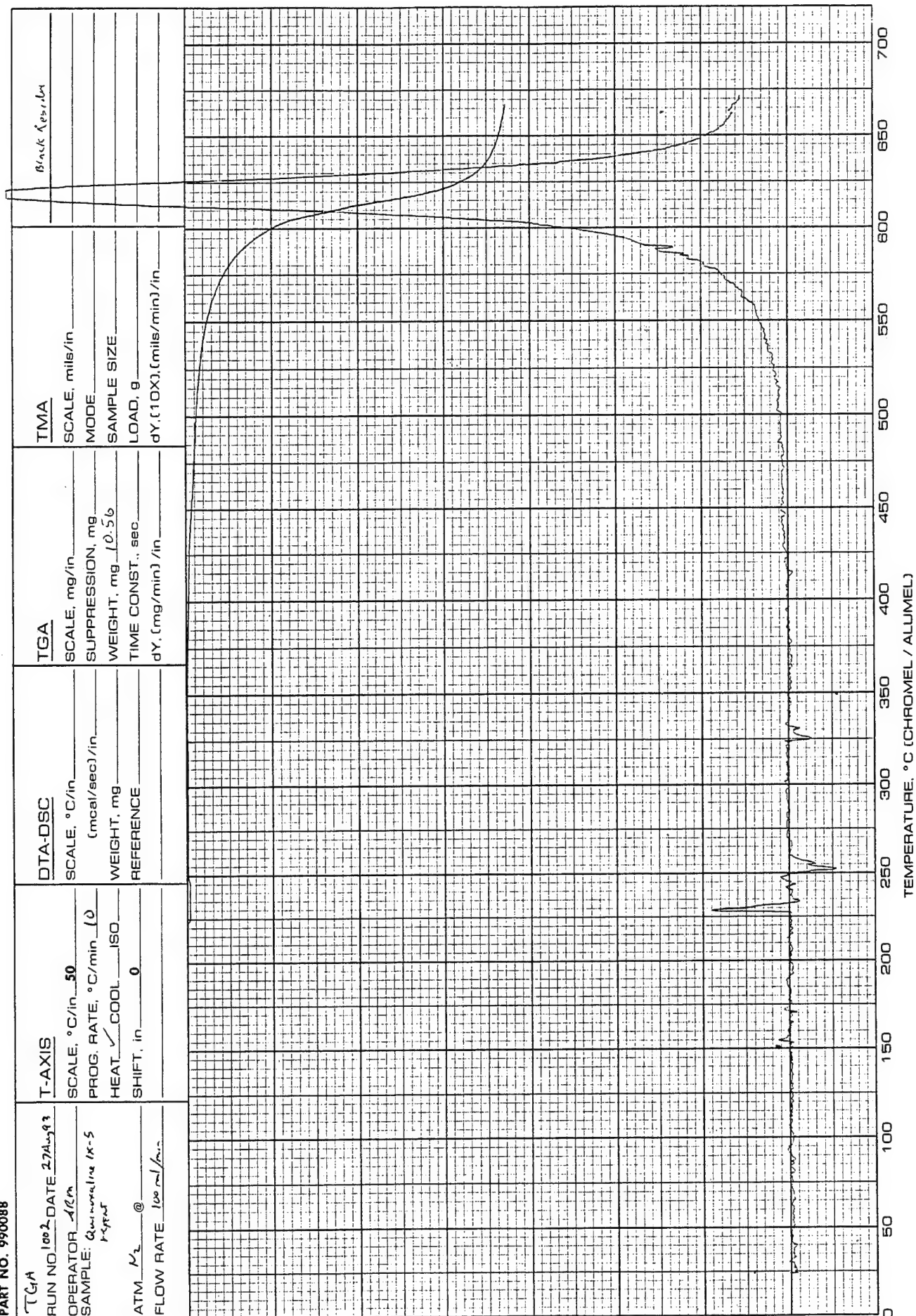


Figure 54. Infrared spectrum of Quinoxaline IX-5 (in C₆F₆; solvent subtracted).

Figure 55. TGA scan of Quinoxaline IX-5 in N₂.

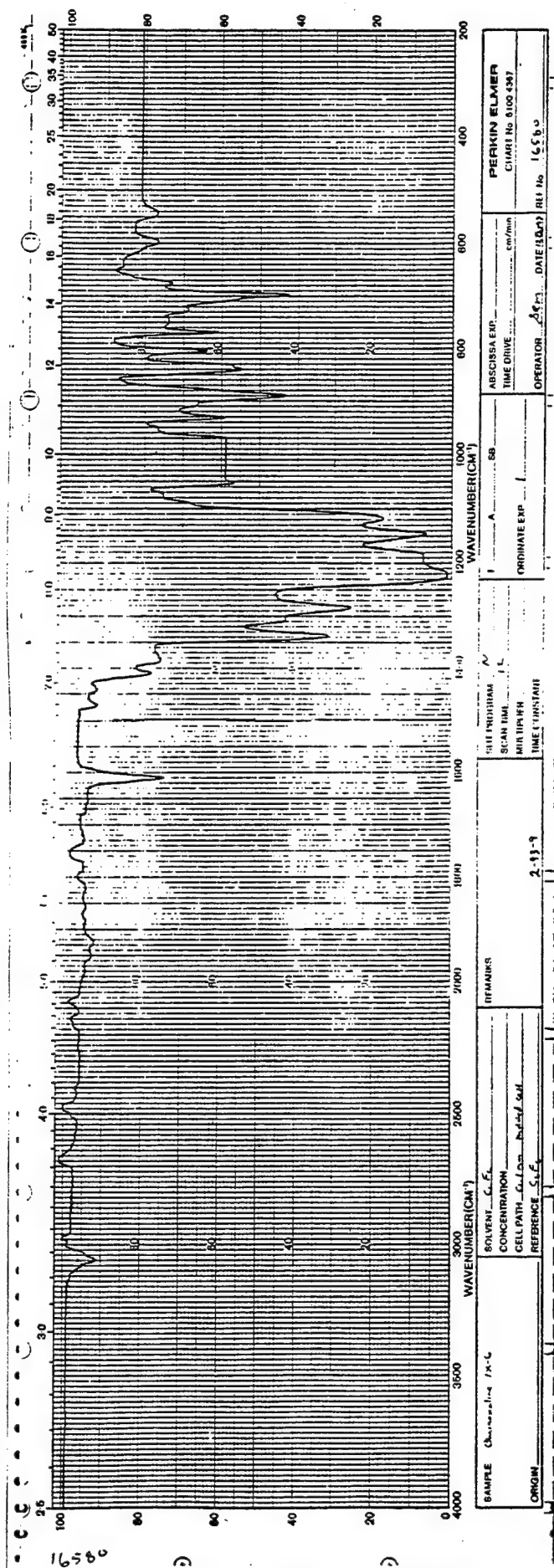
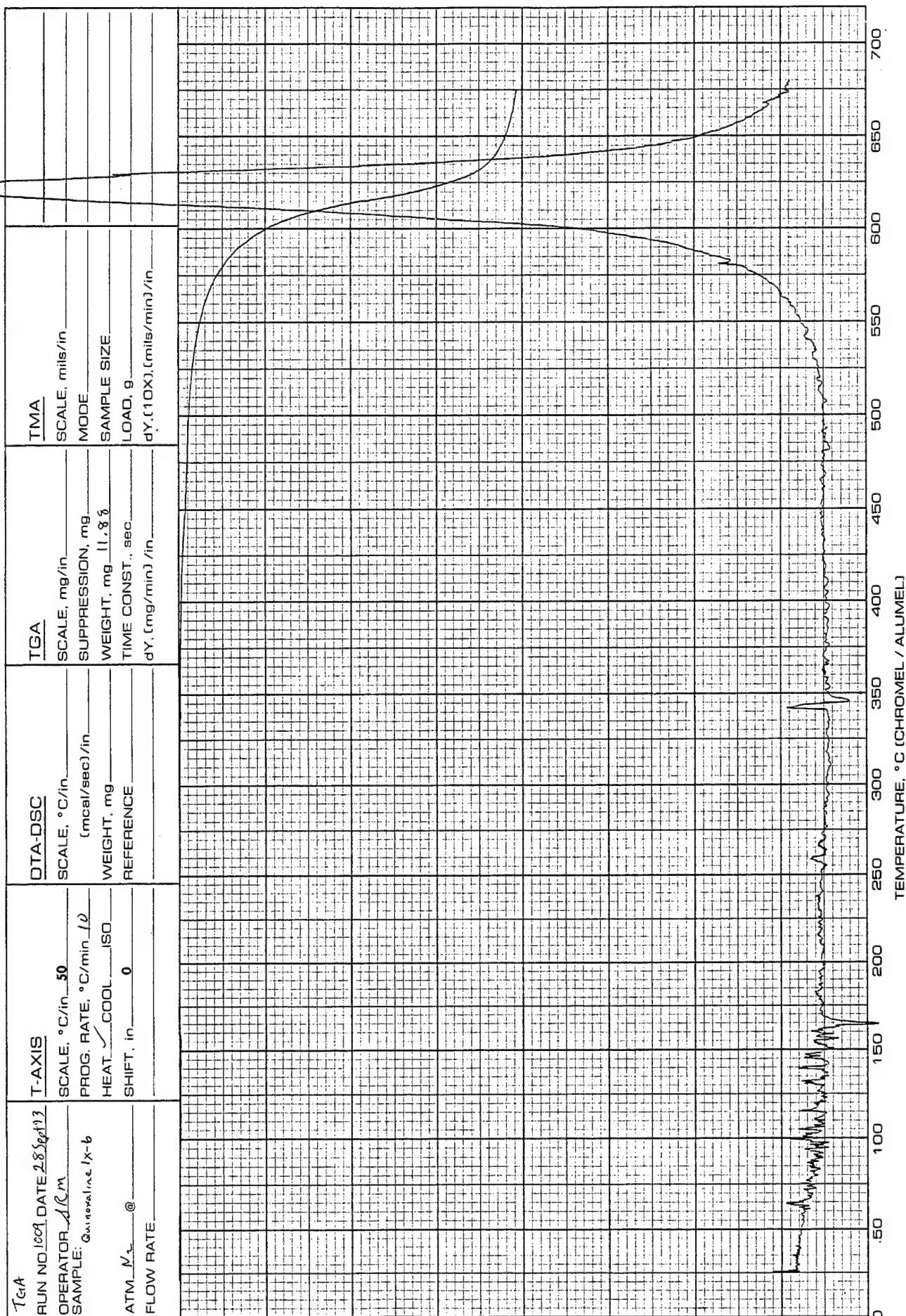


Figure 56. Infrared spectrum of quinoxaline IX-6.

Figure 57. TGA scan of Quinoxaline IX-6 in N₂.

6.3% $\text{C}_3\text{F}_7\text{O}[\text{CF}(\text{CF}_3)\text{CF}_2\text{O}]_2\text{CF}(\text{CF}_3)\text{C}(\text{O})\text{C}_6\text{H}_4\text{Br}$ (HFPO tetramer-substituted material). The compounds were characterized by MS spectra presented in Tables 28 and 29.

Preparation of $\text{C}_3\text{F}_7[\text{OCF}(\text{CF}_3)\text{CF}_2]_2\text{C}_6\text{H}_4\text{Br}$

$\text{C}_3\text{F}_7\text{OCF}(\text{CF}_3)\text{CF}_2\text{OCF}(\text{CF}_3)\text{C}(\text{O})\text{C}_6\text{H}_4\text{Br}$ (16.3 g, 25.7 mmol) was weighed into a 125 mL stainless steel Parr bomb. After adding water (1.5 mL) and Freon-113 (30 mL) the bomb was closed. The water was added to generate the HF catalyst. Subsequently, SF_4 (36.9 g, 342 mmol) was condensed at -78°C into a 95 mL monel bomb, weighed, then transferred into the 125 mL Parr bomb at -78°C . The Parr bomb was allowed to warm to room temperature followed by heating (in a sand bath, while shaken) for 42 hours at 220°C . After cooling to 0°C the bomb was vented and the reaction mixture poured into Freon-113 (100 mL) containing some sodium fluoride. Subsequently, the Freon-113 solution was washed with water (3 x 50 mL), dried over anhydrous magnesium sulfate and the solvent removed in vacuo. The residue (16.5 g) was distilled to give $\text{C}_3\text{F}_7\text{OCF}(\text{CF}_3)\text{CF}_2\text{OCF}(\text{CF}_3)\text{CF}_2\text{C}_6\text{H}_4\text{Br}$ (11.5 g, 68% yield) BP $94-95^\circ\text{C}/0.001$ mm Hg (purity 96%, GC). The MS is presented in Table 30.

Preparation Imide II

In an inert atmosphere enclosure CuI (0.30 g, 1.58 mmol; dried under vacuum <0.001 mm Hg, at $110-150^\circ\text{C}$ for 4 hours), potassium phthalimide (0.30 g, 1.62 mmol), and $\text{C}_3\text{F}_7[\text{OCF}(\text{CF}_3)\text{CF}_2]_2\text{C}_6\text{H}_4\text{Br}$ (1.01 g, 1.54 mmol) were introduced into dimethylacetamide (15 mL) in a 25 mL round bottom flask equipped

TABLE 28

ION FRAGMENTS AND INTENSITIES RELATIVE TO BASE PEAK OF



m/e	%	m/e	%	m/e	%	m/e	%
20	7.8	80	14.5	150	20.0	204	20.2
28	22.2	81	20.0	151	7.2	205	20.1
31	23.0	82	14.0	154	7.0	207	18.5
37	5.6	92	6.4	155	67.7	255	24.4
38	10.7	93	5.3	156	20.4	256	6.8
47	18.0	94	5.2	157	67.0	257	24.3
49	6.8	95	13.0	158	18.6	258	5.8
50	70.1	97	13.8	169	47.0	283	10.6
51	18.9	100	36.7	170	6.4	285	12.3
52	6.0	103	7.4	174	9.2	335	7.0
53	6.4	104	44.4	176	12.4	349	11.3
62	6.6	105	30.7	177	5.0	351	11.8
66	10.3	106	6.8	182	7.2	449	18.4
69	68.0	107	9.4	183	100.0	450	5.4
70	6.1	119	25.3	184	46.8	451	16.4
73	9.1	123	9.0	185	92.8	452	5.2
74	26.8	126	8.0	186	45.4	615	9.1
75	58.7	129	7.5	187	9.1	617	8.9
76	65.8	131	23.4	195	5.0	634	7.0M ⁺
77	23.2	133	6.0	201	5.0	636	7.3
78	12.9	145	5.8	202	10.4		
79	9.2	147	9.0	203	5.5		

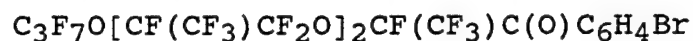
Peaks having intensities lower than 5% of the base peak and lower than m/e 20 are not reported.

Significant Ions in Support of Structure and Composition

m/e76 - C_6H_4^+ 155 - $\text{C}_6\text{H}_4\text{Br}^+$ 169 - C_3F_7^+ m/e183 - $\text{C}(\text{O})\text{C}_6\text{H}_4\text{Br}^+$ 283 - $\text{CF}(\text{CF}_3)\text{C}(\text{O})\text{C}_6\text{H}_4\text{Br}^+$ 615 - $[\text{M}-\text{F}]^+$

TABLE 29

ION FRAGMENTS AND INTENSITIES RELATIVE TO BASE PEAK OF



m/e	%	m/e	%	m/e	%	m/e	%
20	6.9	103	5.6	174	8.5	301	6.6
28	20.1	104	31.5	176	14.6	304	6.8
31	17.5	105	24.0	177	5.1	335	11.5
38	7.2	106	5.4	183	100.0	349	15.0
47	18.4	107	6.9	184	46.1	351	15.7
50	48.6	119	26.2	185	97.9	449	24.1
51	15.3	123	11.3	186	36.7	450	7.5
66	10.5	126	7.0	187	9.6	451	23.7
69	71.6	129	6.4	195	7.3	452	7.9
70	5.0	131	20.8	201	5.0	515	7.7
73	6.9	145	6.9	202	10.8	517	8.4
74	21.5	147	18.2	203	5.7	615	12.0
75	55.8	150	29.0	204	20.8	617	11.4
76	57.7	151	7.1	205	21.5	681	6.5
77	20.5	154	6.7	207	21.0	683	5.9
78	9.4	155	63.3	235	5.8	731	7.3
79	10.6	156	17.5	236	6.3	733	7.7
80	16.6	157	59.5	255	27.6	781	12.5
81	19.4	158	17.7	256	7.4	783	13.6
82	15.6	160	6.8	257	28.1	800	7.7M ⁺
95	11.1	162	5.0	258	6.7	802	7.1
97	18.0	169	62.6	283	12.7		
100	31.8	170	8.3	285	15.2		

Peaks having intensities lower than 5% of the base peak and lower than m/e 20 are not reported.

Significant Ions in Support of Structure and Composition

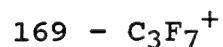
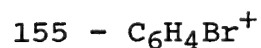
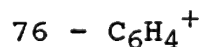
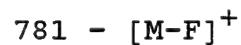
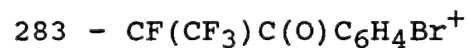
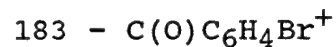
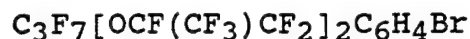
m/em/e

TABLE 30

ION FRAGMENTS AND INTENSITIES RELATIVE TO BASE PEAK OF



m/e	%	m/e	%	m/e	%	m/e	%
18	3.2	80	6.6	150	9.1	255	16.5
20	6.5	81	10.1	155	3.6	256	3.2
28	13.4	82	5.2	156	4.2	257	16.6
31	15.3	87	4.2	157	11.1	285	8.9
32	4.0	95	3.0	169	31.0	287	8.3
38	4.4	97	7.2	170	3.9	302	5.0
39	3.9	99	6.2	176	8.7	304	5.1
47	12.4	100	21.2	187	3.7	305	27.6
50	27.5	104	3.0	195	10.6	306	7.5
51	11.0	106	3.6	204	4.7	307	28.5
57	5.3	107	13.2	205	96.2	308	7.5
62	6.1	119	17.0	206	30.8	471	7.9
63	5.1	125	22.1	207	100.0	473	7.9
66	5.7	126	38.7	208	31.5	627	3.3
69	55.7	127	16.4	223	5.1	637	5.4
70	3.7	131	8.5	225	9.0	639	5.3
74	11.4	137	5.7	226	13.9	656	23.1M ⁺
75	21.2	138	5.1	227	3.4	657	7.6
76	15.8	144	3.2	236	6.9	658	23.1
77	3.6	145	14.5	238	6.6	659	7.8
78	3.9	147	5.4	245	4.4		

Peaks having intensities lower than 3% of the base peak and lower than m/e 18 are not reported.

Significant Ions in Support of Structure and Composition

m/e76 - C₆H₄⁺169 - C₃F₇⁺205 - CF₂C₆H₄Br⁺m/e305 - CF(CF₃)CF₂C₆H₄Br⁺471 - [M-C₃F₇O]⁺637 - [M-F]⁺

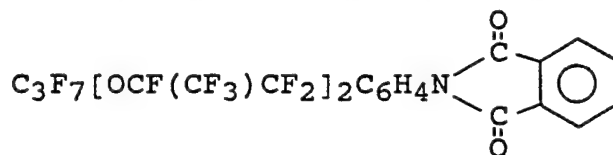
with a magnetic stirrer, reflux condenser, and nitrogen inlet. The reaction mixture was refluxed under nitrogen bypass for 24 hours. After cooling, it was precipitated into hydrochloric acid (15 mL, 4N). The precipitate was taken up into methylene chloride; the organic layer washed with water (7 x 10 mL) and dried over anhydrous magnesium sulfate. The crude product (1.05 g), left after solvent evaporation, was dissolved in benzene and purified by silica gel column chromatography (50 g, 21 cm x 2.8 cm). The following solvents were employed: hexanes (165 mL), benzene (135 mL), and ether (225 mL). This process resulted in Imide II (0.57 g, 51% yield) MP 82.5-85°C (purity 99%, GC; includes 2% HFPO tetramer-substituted analogue). The MS is presented in Table 31 (MS of the HFPO tetramer-substituted analogue is given in Table 32). The IR is presented in Figure 58 and the TGA scans, in nitrogen and air, in Figures 59 and 60, respectively.

Preparation of $\text{BrC}_6\text{H}_4\text{C}(\text{O})\text{CF}_2\text{CF}_2(\text{OCF}_2\text{CF}_2)_5\text{C}(\text{O})\text{C}_6\text{H}_4\text{Br}$

p-Dibromobenzene (17.7 g, 75.0 mmol) in diethyl ether (150 mL) was introduced into a 250 mL, 3-neck round bottom flask equipped with a magnetic stirrer and two 50 mL addition funnels. One addition funnel contained $\text{MeO}_2\text{C}(\text{CF}_2\text{CF}_2\text{O})_5\text{CF}_2\text{CF}_2\text{CO}_2\text{Me}$ (29.9 g, 37.5 mmol) and the other n-butyllithium (31 mL, 2.5 M) (transferred via a syringe). Under nitrogen bypass to the p-dibromobenzene solution, cooled to -6°C in an ice/salt bath n-butyllithium was added dropwise over 25 minutes. The reaction mixture was then stirred at -6°C for 1 hour. Subsequently, it

TABLE 31

ION FRAGMENTS AND INTENSITIES RELATIVE TO BASE PEAK OF



m/e	%	m/e	%	m/e	%	m/e	%
20	6.8	100	10.3	135	2.8	353	3.2
28	4.5	102	8.5	136	7.7	372	11.9
31	10.9	103	6.6	140	3.8	373	3.2
39	2.4	104	19.5	150	4.0	418	4.1
47	8.4	105	2.8	151	5.5	438	4.3
50	22.5	112	2.1	152	2.8	468	2.2
51	4.5	113	5.5	168	16.6	538	6.5
62	2.9	114	7.2	169	19.3	604	8.4
63	5.5	119	8.8	170	2.0	605	2.5
66	2.9	120	2.1	215	2.5	654	2.3
69	34.8	122	2.4	228	2.2	684	2.0
74	5.8	125	4.1	271	4.8	704	13.3
75	11.5	126	16.6	272	100.0	705	4.5
76	28.5	127	2.7	273	34.8	723	40.4M ⁺
77	5.3	130	31.7	274	8.9	724	16.3
90	2.1	131	9.7	322	5.6	725	4.1
97	3.1	132	2.9	352	8.6		

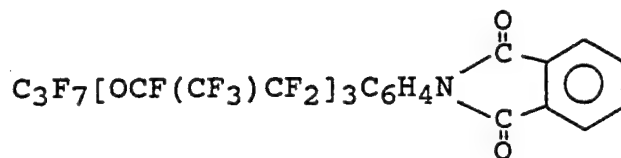
Peaks having intensities lower than 2% of the base peak and lower than m/e 20 are not reported.

Significant Ions in Support of Structure and Composition

m/e76 - C₆H₄⁺104 - C₆H₄C(O)⁺169 - C₃F₇⁺m/e272 - CF₂C₆H₄N(CO)₂C₆H₄⁺372 - CF(CF₃)CF₂C₆H₄N(CO)₂C₆H₄⁺704 - [M - F]⁺

TABLE 32

ION FRAGMENTS AND INTENSITIES RELATIVE TO BASE PEAK OF



m/e	%	m/e	%	m/e	%	m/e	%
17	5.7	103	4.4	169	28.2	355	2.5
18	8.3	104	16.2	177	2.3	357	2.0
20	6.5	112	2.3	191	3.9	372	14.7
28	13.4	113	3.1	193	3.1	373	3.4
31	7.0	114	4.8	207	21.9	418	4.1
32	7.7	119	14.1	208	9.1	429	2.0
47	8.2	125	2.3	209	6.6	438	4.2
50	12.0	126	14.6	219	2.2	503	3.1
51	2.4	127	2.5	221	2.4	538	10.2
66	2.9	130	32.4	271	3.5	539	2.2
69	38.4	131	9.5	272	100.0	604	11.7
73	9.4	133	3.7	273	42.5	605	2.4
74	3.1	135	3.5	274	10.3	701	3.1
75	8.1	136	10.1	281	11.4	704	3.6
76	19.7	140	2.8	282	6.3	723	7.7
77	3.1	145	2.3	283	3.7	754	4.1
79	2.7	147	13.5	290	2.3	770	6.9
85	4.0	149	2.0	322	5.7	773	17.0
96	3.9	150	5.9	335	2.0	774	4.3
97	4.4	151	7.1	341	2.1	820	4.1
100	10.5	152	2.6	352	10.7		
102	4.0	168	13.4	353	2.5		

Peaks having intensities lower than 2% of the base peak and lower than m/e 17 are not reported. Peaks above m/e 831 are not present because they are above the scanning range used.

Significant Ions in Support of Structure and Composition

m/e	m/e
76 - C_6H_4^+	272 - $\text{CF}_2\text{C}_6\text{H}_4\text{N}(\text{CO})_2\text{C}_6\text{H}_4^+$
104 - $\text{C}_6\text{H}_4\text{C}(\text{O})^+$	372 - $\text{CF}(\text{CF}_3)\text{CF}_2\text{C}_6\text{H}_4\text{N}(\text{CO})_2\text{C}_6\text{H}_4^+$
169 - C_3F_7^+	604 - $[\text{M} - \text{C}_3\text{F}_7\text{OCF}(\text{CF}_3)]^+$

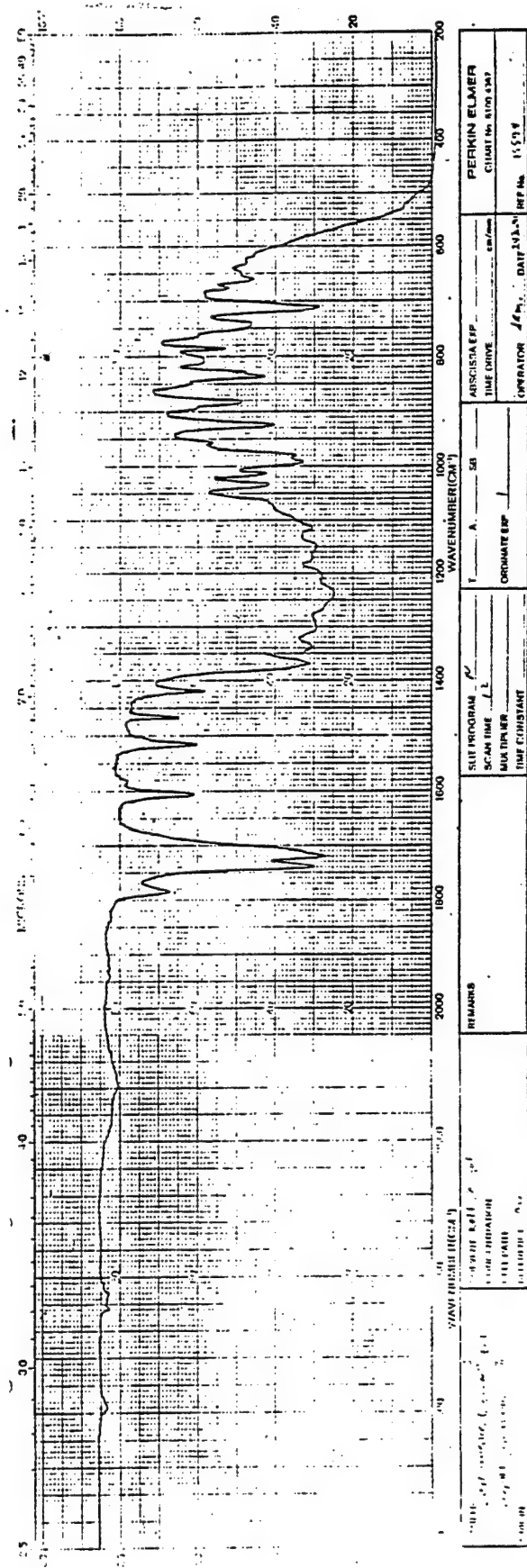
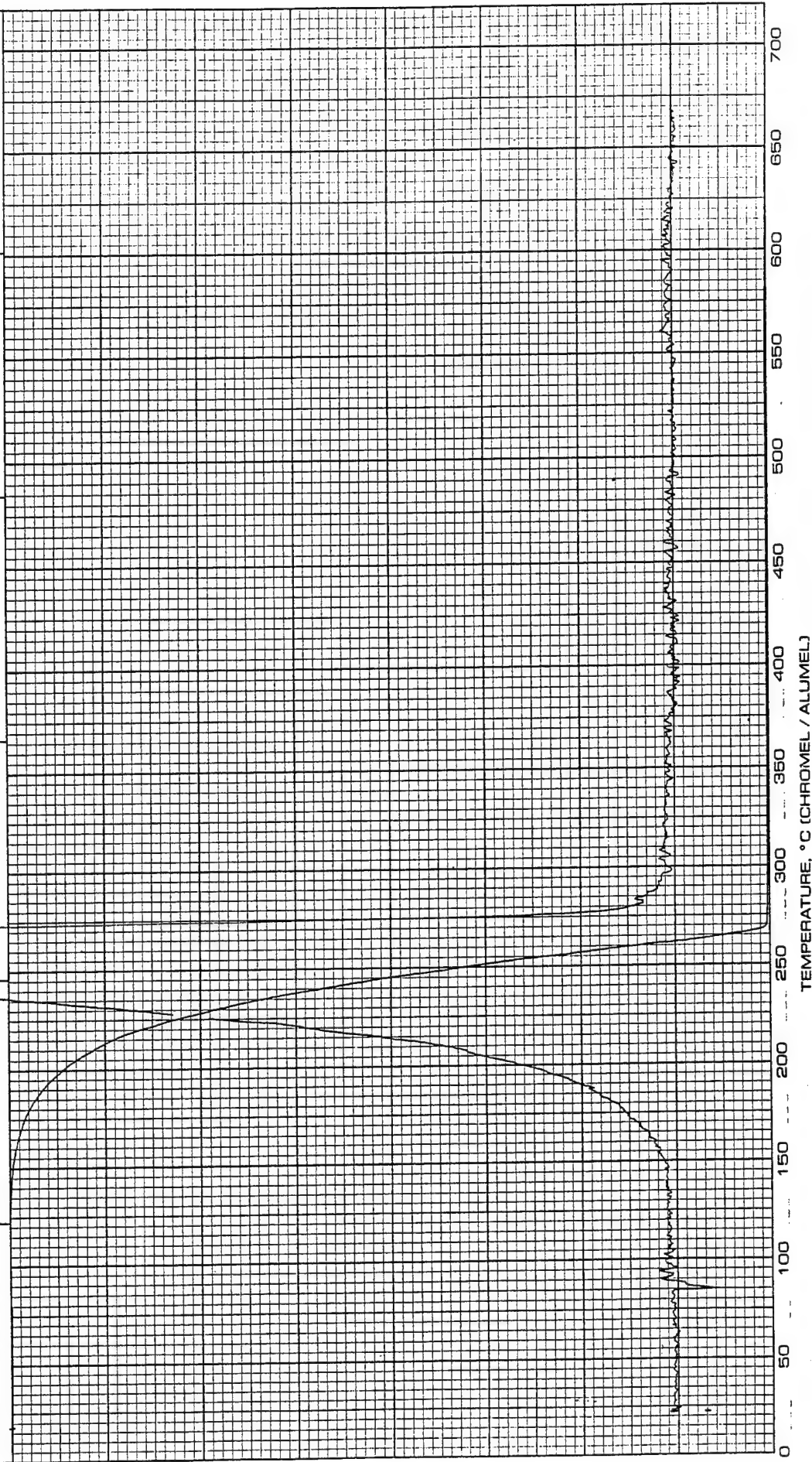


Figure 58. Infrared spectrum of Imide II.

TGA RUN NO. <u>1023</u> DATE <u>7 Oct 1993</u> OPERATOR _____ SAMPLE: <u>Imide II</u> ATM. <u>N₂</u> @ _____ FLOW RATE _____		T-AXIS SCALE, °C/in. <u>50</u> PROG. RATE, °C/min. <u>10</u> HEAT <input checked="" type="checkbox"/> COOL <input type="checkbox"/> ISO SHIFT, in. <u>0</u>		DTA-DSC SCALE, °C/in. _____ (mcal/sec)/in. _____ WEIGHT, mg _____ REFERENCE _____		TGA SCALE, mg/in. _____ SUPPRESSION, mg _____ WEIGHT, mg <u>10.93</u> TIME CONST., sec _____ dY, (mg/min) / in. _____		TMA SCALE, mils/in. _____ MODE _____ SAMPLE SIZE _____ LOAD, g _____ dY, (10X), (mils/min) / in. _____		<u>1-96-116</u>
---	--	--	--	--	--	---	--	--	--	-----------------

Figure 59. TGA scan of Imide II in N₂.

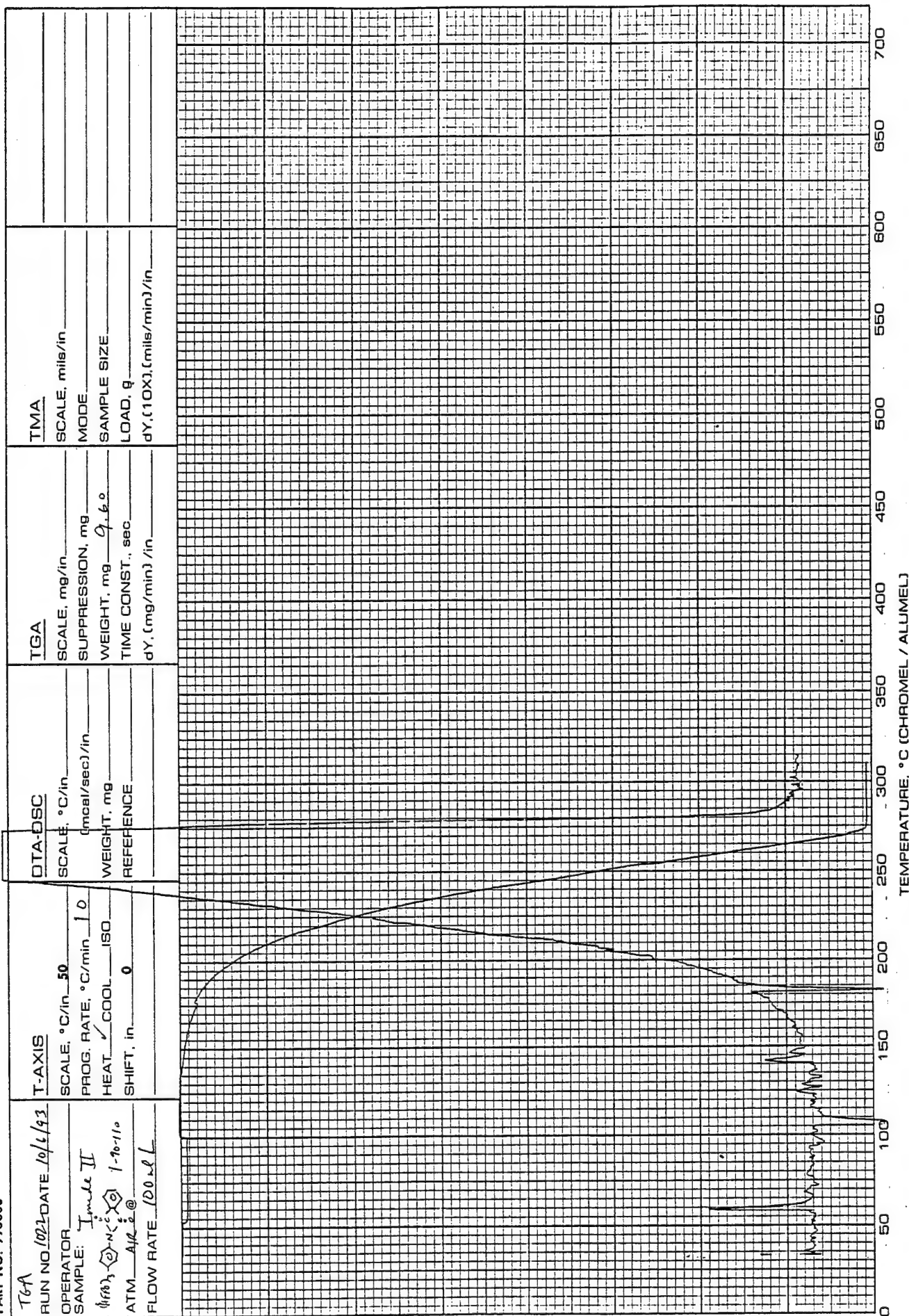


Figure 60. TGA scan of Imide II in air.

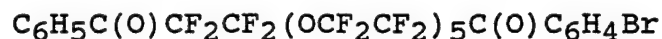
was cooled to -78°C (with a dry ice/acetone bath) and the methyl ester was added over a period of 45 minutes. The reaction mixture was maintained successively at -78 , -40 , and -20°C for 1 hour at each temperature. Following recooling to -78°C , it was quenched with hydrochloric acid (50 mL, 2 N). After warming to room temperature, the ether layer was separated, washed with water (3 x 50 mL), and dried over anhydrous magnesium sulfate, and the solvent removed in vacuum. The solid (37.2 g, 95% yield) consisted of 82% of the desired product based on GC analysis. The major impurity was $\text{C}_6\text{H}_5\text{C}(\text{O})\text{CF}_2\text{CF}_2(\text{OCF}_2\text{CF}_2)_5\text{C}(\text{O})\text{C}_6\text{H}_4\text{Br}$ (MS, Table 33). Crystallization from ether gave pure $\text{BrC}_6\text{H}_4\text{C}(\text{O})\text{CF}_2\text{CF}_2(\text{OCF}_2\text{CF}_2)_5\text{C}(\text{O})\text{C}_6\text{H}_4\text{Br}$, MP $65-66^{\circ}\text{C}$; IR is presented in Figure 61, MS is presented in Table 34.

Preparation of $\text{BrC}_6\text{H}_4\text{C}_3\text{F}_6\text{O}(\text{CF}_2\text{CF}_2\text{O})_4\text{C}_3\text{F}_6\text{C}_6\text{H}_4\text{Br}$

$\text{BrC}_6\text{H}_4\text{C}(\text{O})\text{CF}_2\text{CF}_2(\text{OCF}_2\text{CF}_2)_5\text{C}(\text{O})\text{C}_6\text{H}_4\text{Br}$ (16.5 g, 15.7 mmol) was weighed into a 125 mL Parr stainless steel pressure reactor, followed by addition of Freon-113 (25 mL). Under nitrogen atmosphere, the reactor was cooled in a dry ice/acetone bath to below room temperature, and then hydrogen fluoride (20 mL) at -20°C was quickly poured into the reactor which was closed immediately with a head assembly equipped with a gauge. Sulfur tetrafluoride (10.1 g, 93.5 mmol) was then condensed into the reactor via a pressure hose. The sealed reactor was next heated in a sand bath at $148-158^{\circ}\text{C}$ for 18 hours while agitated by a mechanical shaker. It should be noted that conducting the process at 220°C gave disulfide by-product identified by its MS

TABLE 33

ION FRAGMENTS AND INTENSITIES RELATIVE TO BASE PEAK OF



m/e	%	m/e	%	m/e	%	m/e	%
18	3.1	96	3.5	183	84.9	399	11.2
20	14.5	97	6.9	184	21.3	401	11.3
28	8.2	100	16.3	185	78.0	437	15.9
31	7.3	104	11.5	186	21.1	515	8.7
47	15.4	105	<u>100.0</u>	205	18.6	517	8.6
50	12.1	106	33.2	206	3.8	553	7.2
51	20.5	107	4.1	207	8.8	631	3.5
66	8.9	119	29.8	208	5.7	633	3.7
74	6.5	123	5.0	221	5.2	784	4.6
75	15.8	127	8.6	225	5.5	869	3.3
76	8.9	151	3.3	263	8.1	888	26.7
77	42.6	155	26.9	264	4.5	889	9.1
78	11.2	156	4.1	271	4.5	949	3.2
79	4.2	157	23.7	283	8.8	968	21.9M ⁺
80	11.5	158	3.5	285	7.7	969	7.2
81	6.7	180	3.0	301	3.3	970	19.6
82	11.0	181	4.2	321	19.5	971	6.0

Peaks having intensities lower than 3% of the base peak and lower than m/e 18 are not reported.

Significant Ions in Support of Structure and Composition

m/e	m/e
77 - C_6H_5^+	283 - $\text{BrC}_6\text{H}_4\text{C}(\text{O})\text{CF}_2\text{CF}_2^+$
105 - $\text{C}_6\text{H}_5\text{CO}^+$	321 - $\text{C}_6\text{H}_5\text{C}(\text{O})\text{CF}_2\text{CF}_2\text{OCF}_2\text{CF}_2^+$
155 - BrC_6H_4^+	399 - $\text{BrC}_6\text{H}_4\text{C}(\text{O})\text{CF}_2\text{CF}_2\text{OCF}_2\text{CF}_2^+$
183 - $\text{BrC}_6\text{H}_4\text{CO}^+$	888 - $[\text{M} - \text{HBr}]^+$
205 - $\text{C}_6\text{H}_5\text{C}(\text{O})\text{CF}_2\text{CF}_2^+$	949 - $[\text{M} - \text{F}]^+$

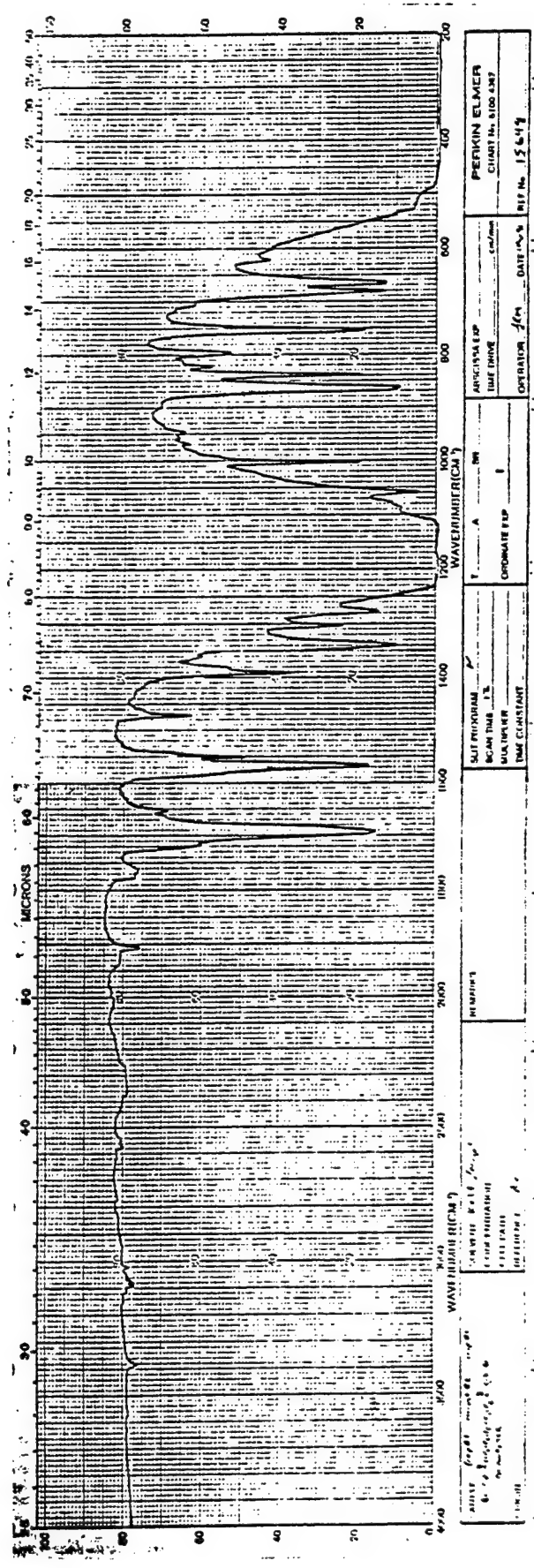


Figure 61. Infrared spectrum of $\text{BrC}_6\text{H}_4\text{C}(\text{O})\text{CF}_2\text{CF}_2(\text{OCF}_2\text{CF}_2)_5\text{C}(\text{O})\text{C}_6\text{H}_4\text{Br}$ (1-90-126).

TABLE 34

ION FRAGMENTS AND INTENSITIES RELATIVE TO BASE PEAK OF



m/e	%	m/e	%	m/e	%	m/e	%
20	9.8	104	19.1	184	36.5	351	7.1
28	16.2	105	7.2	185	98.5	399	18.9
31	16.1	119	41.0	186	36.3	401	18.5
47	19.7	123	9.5	187	7.5	515	16.6
50	26.1	125	6.9	201	10.1	517	15.8
51	10.8	126	7.9	202	9.1	631	8.8
66	14.6	131	6.6	203	6.6	633	8.9
69	15.2	145	5.2	204	9.2	784	5.9
74	15.8	151	7.2	205	15.2	860	5.9
75	30.6	152	6.7	207	11.2	888	14.6
76	30.8	154	8.6	223	5.0	889	6.6
77	9.6	155	38.7	257	5.3	966	18.5
78	6.0	156	12.6	259	6.7	967	10.1
79	15.2	157	37.6	261	7.0	968	16.0
80	16.7	158	11.9	282	5.3	969	9.2
81	21.3	173	5.9	283	17.8	1029	6.7
82	17.5	174	7.4	284	7.2	1046	19.9M ⁺
95	8.3	176	10.5	285	17.6	1048	37.4
97	15.3	179	5.6	299	9.0	1049	13.6
100	22.0	182	5.2	301	9.1	1050	16.6
101	5.1	183	<u>100.0</u>	349	7.0	1051	7.5

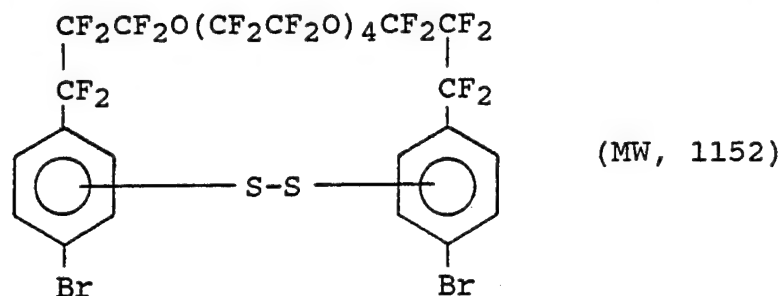
Peaks having intensities lower than 5% of the base peak and lower than m/e 20 are not reported.

Significant Ions in Support of Structure and Composition

m/e	m/e
155 - BrC_6H_4^+	888 - $[\text{M} - 2\text{Br}]^+$
183 - $\text{BrC}_6\text{H}_4\text{CO}^+$	966 - $[\text{M} - \text{HBr}]^+$
283 - $\text{BrC}_6\text{H}_4\text{C}(\text{O})\text{CF}_2\text{CF}_2^+$	967 - $[\text{M} - \text{Br}]^+$
399 - $\text{BrC}_6\text{H}_4\text{C}(\text{O})\text{CF}_2\text{CF}_2\text{OCF}_2\text{CF}_2^+$	1027 - $[\text{M} - \text{F}]^+ (3.7\%)$
515 - $\text{BrC}_6\text{H}_4\text{C}(\text{O})\text{CF}_2\text{CF}_2(\text{OCF}_2\text{CF}_2)_2^+$	

TABLE 35

ION FRAGMENTS AND INTENSITIES RELATIVE TO BASE PEAK OF



m/e	%	m/e	%	m/e	%	m/e	%
31	17.3	125	6.8	255	4.0	866	7.9
32	6.0	131	4.1	257	17.4	928	7.1
44	7.0	157	49.8	263	8.6	962	8.0
45	5.0	158	14.9	269	6.1	975	8.1
47	28.9	159	4.9	282	4.4	985	8.5
50	17.5	160	7.8	313	14.1	987	14.2
51	5.8	163	4.6	314	6.2	988	5.4
63	11.4	176	5.3	333	6.8	989	8.3
64	4.4	188	13.0	335	7.1	994	<u>100.0</u>
66	19.3	189	10.7	336	9.6	995	38.6
69	25.2	192	4.1	338	9.7	996	22.6
75	6.1	194	4.6	373	4.3	997	6.5
79	16.6	204	5.6	381	5.0	1022	6.4
80	18.9	206	8.9	452	6.1	1040	6.3
81	21.9	207	9.7	454	5.2	1042	5.7
82	24.5	225	4.3	568	4.7	1054	6.2
97	8.9	236	30.1	570	4.3	1056	6.5
100	19.9	237	13.0	577	9.9		
113	4.8	238	34.8	762	5.1		
119	46.0	239	8.8	861	5.3		

Peaks having intensities lower than 4% of the base peak and lower than m/e 31 are not reported.

Significant Ions in Support of Structure and Composition

m/e	m/e
157 - $\text{CF}_2\text{C}_6\text{H}_3\text{S}^+$	257 - $\text{C}_3\text{F}_6\text{C}_6\text{H}_3\text{S}^+$
189 - $\text{CF}_2\text{C}_6\text{H}_3\text{SS}^+$	994 - $[\text{M}-2\text{Br}]^+$
236 - $\text{CF}_2\text{C}_6\text{H}_3(\text{S})\text{Br}^+$	

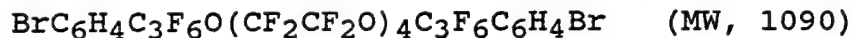
given in Table 35. After cooling to room temperature, the pressure was released by venting and the contents were poured onto crushed ice. The reactor was rinsed with additional Freon-113. The reaction mixture was neutralized with aqueous sodium bicarbonate solution; and following separation of the organic phase, the aqueous layer was extracted with ether (100 mL) and combined with the Freon-113 layer. The combined organic layer was dried over anhydrous magnesium sulfate and the solvent removed in vacuum. The residue, a brown liquid (14.5 g), contained 86% of the desired product as determined by GC. After removal of sulfur (by sublimation), the residue was distilled to give $\text{BrC}_6\text{H}_4\text{C}_3\text{F}_6\text{O}(\text{CF}_2\text{CF}_2\text{O})_4\text{C}_3\text{F}_6\text{C}_6\text{H}_4\text{Br}$ (6.9 g, 40% yield), BP 108-112°C/0.001 mm Hg. The MS is presented in Table 36 and the IR in Figure 62. The major byproduct formed was $\text{C}_6\text{H}_5\text{C}_3\text{F}_6\text{O}(\text{CF}_2\text{CF}_2\text{O})_4\text{C}_3\text{F}_6\text{C}_6\text{H}_4\text{Br}$, its MS is given in Table 37.

Preparation of Imide III

The dibromide, $\text{BrC}_6\text{H}_4\text{C}_3\text{F}_6\text{O}(\text{CF}_2\text{CF}_2\text{O})_4\text{C}_3\text{F}_6\text{C}_6\text{H}_4\text{Br}$, (3.1 g, 2.8 mmol) was mixed with potassium phthalimide (1.1 g, 5.6 mmol) and CuI (1.04 g, 5.5 mmol) in dimethylacetamide (50 mL). The reaction mixture was refluxed for 24 hours. After cooling, a 0.5 mL aliquot was quenched with 3N hydrochloric acid, extracted with methylene chloride, and analyzed by gas chromatography. GC analysis showed a trace of unreacted dibromide, so an additional quantity of potassium phthalimide (0.3 g, 1.8 mmol) was added and refluxing continued for 16 hours. Based on GC, the above procedure failed to remove the last traces of the dibromide. The

TABLE 36

ION FRAGMENTS AND INTENSITIES RELATIVE TO BASE PEAK OF



m/e	%	m/e	%	m/e	%	m/e	%
31	8.3	100	16.1	223	3.9	421	15.3
32	11.5	107	3.3	224	3.5	423	14.3
44	4.3	119	60.6	225	3.9	537	7.5
47	17.6	125	7.8	226	5.6	539	6.8
50	14.4	126	23.0	236	3.6	652	4.1
51	4.4	127	4.4	238	3.2	654	3.8
64	24.0	128	7.1	251	4.1	932	34.9
66	17.7	131	6.3	255	5.6	933	11.0
69	20.3	145	13.9	256	8.4	993	19.5
75	8.0	157	3.7	257	5.9	994	4.6
76	7.3	160	6.5	258	3.2	1010	20.2
79	8.6	169	3.8	283	4.4	1011	7.9
80	17.5	176	6.2	285	10.8	1012	20.1
81	12.5	192	3.9	287	7.6	1013	9.2
82	17.0	205	97.2	305	25.2	1053	3.4
85	3.7	206	21.5	306	4.9		
96	4.1	207	<u>100.0</u>	307	25.2		
97	8.8	208	21.2	308	3.1		

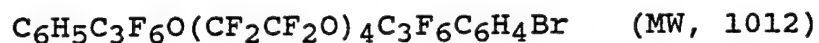
Peaks having intensities lower than 3% of the base peak and lower than m/e 31 are not reported.

Significant Ions in Support of Structure and Composition

m/e	m/e
205 - $\text{CF}_2\text{C}_6\text{H}_4\text{Br}^+$	932 - $[\text{M}-2\text{Br}]^+$
305 - $\text{C}_3\text{F}_6\text{C}_6\text{H}_4\text{Br}^+$	1010 - $[\text{M}-\text{HBr}]^+$
421 - $\text{CF}_2\text{CF}_2\text{OC}_3\text{F}_6\text{C}_6\text{H}_4\text{Br}^+$	

TABLE 37

ION FRAGMENTS AND INTENSITIES RELATIVE TO BASE PEAK OF



m/e	%	m/e	%	m/e	%	m/e	%
31	12.4	125	13.9	226	8.6	537	4.7
47	16.0	126	33.7	227	36.5	539	4.8
50	21.5	127	95.5	228	6.5	575	6.1
51	14.8	128	28.3	245	7.5	913	5.3
66	10.1	145	15.5	251	7.8	932	46.0
69	14.2	146	5.7	252	6.7	933	23.7
74	6.2	157	5.6	255	6.7	934	6.2
75	17.0	158	9.2	257	6.3	973	4.8
76	6.6	176	9.7	283	7.0	975	4.7
77	17.6	177	14.3	285	8.6	993	8.3
78	4.3	185	4.3	287	6.8	995	7.9
79	7.0	195	6.4	305	17.6	1009	4.3
80	8.2	201	4.4	306	4.0	1012	<u>100.0M</u> ⁺
81	14.2	205	86.9	307	18.0	1013	37.8
82	7.1	206	19.3	321	5.0	1014	89.2
97	14.6	207	91.3	343	13.2	1015	34.4
100	28.0	208	21.7	351	7.4	1016	8.2
107	10.1	223	4.6	421	9.0		
119	50.4	224	4.5	423	10.5		
120	5.1	225	5.0	459	9.1		

Peaks having intensities lower than 4% of the base peak and lower than m/e 31 are not reported.

Significant Ions in Support of Structure and Composition

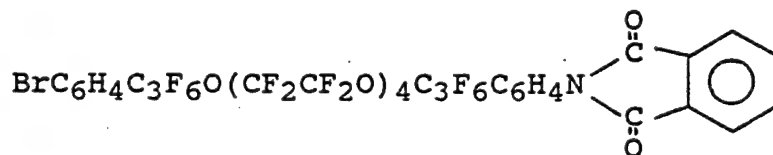
m/e

77 - C_6H_5^+
 127 - $\text{CF}_2\text{C}_6\text{H}_5^+$
 177 - $\text{CF}_2\text{CF}_2\text{C}_6\text{H}_5^+$
 205 - $\text{CF}_2\text{C}_6\text{H}_4\text{Br}^+$
 227 - $\text{C}_3\text{F}_6\text{C}_6\text{H}_5^+$

m/e

305 - $\text{C}_3\text{F}_6\text{C}_6\text{H}_4\text{Br}^+$
 343 - $\text{CF}_2\text{CF}_2\text{OC}_3\text{F}_6\text{C}_6\text{H}_5^+$
 421 - $\text{CF}_2\text{CF}_2\text{OC}_3\text{F}_6\text{C}_6\text{H}_4\text{Br}^+$
 932 - $[\text{M}-\text{HBr}]^+$
 993 - $[\text{M}-\text{F}]^+$

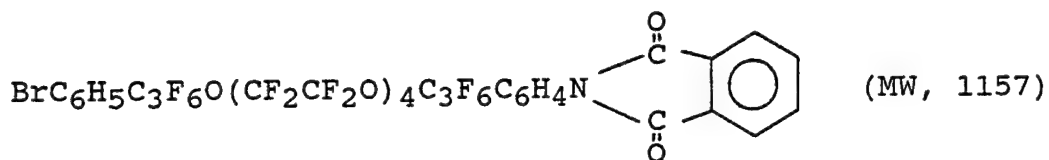
reaction mixture was thus poured into 4N hydrochloric acid (50 mL). The precipitate which formed was dissolved on addition of methylene chloride (50 mL); the methylene chloride layer was separated from the aqueous layer and washed with water (5 x 25 mL). Washing with water resulted in more precipitation. Part of the precipitate was suspended in the water layer and was removed with the aqueous layer. The rest of the precipitate settled to the bottom of the organic layer and was removed by centrifuging the sample. The organic layer was dried over anhydrous magnesium sulfate and the solvent removed in vacuum, leaving 3.83 g of a reddish brown solid. GC/MS analysis showed traces of unreacted dibromide and the monosubstituted imide (MS Table 38).



A portion of the crude product (1.1 g) was purified by column chromatography using silica gel (25 g, 19 cm x 2.2 cm) and elution with benzene (100 mL), followed by ether (170 mL). The benzene fraction (0.56 g) was recrystallized from ether/hexanes (2 mL/20 mL) and resulted in 0.38 g (38 % yield) of Imide III, MP 136-138°C. Anal. Calcd for $C_{42}H_{16}F_{28}N_2O_9$: MW, 1224.60. Found: 1250. The IR is given in Figure 63, the TGA scans, in nitrogen and air, in Figures 64 and 65, respectively, and the DSC scan in Figure 66. The DSC scan of the Imide III following a 72 hour exposure at 316°C is presented in Figure 67.

TABLE 38

ION FRAGMENTS AND INTENSITIES RELATIVE TO BASE PEAK OF



m/e	%	m/e	%	m/e	%	m/e	%
31	6.7	81	5.7	152	2.0	352	4.1
32	5.6	82	3.9	168	6.9	372	8.4
36	3.0	97	3.4	176	2.1	373	2.1
47	16.6	100	8.3	205	20.9	488	6.0
50	13.0	104	14.2	206	2.1	554	2.8
51	3.1	119	28.9	207	22.4	604	5.8
66	11.8	125	3.1	208	2.1	670	2.6
69	14.2	126	10.2	272	<u>100.0</u>	720	3.9
74	2.5	127	5.9	273	29.1	836	2.4
75	5.6	130	15.5	274	4.2	932	2.1
76	13.5	131	3.9	290	3.5	952	2.1
79	3.3	145	3.2	305	3.6	1060	3.9
80	3.4	151	2.9	307	3.1		

Peaks having intensities lower than 2% of the base peak and lower than m/e 31 are not reported.

Significant Ions in Support of Structure and Composition

m/e

76 - C_6H_4^+
 104 - $\text{C}_6\text{H}_4\text{C}(\text{O})^+$
 205 - $\text{CF}_2\text{C}_6\text{H}_4\text{Br}^+$

m/e

272 - $\text{CF}_2\text{C}_6\text{H}_4\text{N}(\text{CO})_2\text{C}_6\text{H}_4^+$
 372 - $\text{C}_3\text{F}_6\text{C}_6\text{H}_4\text{N}(\text{CO})_2\text{C}_6\text{H}_4^+$
 952 - $[\text{M}-\text{CF}_2\text{C}_6\text{H}_4\text{Br}]^+$

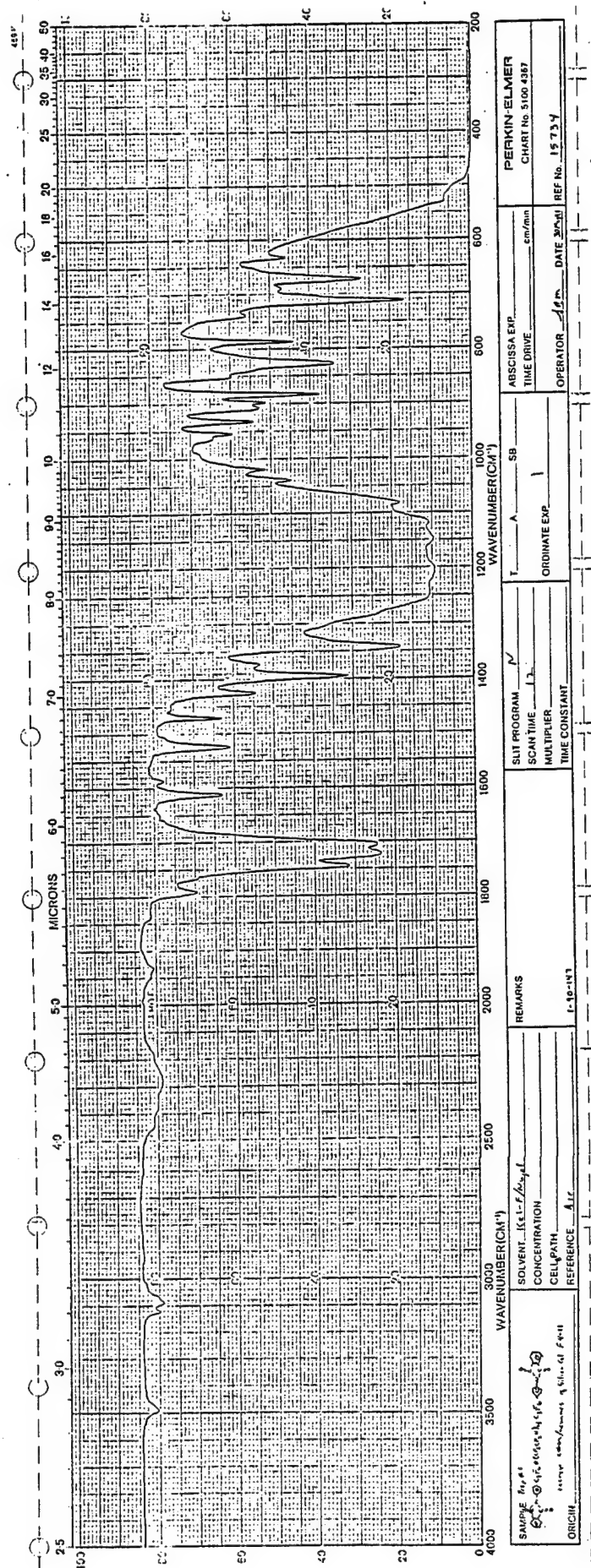


Figure 63. Infrared spectrum of Imide III.

TGA RUN NO 1015 DATE 130492 OPERATOR AKM SAMPLE: 78.5734 1-10-147 ATM. N ₂ @ FLOW RATE 100 mL/min		T-AXIS SCALE, °C/in 50 PROG. RATE, °C/min 10 HEAT <input checked="" type="checkbox"/> COOL <input type="checkbox"/> ISO SHIFT, in 0		DTA-DSC SCALE, °C/in (mcal/sec)/in WEIGHT, mg REFERENCE		TGA SCALE, mg/in SUPPRESSION, mg WEIGHT, mg 11.03 TIME CONST., sec dY, (mg/min)/in		TMA SCALE, mils/in MODE SAMPLE SIZE LOAD, g dY, (10X), (mils/min)/in	
---	--	--	--	--	--	--	--	--	--

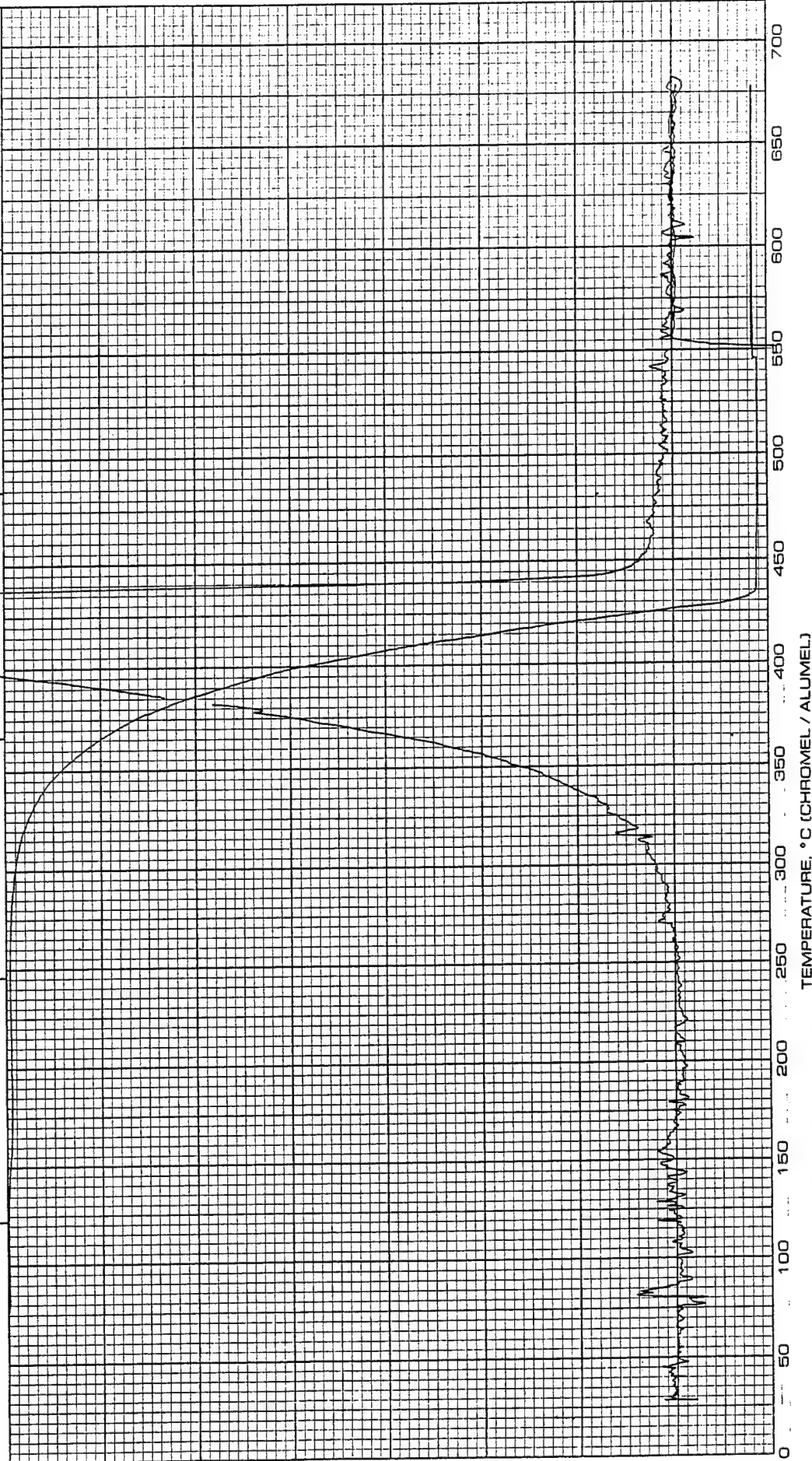


Figure 64. TGA scan of Imide III in N₂.

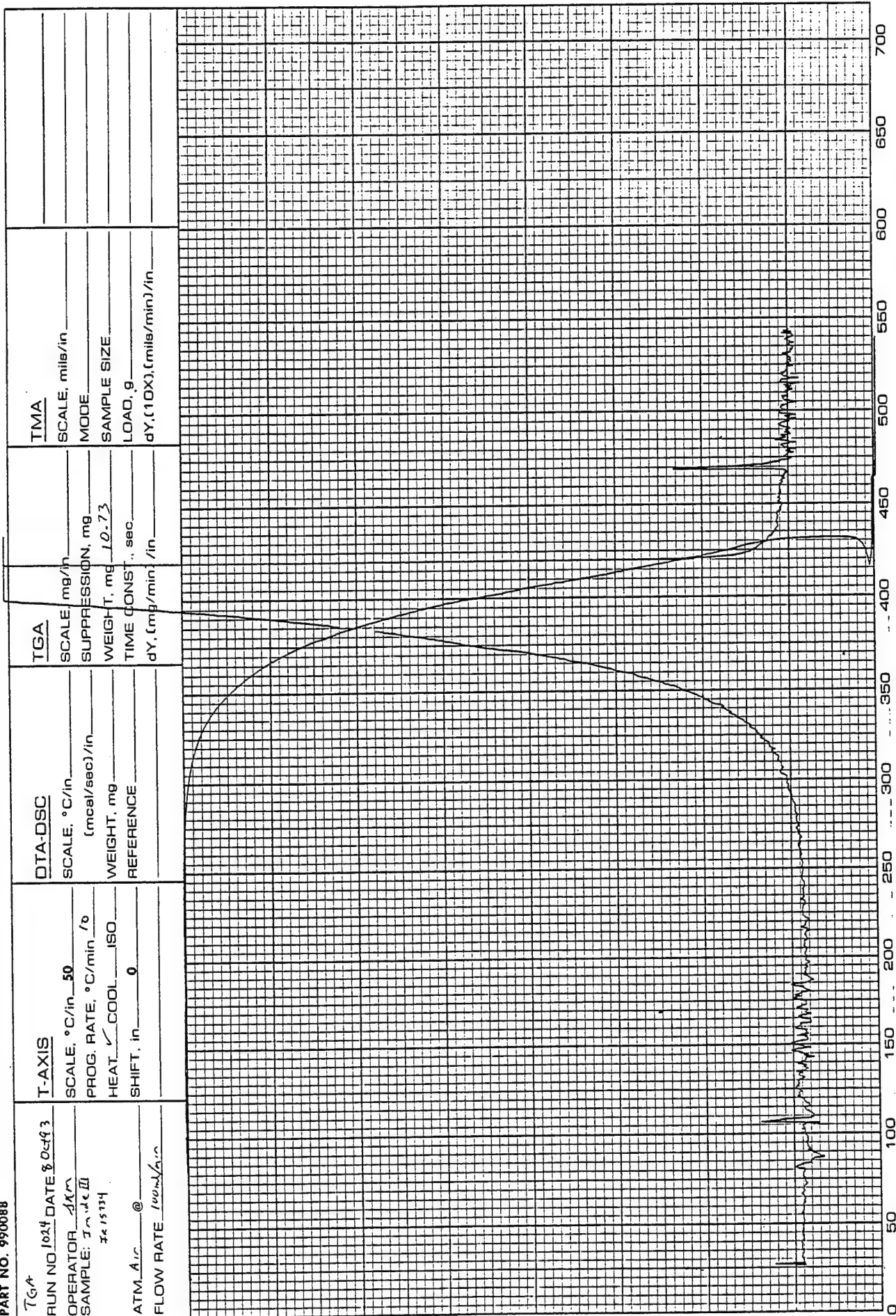


Figure 65. TGA scan of Imide III in air.

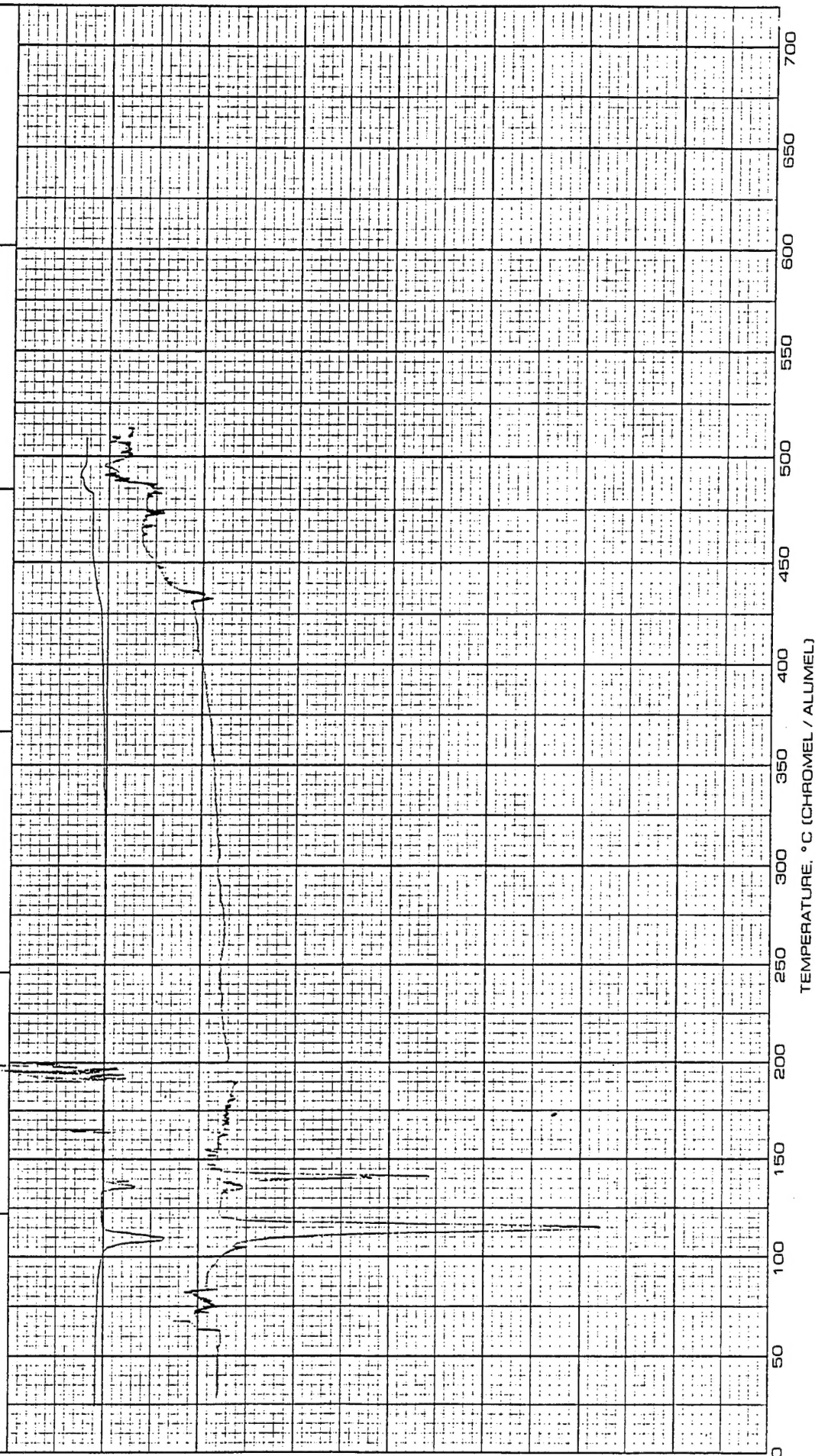


Figure 66. DSC scan of Imide III.

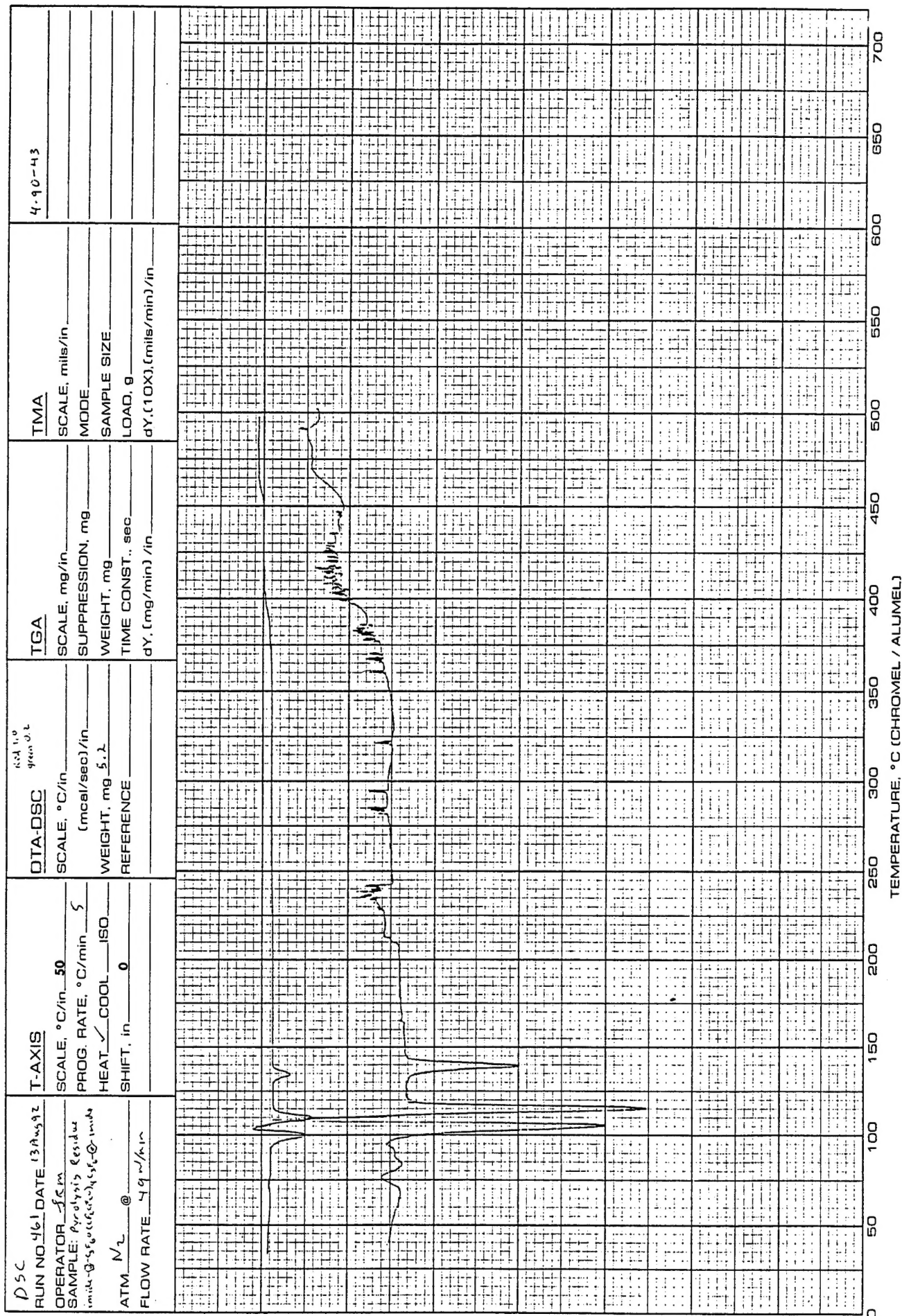


Figure 67. DSC scan of Imide III exposed in vacuo to 316°C for 72 hours.

5. REFERENCES

1. K.L. Paciorek, K.K. Johri, K.G. Podejko, J.G. Shih, and J.S. Wroblewski, "High Performance Elastomers," Interim Report February 1987-February 1988, AFWAL-TR-88-4129, October 1988.
2. K.L. Paciorek, K.K. Johri, J.G. Shih, J.S. Wroblewski, and J.H. Nakahara, "High Performance Elastomers," Interim Report February 1988-February 1989, WRDC-TR-89-4067, August 1989.
3. K.L. Paciorek, S.R. Masuda, J.G. Shih, J.S. Wroblewski, and J.H. Nakahara, "High Performance Elastomers," Interim Report February 1989-February 1990, WRDC-TR-90-4015, November 1990.
4. L.S. Chen and C. Tamborski, J. Fluorine Chem., 26, 269-279 (1964).
5. V.C.R. McLoughlin and J. Thrower, Tetrahedron, 25, 5921-5940 (1969).
6. P.L. Heinze and D.J. Burton, J. Fluorine Chem., 29, 359-361 (1985).
7. D.J. Burton, "Organometallics in Synthetic Organofluorine Chemistry," paper presented at Loker Hydrocarbon Research Institute Symposium on Synthetic Fluorine Chemistry, February 1990.
8. Dr. Donald J. Burton, private communication.
9. K.L. Paciorek, R.H. Kratzer, J. Kaufman and R.W. Rosser, J. Fluorine Chem., 6, 241-258 (1975).

10. K.J.L. Paciorek, J. Kaufman, J.H. Nakahara, T.I. Ito, R.H. Kratzer, R.W. Rosser and J.A. Parker, J. Fluorine Chem., 10, 277-288 (1977).
11. K.J.L. Paciorek, "Phospha-s-triazines of Improved Hydrolytic and Thermal Oxidative Stability," Contract No. NAS3-26508, NASA SBIR Phase I Report, July 1992.
12. E. Strepparola, G. Caporiccio, and E. Monza, Ind. Eng. Chem. Prod. Res. Dev., 23, 600-605 (1984).
13. R.G.R. Bacon and Anna Karim, J. C. S. Perkin I 272-280 (1973).